Late Miocene continental slope evolution in the Gulf of Cádiz: decoding the importance of bottom currents in sedimentation and morphology

Zhi Lin Ng 黃志麟

Doctoral Thesis

Royal Holloway University of London

2022

THE **DRIFTERS** RESEARCH GROUP
BOTTOM CURRENTS & DEEP-WATER SEDIMENTATION

ROYAL HOLLOWAY UNIVERSITY OF LONDON

Department of **Earth Sciences**

Late Miocene continental slope evolution in the Gulf of Cádiz: decoding the importance of bottom currents in sedimentation and morphology

Zhi Lin Ng

A dissertation submitted to
Royal Holloway University of London
in accordance with the requirements for award of
the degree of Doctor of Philosophy (PhD)
in Earth Sciences/Geology

January 2022

Declaration of Authorship

I _____*Zhi Lin Ng*_____ hereby declare that this thesis and the work presented in it is entirely my own. Where I have consulted the work of others, this is always clearly stated.

Signed: _____

Date: _____*25/12/2021*_____

Abstract

The Gulf of Cádiz is home to the well-studied modern contourite depositional system, which was deposited through the influence of bottom currents sourced from the Mediterranean Outflow Water exiting the Straits of Gibraltar since Pliocene to present. However, the Late Miocene sedimentary evolution and Mediterranean-Atlantic water-mass exchange prior and during the Messinian salinity crisis are poorly understood. Some progress on the characterisation of an ancient Late Miocene contourite depositional system were established from field studies onshore in the Betic and Rifian corridors albeit limited due to outcrop availability, but their downstream continuation in the Gulf of Cádiz has yet to be identified. This is partially due to the complexity of the area resulting from tectonic deformation, whose effect on contourite deposition are ambiguous. Consequently, identification and characterisation of the Tortonian to Messinian interval in the Gulf of Cádiz could answer questions related to the relationship between the Mediterranean and Atlantic during that period, as well as increase our knowledge of contourite deposition in tectonically active settings. This thesis presents a regional-scale study on the Late Miocene evolution of the Gulf of Cádiz, focusing on the role of bottom currents in sedimentation. A detailed seismic stratigraphic analysis was carried out for the available seismic and borehole data acquired from scientific and industry sources, to characterise the sedimentary and paleoceanographic evolution during the later parts of the Late Miocene, assisted by chronostratigraphic correlation. An ancient contourite depositional system is identified consisting of three evolutionary stages: initial-drift, growth-drift, and maintenance-drift, prior to its burial in the latest Miocene. The formation of the Late Miocene contourite depositional system occurred following the main emplacement of the regional Gulf of Cádiz allochthonous unit and can be traced towards southern West Iberian margin. The results allowed us to reconstruct the evolution of the paleo-Mediterranean Outflow Water responsible for the bottom current activity depositing the ancient contourite depositional system until its severe weakening or cessation during the latest Miocene, which led to the Messinian salinity crisis, as well as to suggest its impact on North Atlantic paleoceanographic and climate. This is mainly controlled by continuous uplifting and subsequent closure of the Mediterranean-Atlantic paleo-gateways. These findings also allowed us to understand the influence of tectonic and orbital control on gateway evolution and gravitational processes, and thus on contourite deposition. By unravelling these control factors, they enable us to propose diagnostic criteria of contourite depositional system in tectonically active margins.

Acknowledgement

Last but not least, I would like to show my appreciation to my fellow colleagues in *The Drifters Research Group*: Sandra de Castro, Wouter de Weger, Javier Dorador, Débora Duarte, Tatiana Glazkova, Adam Kirby, Oswaldo Mantilla, Alex Mason, Sara Rodrigues, and Antoine Thiéblemont for their company throughout the four years; to my family: my parents, brother, and sister for their relentless support, patience, and encouragement, especially during the difficult times; and to my friends at *North Mews*: Adrian, Wayne, Justin, and Por for their generous assistance and accompaniment, particularly during the lockdown period of the COVID-19 pandemic.

Table of Contents

List of Tables

List of Figures

Figure 4-2   Seismostratigraphy and regional distribution of the middle-upper Messinian unit in (a) Southwest Iberian (SWIM) and (b) Northwest Moroccan margins regional profile (uninterpreted seismic profile in Fig. S2 - supplementary material) with borehole correlations to U1387 (van der Schee et al., 2016), Algarve-2 (Hernández-Molina et al., 2016), Atlantida-3 and GCB-3 (Ledesma, 2000), and GCMPC-1 (Hernández-Molina et al., 2014) (Table S1 in supplementary material).

Figure 4-3   Seismic profiles indicating the distribution of the middle-upper Messinian unit across southern West Iberian margin (WIM): (a) PD00-608; (b) Southwest Iberian margin (SWIM): S81-N27 and S81-N25; and (c) Northwest Moroccan margin (NWMM): GHR10-6. Uninterpreted seismic profiles in Fig. S3 (*supplementary material*).

Figure 4-4   Time thickness (TWT) map of the middle-upper Messinian unit across Northwest Moroccan (NWMM), Southwest Iberian (SWIM), and southern West Iberian (WIM) margins (Contour interval: 100 ms TWT).

Figure 4-5   Chronology of middle-upper Messinian unit (right) and correlation with Mediterranean and Atlantic chronostratigraphy (Flecker et al., 2015; Krijgsman et al., 2018), 100 kyr and filtered 400 kyr eccentricity curves based on orbital solution La04 (Laskar et al., 2004), gamma ray logging in measured depth (MD) with biostratigraphy of well GCB-3 (Ledesma, 2000) in MD and meters below sea level (mbsl).

Figure 4-6   Scheme of the effect of Mediterranean-Atlantic restriction on the Atlantic Meridional Overturning Circulation (AMOC) during the (a) Tortonian, (b) Messinian, and (c) Pliocene. Paleogeographic reconstruction and Mediterranean-Atlantic gateway configuration adapted from Scotese (2014) and Krijgsman et al. (2018), respectively (NACW: North Atlantic Central Water; MOW: Mediterranean Outflow Water; LSW: Labrador Sea Water; NADW: North Atlantic Deep Water; AABW: Antarctic Bottom Water; AMW: Atlantic-Mediterranean Water.

Figure 4-S1   Relationship between mixing coefficient Φ (Phi) and velocity.

Figure 4-S2   Uninterpreted regional seismic profile, as shown in Fig. 2, of (a) Southwest Iberian margin (SWIM) including location of boreholes Algarve-2, Atlantida-3, GCB-3, GCMPC-1 and U1387, and (b) Northwest Moroccan margin (NWMM), including location of boreholes Anchois-1 and Merou-1.

Figure 4-S3   Uninterpreted seismic profiles as shown in Fig. 3, across (a) southern West Iberian margin (WIM): PD00-608; (b) Southwest Iberian margin (SWIM): S81-N27 and S81-N25; and (c) Northwest Moroccan margin (NWMM): GHR10-6.

Figure 5-1   Geological map showing the main structural units of the Betic-Rif orogeny (AUGC: allochthonous unit of the Gulf of Cádiz; GCAW: Gulf of Cádiz accretionary wedge), tectonic features of the Gulf of Cádiz (AH: Albufeira high; CF: Cádiz fault; CPS: Coral Patch seamount; DS: Descobridores seamount GB: Guadalquivir bank; GEF: Gil Eanes fault; GF: Grandola fault; HAP: Horseshoe abyssal plain; HF: Horseshoe fault; HGU: Horseshoe Gravitational Unit; MPF: Marquês de Pombal fault; MPP: Marquês de Pombal plateau; PAS: Príncipe de Avis seamount; PDE: Pen Duick escarpment; PF, Portimão fault; PH: Portimão High: PSF: Pereira de Sousa fault; SAP: Seine abyssal plain; SMQF: São Marcos-Quarteira fault; SVF: São Vicente fault; TAP: Tagus abyssal plain), associated Neogene sedimentary

basins (AlB: Alentejo basin; DAB: Deep Algarve basin; DB: Doñana basin; CB: Cádiz basin; OGB: Offshore Gharb basin; RdLB: Rincão do Lebre basin; SB: Sanlúcar basin) and sedimentary features (FC: Faro canyon; LC: Lagos canyon; PC: Portimão canyon; SC: Sagres canyon; SeC: Setúbal canyon; SVC: São Vicente canyon) (Adapted from Hernández-Molina et al., 2016).

Figure 5-2   Map of the dataset (including seismic surveys, boreholes, and bathymetry).

Figure 5-3   Regional profiles of the study area showing the distribution of the Neogene sedimentary basins (Alentejo basin, Cádiz basin, Deep Algarve basin, Doñana basin, Offshore Gharb basin, Sanlúcar basin), tectonic domains (Betic-Rif orogeny, Gulf of Cádiz accretionary wedge, Iberian Massif, Moroccan Meseta and West Iberian passive margin) and seismic units (PQ, LM and B): a. N-S southern West Iberian margin (WIM), b. W-E Gulf of Cádiz, c. N-S Gulf of Cádiz.

Figure 5-4   Stratigraphic correlation of the main sequences (PQ, LM, B), units (Upper and Lower LM) and sub-units (M1, M2 and M3) described in the present work, including stratigraphic correlations interpreted by previous authors and main tectonic and sedimentary events in the region (Abbreviation for discontinuities, BFU: basal foredeep unconformity; IMU: intra-Messinian unconformity; ITU; intra-Tortonian unconformity; MPB: Miocene-Pliocene boundary; Top AUGC: top allochthonous unit of the Gulf of Cádiz).

Figure 5-5   Thickness map of Unit LM showing (*a*) the distribution of contourite deposits (D1-D7), and (*b*) their relationship with tectonic and sedimentary features in the Gulf of Cádiz (Structural features adapted from Hernández-Molina et al., 2016; abbreviations given in Fig. 5-1).

Figure 5-6   Structure maps and locations of key tectonic and sedimentary features in the Gulf of Cádiz: (*a*) Top LM (MPB), and (*b*) Base LM (combination of Top AUGC, BFU and ITU) (Structural features adapted from Hernández-Molina et al., 2016; abbreviations given in Fig. 5-1)

Figure 5-7   Seismic profile in the middle slope of southern West Iberian margin (PD00-517) showing an elongated separated drift (D1) associated with a contourite channel west of the Príncipe de Avis seamount (PAS). Profile location given in Fig. 5-2. Shown are major sequences (PQ, LM and B2), subunits of Lower LM (M3 and M2) and main boundaries or discontinuities (SF: seafloor; other abbreviations given in Fig. 5-4; red arrows: stratal terminations).

Figure 5-8   Seismic profile of Alentejo basin (AlB), southern West Iberian margin (PD00-610) showing an elongated separated drift (D2) west of a contourite channel. Profile location given in Fig. 5-2. Major sequences (PQ, LM and B2), subunits of Lower LM (M3 and M2) and the main boundaries or discontinuities (SF: seafloor; other abbreviations given in Fig. 5-4; red arrows: stratal terminations).

Figure 5-9   Seismic profile across Sagres canyon (SC), southern West Iberian margin (PD00-602 & PD00-602A) showing an asymmetric levee and the Sagres submarine canyon associated with a mixed system (D3), as well as sediment waves and erosional scour on the middle slope. Profile location given in Fig. 5-2. Major sequences (PQ, LM and B2), subunits of Lower LM (M3? and M2?) and the main boundaries or discontinuities (SF: seafloor; other abbreviations given in Fig. 5-4; red arrows: stratal terminations).

Figure 5-10   Seismic profile across Faro canyon (FC), Southwest Iberian margin (PD00-707) showing a mounded confined drift (D4) and sediment waves. Profile location given in Fig. 5-2. Major sequences (PQ, LM and B1), subunits of Lower LM (M3, M2 and M1) and main boundaries or discontinuities (SF: seafloor; other abbreviations given in Fig. 5-4; red arrows: stratal terminations).

Figure 5-11   Seismic profile in Cádiz basin (CB), Southwest Iberian margin (S81-N14) showing a mounded drift (D5) west of a fault scarp. Profile location given in Fig. 5-2. Major sequences (PQ, LM and B0), subunits of Lower LM (M3, M2 and M1) and main boundaries or discontinuities (SF: seafloor; other abbreviations given in Fig. 5-4; red arrows: stratal terminations)

Figure 5-12   Seismic profile in eastern Offshore Gharb basin, Northwest Moroccan margin (NWM03-F002) showing a plastered to mounded drift (D6) west of a fault scarp. Profile location given in Fig. 5-2. Major sequences (PQ, LM and B0), subunits of Lower LM (M3, M2 and M1) and main boundaries or discontinuities (SF: seafloor; other abbreviations given in Fig. 5-4; red arrows: stratal terminations)

Figure 5-13   Seismic profile in western Offshore Gharb basin, Northwest Moroccan margin (LAR04-5) showing an asymmetric confined drift (D7) bounded by basement highs and flanked by erosional scar and channels. Profile location given in Fig. 5-2. Major sequences (PQ, LM and B0), subunits of Lower LM (M3, M2 and M1) and main boundaries or discontinuities (SF: seafloor; other abbreviations given in Fig. 5-4; red arrows: stratal terminations)

Figure 5-14   Schematic model for the relationship between contourite distribution (Fig. 5-5a, D1-D7) and potential pathway of the paleo-Mediterranean Outflow Water (MOW) for the late Miocene Gulf of Cádiz CDS, superposed on the Base LM structure map (Fig. 5-6b) loosely representing the paleobathymetry of the late Miocene. (NWMM: Northwest Moroccan margin, SWIM: Southwest Iberian margin, WIM: West Iberian margin; other abbreviations given in Fig. 5-1)

Figure 5-15   (*Top*) Seismic profile in western Onshore Gharb basin, subsurface of the Haricha section (85-LK-28), showing the distribution of the Lower LM subunits (M3, M2 and M1), main boundaries and discontinuities, and the presence of elongated separated drifts associated with the late Miocene contourite depositional system in the Rifian corridor. Seismic interpretation adapted from Capella et al. (2017). (T/M boundary: Tortonian-Messinian boundary, other abbreviations available in Fig. 5-4); (*Bottom*) Simplified geological map of the Rifian corridor showing the location of seismic profile 85-LK-28 and sedimentary sections of the Rifian corridor late Miocene CDS, and the paleo-MOW pathway (adapted from Capella et al., 2017) (Location of section indicated in Fig. 5-1).

Figure 6-1   **(A)** Study area in the Gulf of Cádiz. Gray rectangle indicates location of the Algarve-2012 3D seismic reflection survey in B. Modified from Ng et al. (2021a). **(B)** Seafloor of the study area. Red dots indicate location of boreholes (Algarve-2 and U1387); red dotted lines indicate location of cross sections in Figures 3 and 4 (Abbreviations – AGDH: Albufeira-Guadalquivir-Doñana High; ALFZ: Albufeira fault zone; GEFZ: Gil Eanes fault zone; PMFZ: Portimão-Monchique fault zone; SMQF: São Marcos-Quarteira fault zone).

Figure 6-2   Stratigraphic correlation of the seismic units (U1-U6) and boundaries (D1-D7) described in the present work, with previous authors in the Deep Algarve, onshore Algarve, and Guadalquivir basins (Abbreviations for stratigraphic discontinuities - BFU: basal foredeep

unconformity; IMU: intra-Messinian unconformity; LMU; Late Miocene unconformity; MPB: Miocene-Pliocene boundary; MPU: Miocene-Pliocene unconformity).

Figure 6-3 **(A)** Representative seismic reflection profile (IL 2954) across the study area (top) and their interpreted unit boundaries (D1-D7) (bottom). Profile locations are given in Figure 1(B). **(B)** Enlarged cross-section profile (IL 3150) across the southern sub-basin and interpreted seismic units (U1-U6) and evolutionary stages (I-IV).

Figure 6-4 Borehole and facies correlation between **(A)** eastern and **(B)** far eastern Deep Algarve basin. Location given in Figure 1(A).

Figure 6-5 RMS amplitude and variance attributes blend, and time top structure and time thickness maps for the units U1 to U6 and respective boundaries D1 to D7 – **(A)** U1: D1 to D2, **(B)** U2: D2 to D3, **(C)** U3: D3 to D4, **(D)** U4: D4 to D5, **(E)** U5: D5 to D6, and **(F)** U6: D6 to D7.

Figure 6-6 Distribution of Stage I and II (Unit U1, U2 & U3) deposits in the southern sub-basin of the Deep Algarve basin and their relationship with bottom currents, illustrated using seismic profiles **(A)** IL 3600, **(B)** IL 3150 and **(C)** 2700 from the Algarve-2012 3D seismic survey, and **(D)** thickness maps of Unit U1 and U3.

Figure 6-7 Evidence of turbidity and bottom current influence during Stage I (Unit U1) with the identification of erosional and depositional feature related to contourite depositional systems, illustrated using seismic profiles **(A)** XL 3142, **(B)** XL 2490, **(C)** IL 1144, **(D)** IL 1771, from the Algarve-2012 3D seismic survey, and **(E)** RMS amplitude extraction of internal horizons 1 and 2 of Unit U1. Location given in Figure 6(D).

Figure 6-8 Evolution of the Guadalquivir Sands turbidite system (1 to 5) in the southern sub-basin of the Deep Algarve basin during Stage III and IV (Unit U4, U5 & U6), illustrated using seismic profiles IL 2354, 2554, 2754, 2954, 3154, 3354, and 3554 from the Algarve-2012 3D seismic survey (Abbreviation – AUGC: Allochthonous unit of the Gulf of Cádiz).

Figure 6-9 Schematic 4-stage evolutionary block model of the eastern Deep Algarve basin, with **(A)** Stage I (Unit U1), **(B)** Stage II (Unit U2 and U3), **(C)** Stage III (Unit U4 and U5), and **(D)** Stage IV (Unit U6).

Figure 7-1 The distinct stages of the Late Miocene contourite depositional system correlated to the paleogeography of Mediterranean-Atlantic gateways: **(A)** Initial-drift stage during the middle to late Tortonian; **(B)** Growth-drift stage during the latest Tortonian to earliest Messinian; **(C)** Maintenance-drift stage during the early to middle Messinian; and **(D)** Buried-drift stage during the late Messinian (adapted from Martín et al., 2009).

Figure 7-2 The evolution of the Late Miocene contourite depositional system correlated to the eccentricity orbital cycle (Laskar et al., 2004); global sea level (Miller et al., 2011); diapiric activity and tectonic events (Duarte et al., 2021); and oceanographic changes during the late Tortonian to late Messinian.

Chapter 1
Introduction

1.1 Prologue

The Southwest Iberian and Northwest Moroccan continental margins, collectively known as the Gulf of Cádiz, are located west of the Strait of Gibraltar. Their proximity to the Gibraltar Arc makes them ideal for basin studies to understand the geodynamic evolution of the region. The sedimentary record in the Neogene basins of the Gulf of Cádiz and the Betic Guadalquivir and Rifian Gharb foreland, complemented by the structural features, provide insights into the development of the continental margins from the Miocene to the present day (Maldonado et al., 1999; Medialdea et al., 2004; Vergés and Fernàndez, 2012).

Major changes in the plate tectonics, climate, and oceanography, notably the Betic-Rif orogeny and the Messinian salinity crisis (MSC), have occurred during the Neogene. Nearly half a century since the proposal of a desiccated Mediterranean Sea in the Late Miocene by (Hsü et al., 1973), the Messinian salinity crisis remains one of the most controversial scientific topics debated today (Rouchy et al., 2006; Roveri et al., 2014; Lugli et al., 2015). The nature of the isolation of the Mediterranean Sea, as a subsequence of the Betic-Rif orogenic uplift and or the glacio-eustatic lowering of sea-level (Weijermars, 1988; Hodell et al., 1994; Krijgsman et al., 1999) is still widely disputed (Roveri et al., 2014). Nevertheless, the restriction of the Mediterranean-Atlantic connection resulting in the interruption of the Mediterranean Outflow Water (MOW) would have an impact on the bottom-current circulation in the Atlantic (Pérez-Asensio et al., 2012), and the sedimentary distribution within the Gulf of Cádiz.

The presence of contourite and turbidite depositional systems, along with other deep marine deposits, are well documented within the Gulf of Cádiz for the Neogene and Quaternary (Maldonado et al., 1999; Lopes et al., 2006; Llave et al., 2007; Marchès et al., 2010; Roque et al., 2012; Brackenridge et al., 2013; Hernández-Molina et al., 2016). However, the sedimentary distribution and evolution prior to the Late Miocene are not well constrained. A detailed understanding of the Late Miocene sedimentary evolution in the Gulf of Cádiz could unravel the interaction between the Atlantic and the Mediterranean, and the effects of bottom current dynamics on the development of the Southwest Iberian and Northwest Moroccan margins prior, during and after the Messinian salinity crisis.

1.2   Objectives

This work aims to understand the Late Miocene continental slope evolution in the Gulf of Cádiz, including the Southwest Iberian and Northwest Moroccan continental margins.

The primary objective is the definition of major sedimentary and stratigraphic changes in both Southwest Iberian and Northwest Moroccan continental margins during the Late Miocene, which includes the Tortonian to Messinian period prior and during the Messinian salinity crisis, as well as its relationship with the period since the end of the Messinian salinity crisis, which is correlated to the Pliocene to Quaternary. The tasks associated are the seismostratigraphic analysis of the Neogene basins in the Gulf of Cádiz and the correlation with drilling data and the onshore foreland basins for the establishment of a regional chronostratigraphy, followed by the construction of a depositional model to describe the slope evolution of the continental margins.

The secondary objective is the evaluation of the effects of bottom currents to Late Miocene sedimentary and slope morphology evolution of the Southwest Iberian and Northwest Moroccan margins. This involved the identification of the erosional and depositional features of the contourite depositional system and the analysis of its spatial distribution and temporal evolution during the Tortonian to Messinian. The conceptual and economic implications of contourite deposition in the Gulf of Cádiz during the Late Miocene are also discussed.

1.3   Thesis structure

Results of this work are published or submitted for publication in peer-reviewed journals, where the published articles are maintained in the results chapters in this thesis with their guidelines and formats of the respective journals. Repetition and overlapping of regional information and implications are inevitable more commonly in the introduction, literature review and occasionally discussion and conclusion sections of the results chapter. Therefore, the thesis is structured in the following format:

Chapter 1   Introduction

This chapter presents the preface of the work, including the research history and motivation, and highlighting the main objective and the structure of the thesis.

Chapter 2   Geological and Oceanographic Framework

This chapter explains the background of the study, firstly the regional understanding of the research area, including the geological and oceanographic context, and secondly the conceptual understanding of deep marine sedimentology in consideration to basin analysis, including the main processes and their respective deposits.

Chapter 3   Methodology

This chapter catalogues the dataset and methods used, and the dynamics in which the work is carried out in relation to research collaborations.

Chapter 4   Latest Miocene restriction of the Mediterranean Outflow Water: a perspective from the Gulf of Cádiz

This chapter focuses on latest Miocene sedimentary evolution in the Gulf of Cádiz, simultaneous to the evolution of the Messinian salinity crisis, and its paleoceanographic implications for the Mediterranean-Atlantic gateway exchange. It is presented in the form of a research article published in *Geo-Marine Letters **41**, 23 - doi:10.1007/s00367-021-00693-9.*

Chapter 5   Late Miocene Contourite Depositional System of the Gulf of Cádiz: The sedimentary signature of the paleo-Mediterranean Outflow Water

This chapter focuses on the Late Miocene seismostratigraphic work of Gulf of Cádiz, and the discovery of its Late Miocene contourite depositional system. It is presented in the form of a research article published in *Marine Geology **442**, 106605 - doi:10.1016/j.margeo.2021.106605.*

Chapter 6   Late Miocene evolution of the eastern Deep Algarve basin: interaction of bottom currents and gravitational processes in a foredeep setting

This chapter focuses on the Late Miocene evolution of the Deep Algarve basin, depicting the interaction of the paleo-Mediterranean Outflow Water with the Guadalquivir Sands turbidite depositional system. It is presented in the form of a research article ready for submission to SCI journals.

Chapter 7   Discussion and Critical Evaluation

This chapter discusses the results in chapters 4, 5 and 6 and correlates the stratigraphic changes towards a regional evolution for the Gulf of Cádiz during the Late Miocene and its conceptual and economic implications.

Chapter 8   Conclusion

This chapter recapitulates the work, including the summary of main findings and suggestions for future research efforts.

Chapter 2

Geological & Oceanographic Framework

2.1 Morphological setting

The physiography of the continental slope margins of the Gulf of Cádiz below the shelf break at 100-140 m is made up of a steeper upper slope (2°-3°) between the depths of 150-400 m, a gentler middle slope (1°-2°) which is separated into two wide terraces between depths of 500-750 m and 800-1200 m by a northeast trending ridge, and a smooth lower slope (0.5°-1°) (Hernández-Molina et al., 2006). Below we summarised the main morphostructural domains and morphosedimentary sectors:
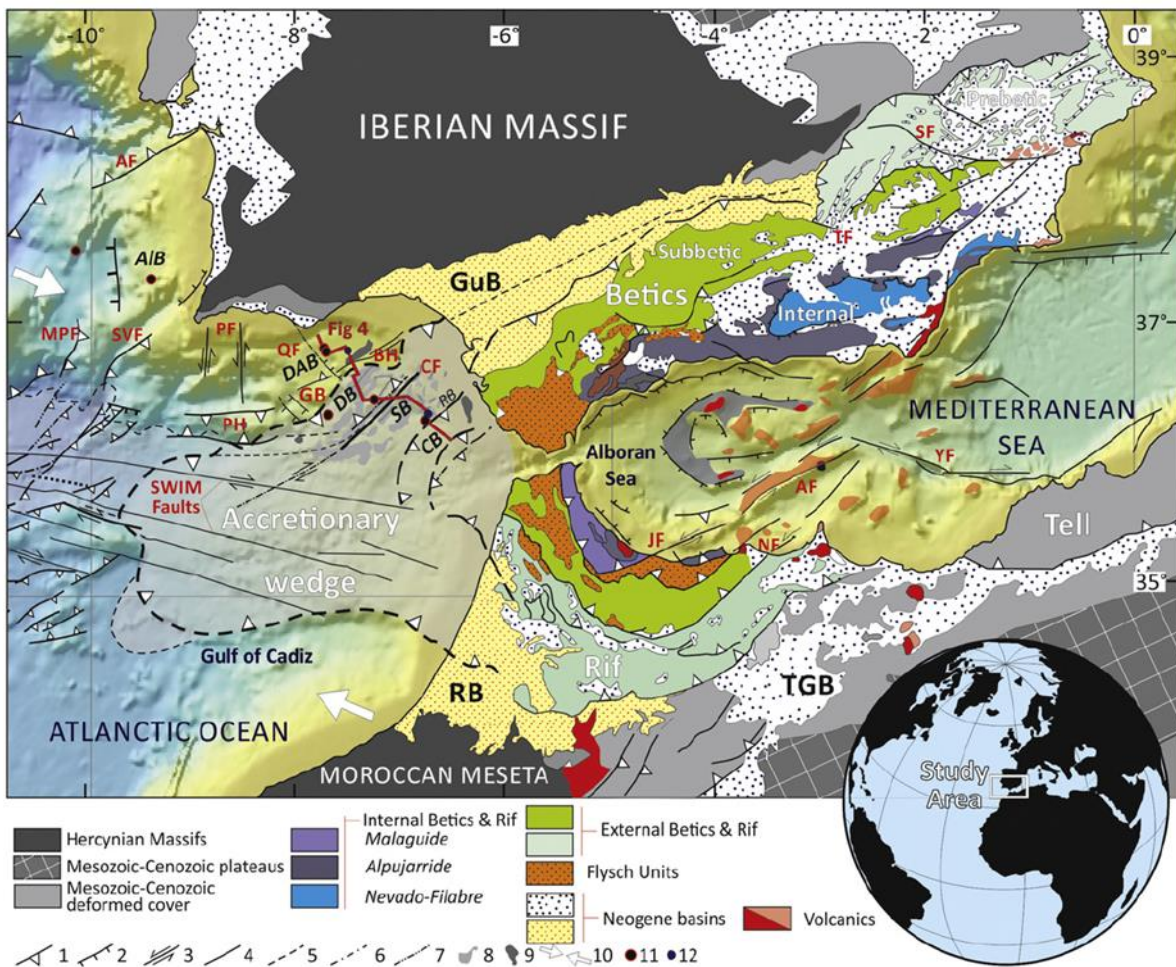
Figure 2-1: Geological map showing key structures and domains of the Betic–Rif Orogen and the Gulf of Cádiz (Hernández-Molina et al., 2016). Key: (*Neogene basins*) DAB – Deep Algarve basin; AlB – Alentejo basin; CB – Cádiz basin; DB – Doñana basin; GuB – Guadalquivir basin, RB – Rharb/Gharb basin; SB – Sanlúcar basin; TGB – Taza-Guercif basin; (*Faults) Betics* - SF – Socovos Fault; TF – Tiscar Fault; *Rif* - JF – Jehba Fault; NF – Nekor Fault; *Alboran* - AF – Alboran Ridge Fault; YF – Yusuf Fault; *Atlantic* - CF – Cádiz Fault; QF – Quarteira Fault; PH – Portimão High; BH – Basement High; SVF – São Vicente Fault; PF – Portimão Fault; MPF – Marquês de Pombal Fault; AF – Arrábida Fault; (*Map annotations*) 1 – reverse and thrust faults; 2 – normal faults; 3 – strike slip faults; 4 – faults; 5 – contact below sediment; 6 – inferred faults; 7 – blind faults; 8 – AUGC ; 9 – salt diapirs; 10 – Nubia–Iberia plate convergence; 11 – Integrated Ocean Drilling Program (IODP) Expedition 339 sites; 12 - exploration wells.

2.1.1 Morphostructural features

The Southwest Iberian and Northwest Moroccan margins consist of three main morphostructural domains (Maldonado et al., 1999; Zitellini et al., 2009; Hernández-Molina et al., 2016): a. The Hercynian Massif basement, including the South-Iberian paleomargin of the Iberian Massif and the North-Moroccan paleomargin of the Moroccan Meseta; b. Neogene basins, including the onshore Guadalquivir and Gharb foreland basins and the offshore foredeep Deep Algarve, and wedge-top Doñana, Sanlúcar, and Cádiz basins in the Gulf of Cádiz; and c. the external front of the Betic-Rif orogeny engulfing the Gulf of Cádiz accretionary wedge (GCAW) (Duarte et al., 2011), firstly introduced as the "olistostrome unit" (Maldonando et al., 1999), later known as the allochthonous unit of the Gulf of Cádiz (AUGC) (Medialdea et al., 2004); or the Atlantis accretionary wedge (Gutscher et al., 2002).

The Iberian Massif and the Moroccan Meseta are representations of the Variscan orogeny between the Baltica-Laurentia and Gondwana (Palomeras et al., 2017) in the Devonian to Carboniferous (Matte, 1986). The separation of the two Hercynian Massifs occurred with the break-up of Pangaea forming the paleomargins of the westernmost segment of the Neo-Tethys Ocean (Sallarès et al., 2011; Palomeras et al., 2017). In the Gulf of Cádiz, there are also the presence of Paleozoic-Mesozoic basement highs: Guadalquivir, Portimão, and Albufeira banks, as offshore prolongation of the Hercynian basement (Medialdea et al., 2004) (Fig. 2-1).

The Neogene basins of the Gulf of Cádiz are basins formed above the AUGC and Mesozoic and Paleogene paleomargins underlain by the Hercynian continental crust (González et al., 1998), juxtaposed against the external fronts of the Betic-Rif orogeny. These basins, formed from the foredeep subsidence within the Gulf of Cádiz, are consisted of Late Miocene, Pliocene, and Quaternary sedimentary deposits (Maldonado et al., 1999). In the Southwest Iberian margin, the Algarve, Doñana, Sanlúcar, and Cádiz basins are separated by basement highs and NE-trending diapiric ridges: Doñana, Guadalquivir, and Cádiz Diapiric Ridges (Hernández-Molina et al., 2016). The eastern part of the Algarve basin is a continuation of the Guadalquivir foreland basin of the Betic Cordillera into the Southwest Iberian margin and the Gulf of Cádiz, where its larger part is located offshore as the foredeep Deep Algarve basin, bounded by both the Guadalquivir bank, and the Guadalquivir or Gulf of Cádiz allochthonous front (Lopes et al., 2006; Hernández-Molina et al., 2016). Whereas the Doñana, Sanlúcar, and Cádiz basins are

known as wedge-top basins, located on top of the allochthonous unit or accretionary wedge (Fig. 2-1).

The external front of the Gulf of Cádiz allochthonous unit consist of westward advancing imbricated sheets or wedges, which can be divided into features of three distinct phases: the thrusting of the Betic-Rif orogenic front; followed by gravitational sliding of the chaotic masses, while extensional collapse occurs at the back of the advancing sheets. The tectonic and gravity transport facilitated thrust sheets development westward leading to new cycles of the emplacement of the allochthonous unit (Medialdea et al., 2004).

Further east, the Gibraltar Arc is divided into external and internal zones. The horseshoe shaped external thrust belts extend from the Prebetic and Subbetic of Spain, the Prerif, Mesorif and Intrarif of Morocco, towards the Tell Mountains of NW Algeria, with Triassic to Lower Miocene deposits (Medialdea et al., 2004; Vergés and Fernàndez, 2012; Flecker et al., 2015). Whereas, the internal arc consists of mainly Paleozoic to Triassic metamorphic complexes of the Internal Betics of Spain and the Internal Rif of Morocco, and the extensional Alborán basin (Comas et al., 1999; Medialdea et al., 2004; Flecker et al., 2015). Upper Cretaceous to Lower Miocene deep marine Flysch of Campo de Gibraltar complexes are sandwiched in between the two zones by overthrusting (Medialdea et al., 2004; Vergés and Fernàndez, 2012; Flecker et al., 2015).

Further west lies the transition from continental slope to the basin plains of African oceanic crust (Medialdea et al., 2004). At the base of the lower slope and rise are the deeper Horseshoe (~4800 m) and shallow Seine (~4300-4400 m) abyssal plains, separated in between by the Coral Patch Ridge and Seamount of NE-SW orientation (Medialdea et al., 2004). The seaward migration of the allochthonous unit of the Gulf of Cádiz is constrained by this ridge and further diverged into two lobes and progressively thins into the respective basin plains (Medialdea et al., 2004). The Horseshoe abyssal plain is also bounded in the north by the NE-SW Gorringe bank and the São Vicente cape (Medialdea et al., 2004; Lopes et al., 2006).

2.1.2 *Morphosedimentary features*

The present day morphosedimentary features in the middle slope of the Gulf of Cádiz is mapped into five different sectors in relation to the contourite depositional system (Hernández-Molina et al., 2003): a. proximal scour and sand-ribbons sector; b.

overflow-sedimentary lobe sector; c. channels and ridges sector; d. contourite-deposition sector; and e. submarine canyon sector. The spatial distribution of these features is largely controlled by the interaction between the middle slope of the Gulf of Cádiz with the evolving oceanographic processes, notably the Mediterranean Outflow Water (Hernández-Molina et al., 2003).

The proximal scour and sand ribbons sector is located at the eastern most section of the Gulf of Cádiz, just off the Straits of Gibraltar (Kenyon and Belderson, 1973). This sector consists of a southeastern erosional domain of mainly erosive scour alignments and abrasion surface, and a northwestern depositional domain of sand dunes and sand-ribbon fields (Hernández-Molina et al., 2003).

Adjoining to this sector in the seaward direction at depths of 750-1600 m above the Cádiz basin is the overflow sedimentary lobes. The sand and mud fan-shaped sedimentary lobes and wave fields in this sector resulted from the erosional and depositional process, with downslope gravitational influence (Nelson et al., 1993; Hernández-Molina et al., 2003). These processes gave rise to sedimentary features such as mega-sedimentary lobes with bedforms, scours and furrows, notably the 55 km long and 0.8-1.7 km wide Gil Eanes channel (Kenyon and Belderson, 1973; Hernández-Molina et al., 2003).

The channels and ridges sector are located centrally in the Neogene basins of the Southwest Iberian margin (Algarve, Doñana, Sanlúcar, and Cádiz basins) (Nelson et al., 1993). The main features here include the five main contourite channels of 10 to more than 100 km in length: Cádiz, Guadalquivir, Huelva, Diogo Cão, and Gusano Channels (García, 2002; Hernández-Molina et al., 2003). These erosive features can be incised till up to 350 m in depth and 10 km in width and are generally positioned along the slope margins of the Gulf of Cádiz or diverted downslope into the valley along the southwestern flanks of basement highs and diapiric ridges in the Gulf of Cádiz (Nelson et al., 1993; Hernández-Molina et al., 2003). The channels are established above relict drifts, which were affected by tectonism and diapirism (Hernández-Molina et al., 2003).

Located along the slope margin south off the coast of Portugal, the 80 km long Alvarez Cabral moat bounds the contourite deposition sector (Hernández-Molina et al., 2003). This sector is composed of the Faro-Albufeira elongated and separated mounded drift, and the Faro-Cádiz and Bartolomeu Dias sheeted drifts (Llave et al., 2001). Erosional features over the drift make up the fifth morphological element in this sector

(Hernández-Molina et al., 2003). The morphological contrast between the channels and ridges, and contourite deposition sectors is controlled by the complex pattern of contour-parallel or valley-perpendicular flow paths of the Mediterranean Outflow Water (Nelson et al., 1993).

The final morphosedimentary sector in the Gulf of Cádiz is the submarine canyons sector, which lies west of the Alvarez Cabral moat until around the São Vicente Cape. They are the Portimão, the Lagos, the Sagres, and the São Vicente Canyons. Separated by the canyons are the Portimão, Lagos, and Sagres sheeted drifts arranged from east to west respectively (Hernández-Molina et al., 2003).
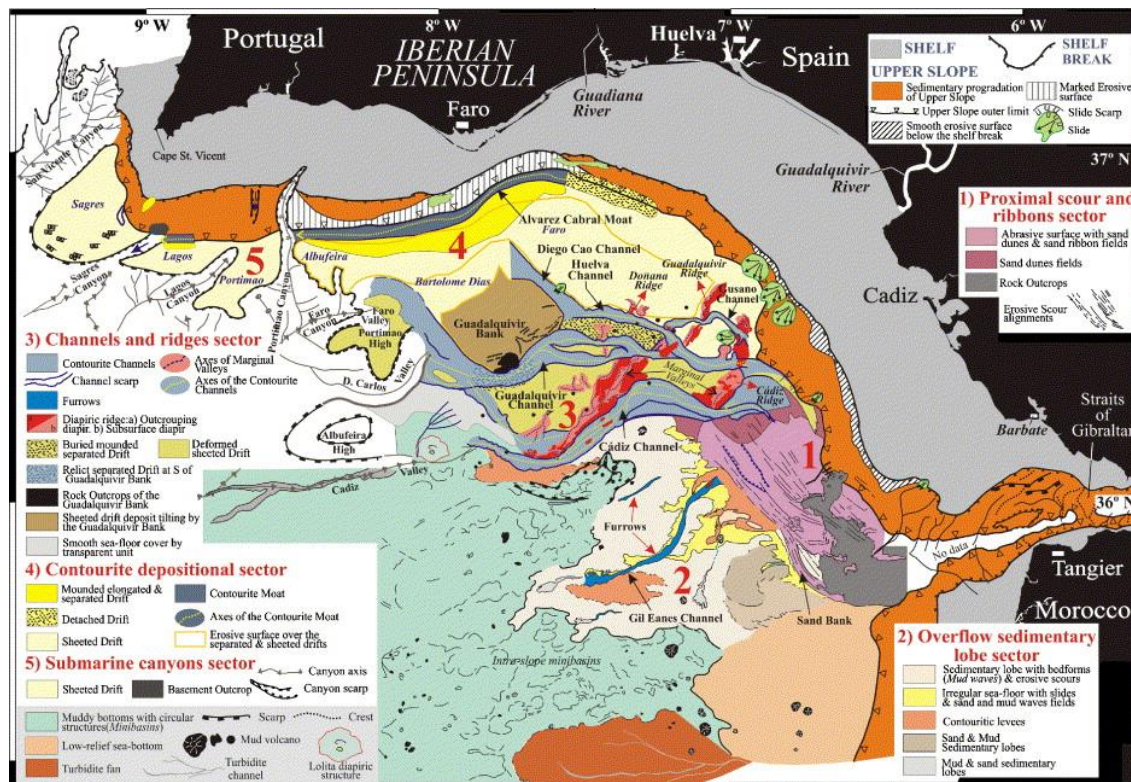
Figure 2-2   Morphosedimentary map of contourite depositional system on middle slope of Gulf of Cádiz. Sedimentary deposit types and bedforms are shown for five morphosedimentary sectors (Hernández-Molina et al., 2003; 2006).

2.2   Stratigraphic framework

2.2.1 Mesozoic - Paleogene

Above the Paleozoic basement rocks of the Hercynian Massif, seven pre-Miocene seismostratigraphic units, correlated to commercial wells drilled offshore in the Gulf of Cádiz, are described in Maldonado et al. (1999). In the order of older to younger units,

the Triassic to Early Jurassic Units TR1 and TR2 consists of halite and clay-anhydrite evaporitic deposits of early rift-sag succession; followed by dolomites and limestones of Lower to Middle Jurassic Unit LJ from carbonate platforms developed on Tethyan rift tilted crustal blocks (Lopes et al., 2006; Terrinha et al., 2019a). The Upper Jurassic to Lower Cretaceous Units UJ-LK1 (~157-125 Ma) and Middle Cretaceous unit LK2 (~125-94 Ma) consists of half-graben fillings of progradational to aggradational carbonate fans, debris apron, and slope facies separated by an angular uniformity (~125-113 Ma). In the Deep Algarve basin, the Lower Cretaceous sediments consist of dolomites, sandstones, and interbedded limestones and marly limestones (Lopes et al., 2006).

The Upper Cretaceous to Uppermost Eocene Unit UK-UE represents the final phase of the extension and the evolution to passive margin with thin to absent limestone, marls, and clays, filling the half-graben, onlapping underlying deposits, and draping over structural highs. This unit can be correlated with Unit B of (Lopes et al., 2006), and the Guia Conglomerate onshore Algarve (Pais et al., 2000). However, Terrinha et al., (2019b) argued for a lack of Cenomanian to Burdigalian sedimentary deposits onshore. Whereas separated by a hiatus, the Eocene to Lower Miocene Unit UO-LM consists of the basinward progradation and aggradation of carbonate shelf platform over the margins, forming the paleoslope for the Neogene depositional system. (Lopes et al., 2006), interpreted this micritic to dolomitic limestone sequence, named Unit C, as bounded by a regional unconformity at the Oligocene-Miocene boundary (OMB). These Paleogene sediments are absent in the onshore Algarve basin (Lopes et al., 2006).

2.2.2 Neogene - Quaternary

The Neogene stratigraphy of the Gulf of Cádiz has been less studied compared to the Quaternary deposits. Maldonado et al. (1999) divided the Neogene deposits into four seismostratigraphic units in the Miocene, with reference to the allochthonous unit of the Gulf of Cádiz or the "olistostrome": Pre-olistostrome Unit M1; Syn-olistostrome Unit M2 (Upper Tortonian); the Olistostrome Unit (AUGC); and the Post-olistostrome Unit M3 (Messinian), and two units in the Pliocene: Unit P1 (Lower Pliocene) and Unit P2 (Upper Pliocene).

Unit M1 consists of Langhian, Serravallian, to Lower Tortonian deposits, equivalent to the Atlántida group described by (Riaza and Martínez del Olmo, 1996). Whereas the Aquitanian to Lower Tortonian Unit D of (Lopes et al., 2006) correspond to

this unit combined with the previously mentioned Unit LM. This unit is characterised by wedge geometry depression filling with progradational to aggradational reflector configurations, evolving from carbonate to siliciclastic in character with age increasing landwards (Maldonado et al., 1999; Lopes et al., 2006). They are also correlated to the onshore Lagos-Portimão Formation dated from Lower Burdigalian to Upper Serravallian and the Lower Tortonian Fine Sands and Sandstones Unit (Antunes et al., 1981). Unit M1 is bounded at the top by the intra-Tortonian basal foredeep unconformity (BFU) (Maldonado et al., 1999; Lopes et al., 2006). The Upper Tortonian Unit M2 is deposited as a wedge on top of the basal foredeep unconformity and interfingers with the allochthonous unit at its front, while the basal foredeep unconformity becomes obscure under the chaotic mass of the allochthonous unit, which is characterised by diffractions and hyperbolic reflections (Maldonado et al., 1999; Lopes et al., 2006). Coevally, active overthrusting occurred within the allochthonous unit of Gulf of Cádiz which caused deposition of slope facies at its front, before merging into hemipelagic facies away from the allochthonous unit of Gulf of Cádiz in the northwest. Unit M2, which is the equivalent of the Bética group in Riaza and Martínez del Olmo (1996), is also found within the depression on top the allochthonous unit. The emplacement of the Gulf of Cádiz allochthonous unit ended in the late Tortonian (Gràcia et al., 2003). Separated by an erosional unconformity, the Messinian Unit M3 is draped over both the Unit M2 and the allochthonous unit of the Gulf of Cádiz, filling the depressions formed by the overthrusting and backthrusting. Unit M3 is equivalent to the Andalucía group, consisting of the siliciclastic Guadiana and the Guadalquivir sands (Riaza and Martínez del Olmo, 1996; Lopes et al., 2006). The Guadiana sands represents depositional fan lobe which originated from the northern margin, whereas the Guadalquivir sands originated from the Guadalquivir valley in the northeast, prograding southwestwards into the Gulf of Cádiz. Onshore Algarve basin, Unit M2 and M3 are correlated to the uppermost Tortonian to Messinian Cacela Formation (Antunes et al., 1981). In Lopes et al. (2006), the olistostromic-allochthonous unit, Units M2 and M3 are interpreted as a single Unit E, divided into subunits E0, E1 and E2 respectively.

The Lower Pliocene Unit P1 is consisted of interbedded clays and sandy clays hemipelagites, with minor sandy turbidites of deep-sea fans sourced from the Guadiana and the Guadalquivir (Riaza and Martínez del Olmo, 1996). It is equivalent to the alluvial Galvana Conglomerates onshore Algarve (Pais et al., 2000) and the Zanclean Unit F of (Lopes et al., 2006). Deposition of Unit P1 is controlled by the basin morphology at the

end of the Miocene. The base of this unit is interpreted as a basin-wide erosional unconformity (Nelson et al., 1993) of uppermost Messinian age (Lopes et al., 2006). The Upper Pliocene Unit P2 is consisted of sand and clay deposits from hemipelagic and turbiditic processes, separated from Unit P1 by an intra-Pliocene unconformity (Lopes et al., 2006). This unit is equivalent to the Olhos de Agua Sands onshore Algarve (Pais et al., 2000), and the Piacenzian Unit G1 of Lopes et al. (2006). The onset of contouritic deposits due to the is also witnessed within this unit. This unit is also bounded at the top by a late Pliocene unconformity. The Pliocene (P) units were also studied in detail by Hernández-Molina et al. (2016), where they are also divided into three main units (PI, PII and PIII) separated by the early Pliocene discontinuity (EPD) and intra-Pliocene discontinuity (IPD) respectively. These units are further divided into two subunits each (P1 to P6). The basal Miocene-Pliocene boundary (MPB) is identified from biostratigraphic data and cyclostratigraphic tuning of resistivity logs for both the Algarve-2 exploration well and the U1387 site of the Integrated Ocean Drilling Program (IODP) Expedition 339 (Hernández-Molina et al., 2016), replacing previous interpretations from the lithologic transitions of clay-sand with no robust justification in Expedition 339 Scientists (2013) and Hernandez-Molina et al., (2014). The Pliocene units (PI to PIII) in the Deep Algarve basin consists of basal high amplitude reflections with lobate and tabular geometry interbedded with wedge-shaped chaotic seismic facies and evolve upward into weaker acoustic response, which represented turbiditic and debritic sands proximal to the margins (Hernández-Molina et al., 2016). This trend is opposite for the wedge-top basins, which indicated the development of large, muddy sheeted drifts due to the strengthening of the Mediterranean Outflow Water, representing the initial-drift stage of the Gulf of Cádiz contourite depositional system (Hernández-Molina et al., 2016).

The latest Pliocene to Quaternary deposits of Unit P/Q onlap and prograde basinward above the late Pliocene basal unconformity (Maldonado et al., 1999), and is equivalent to Units G2 and G3 of Lopes et al. (2006). These deposits also show significant facies and thickness variations controlled by the structure of the margin, the sediment sources and the Pliocene-Quaternary eustatic sea-level fluctuations (Rodero et al., 1999). Distribution of contouritic drift deposition and erosional features are influenced by the bottom currents of Mediterranean outflow (Nelson et al., 1993). According to Hernández-Molina et al. (2016) the latest Pliocene to earliest Quaternary units (PQ) is represented by the transitional-drift stage, bounded by two prominent hiatuses, late Pliocene discontinuity (LPD) and early Quaternary discontinuity (EQD), which eroded or

interrupted deposition of interbedded contourites and turbidite indicated by the cyclic swings in amplitudes. The Quaternary sequence (QI to QIII), on the other hand, consists of mounded geometry with repetitive trend with weak to transparent acoustic facies which evolve upwards into high amplitude facies truncated by an erosional surface (Hernández-Molina et al., 2016). In the Deep Algarve basin, the seismic trend together with upslope progradation reflections, represent a mounded elongated and separated drift in the growth-drift stage. Whereas in the wedge top basins, high to very high amplitude aggrading sandy sheeted drifts with lateral progradation resulted from Mediterranean Outflow Water intensification following tectonic constriction and deformation in the basins (Hernández-Molina et al., 2016).

2.3   Geodynamic evolution

The Southwest Iberian and Northwest Moroccan continental margins are located on the eastern end of the Azores-Gibraltar fracture zone (AGFZ) and are formed during the continental break-up of the North America with Iberia and Africa respectively (Newfoundland-Iberia & Nova Scotia-Morocco E-W trending rifts) in the Early Jurassic (~190 Ma) (Srivastava et al., 1990; Sibuet et al., 2012). Sinistral transtension of the Neo-Tethys transfer zone separated Africa from Iberia in a NW-SE transtensional setting, forming the Algarve basin (Dewey et al., 1989; Srivastava et al., 1990; Terrinha, 1998; Terrinha et al., 2002; Ramos et al., 2016). This regime lasted from the Early Jurassic until at least the Cenomanian (~92 Ma) (Dewey et al., 1989; Terrinha et al., 2019a), interrupted by short-lived compressional episodes (Terrinha et al., 2019b). Five phases of extension were recorded for the Southwest Iberian margin, including: Triassic to Early Jurassic (Hettangian), Early to Middle Jurassic (Sinemurian-Toarcian), Middle Jurassic (Aalenian-Bajocian), Middle to Late Jurassic (Callovan-Oxfordian), Early Cretaceous (Cenomanian) (Terrinha et al., 2019a).

At present, a WNW-ESE convergence at a rate of approximately 4-5 mm/y is active between the Iberian sub-plate of Eurasia and the Nubian sub-plate of Africa (Argus et al., 1989; Fernández-Ibáñez et al., 2007), where the lineaments within the SWIM Fault Zone are interpreted as the Nubian-Iberian plate boundary (Zitellini et al., 2009). The interaction between these two plates has been driven by two mechanisms since the Late Cretaceous (Zitellini et al., 2009): a. an oblique lithosphere collision which has

accommodated by dextral wrenching across the SWIM Fault Zone; and b. subduction associated to the emplacement of Gibraltar Arc and the formation of the GCAW.

The onset of N-S convergence for Iberia and Africa occurred in the Santonian (~85 Ma), continuing throughout the Paleocene and Early Eocene at a rate of about 2 mm/y (Terrinha, 1998; Vergés and Fernàndez, 2012), and even into the Middle Eocene in the Alentejo basin (Pereira et al., 2011). Alpine deformation migrated from the north to south of Iberia as it collides with Europe towards the north building up the Pyrenean orogenic system (Vergés and Fernàndez, 2012; Ramos et al., 2017). The compressional setting in the Southwest Iberian and Northwest Moroccan margins is observed in the sedimentary record with basin inversion structures (Terrinha et al., 2002). Due to the regional compression during this period, halokinesis of Upper Triassic evaporites (Lopes et al., 2006) caused the thin-skinned decoupling of the External and Internal Betics. Simultaneously, the compression also produced a SE dipping partial subduction of the Ligurian-Tethys Ocean (Vergés and Fernàndez, 2012).

From the Oligocene until the Early Miocene (~30-20 Ma), subduction and rollback of the Ligurian-Tethys oceanic slab sped up until the continental collision, which had rapidly developed the fold and thrust belt of the Betic-Rif orogenic system, coeval to the opening of the Alborán basin (Vergés and Fernàndez, 2012). As subduction was inhibited by the continental-oceanic transition at the Betics (McKenzie, 1969; Buiter, 2000), there was a shift to an eastward dipping subduction for the consumption of Ligurian-Tethys Ocean at the west, and the westward rollback of the subduction slab from its initial NW direction (Martínez del Olmo et al., 2008; Vergés and Fernàndez, 2012). Consequently, the lateral tearing occurred at the eastern end of the subduction slab in the Middle Miocene (~18-16 Ma) (Wortel and Spakman, 2000). The orogenic build-up of the Betic-Rif fold and thrust belt went through its denudation and deposited the Guadalquivir Allochthon in the Guadalquivir foreland basin, and the Prerifaine nappes in the Gharb foreland basin (Torelli et al., 1997; Berástegui et al., 1998; Flinch and Vail, 1998; Maldonado et al., 1999; Gràcia et al., 2003; Medialdea et al., 2004). Whereas the Gibraltar arc started to migrate westwards and partially developed the Gulf of Cádiz accretionary wedge (Berástegui et al., 1998; Vergés and Fernàndez, 2012) and initiated radial expulsion of the Gulf of Cádiz allochthonous unit from the Early-Middle Miocene (Maldonado et al., 1999; Medialdea et al., 2004; Terrinha et al., 2009) (Fig. 2-3).

2.3.1 Late Miocene

During the late Tortonian (~8 Ma), the continuous westward slab rollback drove compression in the Gulf of Cádiz accretionary wedge and the westward drift of the Alborán Domain (Lonergan and White, 1997; Gutscher et al., 2002; Duggen et al., 2003; van Hinsbergen et al., 2014), before slab detachment with a lateral rupture propagation westward from the central-eastern Betic region (Zeck, 1997; Wortel and Spakman, 2000; Spakman and Wortel, 2004; Garcia-Castellanos and Villaseñor, 2011). However, other modes such as lithospheric delamination (Seber et al., 1996; Calvert et al., 2000) and convective removal (Platt and Vissers, 1989) have also been proposed. These eventually led to lithospheric thinning and the regional exhumation of the Gibraltar Arc, firstly in the Betic (~7.8 Ma) (Krijgsman et al., 2006; Betzler et al., 2006) and slightly later in the Rif (~7 Ma) (Capella et al., 2017b; Tulbure et al., 2017), forming various small intramontane basins in the Betics and the Rif (Iribarren et al., 2009). The external fronts and the allochthonous units of the Betic, Rif and Gulf of Cádiz were fossilised around the late Tortonian (Berástegui et al., 1998; Negro et al., 2007; Iribarren et al., 2007), but reactivation in the Gulf of Cádiz due to a Late Miocene initiation of NW-SE convergence emplaced new allochthonous wedges by gravitational sliding, with the Triassic salt and uncompacted Middle Miocene marls or mud acting as the detachment layer (Argus et al., 1989; Medialdea et al., 2004). The overloading and overpressure of the Gulf of Cádiz allochthonous unit also enhanced diapirism of these evaporites and marls from the late Tortonian to the Messinian (Maestro et al., 2003; Medialdea et al., 2004; Lopes et al., 2006). As the thrust imbrication advanced basinward, extensional collapse and roll-over structures developed coevally as reactivation of landward thrust fronts (Maestro et al., 2003), causing high rates of subsidence since the late Messinian (Maldonado et al., 1999). This increasing subsidence formed the flexural depocentres in the Algarve basin (Lopes et al., 2006), and the creation of the Cádiz basin (Medialdea et al., 2004).

2.3.2 Pliocene - Quaternary

The sedimentary record since the early Pliocene is undeformed (Zitellini et al., 2009) as the Betic-Rif orogeny slowed down in the Late Miocene (Vergés and Fernàndez, 2012). Coevally, the flexural subsidence since late Messinian lasted until the Quaternary (Terrinha, 1998; Lopes et al., 2006). The Gulf of Cádiz also consists of the location of the African-Eurasian plate boundary which has been considered as diffuse (Sartori et al., 1994), where the SWIM Fault Zone were identified as making this boundary (Zitellini et

al., 2009). The SWIM dextral strike slip faults cut through the Gulf of Cádiz accretionary wedge producing a counter-clockwise rotation, shifted from the N-S orientation since at least the beginning of the Calabrian age (1.8 Ma) (Rosas et al., 2009; Zitellini et al., 2009; Duarte et al., 2011). Whereas west of the Gulf of Cádiz, compressional features such as the Gorringe Thrust, Horseshoe Thrust, Marquês de Pombal Thrust, and the Coral Patch Ridge, are found deeply rooted into the basement (Terrinha et al., 2003; Gràcia et al., 2003; Zitellini et al., 2004; Sallarès et al., 2013; Ramos et al., 2017). The thick-skinned deformation led to margin inversion, and are accommodated by buttressing, thrusting and reactivation of diapirs (Ramos et al., 2017).
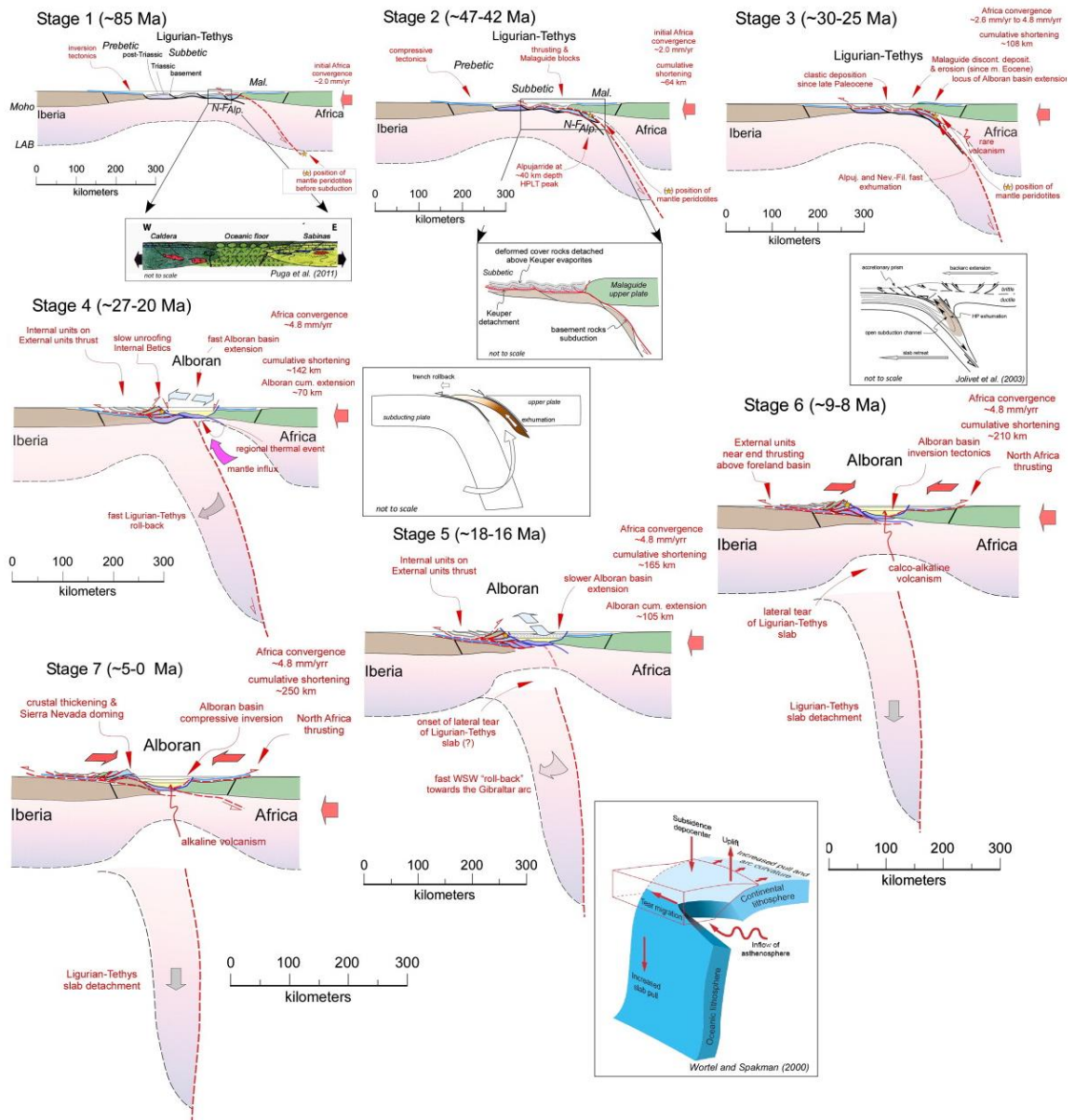
Figure 2-3 Crustal kinematic model showing evolution of the Betic–Rif orogenic system and its timing, with a constant rate of Africa convergence from Late Cretaceous to present (Vergés and Fernàndez, 2012)

2.4 Oceanographic setting

2.4.1 Present-day setting

At present, the water circulation in the Gulf of Cádiz is closely related to the anti-estuarine exchange of water masses between the Atlantic Ocean and the Mediterranean Sea (Sánchez-Leal et al., 2017) through the Strait of Gibraltar, henceforth referred to as the Gibraltar Gateway. This configuration has been established since the end of the Messinian salinity crisis, the Miocene-Pliocene boundary (5.332 Ma) (Duggen et al., 2003; Roveri et al., 2014). At the surface, the cool and less saline Atlantic Inflow Water (AIW) flows eastwards into the Mediterranean Sea through the Gibraltar Gateway; while near the bottom the warmer and more saline Mediterranean Outflow Water exits the Mediterranean Sea into the Gulf of Cádiz before flowing westward (Rogerson et al., 2012; Sánchez-Leal et al., 2017). Whereas westward of the Gulf of Cádiz, the Mediterranean Outflow Water flows in between the Modified Antarctic Intermediate Water (AAIW) (Louarn and Morin, 2011) and the North Atlantic Deep Water (NADW) (Ambar et al., 2002; Criado-Aldeanueva et al., 2006) (Fig. 2-3).

The Atlantic Inflow Water is composed of the North Atlantic Superficial Water (NASW) (0-100 m) and the Eastern North Atlantic Central Water (ENACW) (100-700 m; 12-16 °C, 34.7-36.25‰ TDS - *total dissolved solids*) (Criado-Aldeanueva et al., 2006). Below the Atlantic Inflow Water, the Modified Antarctic Intermediate Water (AAIW) circulates above the Mediterranean Outflow Water with an average of 10 °C, 35.62‰ TDS and ~4.16 ml/L dissolved oxygen (Louarn and Morin, 2011). Whereas flowing beneath the Mediterranean Outflow Water, the North Atlantic Deep Water is a colder (3-7 °C) and less saline (34.95-35.2‰) water mass (O'Neill-Baringer and Price, 1999; Criado-Aldeanueva et al., 2006). Beyond the Gulf of Cádiz, the Antarctic Bottom Water (AABW) circulates in the abyssal plains of the Central Atlantic (Fig. 2-3).

a.   Mediterranean Outflow Water (MOW)

The Mediterranean Outflow Water is composed of mainly the Levantine Intermediate Water (LIW) and Western Mediterranean Deep Water (WMDW), produced by downwelling of warm, dense, and highly saline water masses in the constricted east and west basins of the arid Mediterranean Sea (Ambar and Howe, 1979; Millot, 2009). With a pressure gradient existing between the denser Mediterranean Sea and the less dense Atlantic Ocean, juxtaposed through the Gibraltar Gateway, the Mediterranean

Outflow Water accelerates through the lower half of this 300 m deep and 13 km wide strait with a velocity of approximately 300 cm/s (Ambar and Howe, 1979; Mulder et al., 2003) and cascades into the Gulf of Cádiz as a strong bottom current with an overflow rate of 0.67 ± 0.28 Sv (Serra et al., 2010; Rogerson et al., 2012).

The Mediterranean Outflow Water enters the Gulf of Cádiz at 250-300 m before being deflected northward at the Camarinal Sill due to Coriolis Effect (Ambar and Howe, 1979; Mulder et al., 2003) before settling within the mid-slope as an intermediate water mass (Hernandez-Molina et al., 2014) towards the NW with velocities of 60-100 cm/s (Cherubin et al., 2000). It flows between 500 and 1400 mbsl (meters below sea level) below the surficial Atlantic Inflow Water and above the North Atlantic Deep Water further westward into the Atlantic Ocean. Systematically decelerating along the Southwest Iberian margin (Hernández-Molina et al., 2003) due to decreasing salinity as it descends and mixed with overlying waters, the Mediterranean Outflow Water reaches neutral buoyancy off the São Vicente Cape at a depth of ~1400 m (O'Neill-Baringer and Price, 1997), and exits the Gulf of Cádiz through 3 branches: a. northward along the mid-slope of Portuguese Margin; b. westward into the Atlantic Ocean; and c. southward to the Canary Islands before veering west. The Mediterranean Outflow Water increases the density of the North Atlantic, drives the Atlantic Meridional Overturning Circulation (AMOC) deep convection by ~15%, and increases the surface temperature by 1 °C (Rogerson et al., 2012; Hernandez-Molina et al., 2014).

In the Gulf of Cádiz, the flow pathway of the Mediterranean Outflow Water is controlled by the complex morphology of the Southwest Iberian margin continental slope and locally enhanced where diapiric ridges and basement highs existed obliquely to the flow direction (Hernández-Molina et al., 2016). These NE-SW oriented ridges and margin uplifts are responsible for splitting up the Mediterranean Outflow Water into multiple cores and vertical layering (Nelson et al., 1999; Maestro et al., 2003; Millot, 2009). The Mediterranean Outflow Water splits into two cores after exiting the Gibraltar Gateway (Fig. 2-4): a. the warmer and less saline Mediterranean Upper Core (MU) (13-14 °C; 35.7-37‰), and b. the cooler and more saline Mediterranean Lower Core (ML) (10.5-11.5 °C; 36.6-37.5‰) (Madelain, 1970; Ambar and Howe, 1979). The MU flows parallel along the slope of the Southwest Iberian margin at a depth between 500-800 m, whereas ML flows NW at 20-30 cm/s between 800-1400 m (Marchès et al., 2007; Llave et al., 2007). At 7° W, a minor branch detaches from the ML towards the southwest (Madelain, 1970), while the major flow concentrates westwards before further parting into three

branches at 7° 20′ W: the Southern (SB), the Principal (PB), and the Intermediate (IB) branches (Madelain, 1970). The Mediterranean Outflow Water, acting as bottom current in the Gulf of Cádiz, generates the world's most extensive contourite depositional system along the Southwest Iberian margin during the Pliocene and Quaternary (Hernández-Molina et al., 2016) (Fig. 2-3).
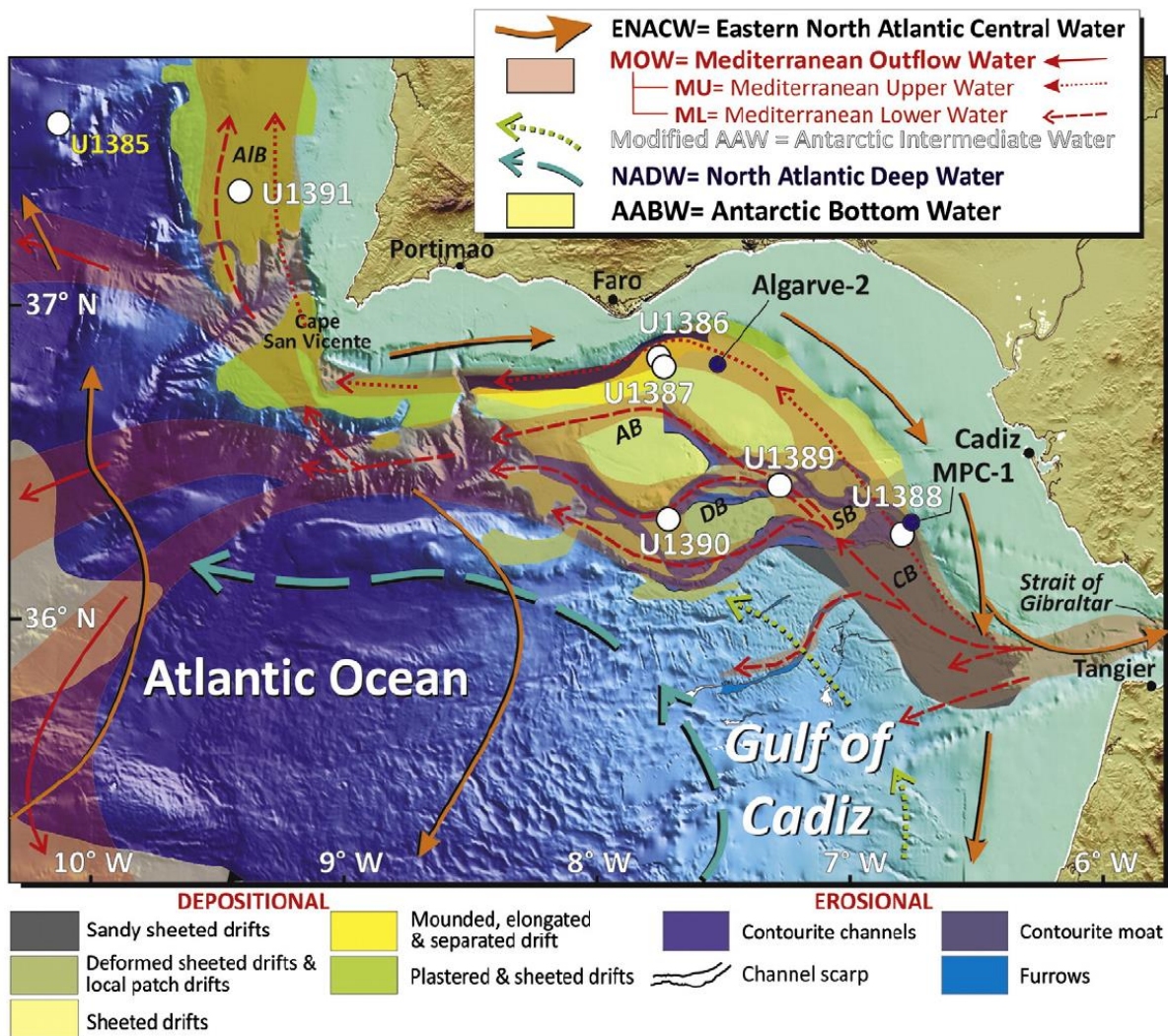
Figure 2-4   The pathway of Mediterranean Outflow Water (MOW) in the Gulf of Cádiz after it exits Gibraltar Gateway, with the distribution of depositional and erosional along the mid-slope. Seven Integrated Ocean Drilling Program (IODP) Exp. 339 sites shown as solid white circles and two exploration wells shown as blue circles. Key: (*Neogene basins*) AB – Algarve basin; AlB – Alentejo basin; CB – Cádiz basin; DB – Doñana basin; SB – Sanlúcar basin (Hernández-Molina et al., 2016).

2.4.2 Palaeoceanographic setting

The Mediterranean and the Paratethys were linked with the Indian Ocean up until the Late Burdigalian (~17Ma), where it then opened and closed intermittently due to the collision of the Arabian and African plates with Eurasia (Rögl, 1999; Hüsing et al., 2009).

After the final closure of the eastern Tethys gateway during the Middle Miocene Climate Transition (14-11 Ma), the Tethyan Indian Saline Water (TISW) that fed into the circum-equatorial current of the Indian Ocean was terminated (Woodruff and Savin, 1989; Rögl, 1999) and redirected westwards into the Atlantic as the Mediterranean Outflow Water and became more stratified (Hüsing et al., 2009; Hamon et al., 2013).

a.   *Pre-Messinian salinity crisis*

Before the Messinian salinity crisis, the Mediterranean-Atlantic connection cut through the Betic Corridor in the south of Spain and the Rifian Corridor in the north of Morocco (Santisteban and Taberner, 1983; Simon, 2017; Krijgsman et al., 2018), henceforth referred to as the Betic and Rifian Gateway respectively (Fig. 2-5). The Betic Gateway consisted of the Guadalquivir basin in the west, divided into four separate sub-gateways: a. the North-Betic Strait; b. the Guadix Strait; c. the Zagra Strait; and d. the Guadalhorce Strait, whereas the Rifian Gateway is separated into two main gateways: the North- and South-Rifian Corridors (Capella et al., 2018) (Fig. 2-4).

These complex gateways became closed progressively due to a combination of tectonic, eustatic and climatic factors during the latest Miocene (Flecker et al., 2015). Evident from the biostratigraphic constraint on marine to continental transitions and hiatuses in these gateways, the Betic Gateway connection was terminated in the late Tortonian (Krijgsman et al., 2018), starting from the North-Betic Strait at 7.6 Ma (Garcés et al., 2001). In the Guadix Strait, a hiatus separates marine deposits last dated ~7.8 Ma from the continental deposits of ~5.5 Ma (Hüsing et al., 2010); while in the Zagra Strait, marine-continental transition occurred at 7.37-7.24 Ma within the Granada basin (Garcia-Garcia et al., 2009; Corbí et al., 2012). The Guadalhorce Strait was the last connection to close in the Betic Gateway during the late Tortonian (van der Schee et al., 2018), which conforms to the regional uplift of the area (Jiménez-Bonilla et al., 2015). The restriction of the Betic Gateway since the Early Tortonian (Martín et al., 2009) has led to the deposition of evaporites of the Tortonian salinity crisis (TSC) in isolated basins within these gateways (Krijgsman et al., 2000). In the Rifian Gateway, The North-Rifian Corridor became closed roughly in the latest Tortonian (7.35-7 Ma) (Tulbure et al., 2017; Capella et al., 2018), whereas the South-Rifian Corridor became closed later in the earliest Messinian (7.1-6.9 Ma) (Capella et al., 2017b, 2018). As such, there was no direct evidence for a Mediterranean-Atlantic connection through southern Spain nor northern

Morocco (Krijgsman et al., 2018) even one million years or more before the evaporitic precipitation of the Messinian salinity crisis (Flecker et al., 2015).
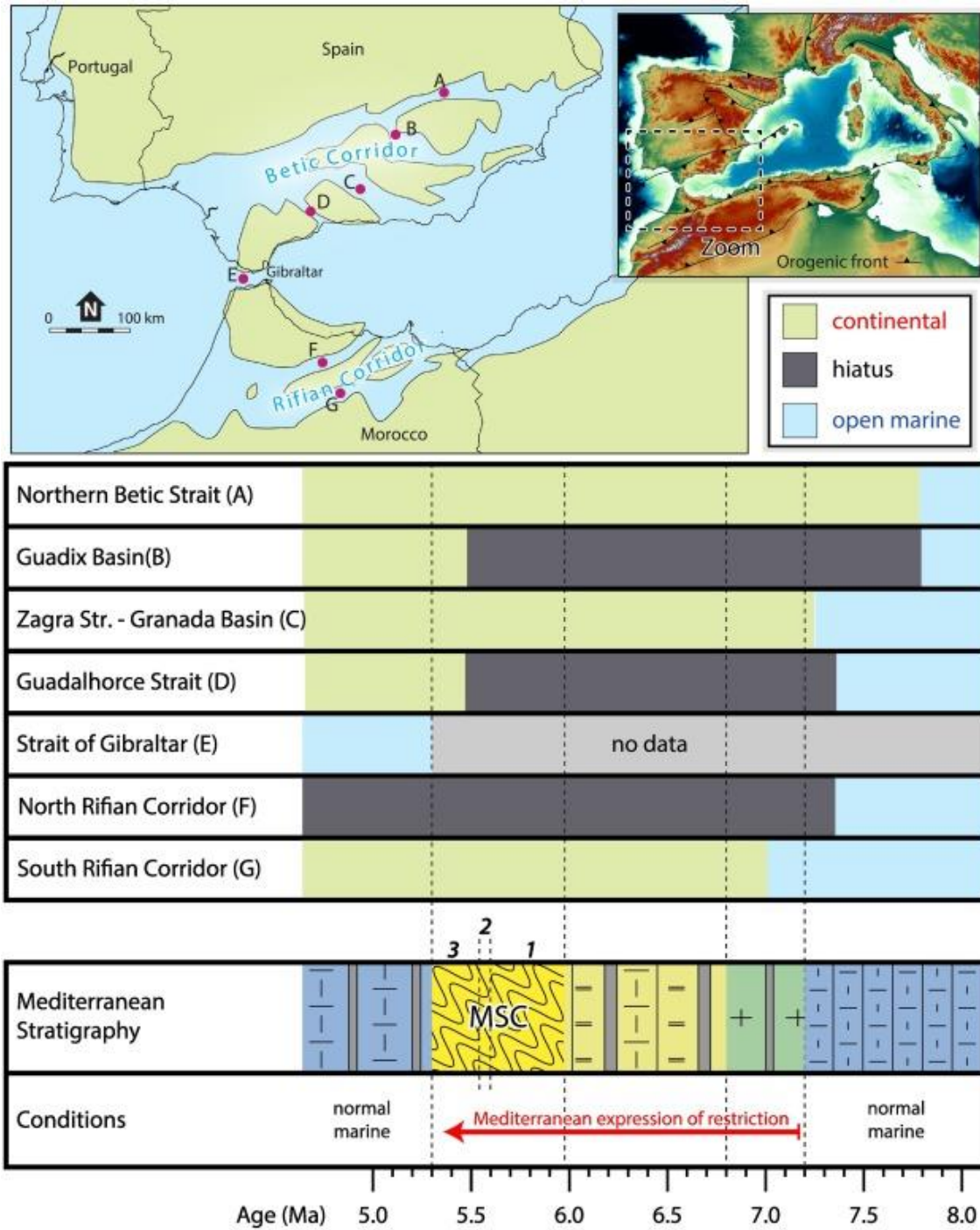
Figure 2-5 (*Top*) The Betic-Rif region indicating locations of all known Mediterranean-Atlantic seaways that existed during late Miocene and Pliocene; (*Bottom*) Temporal evolution of the marine-continental transitions of the gateways and simplified Mediterranean sedimentary succession (Flecker et al., 2015; Krijgsman et al. 2018).

b.   Messinian salinity crisis

As both the Betic and Rifian Gateways became closed in the early Messinian (Martin et al., 2001) as a result of the African-Iberian convergence (Spakman et al., 2018), the exchange between the Atlantic and the Mediterranean became restricted with a near complete disconnection during the late Messinian (5.97-5.33 Ma) (Krijgsman et al., 1999; Simon and Meijer, 2015). There was dramatic change in salinity of the Mediterranean Sea reaching gypsum saturation of ~130‰ or higher (Flecker et al., 2015), leading to the deposition of thick evaporites of the Messinian salinity crisis (Hsü et al., 1973); whereas it was a quiet hemipelagic environment in the Gulf of Cádiz (van der Schee et al., 2016).

The closure of the Betic and Rif Gateways however meant that another marine connection with the open Atlantic Ocean is necessary for preservation of the salt giant within the Mediterranean at least until the end of the halite stage (5.55 Ma) (Krijgsman and Meijer, 2008). It is thought that the Gibraltar Gateway would have been established as the single Atlantic-Mediterranean connection during the late Miocene even before the restriction of the Mediterranean that led to the Messinian salinity crisis (Nelson et al., 1993; Capella et al., 2018). The Gibraltar Gateway would have been consisted of two separate shallow straits (northern & southern) before the Zanclean flood (Garcia-Castellanos et al., 2009).

c.   Post-Messinian salinity crisis

At the end of the Messinian and the beginning of the Pliocene (5.33 Ma), the Atlantic-Mediterranean connection was thought to be re-established through the Gibraltar gateway, ending the Messinian salinity crisis as the Atlantic Ocean immediately penetrated the Mediterranean in the form of the Atlantic Inflow Water (Hsü et al., 1973; Garcia-Castellanos et al., 2009; van der Schee et al., 2016). After the Messinian salinity crisis, warming of the Atlantic Ocean in the earliest Pliocene suggested the immediate onset of weak Mediterranean Outflow Water bottom current from the Mediterranean (van der Schee et al., 2016). However, the onset of the Mediterranean Outflow Water in the seismic reflection profiles only began since the late early Pliocene (~4.5-3.5 Ma) as suggested by the limited degree of contourite deposition in the beginning of the Pliocene (Expedition 339 Scientists, 2013; Hernandez-Molina et al., 2014). The Mediterranean Outflow Water is then enhanced during the late Pliocene to the Quaternary (~3.2-2.1 Ma) indicated by erosional features (Hernandez-Molina et al., 2014). The intensification of

the Mediterranean Outflow Water (Roque et al., 2012) is due to the sea level change from low- to high-stand (Nelson et al., 1993), evident with the change in the sedimentary stacking pattern of the contourite depositional system occurred after 2.1 Ma (Hernandez-Molina et al., 2014). Similar cycle of sea level change can be observed since the last sea level low-stand of Late Pleistocene to the high sea level Holocene (Nelson et al., 1993), establishing the present-day circulation.
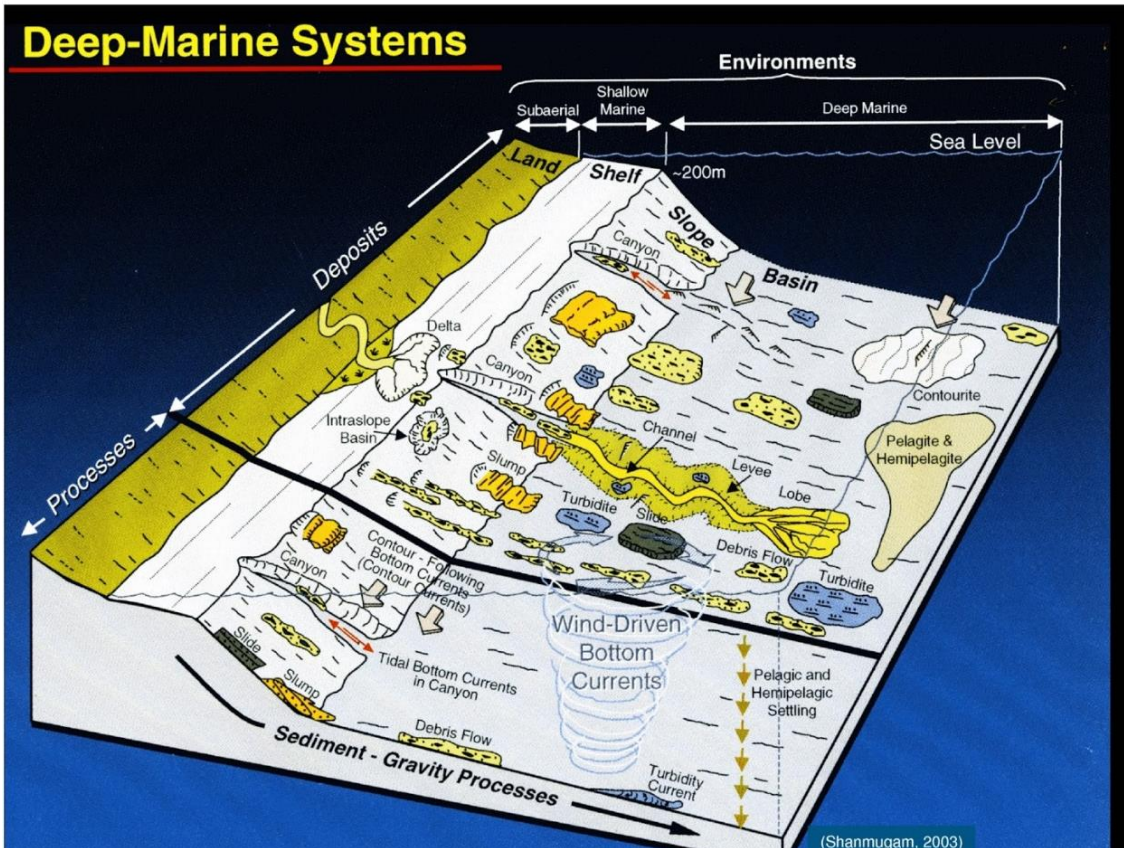
Figure 2-6   Deep marine sedimentary environment encompassing deposits of pelagic settling, density, and bottom current processes (Shanmugam, 2003).

2.5   Deep-marine sedimentary depositional systems

The continental slopes of the Gulf of Cádiz generally consist of mixed contourite and turbidite depositional system (Hernández-Molina et al., 2003). However, there are four main sedimentary deposits of deep-marine environment: pelagites, mass-transport deposits (MTD), turbidites and contourites, shown in association in a conceptual model (Fig. 2-6). The depositional processes associated with the deposits are illustrated in figure 2-7, where contourites are formed from reworking and deposition due to bottom currents, with its facies model based on (Stow and Faugères, 2008); turbidites are deposited from density current with its standard facies model based on (Bouma, 1962a), and pelagites

deposited from the vertical settling of pelagic materials (Rebesco et al., 2014), with mass-transport deposits considered under density current deposits. These deposits are discussed in depth in the following section.
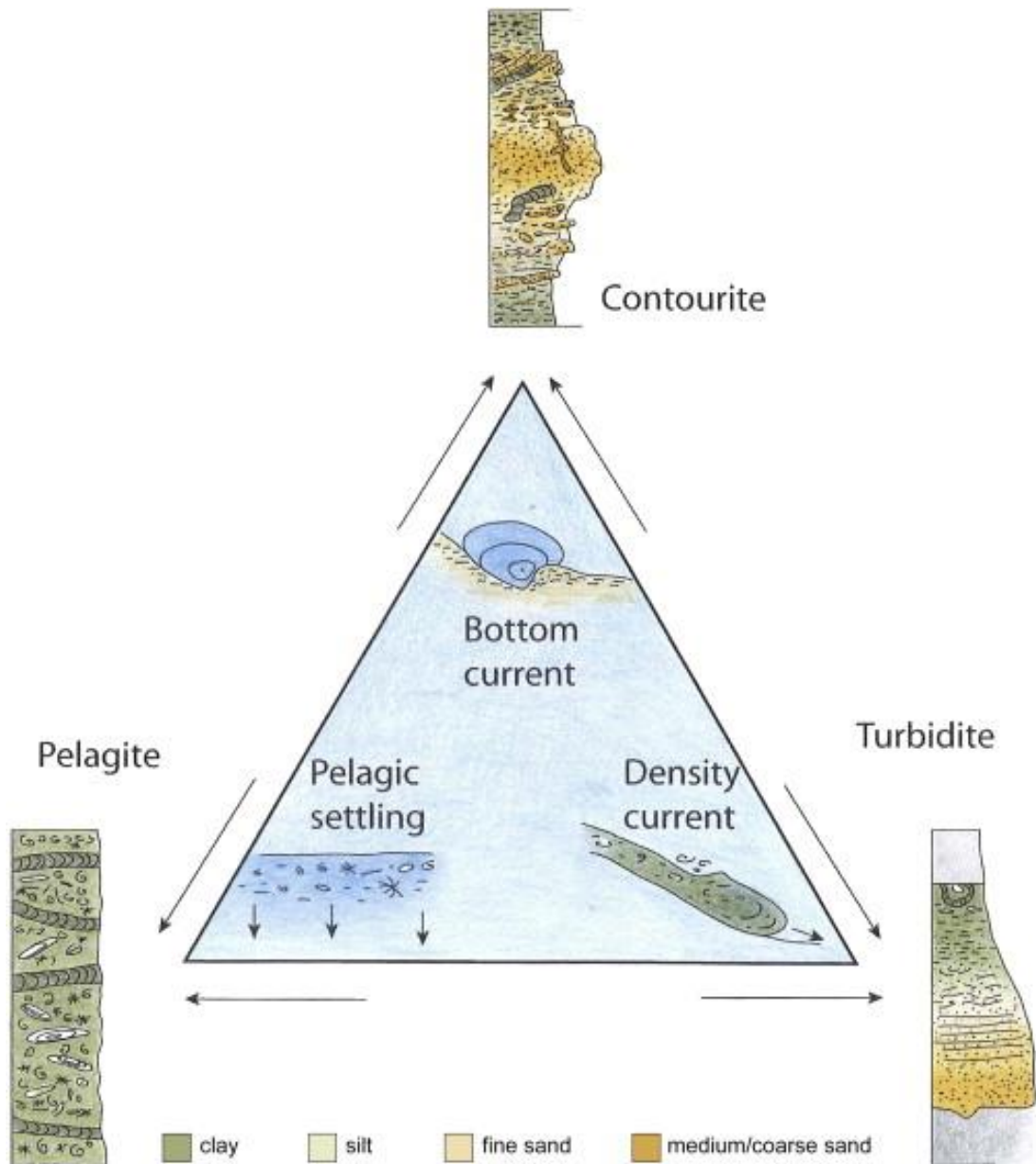
Figure 2-7 Conceptual diagram of the three main deep-marine sedimentary processes and the facies model of their respective depositional products (Rebesco et al., 2014).

2.5.1 *Pelagic and hemipelagic deposits*

Pelagites developed through the process of vertical settling under the influence of gravity, where biogenic and very fine-grained terrigenous material, including other detritus which fall slowly to the seafloor (Stow and Smillie, 2020; Fig. 2-8). Pelagic

settling is continuous, with a very slow accumulation rate of <1 cm ka^{-1}, which can increase through flocculation and organic pelletisation in high productive areas (Stow and Smillie, 2020). Hemipelagites are also fine-grained sediments which involve both vertical settling and additional slow lateral advection of the biogenic and terrigenous material through the water column (Fig. 2-8), which could include calcareous or siliceous mud or marl (Stow and Tabrez, 1998). The driving force behind the lateral advection include inertia from river or turbid layer plumes, diffusion of glacial meltwater, internal tides, waves, and other slow currents. Hemipelagic deposition is a continuous process with huge range of depositional rates, dependant on the nature of sediment inputs, e.g., 2 cm ka−1 with little terrigenous input, 10 cm·ka−1 for black shales with high upwelling, >20 cm·ka−1 for high latitude glaciomarine environment (Stow and Smillie, 2020).
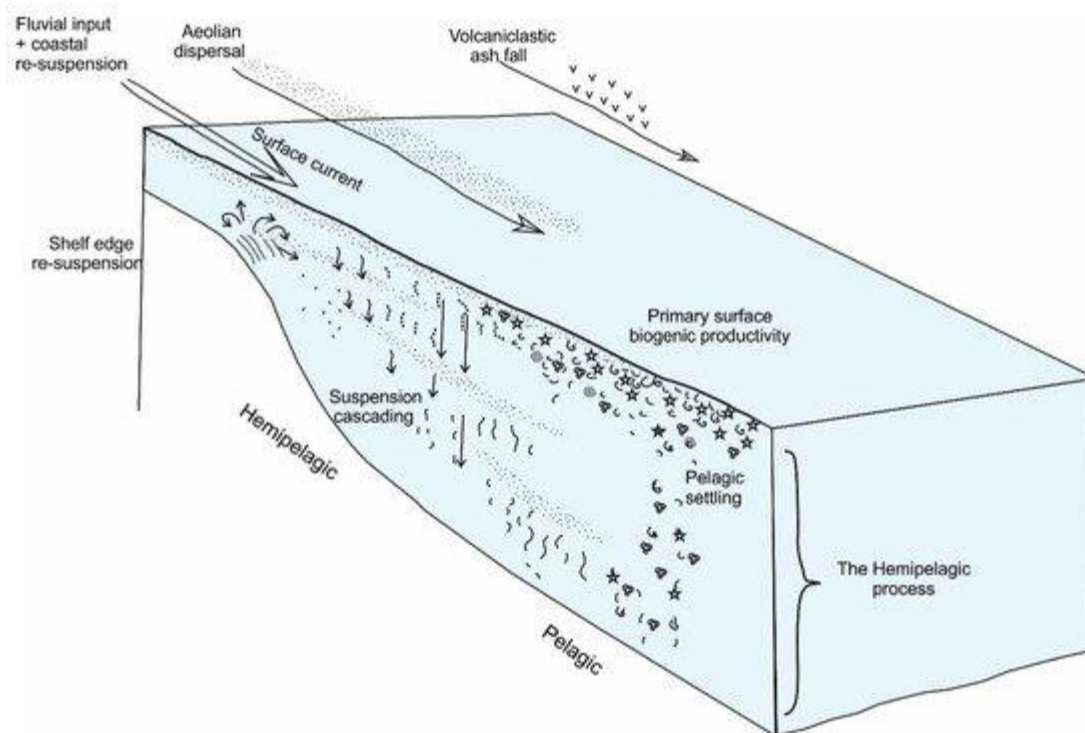
Figure 2-8   Composite model for the hemipelagic and pelagic processes, distinguishing the sediment supply from terrigenous and biological sources, and its dispersion and settling through the water column (Stow and Smillie, 2020).

2.5.2 Turbidite depositional system
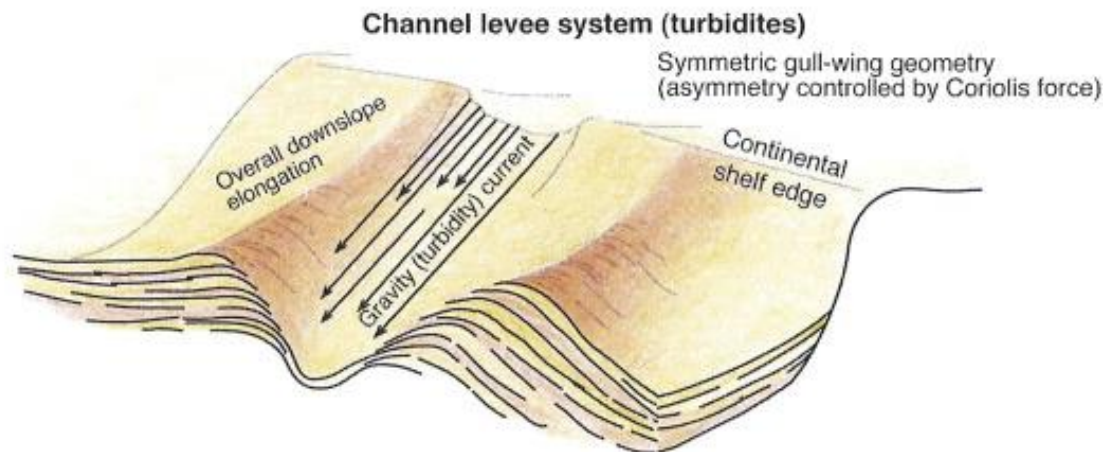
Figure 2-9   Schematic model showing the turbiditic channel-levee system, compared in large-scale differences with the contourite drift in *Figure 2-15* (Rebesco et al., 2014).

a.   Conceptual theory of turbidites

Turbidite studies evolved from the recognition of *flysch* or tectonically induced deposits in the Alpine orogeny since the 1820s (Mutti et al., 2009). This idea was pioneered by Kuenen (1937), which led to the first experiments carried out on turbidity currents, and the discovery of these currents as the cause for graded bedding (Kuenen and Migliorini, 1950). Initially, they were introduced as resedimented shallow marine or fluvial sands deposited in the deep marine environments by turbid density currents triggered by slope instability (Migliorini, 1943). This was followed by overwhelming studies in the 1950s and 1960s which concluded the role of turbidity currents in depositing these deep marine sands (Stanley, 1988). Sanders (1965) defined turbidites strictly as deposits formed from turbulent suspension of turbidity currents. Through time, it has been simplified as "deposits of turbidity currents" (Middleton and Hampton M.A., 1973; Meiburg and Kneller, 2010; Stow and Smillie, 2020). Contrastingly, Mutti et al. (1999) defined turbidites as deposits of sediment-gravity flows, which include turbidity currents among others. Turbidity currents are downslope moving sediment-laden gravity flows due to its density difference with the ambient water (Meiburg and Kneller, 2010; Pohl et al., 2019). They have Newtonian rheology where sediments are supported by fluid turbulence while deposition occurs through suspension settling (Middleton and Hampton M.A., 1973; Shanmugam, 2012). These periodic downslope turbulent flows can produce a broad spectrum of gravity-driven features on the continental slope to the abyssal plain (Mulder, 2011).

The first turbidites facies model was introduced by Bouma (1962) as the Bouma Sequence, which was based on outcrop studies of the Eocene-Oligocene Annot Sandstones in the Maritime Alps. The Bouma Sequence describes a single turbidite bed as consisting of five depositional divisions: Ta, basal massive or normal graded; Tb, lower parallel laminae; Tc, ripples, wavy or convolute laminae; Td, upper parallel laminae; and Te, laminated to homogenous mud, with base missing variations of decreasing thickness and coarseness developing downstream of a submarine fan or "cone" (Fig. 2-10; Bouma, 1962). This model depicts turbidity current as an unsteady and non-uniform waning flow, where it decreases in velocity and competence through time and distance (Allen, 1985; Shanmugam, 2012). This normally graded sequence is attributed to the decay of initial turbulence in the turbidity current (Middleton and Hampton, 1973). As the Bouma Sequence Te was inadequate in representing all the different divisions of the muddy turbidite facies in a low-density turbidity current (Piper, 1985), Stow and Shanmugam (1980) proposed a new facies model for the fine-grained turbidites based on three contrasting areas, equivalent to the (C)DE division of the Bouma Sequence. This sequence consists of nine divisions: T0, silt lamina; T1, silt-mud convolute laminae; T2, silt-mud low-amplitude climbing ripples; T3, silt-mud thin regular laminae; T4, silt-mud thin indistinct laminae; T5, silt-mud thin wispy/convolute laminae; T6, graded mud; T7, ungraded mud; and T8, bioturbated mud (Fig. 2-10; Stow and Shanmugam, 1980). Similarly, Lowe, (1982) proposed a coarse-grained turbidites facies model, where they are deposited by high-density turbidity currents. The Lowe Sequence consists of six divisions: R1, traction gravel; R2, traction carpet gravel; R3, suspension gravel; S1, traction coarse sand-fine gravel; S2, traction carpet coarse sand-fine gravel; and S3 suspension coarse sand-fine gravel (Fig. 2-10; Lowe, 1982). To distinguish the two types of turbidity currents, high density turbidity currents are concentrated, which correspond to the dense basal layer of the frontal (head and body) flow; whereas low density turbidity currents are diluted, which correspond to the trailing (tail) suspension cloud in a turbulent flow (Fig. 2-11; Stow and Smillie, 2020). However, these vertical sequences are still not able to represent the entire spectrum of turbiditic deposits (Walker, 1984), such as the lateral variation between the divisions (Shanmugam, 2016).
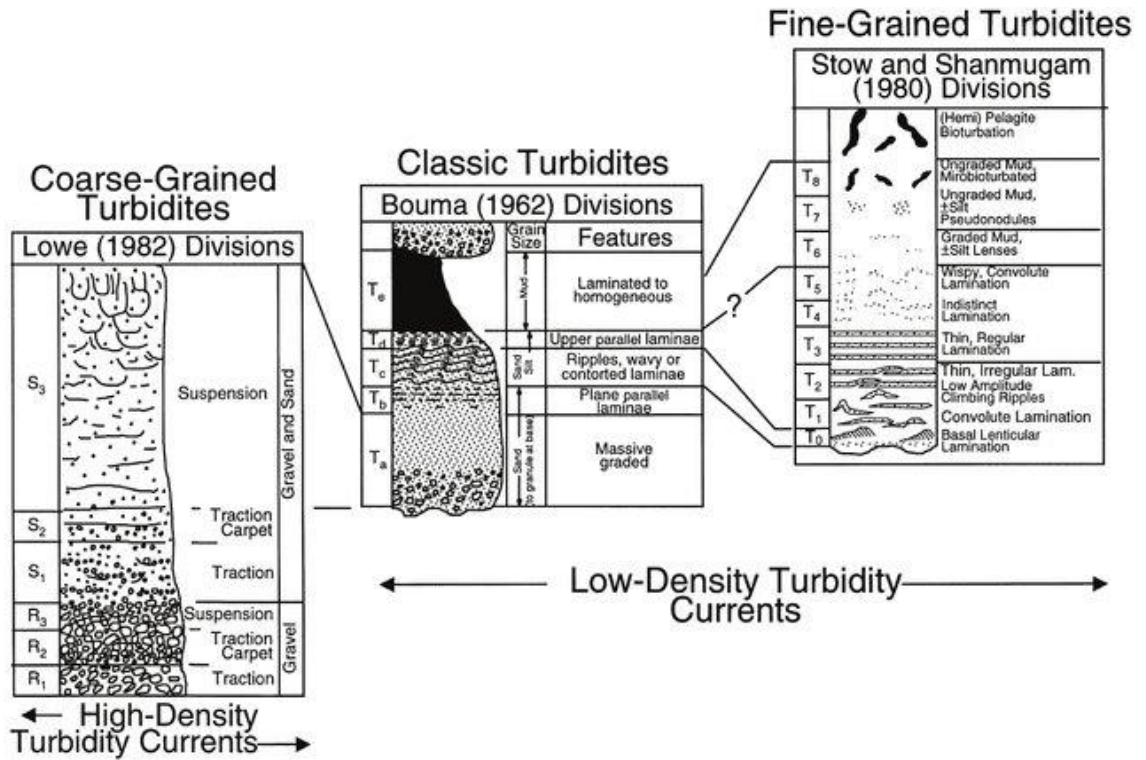
Figure 2-10 Ideal Bouma sequence (centre) showing Ta to Te divisions (Bouma, 1962); fine-grained turbidites (right) showing T0 to T8 divisions (Stow and Shanmugam, 1980), equivalent to the Tc to Te divisions; and coarse-grained turbidites (left) showing R1 to R3 and S1 to S3 divisions (Lowe, 1982) equivalent to Ta division (Shanmugam, 2000).
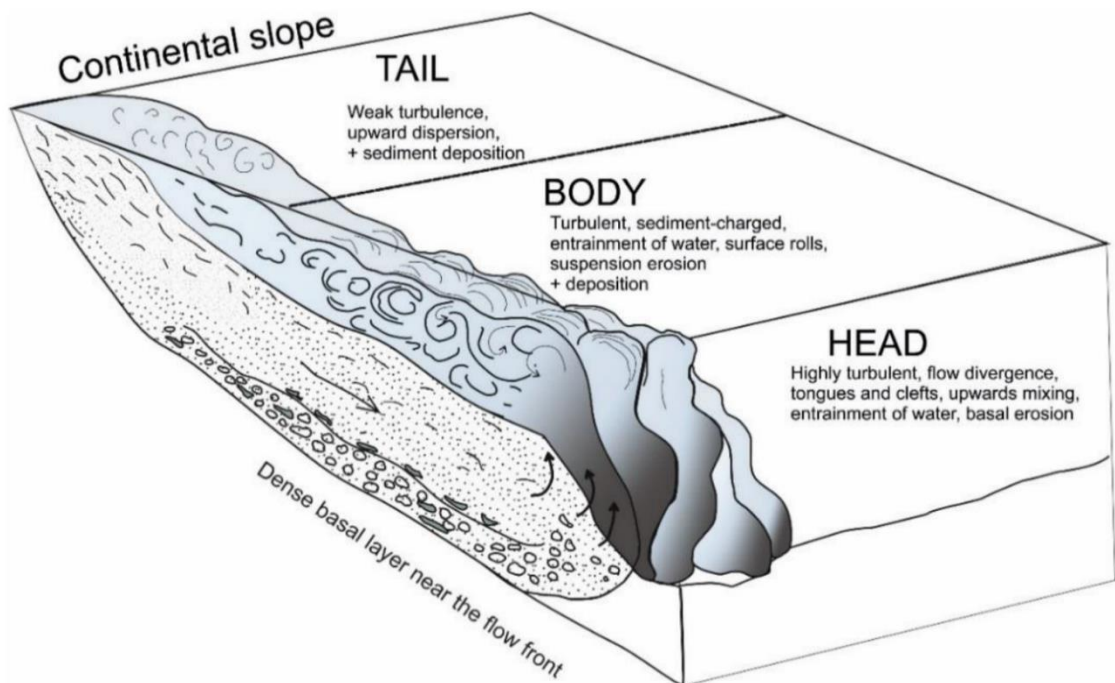
Figure 2-11 Structure of a turbiditic flow, consisting of the head, body, and tail (Stow and Smillie, 2020)

As turbidite research moved towards modern examples, models based on modern suprafan lobe were developed (Normark, 1970; Middleton and Hampton M.A., 1973). However, a universal facies association model for the "Deep Sea Fan" was introduced by Mutti and Ricci Lucchi, (1972), based on outcrop studies of the Miocene Marnoso-Arenacea of northern Apennines and the Eocene Hecho Group of south-central Pyrenees. The model subdivided an ancient submarine fan system into seven facies A-G: slope, canyon, channel, lobe, lobe fringe, levee, and basin plain (Fig. 2-12). Facies associations are then used to distinguish the inner-, middle-, and outer-fan segments of the submarine fan (Mutti and Ricci Lucchi, 1972). A further study by Mutti (1985) added to the different type of turbidite systems: attached lobes, detached lobes, and channel-levee complexes.
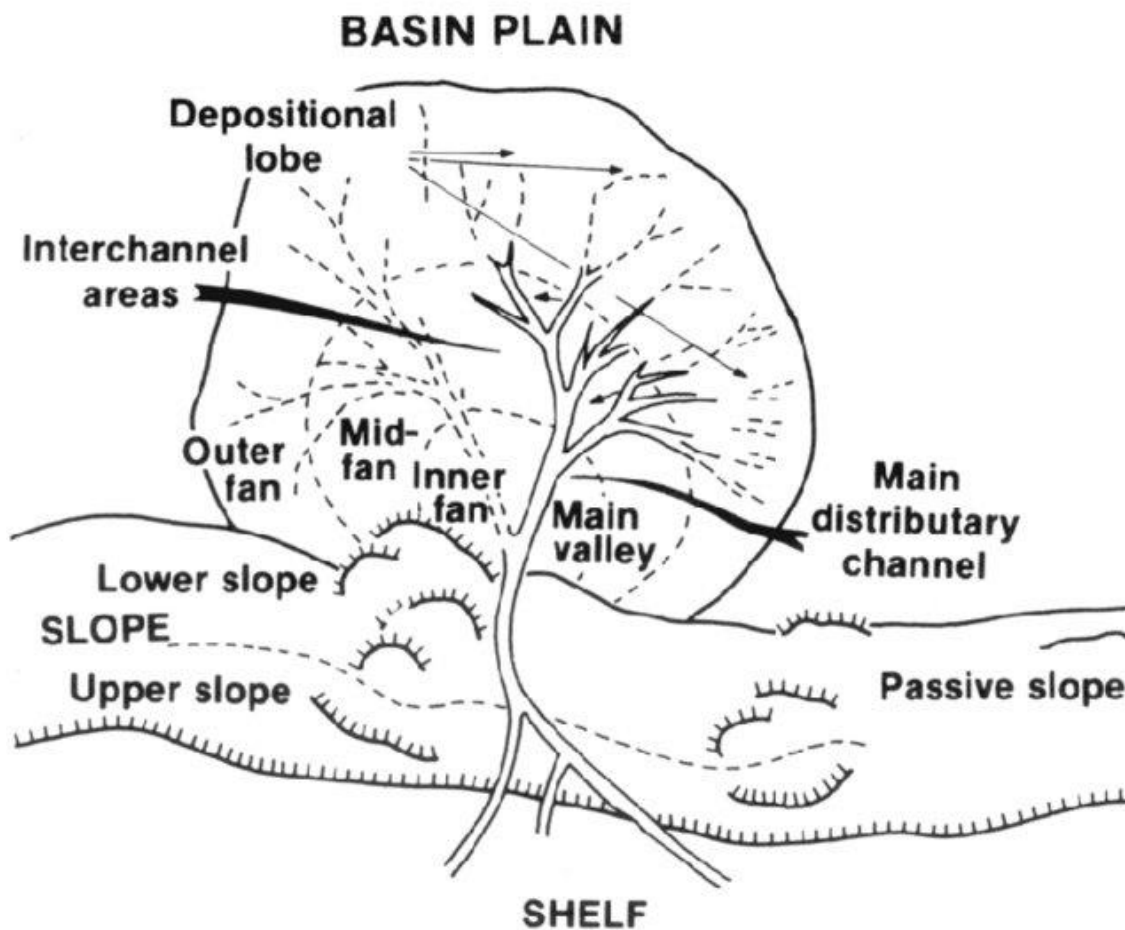
Figure 2-12 Submarine fan system facies and their associations (Mutti and Ricci Lucchi, 1972)

Since the 1970's, significant advances in technology such as seismic surveys and borehole drilling with the rise of the oil and gas industry led to an increase interest in turbiditic processes and systems, especially on sandy turbidites and their exploration potential (Mutti et al., 2009). The introduction of the basin floor fan model by Vail et al. (1991) used in the context sequence stratigraphy for the interpretation of sandy turbidites as reservoir sands (Shanmugam, 2016). However, different perspective from scientific experts on the definition and characteristic of turbidites still exists (Shanmugam, 2012). For example, the deposition of sandy turbidites in the dense basal layer of plastic rheology and laminar flow attributed to high density turbidity currents as opposed to debris flow (Shanmugam, 2016). Whereas Postma and Cartigny (2014) divided the stratified high density and the non-stratified low density turbidity currents in relation to Froude number (Fr): supercritical (Fr>1) and subcritical (Fr<1) flows, which led to idea that the deposition of sandy submarine fan are dominated by the hydraulic jumps in turbidity currents. Nevertheless, the wealth of knowledge on turbidite studies has allowed it to dominate the interpretation for deep-marine sedimentary facies, despite the ever-growing presence of other deep-water processes, such as the ones related to bottom current circulation (Rebesco et al., 2014) and other gravity-driven processes including slides, slumps, and debris flows (Haughton et al., 2009).

The identification of turbidites on the seismic scale has also been studied (Mitchum, 1985; Posamentier and Erskine, 1991; Liu and Watkins, 1992; Prather et al., 1998). Posamentier and Erskine (1991) introduced key recognition criteria for the lowstand or basin floor fans, which includes: lateral pinchout geometry, high-amplitude continuous reflection onlapping highs, internal bidirectional downlapping, low-relief external mounding, and association with unconformity basinward. Whereas Prather et al. (1998) classified seismic facies for turbidites and other deep-water deposits on intraslope basins, calibrated to lithologic information from boreholes (Fig. 2-13). The evolution of accommodation space resulted in the transition from sand prone ponded basin-fill succession (including convergent-baselapping, and localised chaotic and draping facies), to the shale prone slope-bypass succession (including convergent-thinning, and widespread chaotic and draping facies), where turbiditic deposits have been summarised and identified for the convergent and high reflectivity or impedance facies (Prather et al., 1998).
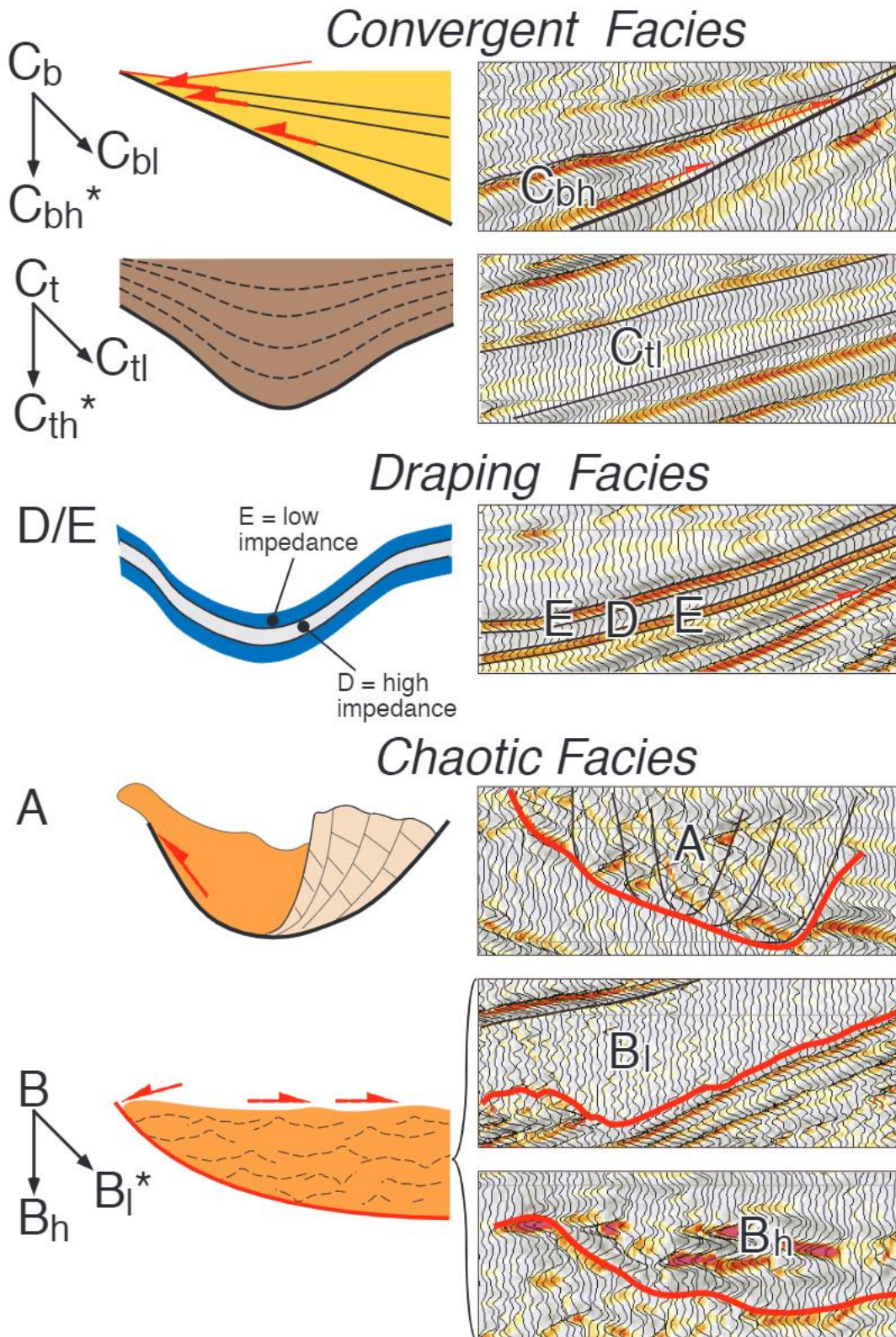
Figure 2-13   Idealised seismic facies and geometries identified in intraslope basins containing turbidites and other deep-water deposits (Prather et al., 1998).

b.   *Mass-transport deposits (MTDs)*

Downslope processes responsible for the sediment gravity-flow deposits are not limited to turbidity currents, but an entire spectrum of gravity-driven processes, such as slides, slumps, and debris flow (Middleton and Hampton, 1973; Haughton et al.,2009). In fact, there is a transition between the different types of sediment gravity-flows, from cohesive, laminar debris flows to non-cohesive, low density turbidity currents of turbulent behaviour (Haughton et al., 2009). However, the definition for "sediment gravity flows" also include that of subaqueous and subaerial environments (Middleton and Hampton, 1973). The term mass-transport deposits (MTD) and mass-transport complexes (MTC) has since been popularised to describe the deposits formed *en masse* or resulting from mass-wasting (Posamentier and Martinsen, 2011). Mass-transport deposits are generally used to refer single event typically in outcrop-scale (Jackson et al., 2009), while mass-transport complexes are used commonly in seismic interpretation to refer features large enough to be imaged (Weimer and Shipp, 2004).

Dott (1963) first proposed a scheme for only the subaqueous mass-transport processes, which classified them based on mechanical behaviour: elastic, elastic and plastic, plastic, and viscous fluid types. The initial classification of mass transport processes by Dott (1963) composed of three basic types: slide, slump, and debris flow; and did not include turbidity currents, whereas creep and rockfall were added later (Posamentier and Martinsen, 2011; Fig. 2-14). Nardin et al., (1979) reclassified mass movement processes according to flow behaviours: elastic (rockfalls, slides and slumps), plastic (debris flows, mudflows, and inertial grain flows), and viscous fluid flows. A slide is "a coherent mass of sediment or a rigid body that moves along a planar glide plane and shows no internal deformation"; whereas a slump is "a coherent mass of sediment that moves on a concave-up glide plane and undergoes rotational movements causing internal deformation" (Dott, 1963). In other words, slides and slumps represent translational and rotational shear-surface movements respectively (Shanmugam, 2016). On the other hand, debris flow is "a sediment mass of plastic rheology in a laminar state primarily supported by the cohesive strength of matrix" (Nardin et al., 1979). These processes can transport coarse grained sediments and travel up to hundreds of kilometres on the continental slope. A list of primary sedimentary structures attained from borehole data and attributed to MTDs include angular bedding contacts, shear zones, faults, partially and fully mixed layers, highly distorted stratified sediments with convoluted folds and clasts of lithified or semi-lithified structures (Tripsanas et al., 2007).

For seismic analysis in deep-water depositional systems, mass-transport complexes are rather distinctive due to their large size, distinct morphology, and chaotic internal character (Embley, 1980; Moscardelli et al., 2006; Moscardelli and Wood, 2008). Their seismic character can be identified by a change in sedimentation patterns from non-chaotic, parallel reflectors to lack of internal reflectors. These can be identified as chaotic, low amplitude or transparent amplitudes (Embley, 1980; Garziglia et al., 2008; Moscardelli and Wood, 2008). Examples from Garziglia et al. (2008) also identified mass-transport complexes with the following traits: pronounced vertical relief, basal scours, chaotic internal reflectivity, and rapid thinning. The different type of mass-transport deposits may be individually recognized by their seismic features: slides are continuous blocks with high-amplitude, continuous reflections; slumps are contorted layers with low- and high-amplitude reflections and deformed geometry, whereas debris flow are detached blocks with low-amplitude to semi-transparent chaotic reflections (Moscardelli et al., 2006). Their external morphology can comprise sheets, lobes and channels fill and reach greater thicknesses when successive flows are amalgamated (Posamentier and Martinsen, 2011). Whereas the staging area of a mass-transport deposit can be characterised by arcuate scars commonly observed at shelf-slope break or mid-slope settings (Posamentier and Martinsen, 2011). On the larger scale classification, three types of mass-transport complexes have been grouped from 32 examples studied (Moscardelli and Wood, 2008): shelf-attached systems, which are fed by shelf-edge deltas; slope-attached systems, which are caused by upper-slope catastrophe; and locally detached systems, which are small collapses triggered by local instabilities in the seafloor. A different classification by Gong et al. (2014) shows only two types: localised detached mass-transport complexes, resulting from small-scale mass-wasting confined to submarine canyons; regional attached mass-transport complexes, resulting from large-scale mass-wasting in a semi-confined or unconfined setting.
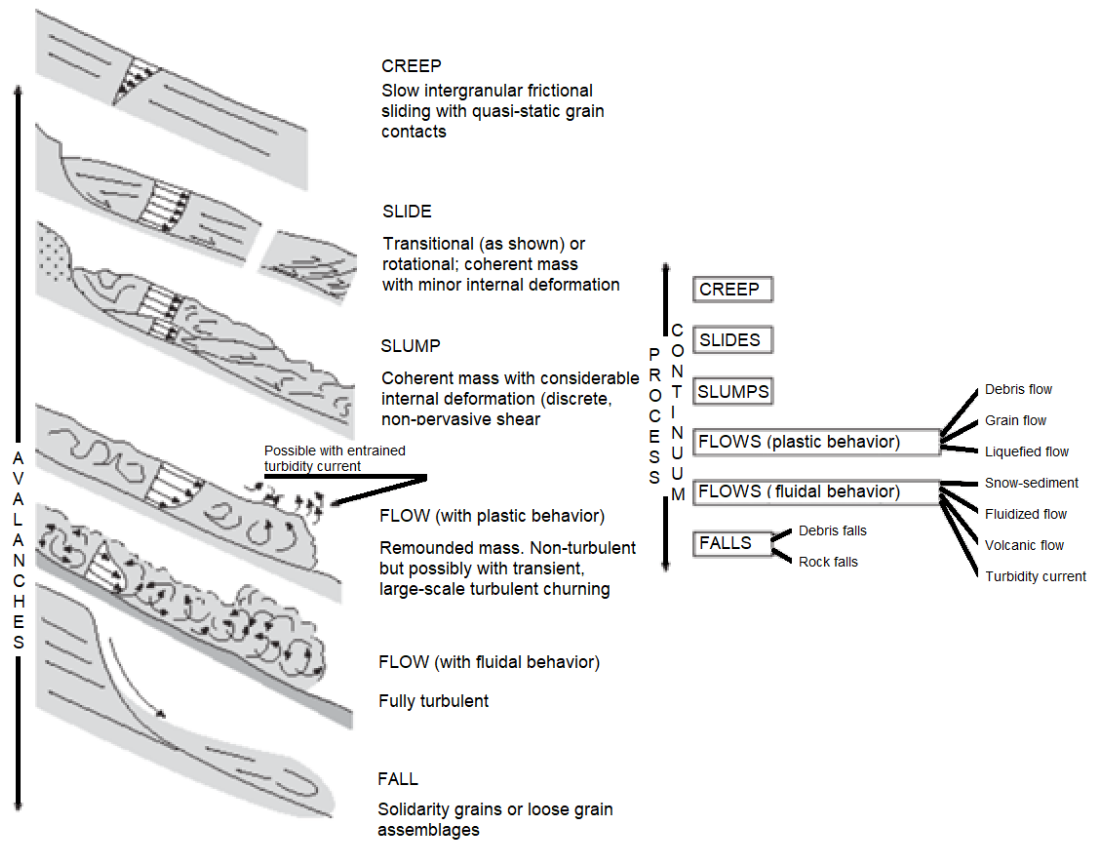
Figure 2-14   Types of mass transport processes, modified after the initial classification of Dott (1963), based on their mechanical behaviour (Posamentier and Martinsen, 2011).

c.   *Turbidites and mass transport deposits in the Gulf of Cádiz*

During the last three decades, the Mediterranean Sea has been at the centre for research for both turbidites and mass transport deposits, including submarine canyons, channels, and fans (Piper and Savoye, 1993; Mulder et al., 2001; Kenyon et al., 2002; Camerlenghi et al., 2010; Mulder and Etienne, 2010; Migeon et al., 2011, 2012; Würtz, 2012; Gamberi et al., 2014, 2015). On the other side of the straits of Gibraltar, the Gulf of Cádiz is known more for its contourite studies (Nelson et al., 1999; Llave et al., 2007; Roque et al., 2012; Hernández-Molina et al., 2016). However, gravity flow deposits have also been well studied. The most obvious features are the submarine canyons on the continental margin south and west of Portugal. Located around the São Vicente Cape, they consist of (from east to west) Faro, Portimão, Lagos, Sagres, and São Vicente Canyons (Hernández-Molina et al., 2003). Dominant downslope processes during the Pliocene-Pleistocene boundary, correlated to erosion linked to sea level lowstand (Llave et al., 2001; Llave, 2004), resulted in the incision of submarine canyons perpendicular to the slope connecting to the deep valleys (Marchès et al., 2007). Tectonic activity also

supported the initiation of gravity processes along zone of weaknesses, such as the N-S Portimão Fault underlying the Portimão Canyon (Lopes et al., 2006). The transition of dominance from downslope gravity processes to Mediterranean Outflow Water-related processes towards present day has led to partial filling within these submarine canyons (Marchès et al., 2007), during which mass wasting process also occurred on the flanks of the canyons (Llave et al., 2007).

Mass movement processes are also present east of these submarine canyons in the Deep Algarve basin, where debrites of different compositions originating from the shelf and upper slope have been identified for two periods, during the early Pliocene and early Pleistocene (Ducassou et al., 2016). The lower Pliocene bioclastic debrites occurred during a phase of dominant gravity flow deposits between 4.5 to 3.5 Ma after an older phase between 5.2 to 4.5 Ma which included terrigenous turbidites and slumps, whereas the lower Pleistocene terrigenous debrites is dated between 1.66 to 1.25 Ma (Ducassou et al., 2016). During the early Pliocene, the downslope mass transport and turbiditic systems are mainly sourced from the Guadalquivir and Guadiana Rivers, northeast and north of the Deep Algarve basin respectively (Riaza and Martínez del Olmo, 1996; Ledesma, 2000), while diapirism could also trigger gravity flows (Roque et al., 2012; Brackenridge et al., 2013). Synchronous gravitational collapse breccias can be found in outcrops in areas adjacent to the Cádiz basin and the Strait of Gibraltar (Esteras et al., 2000), indicating basinwide tectonic activity. The strengthening of Mediterranean Outflow Water -related bottom currents since the late Pliocene would dominate over gravity flow deposits by reworking and redistribution, except in the northeast of the basin where higher clastic influx downslope from the north prevails (Brackenridge et al., 2013).

Another feature of downslope gravitational influence is the Gil Eanes channel and the mega-sedimentary lobes previously described in *2.1.2 Morphosedimentary features* (Kenyon and Belderson, 1973; Hernández-Molina et al., 2003). Four other inactive secondary channels were also identified, where these were also once connected to the deep core of the Mediterranean Outflow Water which spills over the sedimentary levee (Mulder et al., 2003). The Gil Eanes channel drains the downwelling currents and forms debritic or turbiditic depositional lobes at the end, due to mass-wasting at the channel head or transitioned into turbidity currents with loss of flow competence at the channel mouth (Mulder et al., 2003).

The most prominent feature in the Gulf of Cádiz however is the allochthonous unit previously described in *2.1.1 Morphostructural features* (Medialdea et al., 2004).

This allochthonous unit, also known as the "Olistostrome" unit (Maldonado et al., 1999), is formed from the mechanism of mass gravity sliding and collapse along the slope, where it gave rise to thrusting and extensional collapse on the back (Flinch and Vail, 1998; Maestro et al., 2003) and are emplaced in the oceanic domain and tectonically reactivated (Gràcia et al., 2003). Age of emplacement for the allochthonous unit of the Gulf of Cádiz is generally agreed as late Tortonian (Maldonado et al., 1999; Somoza et al., 1999; Gutscher et al., 2002), similar to both the Guadalquivir (Perconig, 1960) and Gharb (Flinch and Vail, 1998) basins. The affected area covers from the Betic-Rif external front, extending along the continental shelf, upper and middle slope, towards the abyssal plain (Medialdea et al., 2004). The allochthonous mass advance was restricted by structural high including the Guadalquivir bank and Portimão basement high in the upper to middle slope, and the Gorringe bank and Coral Patch (Medialdea et al., 2004).

2.5.3 Contourite depositional system
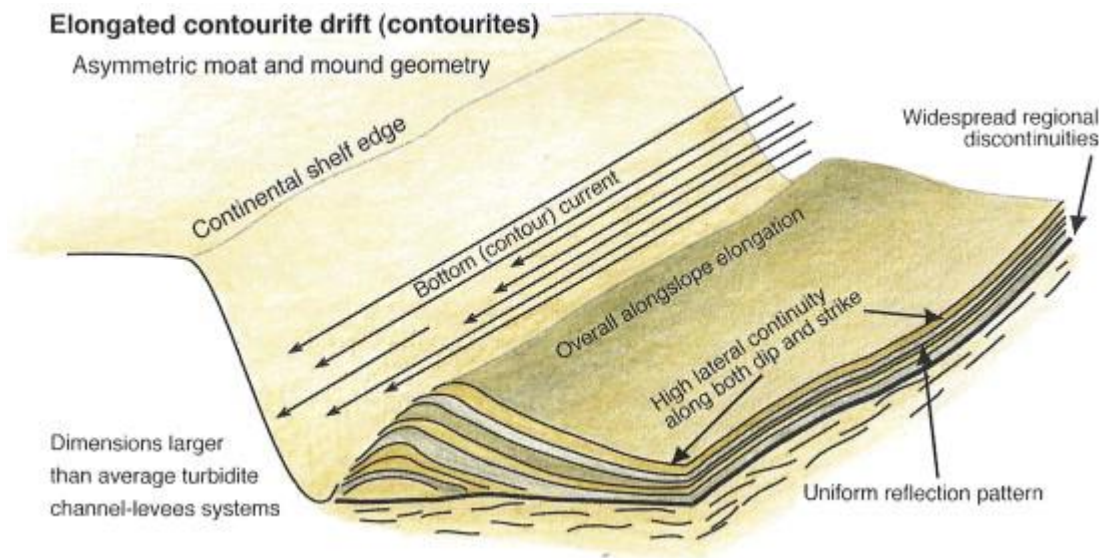
Figure 2-15 Schematic model showing the contourite drift, compared in large-scale differences with the turbiditic channel-levee system in *Figure 2-9* (Rebesco et al., 2014).

a. Conceptual theory of contourites

Contourites were firstly introduced as deep marine deposits of thermohaline-induced contour currents (Hollister, 1967). A recent review by (Rebesco et al., 2008) shows a widely accepted definition for contourites as "deposits of bottom currents". In full, contourites are defined as "sediments deposited or substantially reworked by the persistent action of bottom currents" (Rebesco et al., 2014). According to (Shanmugam, 2012), bottom currents are defined as "a deep-water component of water masses that winnow, rework and deposit sediment on the seafloor for a sustained period of time". Sediments are eroded and transported away when velocity of bottom currents picks up parallel to the margin; and are deposited when velocity drops usually disrupted by topographic highs (Rebesco et al., 2014). Contourite deposits are generally well sorted and composed of less mud due to the winnowing away action of the finer-grained sediments, whereas turbidites in comparison are poorly sorted and are generally mud-rich facies (Shanmugam, 2012, 2017). These alongslope currents are divided into four major types: thermohaline-induced geostrophic, caused by continuous equilibrium between Coriolis and pressure gradient forces resulted from density, temperature and salinity variations in a water mass; wind-driven, caused by sea surface wind-stress which are propagated to the sea floor; tide-driven, caused by flood and ebb currents found within submarine canyon; and internal wave-/tide-driven, caused by baroclinic gravity waves oscillating along a pycnocline (Southard and Stanley, 1976; Shanmugam, 2008, 2017).

They are also affected by climatic or seasonal variability, and their relationship with turbiditic systems in various basin margin settings. Upwelling and downwelling are also important processes in contourite formation at restricted regions and topographic barriers (Rebesco et al., 2008).

	Sketch	Sed. structures	Dominant grain size	Enviromental implications
MAIN TYPES OF PRIMARY SEDIMENTARY STRUCTURES IN CONTOURITE DEPOSITS	1 cm	Horizontal or sinusoidal lamination, stripped, fine-grained deposits; "wispy" lamination	Fine sand, silt & mud < 2 Ø < 0.250 mm	Low current strength Predominance of deposition from suspension
	1 cm	Lenticular bedding starved ripples	Fine sand, silt & mud < 2 Ø < 0.250 mm	Alternating flow conditions, low to moderate current strength, winnowing
	1 cm	Wavy bedding, flaggy chalks	Fine sand, silt & mud < 2 Ø < 0.250 mm	Alternating flow conditions, low to moderate current strength
	1 - 5 cm	Flaser bedding, mud offshoots	Fine sand to silt 8 - 2 Ø 0.004 - 0.250 mm	Alternating flow conditions, Current speed = 10 - 40 cm / s
	1 - 5 cm	Climbing ripples (subcritical to supercritical)	Very fine to medium sands 4 - 1 Ø 0.063 - 0.5 mm	Current speed = 10 - 40 cm / s High suspension load
	10 - 50 cm	Large-scale cross-bedding, megaripples, dunes, sandwaves	Medium sands 2 - 1 Ø 0.250 - 0.5 mm	Current speed = 40 - 200 cm / s Barchan dunes usually form at 40-80 cm / s
	1 cm	Parallel lamination (upper stage plane beds), presence of primary current lamination	Very fine to medium sands 4 - 1 Ø 0.063 - 0.5 mm	Current speed = 40 - 200 cm / s
	1 cm	Minor erosive surfaces, mud rip-up clasts, upper sharp contacts	Sand, silt & mud < -1 Ø < 2 mm	Alternating flow conditions, low to moderate current strength
	1 - 5 cm	Sole marks: flutes, obstacle scours & longitudinal scours, cut & fill structures	Sand, silt & mud < -1 Ø < 2 mm	Flow speed peaks
	5 cm	Longitudinal ripples	Coarse sandy muds (20 % sand)	Low current speed = 2 - 5 cm / s Winnowing
	1 - 10 cm	Bioturbation (strongly variable)	Sand, silt & mud	Low current speed Strong paleoecological control, Low to moderate accumulation rates
	3 - 20 cm	Normal & reverse grading at different scales and within different types of deposits	From coarse sand to mud Usually fine sand, silt & mud	Gradual changes in flow strength
	0.1 - 2 cm	Pebble lags, furrows	Coarse sand, microconglomerate	Current speed over 200 cm / s

Clay and / or mud	Silt	Sand	Pebbles & cobbles

Figure 2-16   Summary of traction sedimentary structures in contourite deposits. (Martín-Chivelet et al., 2008).

On identifying contourites through facies association and their diagnostic sedimentological criteria however, there are two main contrasting perspectives among scientific experts on contourites, which are: firstly, through traction structures; and secondly, bioturbation (Rebesco et al., 2008, 2014). As there is no unique facies sequence for contourites, traction structures which are commonly found within contourites are used as its indication (Rebesco et al., 2014). A summary of traction sedimentary structures by (Martín–Chivelet et al., 2008) is shown in figure 2-16. Bedforms or traction structures are also used to reconstruct the bottom-current velocity, as depicted in the bedform-velocity matrix by (Stow et al., 2009) (Fig. 2-17). They can be divided into longitudinal and transverse bedforms based on their spatial relationship with the flow (Rebesco et al., 2014).
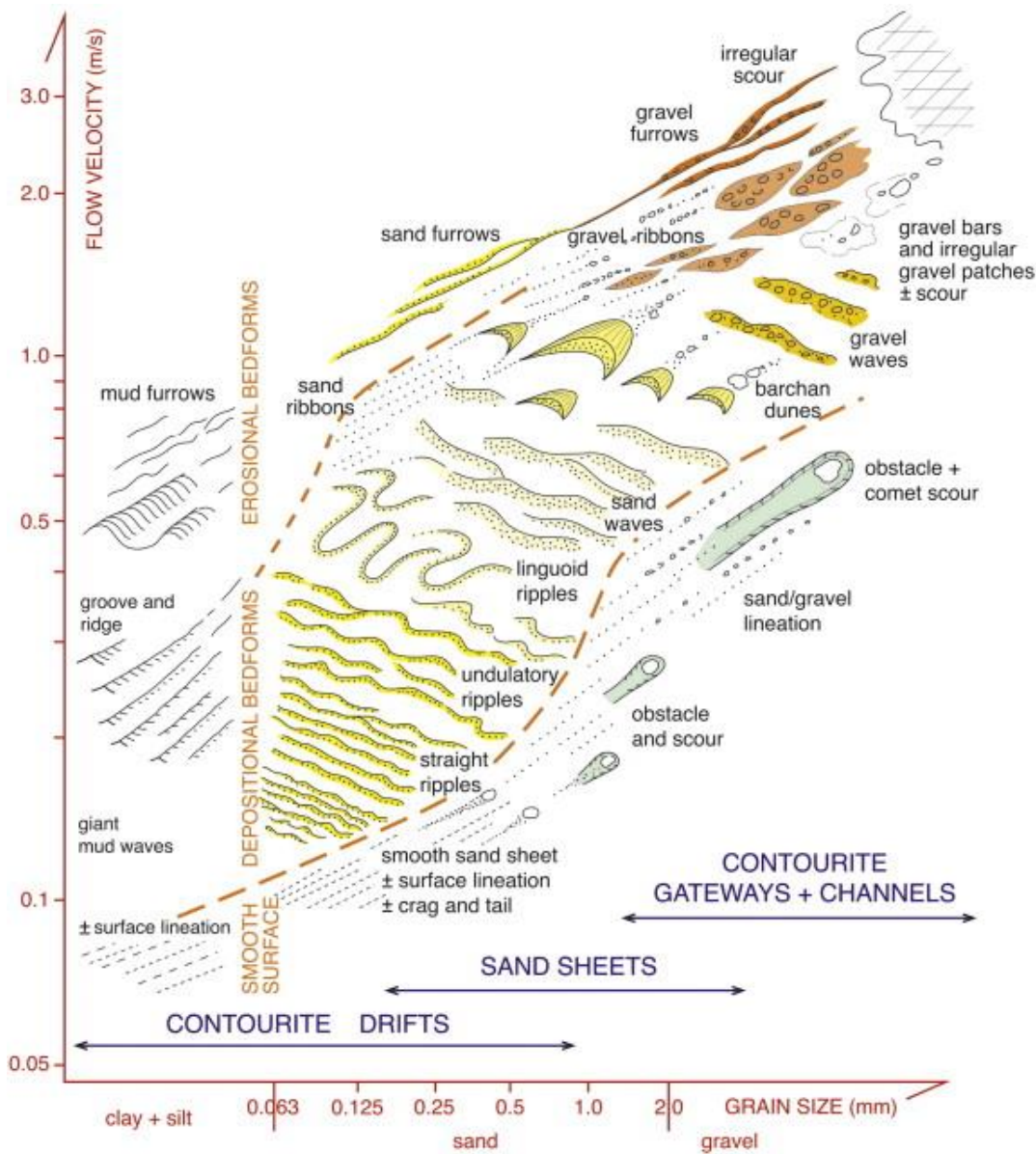
Figure 2-17   Bedform-velocity matrix for bottom current deposits (Stow et al., 2009).
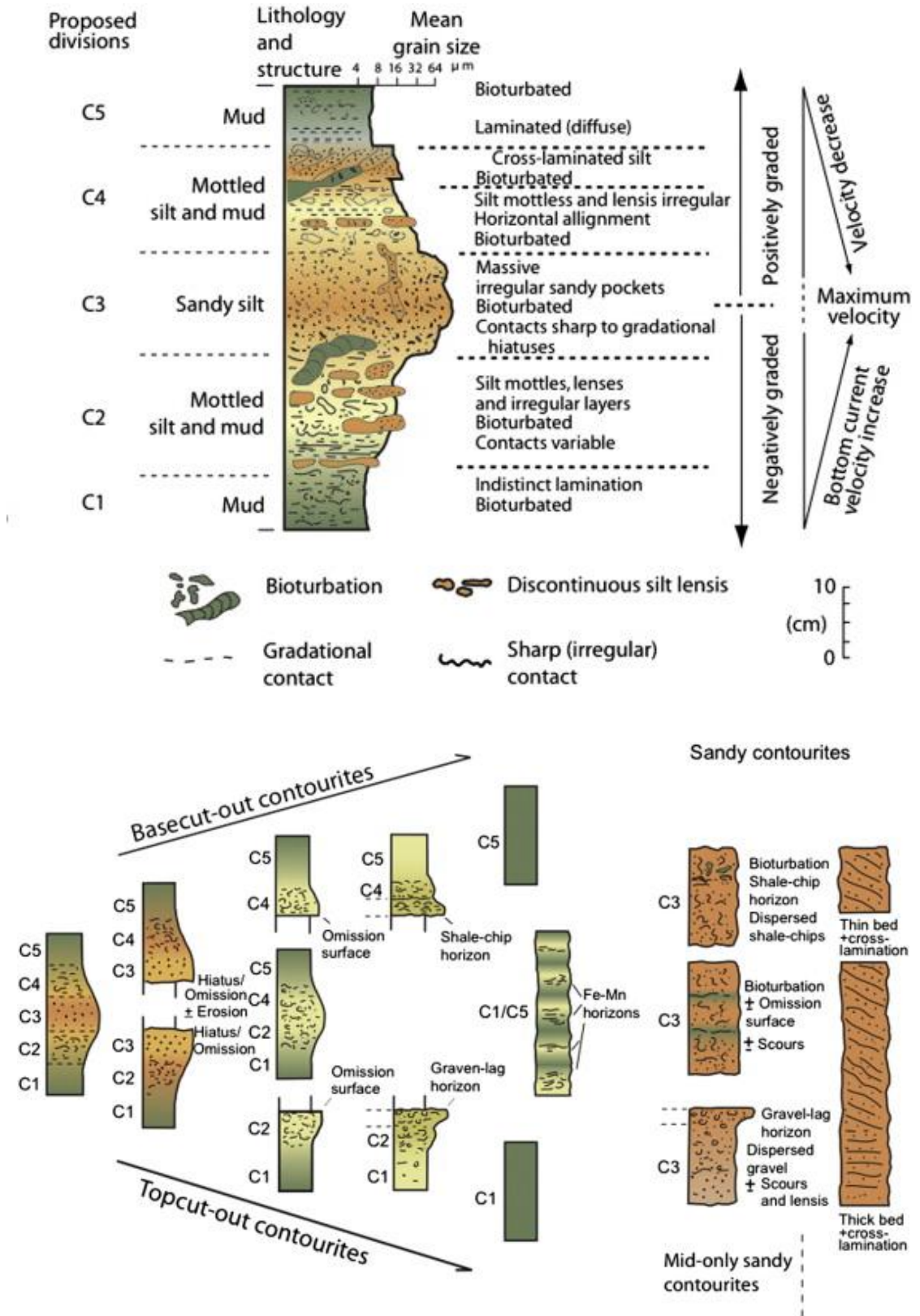
Figure 2-18 The standard contourite facies model with five divisions and modifications with partial sequences from the standard model (Stow & Faugères, 2008, modified after Gonthier et al., 1984).

The standard contourite facies model (Stow and Faugères, 2008; Fig. 2-18), first introduced by Faugères et al. (1984) and Gonthier et al. (1984) supports the diagnosis of bioturbation together with differentiation of sandy and muddy contourite facies initially demonstrated by (Stow and Lovell, 1979) on lithology and texture, which includes three main facies: homogenous mud, mottled silt and mud, and sand and silt. The cyclic bigradational sequence of coarsening then fining upwards in the facies model labelled C1 to C5 (Fig. 2-18, Stow and Faugères, 2008) illustrates the shift of strength of the bottom current flow from weak to strong and back (Hüneke and Stow, 2008). These changes may
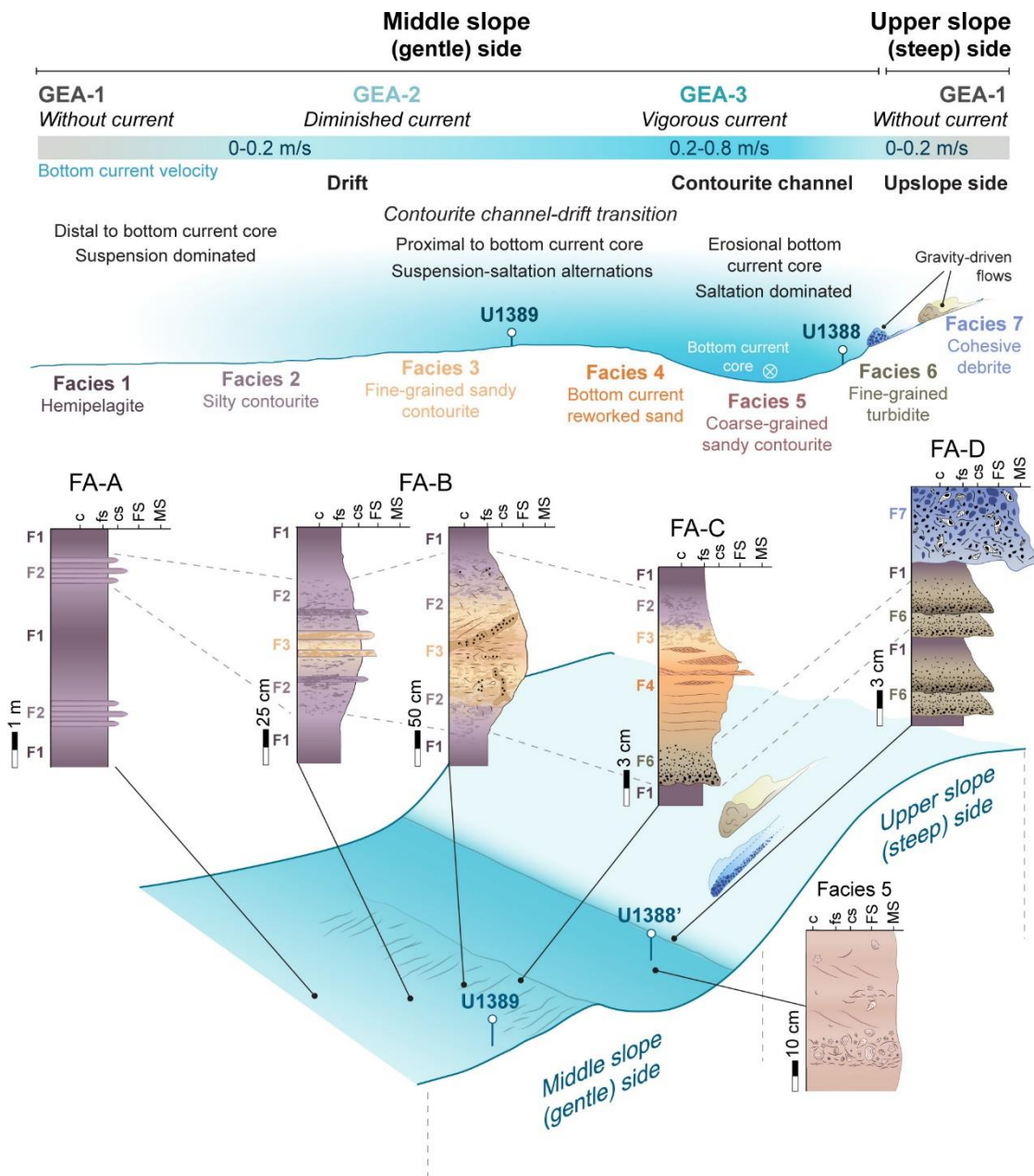
Figure 2-19   Conceptual depositional model for the sedimentary facies (Facies 1 to 7), facies associations (FA-A to FA-D), geochemical element associations (GEA-1 to GEA-3) and depositional processes in different contouritic physiographic domains of a modern contourite drift (de Castro et al., 2021a).

be due to increased erosion on fine-grained particles or increased coarser sediment supply (Mulder et al., 2013). However, (Mulder et al., 2013) recognised sharp contacts between facies as opposed to the transitional change, while (Stow and Faugères, 2008) proposed partial sequences as modifications for the inclusion of coarser contourites facies alongside the generally muddy facies with bioturbation in the standard model (Fig. 2-18).

The latest development on the small (sedimentary facies) scale identification of contourite deposits shows a continuum of facies associations depicting the range of facies from proximal to distal environment in relation to a contourite channel in both modern and ancient contourite depositional systems (de Castro et al., 2021a; de Weger et al., 2021). The six facies recently proposed by de Castro et al. (2021a) based on a modern
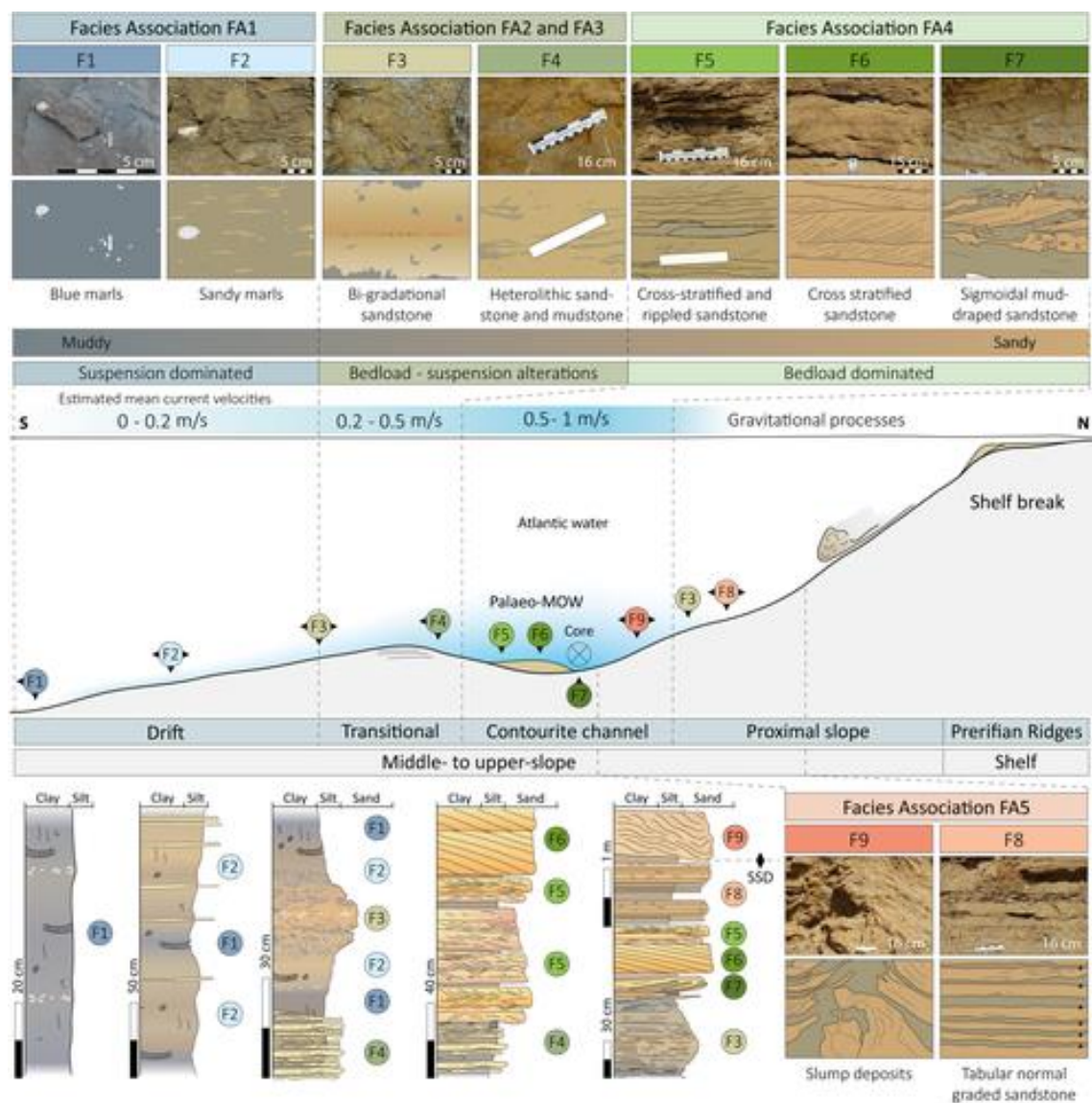
Figure 2-20   Conceptual depositional model with sedimentary facies (F1 to F9) and their associations related to their dominant depositional process and associated current velocities linked to different depositional and erosional elements from the proximal continental slope to an ancient contourite drift (de Weger et al., 2021).

contourite system, the Huelva drift and associated channel in the Gulf of Cadiz (Fig. 2-19), which include: hemipelagites (F1); silty contourite (F2); fine-grained sandy contourite (F3); bottom current reworked sand (F4); coarse-grained sandy contourite (F5); fine-grained turbidite (F6); and cohesive debrite (F7). The association of the sedimentary facies and geochemical elements provide five representative facies models in a continuum of depositional environments: distal contourite drift (FA-A: F1 and F2); channel-drift transition (FA-B: F1, F2 and F3); contourite channel with turbidite influence (FA-C: F1, F2, F3, F and F6); contourite channel core (F5); and upslope side (FA-D: F1, F6 and F7) (de Castro et al., 2021a; Fig 2-19), which also taken into account their relationship with gravity flow processes in the form of bottom current reworked sand (de Castro et al., 2020). Similar facies and their associations, with minor variations, are also identified in ancient contourite outcrops within the Rifian corridor onshore Morocco (de Weger et al. 2021; Fig. 2-20).
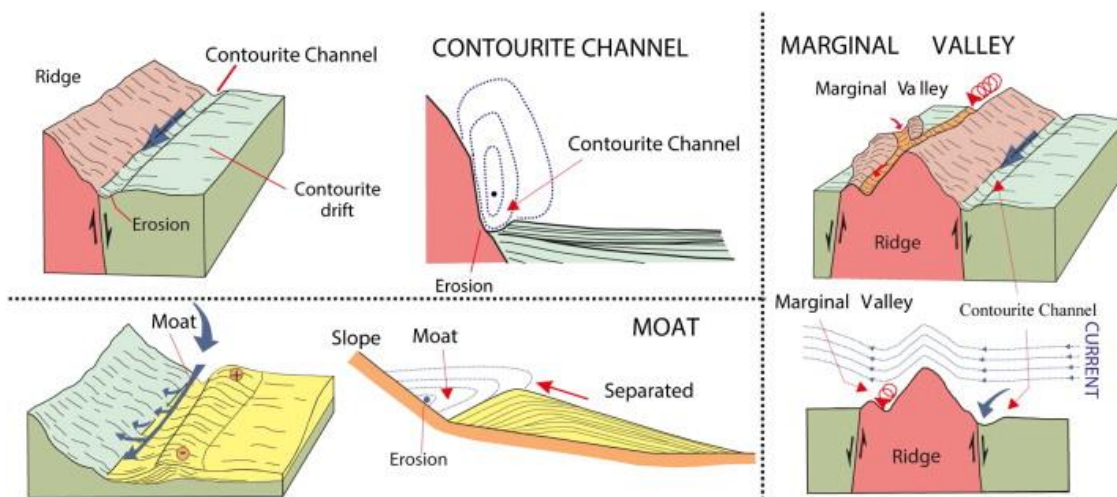
Figure 2-21   Erosional features on slopes associated to bottom current action (Hernández-Molina et al., 2008).

The bottom current deposits can also be identified by depositional and erosional features in large (seismic facies) scale, forming contourite depositional systems (CDS) (Hernández-Molina et al., 2003, 2008). They are associations of contourite drifts which are usually extensively accumulated (Rebesco et al., 2014). A simple classification of these drifts based on morphology by (Faugères and Stow, 2008) comprises of the self-explanatory: sheeted drifts, mounded drifts, and mixed drift systems. On seismic-reflection data, the seismic characteristics of the drifts could be recognised using a triple-stage approach: with an analysis on the overall architecture of the deposit including gross

geometry and large-scale depositional units, the internal architecture including structure and sub-units, and the seismic attributes and facies in the sub-units (Rebesco et al., 2008). The morphology such as erosional (Fig. 2-21) and depositional (Fig. 2-22) features observed on seismic are used as identification criteria for contouritic drifts and deposits (Hernández-Molina et al., 2008), whereas structures and thicknesses are used to identify the distribution of the channels as well as depocentres from the action of bottom currents.
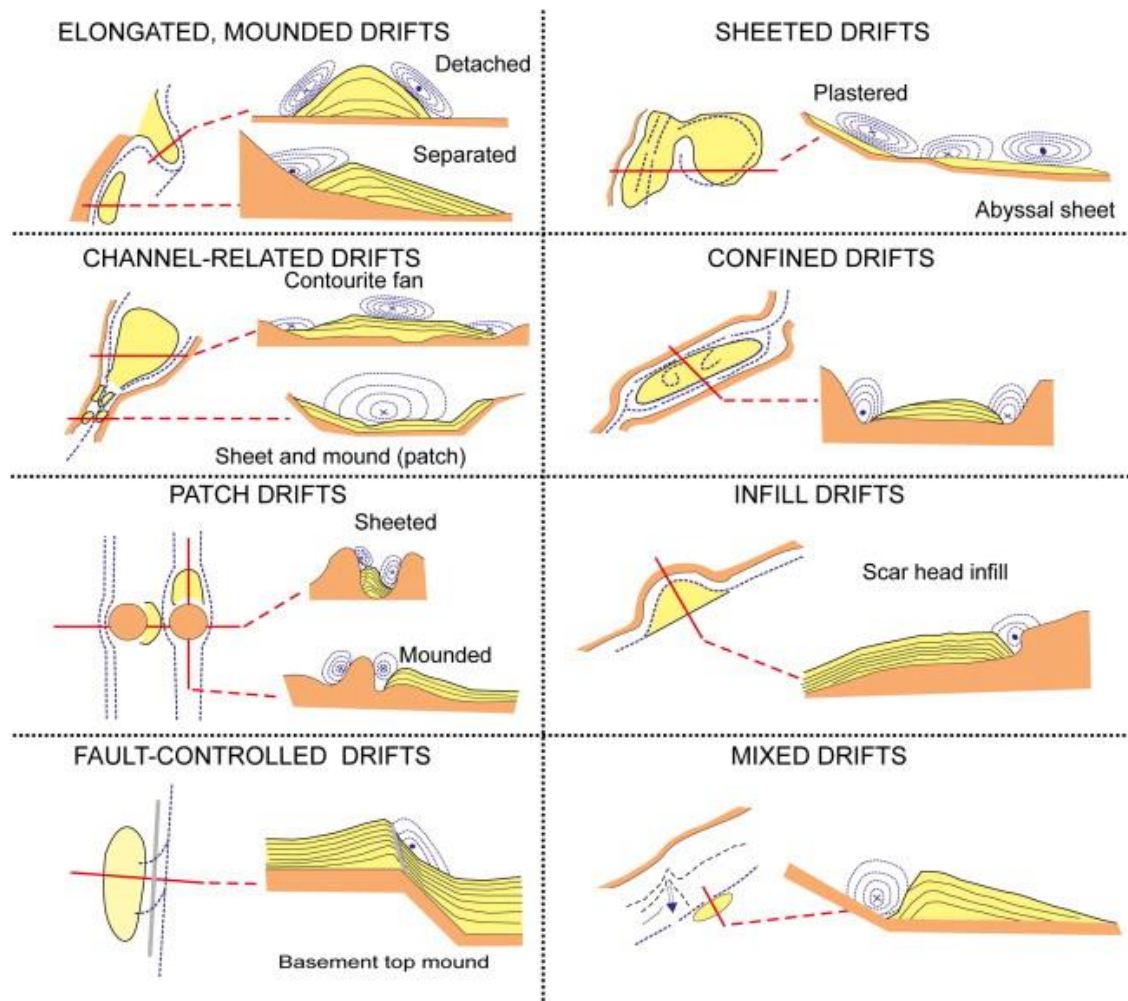
Figure 2-22   Depositional features or drifts associated to contourite deposits and bottom-current action (Hernández-Molina et al., 2008).

b.   *Mixed / hybrid contourite-turbidite deposits*

Contourites and turbidites represent two extreme sedimentary facies when one of the two processes shapes a continental margin. However, other sedimentary and oceanographic processes occur in the same area but with less energy. In mixed systems the interaction between alongslope and downslope processes produces numerous scenarios, since there is a large variability of features and deposits. Alternations of turbidites and contourites are frequent, at different scales, from single decametric beds to large sedimentary bodies (Mulder et al., 2008).

The first model for the interaction between alongslope and downslope currents illustrated that turbidity currents carried the sediments downslope, while the fine-grained particles in suspension were pirated by oblique, alongslope currents (Stanley, 1988). The contouritic levees (e.g., mounded contourite drifts) are formed parallel to the slope trend while turbiditic levee (e.g., deep sea fans) occur perpendicular to the slope (Faugères et al., 1999), where their combination will develop elongated and asymmetric levees with mixed or hybrid traits of both processes, depending on the level of interaction and strength between turbidity and bottom currents. However, it is still not fully understood the interaction between these two processes, as contrasting interpretations of bottom current direction in relation to the downstream turbidity current being raised from recent examples (Gong et al., 2013, 2018; Palermo et al., 2014; Sansom, 2018; Fonnesu et al., 2020, Rodrigues et al., 2021; Fig. 2-23). This is particularly hard for the identification of large-scale features and systems, where there is a lack of unambiguous and widely accepted diagnostic criteria.

Different types of mixed depositional system have been proposed by Mulder et al. (2008), such as low-frequency alternations, high frequency alternations, redistribution of gravity deposits by bottom-currents or synchronous interaction between bottom and turbidity currents. Low-frequency alternation represents bottom current settling on a pre-existing morphology developed by turbidity currents or vice-versa, where deposit distribution controlled by previous configurations at a margin scale. High-frequency alternation, on the other hand, represents intercalations of turbidite and bottom current deposits at individual beds or successions, where the two processes alternate in time. Reworking and redistribution of sediments by bottom-currents require the existence of gravitational or turbiditic processes in the same setting but alternating in time, which

could form sedimentary lobes with massive, clean, well sorted coarse silts to find sands. Synchronous interaction of bottom and turbidity currents can occur when these processes are balanced or at the boundary of the two depositional environments correspond to alternations of contourites, turbidites and their transitional facies.
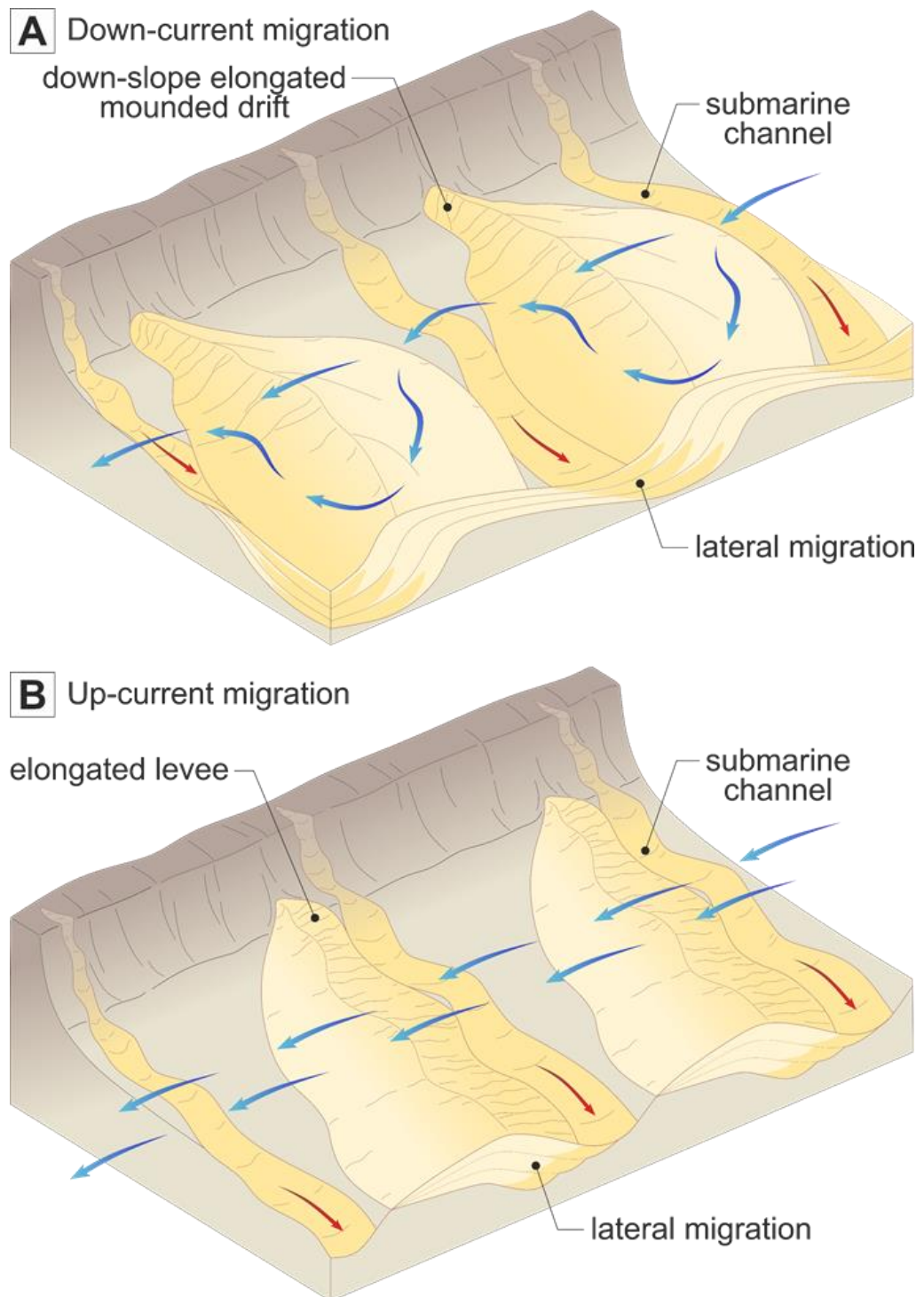
Figure 2-23   Conceptual model for mixed depositional systems, with interpretations for (A) down-current migrating submarine channels and down-slope elongated mounded drifts, and (B) up-current migrating submarine channels and elongated levees (Rodrigues et al., 2021).

c.   Contourites in the Gulf of Cádiz

Contourites and mixed deposits studies in the Gulf of Cádiz has been well documented in the literature, where it has been the focal point of the topic for the past three decades, which includes the scientific cruise Integrated Ocean Drilling Program (IODP) Expedition 339 (Hernández-Molina et al., 2016, 2006; Hernandez-Molina et al., 2014; Hernández-Molina et al., 2014; Llave et al., 2007). In fact, the first contourite facies model was developed here in the 1980s (Gonthier et al., 1984). The interaction of Mediterranean Outflow Water flowing along the middle slope of the Gulf of Cádiz after exiting the Gibraltar Gateway since the Pliocene to present (Hernández-Molina et al., 2014), developed one of the most extensive and complex contourite depositional system described. The Gulf of Cádiz contourite depositional system is classified as a detached combined drift fan which has been partly conditioned by Pliocene-Quaternary tectonics (Hernández-Molina et al., 2003).

The large depositional and erosional features developed within the morphosedimentary sector is generated by a strong current with the highest speeds located close to the Strait of Gibraltar (<300 cm s^{-1}), which decreases systematically towards the Cape São Vincent (~80 cm s^{-1}, Kenyon and Belderson, 1973; Ambar and Howe, 1979; Cherubin et al., 2000) due to interaction with margin bathymetry and the effects of Coriolis. The depositional features include sedimentary wave fields, sedimentary lobes, mixed drifts, plastered drifts, elongated mounded and separated drifts, and sheeted drifts; while the erosional features include contourite channels, furrows, marginal valleys, and moats (Hernández-Molina et al., 2016). These features all indicate clues to palaeoceanographic imprints related to a singular water mass – Mediterranean Outflow Water, or individualized by local behaviour of current, such as sea bottom stresses, secondary flows, filaments, internal waves, local turbulences, overflows, or helicoidal flow (Hernández-Molina et al., 2003). Within the Gulf of Cádiz contourite depositional system, drift deposition is mainly consisted of muddy, silty, and finer sandy sediments of mixed terrigenous and biogenic composition (Gonthier et al. 1984), whereas coarser sands and gravel sediments can be found within channel erosions (Nelson et al., 1993, 1999). In the proximal sector close to the Strait of Gibraltar, sand layers up to 12-15 m can be observed in thick sandy-sheeted drift (-815 m in thickness, Buitrago et al., 2001; Llave et al., 2007).

Along the western Portuguese margin, Alves et al. (2003) described the occurrence of contourite features on the middle continental slope and the continental rise. Contourite drifts on the middle slope are associated with Mediterranean Outflow Water interaction, which the Pliocene-Quaternary section have been studied in detail by Teixeira et al. (2019; 2020) and Rodrigues et al. (2020). Whereas drifts located on the continental rise were interpreted to be influenced by the northeastern circulation of Antarctic Bottom Water (Alves et al., 2003).

Chapter 3
Methodology

3.1   **Dataset**

The dataset used for this work includes bathymetric, seismic, and drilling data, summarised in figure (3-1). Furthermore, input from collaborations of relevant ongoing research is used to calibrate and validate the findings of this work.

3.1.1 *Bathymetric data*

Bathymetric data used in this work include the SWIM multibeam compilation of swath bathymetric data in the Gulf of Cádiz area and the SW Margin of Portugal, produced from Digital Terrain Models (DTM) at 100 m grid spacing available in Zitellini et al. (2009).

3.1.2 *Seismic data*

Seismic surveys used in this work include 2D multi-channel and single channel seismic surveys and 3D seismic surveys (Fig. 3-1), acquired from *Repsol S.A.* and *Office National des Hydrocarbures et d*es Mines (ONHYM). The 3D seismic volumes used include Algarve_3D, Calypso 1, and Calypso 2, whereas the 2D seismic surveys utilised include: GC-D, GHR10, HE-91, LAR04, NWM03, PD00/PDT00, P74, S81 and Tasyo. Relevant acquisition and processing parameters are also included in the *Material and Methods* or *Supplementary Materials* sections of chapters 4, 5 and 6.

3.1.3 *Drilling data*

Drilling data used in this work include those acquired from petroleum exploration wells of *Repsol S.A.* and *OHNYM*, and Integrated Ocean Drilling Program (IODP) scientific expedition sites (Fig. 3-1). They are divided into geophysical data which commonly are available as well logs and geological data in the form of well reports. In the Expedition 339 of the IODP, scientists drilled five scientific sites in the Gulf of Cádiz: e.g., U1386, U1387, U1388, U1389 and U1390, and two on the western Iberian margin, e.g., U1385 and U1391 (Expedition 339 Scientists, 2013; Hernández-Molina et al., 2016). Other than that, exploration wells acquired by the petroleum industry include the following: Algarve-1, Algarve-2, Atlantida-3, Corvina, Golfo de Cádiz B-3 (GCB-3), Golfo de Cádiz E-1 (GCE-1), Golfo de Cádiz Mar Profundo C-1 (GCMPC-1), Imperador Neptuno-1, Neptuno-2 and Ruivo from Southwest Iberian margin; three additional wells: Anchois-1, Deep Thon-1, and Merou-1 from Northwest Moroccan margin, and Pescada-1 from the southern West Iberian margin.
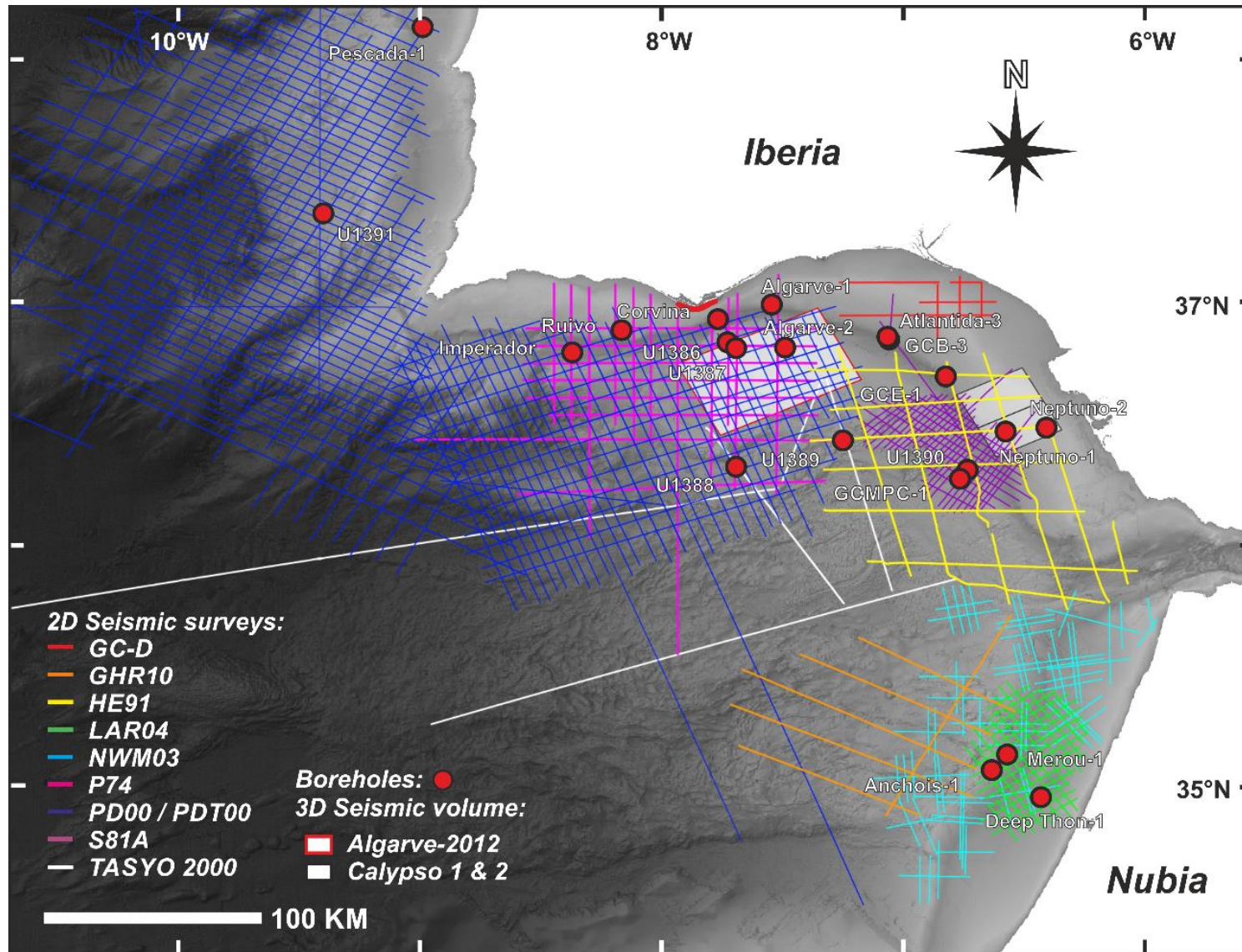
Figure 3-1 Compilation of dataset used in the project, including bathymetric, seismic, and drilling data.

3.1.4 Collaborative input

This research project is conducted in the framework of *The Drifters Research Group, Department of Earth Sciences, Royal Holloway University of London.* Collaborations with other research projects running in parallel within the group, were carried out, where results emerged from these projects has also been incorporated into the discussion of this topic, to provide a dynamic overview of the sedimentary evolution of the Gulf of Cádiz.

Internal collaborators include contemporaneous researches in or around the Gulf of Cádiz, such as the seismic analysis of the tectonostratigraphic & morphostructural controls on sedimentation, led by Débora F.P. Duarte; sedimentary and ichnological facies analysis of the Pliocene-Quaternary contourite depositional system, led respectively by Dr. Sandra de Castro Santos and Dr. Javier Dorador; and sedimentary facies analysis of the Late Miocene contourite depositional system of the Rifian Corridor, Morocco, led by Dr. Wouter de Weger.

External collaborators include Prof. Francisco. J. Sierro (*Universidad de Salamanca*) and Dr. Santiago Ledesma (*Naturgy S.A.*) which assisted with the chronological and seismostratigraphic correlation of the Gulf of Cádiz with the lower Guadalquivir basin, onshore Spain; M. Amine Manar (*ONHYM*), on the seismostratigraphic correlation of the Gulf of Cádiz with the Gharb and Saiss basins, onshore Morocco; Álvaro Arnáiz Giménez-Coral (*Repsol S.A.*), on the sedimentary evolution of the Deep Algarve basin; and the interdisciplinary collaboration with Prof. Mike Rogerson (*Northumbria University*) on the relationship of the sedimentary evolution of the Gulf of Cádiz with the physical oceanography of the Mediterranean-Atlantic gateway exchange.

3.2   Methods

The methods of this work are carried out mainly by seismic analysis. It includes the seismic interpretation of seismostratigraphy, as well as the seismic-to-well correlation to cross-check interpretations and to establish chronostratigraphy of the Neogene basins.

3.2.1 Seismic Analysis

Basin analysis on the continental slope of the Gulf of Cádiz is carried out on seismic data listed in section 3.1.2, using the Petrel E&P software platform by *Schlumberger N.V.*. Seismic interpretation is carried out to evaluate the sedimentary stacking pattern by seismic stratigraphic analysis to understand the sedimentary evolution, which is divided into two steps: a. the identification of seismic units and boundaries through reflection terminations; and b. the interpretation of seismic facies using reflection configurations, based on Mitchum et al., (1977). Specific methods are explained in the *Materials and Methods* section of chapters 4, 5 and 6.

With the identification of seismic units of the basins, the time structure (isobaths) and time thickness (isochron) maps were generated to reconstruct the regional paleogeography and to identify the distribution pattern of the seismic units, and for further analysis. Morphologies of contourite depositional systems such as erosional and depositional features observed on seismic are used as identification criteria for contouritic drifts and deposits (Faugères et al., 1999; Hernández-Molina et al., 2008), as mentioned in section 2.4.4, whereas geometric attributes, such as structures and thicknesses, and amplitude attributes, such as variance and Root Mean Square (RMS) amplitude extraction, can be used to identify sedimentary features (Jackson and Kane, 2011), such as the distribution of the channels as well as depocentres from the action of bottom currents. The interpreted seismic features were compared in terms of their acoustic character and distribution against other deposits of other deep-water sedimentary process, such as gravity flow deposits including turbidites and mass transport deposits, and pelagites or hemipelagites.

This method relies on the resolution of the seismic reflection data and their signal bandwidth, which dictates the minimum spatial or temporal separation between two reflection events for them to be distinguished and resolved separately. The vertical resolution is determined by the dominant wavelength, which is controlled by wave velocity and the dominant frequency. Using the Rayleigh criterion for Ricker wavelets, the vertical resolution limit can be expressed in terms of wavelength of the dominant frequency lambda as approximately $\lambda/4$. Whereas the lateral resolution is the Fresnel zone, which depends on the depth to the reflector, the velocity above the reflector and the dominant frequency. Both these resolutions can be increased through better acquisition and processing techniques, such as deconvolution and migration.

The multi-channel seismic surveys in the study area have an approximate dominant frequency of 30 Hz at the interval of interest. Assuming an average velocity of 2,000 m s^{-1} for the same interval, the average vertical and lateral resolutions are estimated to be 17 and 67 m respectively (Llave et al. 2011). Other high resolution seismic surveys with dominant frequency of 100-1000 Hz are also available, which gives an average vertical resolution of 0.5 - 5 m (Llave et al., 2007). Based on the average hemipelagic sedimentation rate of 5.2-17.5 cm ka^{-1} (Chapter 4) in the study area, each seismic reflection will represent stratigraphic interval of approximately 100-300 kyr. However, input of turbiditic and or contouritic sediments may significantly increase sedimentation rate and reduce the time range for each reflection.

3.2.2 Chronologic Correlation

Bio- and cyclo-stratigraphic data acquired from drilling data listed in 3.1.3 are utilised to construct the chronologic framework and to assign geologic ages based on the correlation through seismic to well ties. The chronology of the studied interval is also correlated to previous works in the study area, including Maldonado et al. (1999), Lopes et al. (2006), Llave et al. (2011), Roque et al. (2012), Hernández-Molina et al. (2016), Ramos et al. (2017) for the Gulf of Cádiz; Alves et al. (2003) and Rodrigues et al. (2020) for the southern West Iberian margin, Ledesma (2000) for the Guadalquivir basin, and Capella et al. (2017a) and de Weger et al. (2021) for the Gharb and Saiss basins.

In the Atlantic domain, the limited well penetration into the interval of interest available led to uncertainties regarding the determination of age constraints for stratigraphic model. The sedimentary description of each stratigraphic unit, on top of the bio- and cyclo-stratigraphic data, are also carried out in less detail for the Late Miocene interval compared to the Pliocene to Quaternary. The research also relied on chronological information available in previous works from the Mediterranean. The bio- and cyclo-stratigraphic, combined palaeomagnetic data allowed for the pre- and post-Messinian salinity crisis evaporite marginal succession onshore Mediterranean to be precisely constrained within an error of ~10 kyr, equivalent to a single precessional cycle (Krijgsman et al., 1999; Flecker et al., 2015). However, in the evaporitic stages, the lack of biostratigraphic markers and weak paleomagnetic signal led to an age determination based solely on the precessional cyclostratigraphy (Hilgen et al., 2007; Roveri et al., 2014). On top of that, the age constraints for the basinal succession are reliant on seismic interpretation with absence of well ties available for correlation (Flecker et al., 2015).

3.2.3 Quantitative Evaluation

Adaptation in the paleoceanographic regime between the Mediterranean and the Atlantic are a synchronous outcome to changes in sedimentary deposition in the Gulf of Cadiz during the Late Miocene. A simplistic representation of the past flow exchange introduced by previous works (Rogerson et al., 2012; Simon and Meijer, 2015) are used to test certain hypothesis with regards to the paleoceanography in agreement with the sedimentary and stratigraphic observations, which are inclusive of the variables related to the Mediterranean-Atlantic gateway exchange. They are:

$$\frac{Q_{MOW}}{Q_{inflow}} = 1 / \left(\frac{S_M}{S_A}\right) \tag{1}$$

$$Q_{AMW} = Q_{MOW} / \Phi \tag{2}$$

$$\Phi = 1 - \frac{B_{geo}^{1/3}}{U_{geo}} \tag{3}$$

$$B_{geo} = \frac{H_{MOW} \, U_{MOW} \, g'}{(1 + 2K_{geo} \, x / w_{MOW})} \tag{4}$$

$$U_{geo} = g' \alpha / f \tag{5}$$

$$g' = \frac{\rho_{AMW} - \rho_{ATL}}{\rho_{AMW}} \tag{6}$$

where, equation 1 represents the relationship between fluxes and salinities, where the ratio of Q_{MOW} to Q_{inflow} (Sv, fluxes of Mediterranean outflow and Atlantic inflow) are inversely affected by proportions of S_M against S_A (PSU, salinities of the Mediterranean and Atlantic water); equation 2 represents the relationship between Q_{AMW} and Q_{MOW} (Sv, fluxes of Atlantic Mediterranean Water and Mediterranean Outflow), controlled by Φ (mixing coefficient of AMW and MOW); equation 3 represents the mixing coefficient of AMW and MOW (Φ), which is determined by the inverse sigmoidal relationship from the ratio of B_{geo} and U_{geo} (m s-1, geostrophic buoyancy flux and velocity); equation 4 represents the geostrophic buoyancy flux (Bgeo), measured by H_{MOW} (m) , U_{MOW} (m s-1), w_{MOW} (m) and g' (height, velocity, and width of MOW at the gateway, and the density anomaly of the plume within the ambient water) against K_{geo}, (geostrophic Ekman number, assumed 0.2 m s-1) and x (m, the distance downslope from which mixing or entrainment occurs, assumed 100,000 m); equation 5 represents the Ugeo is measured by g', α (the slope the water is moving over) and f (acceleration due to Coriolis force, assumed 0.000084 m s-2); and equation 6 represents the density anomaly (g'), determined from ρ_{AMW} and ρ_{ATL} (kg m-3, densities of AMW and ambient Atlantic water).

Chapter 4

Latest Miocene restriction of the Mediterranean Outflow Water: a perspective from the Gulf of Cádiz

*Zhi Lin Ng, F. Javier Hernández-Molina, Débora Duarte, Francisco J. Sierro, Santiago Ledesma, Michael Rogerson, Estefanía Llave, Cristina Roque, M. Amine Manar. 2021. Latest Miocene restriction of the Mediterranean Outflow Water: a perspective from the Gulf of Cádiz. Geo-Marine Letters **41**, 23. doi:10.1007/s00367-021-00693-9*

ORIGINAL

Check for
updates

Latest Miocene restriction of the Mediterranean Outflow Water: a perspective from the Gulf of Cádiz

Latest Miocene restriction of the Mediterranean Outflow Water: A perspective from the Gulf of Cádiz

Zhi Lin Ng[1*], F. Javier Hernández-Molina[1], Débora Duarte[1, 2], Francisco J. Sierro[3], Santiago Ledesma[4], Michael Rogerson[5], Estefanía Llave[6], Cristina Roque[7, 8], M. Amine Manar[9]

[1]Dept. Earth Sciences, Royal Holloway Univ. London, Egham TW20 0EX, UK
[2]Instituto Português do Mar e da Atmosfera (IPMA), 1749-077 Lisboa, Portugal
[3]Dpto. de Geología, Univ. de Salamanca, 37008 Salamanca, Spain
[4]Naturgy Energy Group S.A., 28033 Madrid, Spain
[5]Dept. Geography and Environmental Sciences, Northumbria Univ., Newcastle upon Tyne, NE1 8ST, UK
[6]Instituto Geológico y Minero de España (IGME), 28003 Madrid, Spain
[7]Estrutura de Missão para a Extensão da Plataforma Continental (EMEPC), 2770-047 Paço de Arcos, Portugal
[8]Instituto Dom Luiz (IDL), 1749-016 Lisboa, Portugal
[9]Office National des Hydrocarbures et des Mines (ONHYM), BP 99 Rabat, Morocco
Corresponding author: Zhi Lin Ng (Zhi.Ng.2016@live.rhul.ac.uk)

Abstract

The Mediterranean-Atlantic water-mass exchange provides the ideal setting for deciphering the role of gateway evolution in ocean circulation. However, the dynamics of Mediterranean Outflow Water (MOW) during closure of the Late Miocene Mediterranean-Atlantic gateways are poorly understood. Here, we define the sedimentary evolution of Neogene basins from the Gulf of Cádiz to the West Iberian margin to investigate MOW circulation during the latest Miocene. Seismic interpretation highlights a middle to upper Messinian seismic unit of transparent facies, whose base predates the onset of the Messinian salinity crisis (MSC). Its facies and distribution imply a predominantly hemipelagic environment along the Atlantic margins, suggesting an absence or intermittence of MOW preceding evaporite precipitation in the Mediterranean, simultaneous to progressive gateway restriction. The removal of MOW from the Mediterranean-Atlantic water-mass exchange reorganised the Atlantic water-masses and is correlated to severe weakening of the Atlantic Meridional Overturning Circulation (AMOC) and a period of further cooling in the North Atlantic during the latest Miocene.

Introduction

Gateway evolution plays a significant role in the reorganisation of global ocean circulation (Berggren, 1982; Knutz, 2008; Straume et al. 2020). The Mediterranean-Atlantic water-mass exchange provides the ideal setting for such research. At present, the Mediterranean-Atlantic exchange is characterized by an anti-estuarine circulation (Wüst, 1961) involving a surficial Atlantic inflow and a deeper outflow, known as the Mediterranean Outflow Water (MOW), through the Strait of Gibraltar (Sánchez-Leal et al., 2017). The MOW is predominantly sourced from the intermediate water-mass of the Mediterranean, known as the Levantine Intermediate Water (LIW) (Millot et al., 2006). Upon exiting the Strait of Gibraltar, the dense MOW cascades onto the Gulf of Cádiz continental slope, entraining or mixing with Atlantic ambient water to form the Atlantic Mediterranean Water (AMW) (Rogerson et al., 2012b). The entrained ambient water is mainly sourced from the Azores Current, which originates at the Azores Front, the boundary between the European and African surface water-masses (Rogerson et al., 2004). The resulting AMW water-mass settles along the middle continental slope (~1000–1500 m) and flows northwards above the North Atlantic Deep Water (NADW) (O'Neill-Baringer and Price, 1997; Hernandez-Molina et al., 2016). MOW input into the Atlantic has a significant impact on the formation of the NADW and on the thermohaline circulation (Pérez-Asensio et al., 2012), known as the Atlantic Meridional Overturning Circulation (AMOC). Removal or interruption of MOW would significantly impact the AMOC by ~15% and reduce sea surface temperatures by up to 1°C (Rogerson et al., 2012b). The AMOC plays a vital role in the earth's climate through the northward transport of heat and CO_2, which bears an impact on the Arctic Sea ice volume (Liu et al., 2020) and the ocean-terrestrial carbon cycle (Zickfeld et al., 2008).

The Mediterranean-Atlantic exchange was also active through the Late Miocene gateways (Fig. 4-1; ~11.6 – 6.9 Ma; Krijgsman et al., 2018), which include the Betic and Riffian corridors currently exposed onshore southern Spain and northern Morocco, respectively (Capella et al., 2017), and possibly the Strait of Gibraltar (Krijgsman et al., 2018). It is thought to have ceased or become reduced during the latest Miocene, causing isolation of the Mediterranean Sea from the Atlantic Ocean, hence the Messinian salinity crisis (MSC; 5.97–5.33 Ma; Krijgsman et al., 1999; Manzi et al., 2018). However, since formulating the MSC concept, Selli (1960) also argued for the early Messinian (~7.25 Ma) as the actual beginning of the MSC; it is marked by dystrophic faunal

elements in the Mediterranean as the earliest indication of an ongoing restriction of the exchange. Yet restriction of MOW from the Mediterranean-Atlantic water-mass exchange is one of the prerequisites for hypersaline conditions to deposit MSC evaporites (Flecker et al., 2015). In the Mediterranean, an inferred base-level fall and erosion of its margins during the MSC acme, and subsequent refilling by an open marine connection with the Atlantic, respectively resulted in a regional Messinian erosional surface (MES; 5.61 Ma), and a sharp lithological and paleontological change across the Miocene-Pliocene boundary (5.33 Ma) (Roveri et al., 2014). In turn, the onset of the MSC (5.97 Ma) shows no correlation to glacio-eustatic change and was thought to be controlled dominantly by tectonics (Flecker and Ellam, 2006; Hodell et al., 2001; Krijgsman et al., 2004).

In the Atlantic domain, open marine conditions have prevailed throughout the Miocene to the present (Flecker et al., 2015). Locally, the continental margins surrounding the Gulf of Cádiz were affected by gravitational processes due to rapid regional uplift and tectonic instability after the Middle to Late Miocene Betic-Rif Orogeny (Duggen et al., 2003). The Betif-Rif Orogery, due to convergence between Africa and Eurasia, transformed a wider Middle Miocene gateway (~15 Ma) into several Late Miocene narrow and shallow corridors (~8 Ma) affecting MOW distribution, namely: the North Betic Strait, Guadix Basin, Zagra Strait, Guadalhorce Strait, and the North and South Riffian Corridors. (Fig. 4-1; Capella et al., 2019; Krijgsman et al., 2018). The continuous constriction and closure of these corridors and the reduction of the water-mass exchange are collectively known as the Mediterranean-Atlantic gateway restriction (Krijgsman et al., 2018; Pérez-Asensio et al., 2012). The distribution of contourite depositional systems within these corridors serves as evidence of bottom current influence from the MOW as it exits the Mediterranean (de Weger et al., 2020; Martín et al., 2009). The increase in bottom-current velocities as a consequence of the ongoing restriction of the corridors, and the initiation of an overflow setting for the MOW across the Mediterranean-Atlantic water-mass exchange, resulted in the deposition of sandy contourites in the Betic and Riffian Corridors during the late Tortonian to early Messinian (7.8 – 7.25 Ma; Capella et al., 2017; de Weger et al., 2020; Martín et al., 2009), but has yet to be described for the Gulf of Cádiz. During this period, the Gulf of Cádiz would have represented the downstream continuation of the Betic and Riffian Corridors for MOW circulation after exiting the Mediterranean. Relocation of the contourite depositional system to the Gulf of Cádiz, within the Deep Algarve, Doñana, Sanlúcar and Cádiz basins (Fig. 4-1), occurred from

Pliocene to the present (5.33 Ma onwards), with the MOW flowing through the Strait of Gibraltar (Hernández-Molina et al., 2014; 2016). However, the Strait of Gibraltar might have opened earlier in the early Messinian (Krijgsman et al., 2018). Meanwhile, the Guadalquivir and Onshore Gharb basins (Fig. 4-1), located at the western end of the Betic and Riffian corridors, became marine embayments after the closure of these corridors (Capella et al., 2017; Pérez-Asensio et al., 2012). Despite extensive outcrop studies carried out onshore, the timing of final closure of the gateways remains unknown, due to erosional hiatuses in the sedimentary record (Capella et al., 2017; Hüsing et al., 2010). Some outcrop studies suggest that the closure of the gateways occurred well before the onset of the MSC (Kouwenhoven et al., 1999; Martin et al., 2002), whereas modelling studies suggest that a narrow (~1 km) and shallow (~10m) connection is sufficient to supply the salt for the MSC evaporites (Meijer and Krijgsman, 2005).
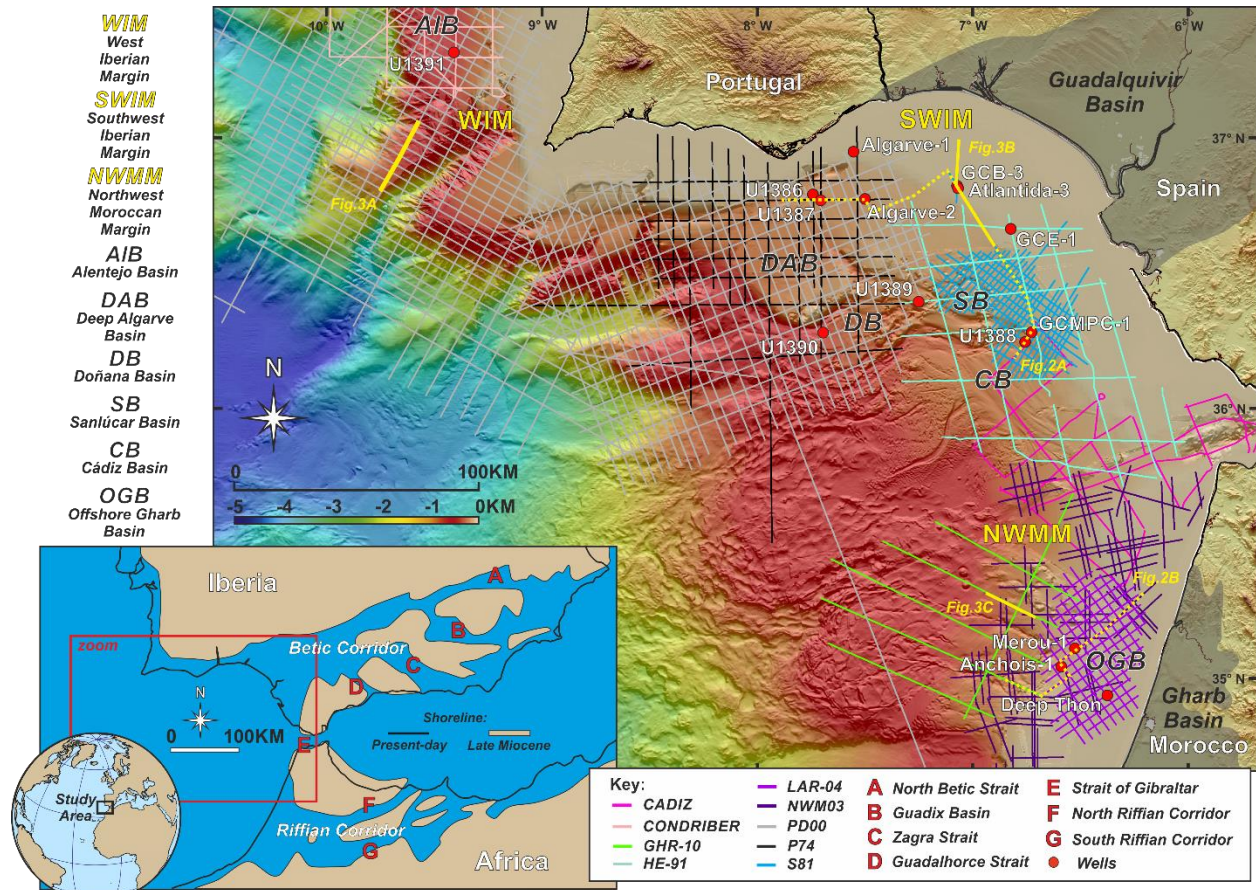
Figure 4-1   Data set including post-stack, time-migrated multichannel two-dimensional (2-D) seismic reflection surveys from ONHYM, Repsol S.A., and TGS-Nopec; borehole data from exploration wells and IODP Expedition 339 scientific sites. Coordinate system: WGS 84 UTM 29N. (Inset) Geographic location of the Gulf of Cádiz and the Late Miocene and present-day gateways.

Figure 4-2 Seismostratigraphy and regional distribution of the middle-upper Messinian unit in (a) Southwest Iberian (SWIM) and (b) Northwest Moroccan margins regional profile (uninterpreted seismic profile in Fig. 4-S2 - supplementary material) with borehole correlations to U1387 (van der Schee et al., 2016), Algarve-2 (Hernández-Molina et al., 2016), Atlantida-3 and GCB-3 (Ledesma, 2000), and GCMPC-1 (Hernández-Molina et al., 2014) (Table 4-S1 in *supplementary material*).

Here, we define the middle to late Messinian sedimentary evolution and its relationship with its upper and lower bounding stratigraphic units in the Neogene basins (Offshore Gharb, Deep Algarve, Doñana, Sanlúcar, Cádiz and Alentejo basins), located on the upper to middle continental slope of the Northwest Moroccan (NWMM), the Southwest Iberian (SWIM), and the southern part of the West Iberian (WIM) margins (Fig. 4-1) using seismic stratigraphic analysis, correlated to chronology and lithology from borehole data (Fig. 4-2). We compared the distribution of the middle to upper Messinian succession with the Guadalquivir and Onshore Gharb basins (Fig. 4-1), based on the literature, to evaluate its significance for the Mediterranean-Atlantic water-mass exchange and its implications for sedimentary and paleoceanographic processes in the Atlantic. For the first time, we investigated the paleoceanographic scenarios for the Late Miocene Mediterranean-Atlantic water-mass exchange through a hypothetico-deductive method, using a simple quantitative representation of the system together with seismostratigraphic evidence and observation.

Materials and Methods

Seismic analysis and borehole correlation

We compiled a regional database of seismic reflection and borehole data in the Gulf of Cádiz to the southern part of the West Iberian Margin (Fig. 4-1). We carried out seismic interpretation of the database, which entailed the identification of seismic facies and boundaries, focusing on the middle to late Messinian unit. We utilized the nomenclature for seismic facies description and interpretation of Prather et al. (1998) based analogously on an intraslope basin setting in the Gulf of Mexico, which characterized three primary seismic facies categories (chaotic, convergent, and draping). The seismic stratigraphy was correlated to borehole data (Fig. 4-2) consisting of lithological and chronological information (Table 4-S1). They include five wells available from the literature: Algarve-2 (Hernández-Molina et al., 2016), Atlantida-3 and Golfo de Cádiz B-3 (GCB-3; Ledesma, 2000), Golfo de Cádiz Mar Profundo C-1 (GCMPC-1; Hernández-Molina et al., 2014), and U1387 (van der Schee et al., 2016); three additional wells: Anchois-1, Deep Thon-1, and Merou-1, were acquired from an internal report for petroleum exploration by Repsol S.A.,

titled *"Tanger-Larache Sedimentological study"* (hereinafter referred to as Repsol S.A., 2013). The chronological information is based on bio- and cyclo-stratigraphic dating acquired from boreholes with top-only penetration of the middle to late Messinian unit in U1387 (van der Schee et al., 2016) and Algarve-2 (Hernández-Molina et al., 2016), while its base is reached in Atlantida-3 and GCB- 3 (Ledesma, 2000), GCMPC-1 (Hernández-Molina et al., 2014), Anchois-1, Deep Thon-1 and Merou-1 (Repsol S.A., 2013) (Table 4-S1).

Quantitative exploration of past flow conditions

We adopted simple quantitative representations below to test three possible scenarios through a hypothetico-deductive method, based on the climatic, paleogeographic and paleoceanographic conditions during the middle to late Messinian, where a two-way water-mass exchange between the Atlantic and the Mediterranean could be active. These experiments directly test hypotheses drawn from seismic and borehole analysis, which is limited to determining the presence or absence of flow on the slope, and the bottom velocity thresholds required for muddy and sandy bedform deposition. Key to the latter is the threshold at which sandy contourite deposition commences, as we expect deposits of this nature to be resolved in seismic data as packages with variable impedance. Field and experimental works (e.g., Culp et al., 2020; McCave et al., 2017; McCave and Hall, 2006) indicate that winnowing of muddy marine sediments and construction of muddy bedforms occur at flow velocities higher than 0.15 m s^{-1}, while winnowing, reworking and accumulation of sandy marine sediments occur at flow velocities higher than 0.2 m s^{-1}. Consequently, the maximum MOW or AMW plume velocity on the Gulf of Cádiz upper to middle slope for the middle to late Messinian, where no contourite deposition is observed within the seismic resolution of our dataset, would be 0.2 m s^{-1}, while the physical oceanography of the exchange must be consistent with generating flow no faster than this value. We also investigated a MOW or AMW plume velocity of 0.15 m s^{-1} for the threshold of silt-rich muddy contourite formation by bottom currents. Three scenarios allowing for a continuing MOW are explored here:

- Scenario A: The flux of exchange (and thus the size of the plume) was so small that the area impacted on the slope could not be resolved by the seismic analysis;

- Scenario B: The flow was slower during the middle to late Messinian than it was during the late Tortonian to early Messinian, where contourite deposition can be observed; and

- Scenario C: The seismic analysis does not cover the region over which the MOW or AMW was flowing during the middle to late Messinian.

Following previous intensive research into these relationships (Rogerson et al., 2012a; Simon and Meijer, 2015), we used *equations 1 – 6* to represent the system,

$$\frac{Q_{\text{MOW}}}{Q_{\text{inflow}}} = 1 \left/ \left(\frac{S_{\text{M}}}{S_{\text{A}}}\right) \right. \tag{1}$$

$$Q_{\text{AMW}} = Q_{\text{MOW}} / \Phi \tag{2}$$

$$\Phi = 1 - \frac{B_{\text{geo}}^{1/3}}{U_{\text{geo}}} \tag{3}$$

$$B_{\text{geo}} = \frac{H_{\text{MOW}} \, U_{\text{MOW}} \, \text{g}'}{(1 + 2K_{\text{geo}} \, \text{x} \, / \, w_{\text{MOW}})} \tag{4}$$

$$U_{\text{geo}} = \text{g}' \alpha / f \tag{5}$$

$$\text{g}' = \frac{\rho_{\text{AMW}} - \rho_{\text{ATL}}}{\rho_{\text{AMW}}} \tag{6}$$

where Q_{inflow}, Q_{AMW} and Q_{MOW} (Sv) are respectively the fluxes of Atlantic inflow, AMW, and MOW; S_{M} and S_{A} (PSU) are the salinities of the Mediterranean and Atlantic water, respectively; Φ is the mixing coefficient of AMW and MOW; B_{geo} and U_{geo} (m s^{-1}) are geostrophic buoyancy flux and velocity, where B_{geo} is measured by H_{MOW} (m), U_{MOW} (m s^{-1}) and w_{MOW} (m), which are the height, velocity and width of pure MOW at the gateway, K_{geo} (m s^{-1}), which is the geostrophic Ekman number (assumed 0.2), and x (m), which is the distance downslope from which mixing or entrainment occurs (assumed 100,000 m,; while U_{geo} is measured by g'$_{\text{,}}$ which is the density anomaly of the plume within the ambient water, α, which is the slope the water is moving over, and f, which is the acceleration due

to Coriolis force (assumed 0.000084 m s^{-2}); g' is determined from ρ_{AMW} and ρ_{ATL} (kg m^{-3}), which are respectively the densities of AMW and ambient Atlantic water (Rogerson et al., 2012b).

Today, the velocity of water (U$_{geo}$) interacting with bedform-dominated sediment surfaces varies between 1.4 m s^{-1} for regions with sandy contourites or abrasion surfaces to 0.3-0.5 m s^{-1} for muddy contourites (O'Neill-Baringer and Price, 1999). The higher velocities in proximal parts of the system reflect the presence of an unmixed core of MOW water which is yet to frictionally entrain ambient Atlantic water, and thus relates directly to the modern salinity difference of Mediterranean and Atlantic water of ~2 PSU (Rogerson et al., 2012b). The lower velocities in the distal part of the system reflect water almost completely mixed to produce AMW (Atlantic Mediterranean Water) composition, and thus relates to the density of the plume of water that lies at neutral density in the Atlantic.

Results

Seismic Analysis

Seismic interpretation of the Gulf of Cádiz continental slope shows three main sedimentary intervals above a basin-wide erosional unconformity known as the Basal Foredeep unconformity (BFU; ~8.2 Ma, *sensu* Maldonado et al., 1999). The BFU is juxtaposed against a thick chaotic body pinching out northwards, known as the Allochthonous Unit of the Gulf of Cádiz (AUGC; Fig. 4-2; *sensu* Medialdea et al., 2004). Above the BFU, an upper Tortonian-lower Messinian (~8.2 – ~6.4 Ma) succession consisting of high-amplitude convergent-by-baselap facies (Fig. 4-3b) is observed along the Southwest Iberian margin. In the Northwest Moroccan margin and the southern part of the West Iberian margin, the upper-Tortonian-lower Messinian succession consists of cyclical alternations of low-to-high-amplitude reflections in sheeted or mounded geometries adjacent to basin margins (Fig. 4-3, a and c). The top of the upper Tortonian-lower Messinian succession is bounded by, or locally truncated against, an unconformity.

Figure 4-3 Seismic profiles indicating the distribution of the middle-upper Messinian unit across southern West Iberian margin (WIM): (a) PD00-608; (b) Southwest Iberian margin (SWIM): S81-N27 and S81-N25; and (c) Northwest Moroccan margin (NWMM): GHR10-6. Uninterpreted seismic profiles in Fig. 4-S3 (*supplementary material*).
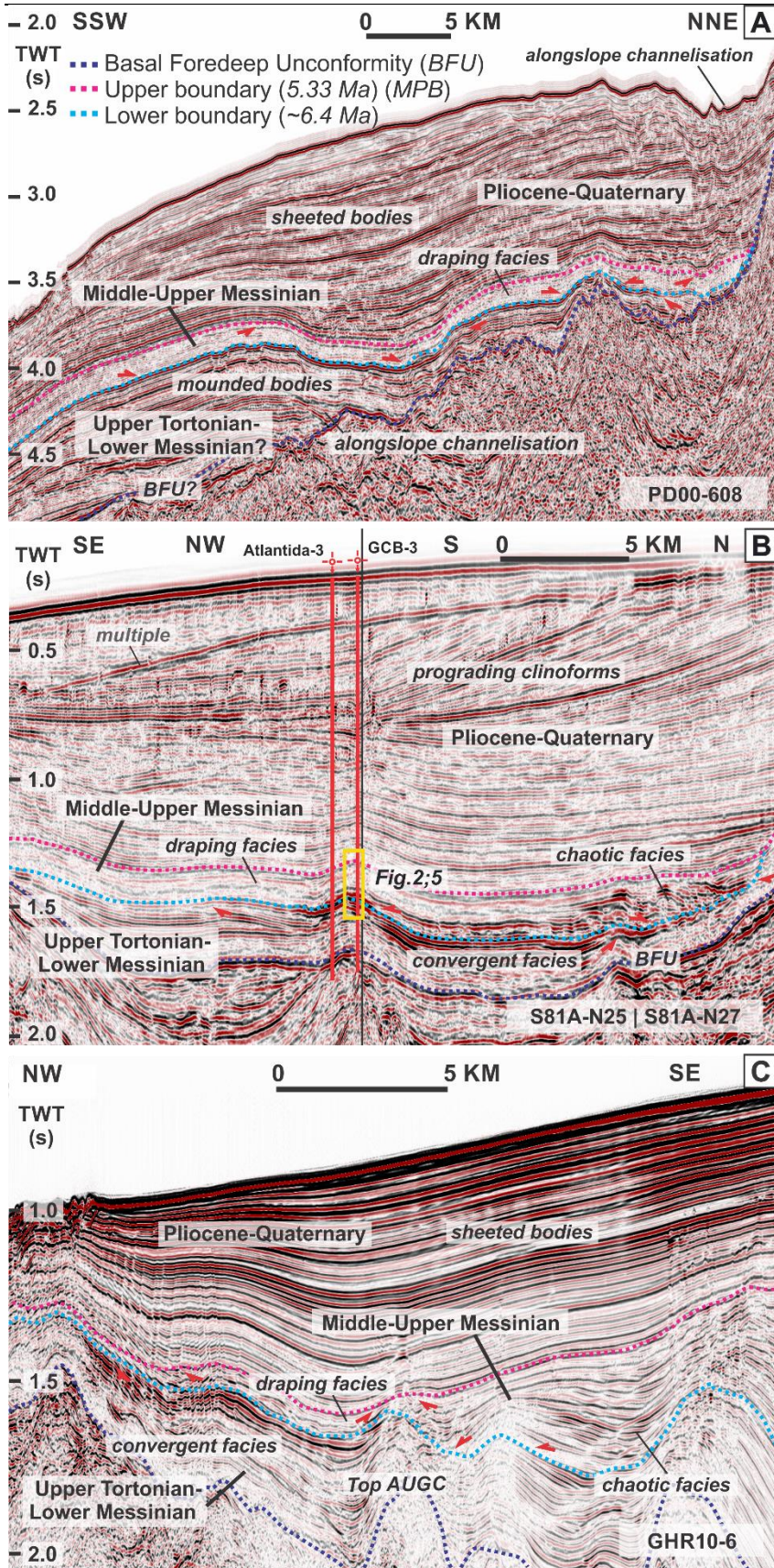
Overlying the upper Tortonian-lower Messinian succession is a middle-upper Messinian seismic unit of transparent seismic facies or with seismic reflections of very low amplitude, locally underlain by high-amplitude reflections (Fig. 4-2 and 4-3). It has a relatively homogenous reflection configuration, in sheeted or draped geometries. The base is erosional at basin margins with locally high-amplitude chaotic facies (Fig. 4-3b) with a "gull-wing" geometry (*sensu* Wynn et al., 2007) and onlap to downlap terminations (Fig. 4-43c). The basal boundary could also be conformable on older successions in the basin centers (Fig. -2b). Within the Offshore Gharb basin, the transparent reflections are interrupted by intervals of high amplitude convergent-by-thinning facies in the basin centre and high amplitude chaotic facies at the basin margin (Fig. 4-2b and 4-3c), whereas away from the basin this unit can be observed as draping facies at the margins (Fig. 4-3c). Across the upper to middle slope of the Gulf of Cádiz, the tabular distribution of the middle to upper Messinian unit is also punctuated by structural highs (Fig. 4-2a) and areas of erosion (Fig. 4-4), or depocenters with the presence of high amplitude chaotic or convergent facies, most prominently the eastern section of the Deep Algarve basin and the Offshore Gharb basin (Fig. 4-2b and 4-3a).

The top boundary of the middle-upper Messinian seismic unit is generally conformable with a change from transparent to relatively continuous seismic facies (Fig. 4-2b and 4-3b), or locally unconformable as truncation surfaces against younger successions (Fig. 4-3a), represented by the Miocene-Pliocene boundary (MPB; 5.33 Ma; *sensu* Hernandez-Molina et al., 2016). The Pliocene-Quaternary (5.33 Ma – present) succession above consists of lowermost Pliocene low- to moderate-amplitude parallel continuous facies in the basin centres, or lower Pliocene high-amplitude chaotic facies on the basin margins truncating the lowermost Pliocene units. They are overlain by upper Pliocene-Quaternary cyclical alternation of low- to high- amplitude sequences in sheeted to mounded geometries associated with alongslope channels (Fig. 4-3, a and c), or prograding clinoforms in the north- and southeast originating from lower Guadalquivir and Onshore Gharb basins, respectively (Fig. 4-3b).

The contrast in seismic facies between the middle-upper Messinian unit with the upper Tortonian-lower Messinian and Pliocene-Quaternary succession below and above,

respectively, provides a distinctive signature for regional stratigraphic correlation across the Gulf of Cádiz towards the southern part of the West Iberian margin (Fig. 4-2 and 4-3) and can be considered as a regional marker horizon or stratigraphic unit. The middle to upper Messinian unit has an average thickness of 100 ms TWT (with a range of 50-150 ms TWT), distributed uniformly across the upper to middle continental slope, as shown by the time thickness map of the middle to late Messinian unit (Fig. 4-4). An exception is observed for the Offshore Gharb basin in the Northwest Moroccan margin, with distribution of the middle to upper Messinian unit reaching up to 1200 ms TWT in thickness (Fig. 4-2b and 4-4). Likewise, a thicker distribution for the upper Tortonian-lower Messinian succession is observed for the Northwest Moroccan margin and the southern part of the West Iberian margin (500-1000 ms TWT), in contrast to the Southwest Iberian Margin (250-500 ms TWT).
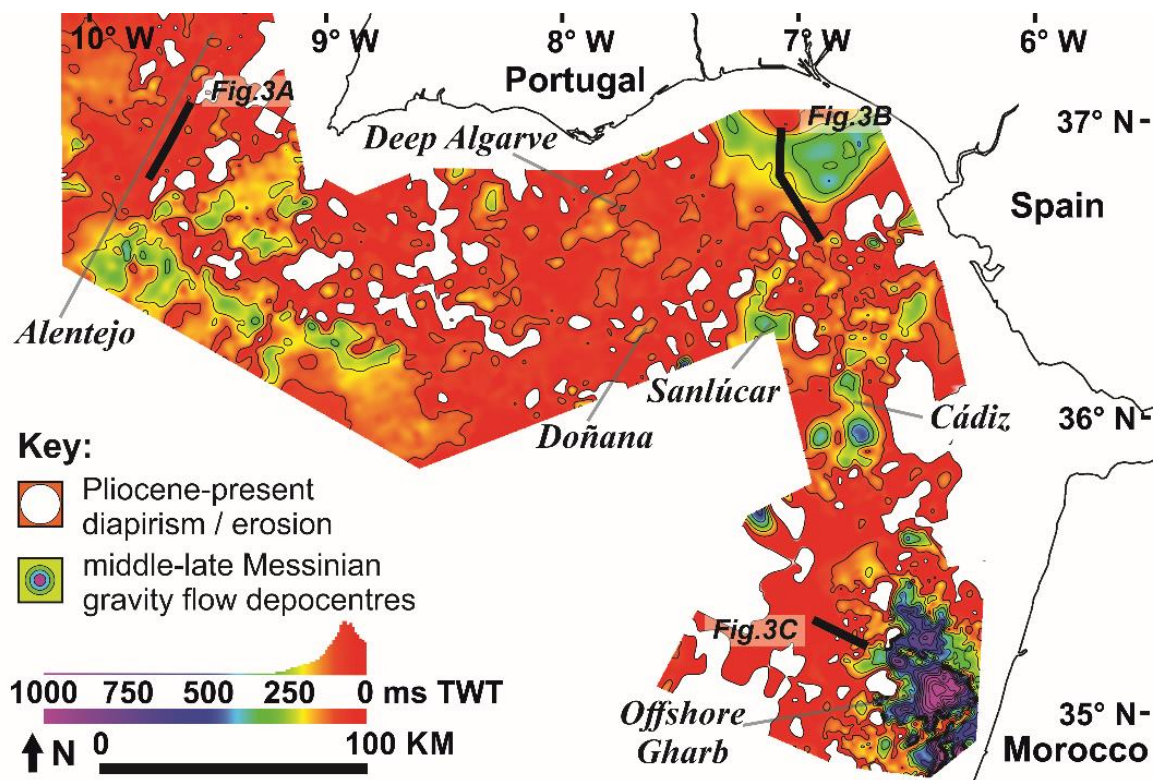
Figure 4-4   Time thickness (TWT) map of the middle-upper Messinian unit across Northwest Moroccan (NWMM), Southwest Iberian (SWIM), and southern West Iberian (WIM) margins (Contour interval: 100 ms TWT).

Borehole Correlation

Correlation of the middle to upper Messinian unit to borehole data indicates fossiliferous marls to clays with distinct bioturbation, containing few lithic coarser particles (Hernandez-Molina et al., 2014; van der Schee et al., 2016), with a mean interval velocity (V_{int}) of ~2290–2570 m s^{-1} based on check-shot data from Algarve-2 and GCMPC-1. In the Offshore Gharb basin, this interval is recorded in Anchois-1, Deep Thon-1 and Merou-1 as very shaly or dirty unconsolidated sands with intercalations of clays (Repsol S.A., 2013). Bio- and cyclo-stratigraphic dating (Fig. 4-2 and 4-5; Table 4-S1) show deposition of the unit spanning an interval of ~1.1 Ma (>6.37–5.33 Ma), with the base predating the First Occurrence (FO) *Globorotalia margaritae,* Last Regular Occurrence (LaO) or Last abundant Occurrence (LaO) *Globorotalia miotumida* events dated 6.31 to 6.35 Ma, and the sinistral to dextral coiling change of the *Neogloboquadrina acostaensis* event dated 6.37 Ma (Krijgsman et al., 2004).

Quantitative Constraint on Changes in the Oceanographic System

Assuming an absence of contourite deposition within the seismic resolution of our dataset, the critical requirement for a continuing MOW in the Gulf of Cádiz is the flow velocity threshold of 0.2 m s-1 for the onset of winnowing and accumulation of sands (McCave and Hall, 2006). Additionally, the 0.15 m s-1 threshold where winnowing and silty bedform construction begins (Culp et al., 2020; McCave et al., 2017) is considered. Three scenarios would permit MOW to continue across the Mediterranean-Atlantic water-mass exchange but be invisible under the resolution of our seismic analysis: A) a very small plume (due to considerably reduced flux), B) a plume flowing very slowly, and C) the plume has moved out of the analyzed area. All three possibilities are investigated. Unless one of these scenarios is capable of producing the sedimentary features observed above, the exchange must have been different from that found today.

Two critical constraints on the system are revealed by *equations 1-6* (presented in *Material and Methods*), which reflect two inverse relationships: firstly, between flux and salinity, and secondly between salinity and ambient water entrainment. During the

salinification of the Mediterranean, small fluxes of the Mediterranean-Atlantic water-mass exchange at the sill correlate to high salinity in the outflowing Mediterranean water (via *equation 1)*. This relationship is explored in detail in Simon and Meijer (2015), and we adopt their conclusions here. Accordingly, a high salinity or density in the outflowing Mediterranean water would result in a high velocity MOW (via *equations 5 and 6)*, an intense frictional mixing with ambient water as it passes over the sill of the Mediterranean-Atlantic gateways (via *equation 3*) and hence a vigorous formation of AMW (Rogerson et al., 2012b). Consequently, as the flux of MOW (Q_{MOW}) falls, its mixing or entrainment behaviour (Φ) also changes (via *equation 2*). Where Q_{MOW} is below modern values (~0.68 Sv), these influences balance, providing the counter-intuitive result that the flux of AMW (Q_{AMW}) is almost invariable. The behaviour is best illustrated via the relationship between Φ (Phi) and velocity (see Fig. 4-S1 *in supplementary material*). Consequently, a very small flux of very saline water would, under a first approximation, generate a geostrophic current similar to today, and hence a contourite depositional system in the Gulf of Cádiz.

This inverse and non-linear relationship between MOW salinity and entrainment of ambient Atlantic water complicates the relationship of the Mediterranean-Atlantic water-mass exchange at the sill, and the expected response in both the Gulf of Cadiz and the Mediterranean to changes in other oceanographic conditions. Under freshening scenarios, a reduced salinity or density, and hence velocity (via *equations 5 and 6*), for the MOW flowing into the Atlantic would suppress entrainment (via *equation 3*), resulting in an almost unchanged AMW compared to pure MOW post-mixing. This control essentially acts as negative feedback to changes in the system, which maintains the physical size of the flux. Consequently, a slower outflow would reflect a less-dense water-mass in the Mediterranean. Overall, the resulting dynamics between the physical properties of the Mediterranean-Atlantic water-mass exchange described above are significant for constraining scenarios to discuss the possibility of a continuing outflow across the Mediterranean-Atlantic gateways, complementary to our observations in the seismic and sedimentary interpretation presented in this study.

Discussion

Stratigraphic and Sedimentary Interpretation

The middle to upper Messinian unit (~6.4 – 5.33 Ma) is equivalent to the previously described lower section of Marismas Sequence in Riaza and Martínez del Olmo (1996), Unit M3 in Maldonado et al. (1999), Unit MW3' in Roque (2007), Subunit U1B in Rodrigues (2017), and Subunit E2 in Lopes et al. (2006). Similar successions are found in the subsurface of the onshore Guadalquivir basin as Gibraleón clays (Sierro et al., 1996) or Unit C in Ledesma (2000), and in the Onshore Gharb basin (Capella et al., 2017) when they were marine embayments following gateway closures (Martín et al., 2009; Ivanovic et al., 2013). These previous works interpreted similar seismic and sedimentary characteristics for the middle to upper Messinian unit (e.g., transparent zones and thick clay deposits) and confirm its stratigraphic position in the margin.

The seismic and sedimentary facies, and the widespread uniform and tabular distribution of the middle to upper Messinian unit across the continental margins (Fig. 4-2 and 4-3), imply dominant deposition of hemipelagic settling in the absence of alongslope transport. A higher estimated rate of accumulation (5.2-17.5 cm ka^{-1}) compared to the average hemipelagic sedimentation rate (2 cm ka-1, McCave and Hall, 2006) could be due to higher influx of allochthonous terrigenous material on the continental slopes (Henrich and Hüneke, 2011). Higher sedimentation rates within the intraslope basins, such as the eastern Deep Algarve (Fig. 4-3b) and Offshore Gharb (Fig. 4-2b and 4-3c) basins, are due to interruption in the background sedimentation by interbedded deposition of deep-water turbidite channel-levees and lobes or debrites by gravity flow originating from the adjacent margins, or from the Guadalquivir and Onshore Gharb basins, respectively (Ledesma, 2000). This is indicated by the interpretation of adjoining development of local intervals of high-amplitude chaotic to channel facies on the basin margin and high-amplitude convergent facies locally within the basin centres, as opposed to the transparent draping facies observed regionally across the margin. In the Offshore Gharb basin, the middle-upper Messinian unit consists of a distal turbidite depositional environment of deep-water

channels or lobes interbedded with hemipelagic drapes, as interpreted in the Anchois-1, Deep Thon-1, and Merou-1 wells (Repsol S.A., 2013).
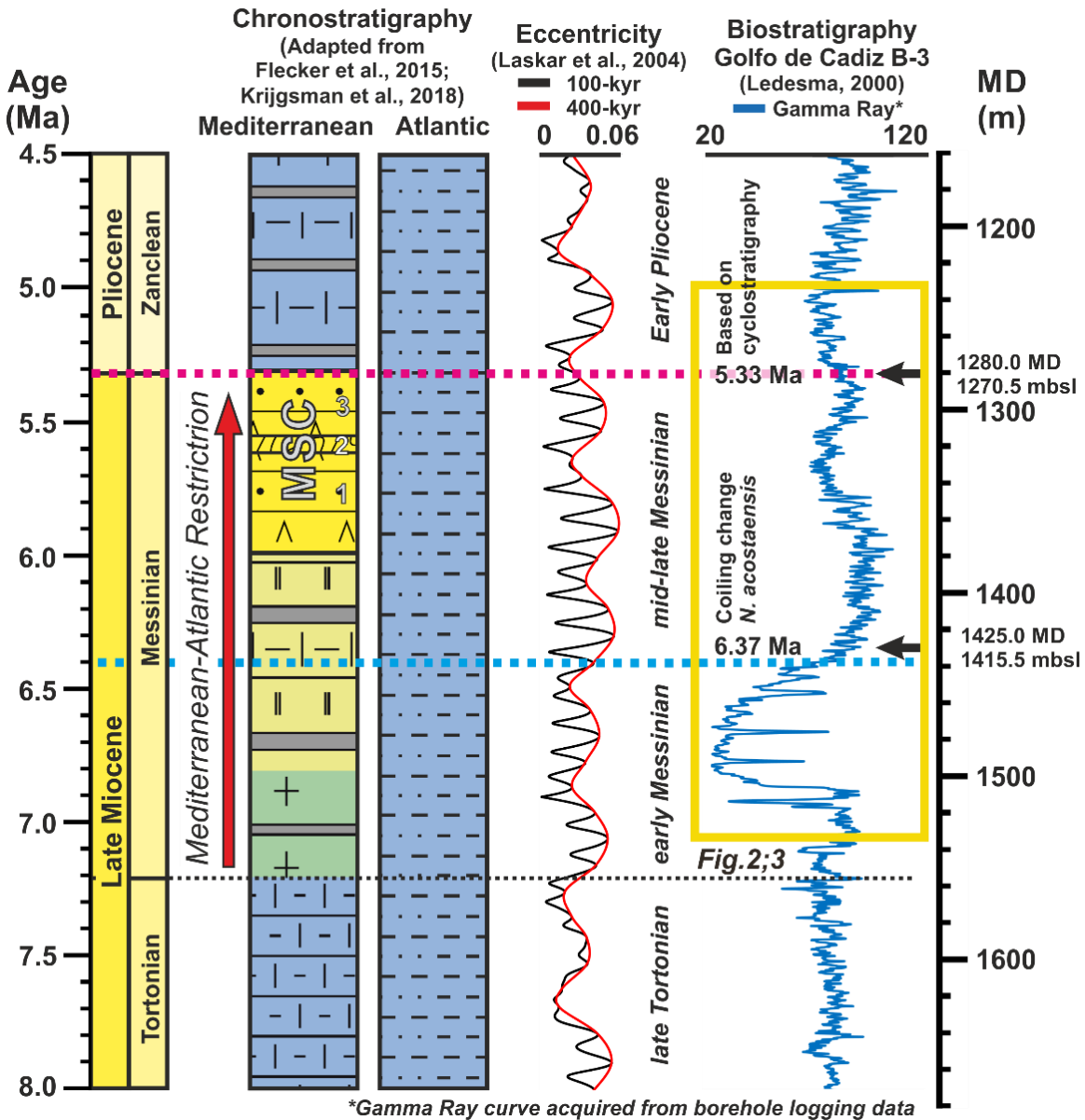
Figure 4-5   Chronology of middle-upper Messinian unit (right) and correlation with Mediterranean and Atlantic chronostratigraphy (Flecker et al., 2015; Krijgsman et al., 2018), 100 kyr and filtered 400 kyr eccentricity curves based on orbital solution La04 (Laskar et al., 2004), gamma ray logging in measured depth (MD) with biostratigraphy of well GCB-3 (Ledesma, 2000) in MD and meters below sea level (mbsl).

Underlying the middle to upper Messinian unit, contourite deposits are distributed onshore and offshore Morocco (Capella et al., 2017; de Weger et al., 2020) as well as in the southern part of the West Iberian margin (Rodrigues, 2017) due to the MOW. This indicates an active exchange through the Riffian Corridor until early Messinian, whereas synchronous MOW influence in the Deep Algarve and Guadalquivir basins has not been reported to date. The fact that the upper Tortonian-lower Messinian sequence in the Northwest Moroccan margin is thicker than in the Southwest Iberian margin could also reflect higher sedimentary input with an active MOW through a connected Riffian but a dormant Betic corridor. However, because of the absence of field evidence onshore Morocco for a marine connection above Lower Messinian deposits (Capella et al., 2019), a shift in MOW circulation through the Strait of Gibraltar cannot be excluded (Krijgsman et al., 2018) with currently available drilling information.

Meanwhile, the top of the middle to upper Messinian unit relates to the end of the MSC, marking a lithological shift from middle to late Messinian hemipelagic conditions into lowermost Pliocene contourite deposits formed by the initiation of weak MOW through the Strait of Gibraltar from 5.33 to 3.2 Ma (Hernández-Molina et al., 2016), with the presence of contourite bigradational sequences directly above the Miocene-Pliocene boundary and an abrupt change in sedimentation rate from 10 to 27 cm ka^{-1} (van der Schee et al., 2016). This change is in agreement with the instantaneous return to open marine connection observed in the Mediterranean (Roveri et al., 2014). The middle to late Messinian and lowermost Pliocene sediments could also be truncated by younger lower Pliocene gravity flow deposits, either channel-filled turbidites, debrites, or slope fans originating from the margins (~5.2–3.8 Ma) (Ducassou et al., 2016; Sierro et al., 2008). They are caused by compressional tectonics superimposed upon glacio-eustatic variation (Pérez-Asensio et al., 2018; Sierro et al., 2008).

Quantitative Testing of Paleoceanographic Conditions through Hypothetico-Deductive Method

The finding that contourite deposition is not evidenced within the Gulf of Cádiz at seismic scale during the deposition of the middle to upper Messinian unit can be interpreted in several ways. It is even possible that MOW flow did continue, despite not being resolved in our body of data. Here, the viability of continuing but changed alongslope flow is explored quantitatively using the simple representation of the plume outlined in *Materials and Methods*, and the physical constraints on the behaviour of the system described in *Results*. Below we discuss the three scenarios put forth in *Results*, and possible no-analog exchanges as an explanation for our observations at the end of this section.

Could there be a very small flux?

Given the necessity for the conservation of salt and mass in marginal basin exchanges like the Mediterranean-Atlantic connection at the Strait of Gibraltar, a reduced flow of water must result in greater density (Bryden et al., 1993). The absolute magnitude of the fluxes would then reflect the underlying control from the net freshwater export flux for the Mediterranean basin, which is 0.05 Sv (Bethoux and Gentili, 1999). This control has been modelled for the Messinian context (Simon and Meijer, 2015), and a small flux exchange is highly consistent with the evolution of a more saline Mediterranean water-mass. Under halite-depositing conditions (Roveri et al., 2014), the flux could be orders of magnitude less than today. As described in *Results*, the small flux would lead to a high density and velocity MOW with more intense mixing, and the subsequent vigorous formation of AMW, generating a geostrophic current capable of forming a contourite depositional system in the Gulf of Cádiz similar to that observed during the Pliocene and Quaternary (Hernández-Molina et al., 2014; 2016). Thus, while superficially attractive, it is not likely that the absence of contourite deposits in the cores and seismic presented in this study can be explained by a very small flux at the gateway.

Could there be a slower flow?

In terms of the paleo-AMW plume, the maximum flow velocity in the region during the middle to late Messinian consistent with our observations (absence of contourite depositional system) is 0.2 m s^{-1} (McCave and Hall, 2006), which represents the maximum geostrophic velocity (U_{geo}) experienced on the slope (O'Neill-Baringer and Price, 1997). This is considerably lower than velocities observed in the region today (Sánchez-Leal et al., 2017), which are ~1 m s^{-1} where sandy contourites are forming and in excess of 1.4 m s^{-1} in regions of abrasion (O'Neill-Baringer and Price, 1999). As shown in *Results*, a low velocity MOW or AMW would directly reflect a less dense Mediterranean water-mass. This implies that the Mediterranean was much less salty during the middle to late Messinian than in the late Tortonian to early Messinian, which is at odds with the empirical evidence. Conceptually, some loss of density could be traced to the warming of the Mediterranean relative to the Atlantic, but such a regional difference would have to be unrealistically large (up to several degrees) and could still not account for the latest Miocene when halite or gypsum were deposited in the Mediterranean. Moreover, a slower maximum flow velocity threshold (0.15 m s^{-1}) would mean a more significant reduction of salinity in the Mediterranean. Hence, we find no conditions under which our seismic observations are explained by a very slow-moving plume.

Could the plume have moved?

As the position of the gateway moved, the contourite deposition downstream of it must have moved as well. The data covers the most northerly (Fig. 4-2a and 4-3b) to the most southerly gateway recognized (Fig. 4-2b and 4-3c), fully capturing the possibility of a change in gateway position, thus eliminating this possibility. It might be that the MOW plume moved deeper down the slope, coming to lie basinward of the seismic data presented. For the Late Quaternary, such alterations have been documented (Schönfeld et al., 2003; Llave et al., 2006; Rogerson et al., 2012a). Given the operations of mixing and/or entrainment to counter changes in the density of outflowing water (see discussion above), such settings would not arise from changes in the Mediterranean basin itself, but rather from a weakening of the Atlantic Meridional Overturning Circulation (Rogerson et al.,

2012a). In order for the AMW to reach water depths beyond the range of the seismic data presented here, the AMOC would have had to weaken to approximately its conditions during the Last Glacial Maximum (Rogerson et al., 2005). A slow AMOC may have occurred in warm periods of the Early Miocene, but there is no evidence in favour of this hypothesis for the Late Miocene (Steinthorsdottir et al., 2020), and the relatively low volume of northern polar ice at the time, as compared to the Late Quaternary Heinrich Events, makes a "thermohaline crisis" scenario in the Atlantic difficult to envisage. We therefore do not speculate about a sustained period of very low AMOC throughout the deposition of the middle to upper Messinian unit (up to several hundreds of thousands of years) in support of a deep-water flow at this time (Steinthorsdottir et al., 2020). Unless such evidence of sustained low Atlantic overturning during the middle to late Messinian is presented, the AMW plume could not be expected to lie lower on the slope than the region of the seismic data we examined.

Was the Mediterranean-Atlantic water-mass exchange different from that of today?

Recent consensus regarding the evaporite-depositing phases in the latest Miocene evokes an extremely stratified Mediterranean basins (Yoshimura et al., 2016), with exceptionally dense brines occupying deep areas below sills connecting with the Atlantic. However, these deep brine bodies would remain within a Mediterranean overturning circulation, where quantitative representations of the basin demonstrate that deep brines would have continued to mix into overlying waters (Simon and Meijer, 2017), and as part of that advection were likely directly drawn up to sill depth by frictional Bernoulli aspiration (Rogerson et al., 2012b). Advection of deep waters is required to balance the water volume provided to finite deep basins by convection (Simon and Meijer, 2017); without the Mediterranean overturning circulation, the mass of salt held in water within the deep basins could rapidly be exhausted and evaporite deposition would be replaced by sapropel deposition. The extreme stratification scenarios provided by Simon and Meijer (2017) are therefore consistent with the quantitative representation of the AMW plume used here, and do not suffice to explain the lack of a contourite depositional system in the Gulf of Cádiz.
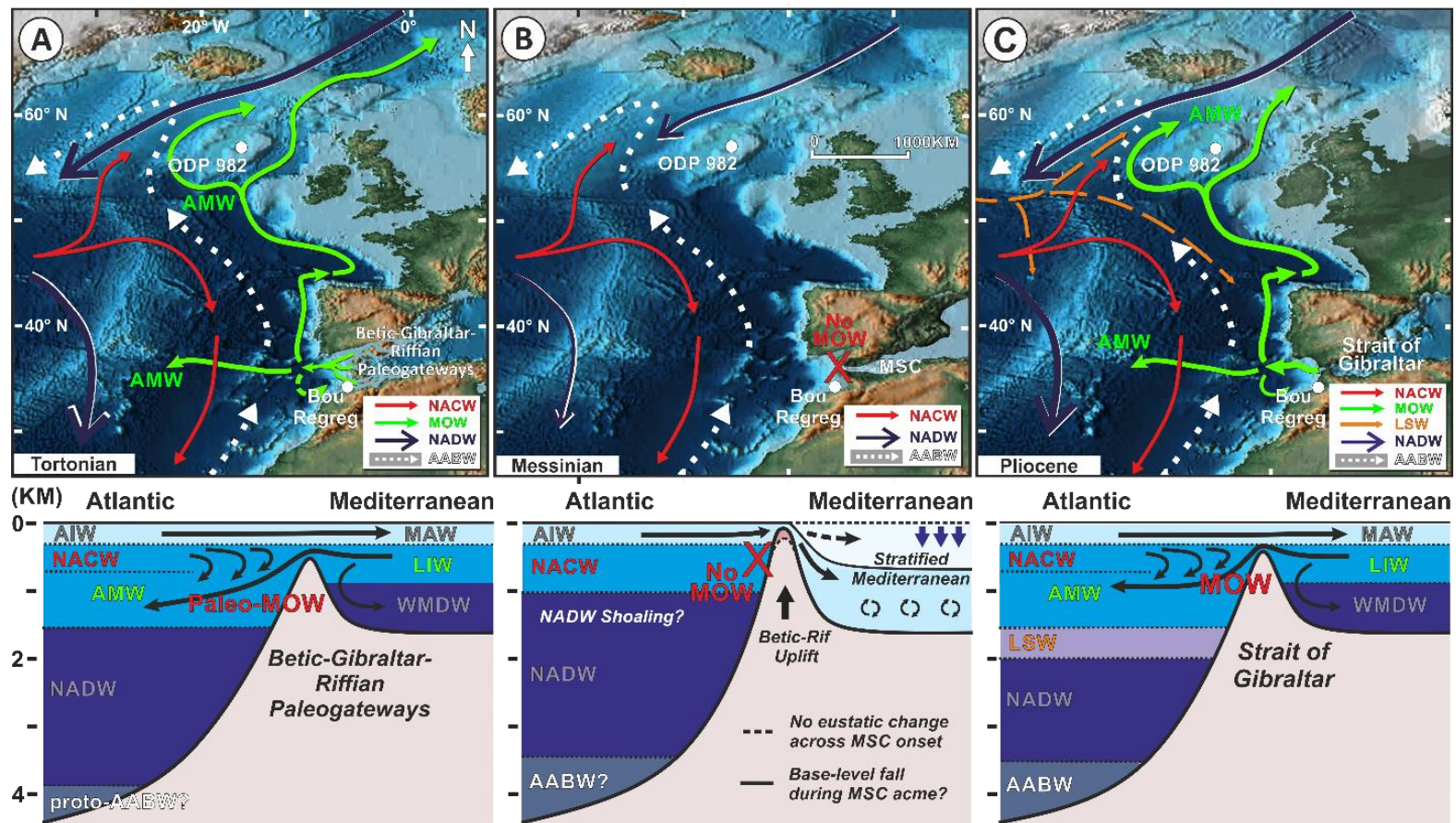
Figure 4-6 Scheme of the effect of Mediterranean-Atlantic restriction on the Atlantic Meridional Overturning Circulation (AMOC) during the (a) Tortonian, (b) Messinian, and (c) Pliocene. Paleogeographic reconstruction and Mediterranean-Atlantic gateway configuration adapted from Scotese (2014) and Krijgsman et al. (2018), respectively (NACW: North Atlantic Central Water; MOW: Mediterranean Outflow Water; LSW: Labrador Sea Water; NADW: North Atlantic Deep Water; AABW: Antarctic Bottom Water; AMW: Atlantic-Mediterranean Water.

By discarding other reasonable scenarios through this hypothetico-deductive method, we find that the most likely explanation for our seismic observations in the Gulf of Cádiz and the non-desiccation of the Mediterranean during the deposition of the middle to upper Messinian unit is inflow-without-outflow. This implies that the interface between the surficial and intermediate (e.g., LIW) water-masses in the Mediterranean had already been drawn to- or below sill depth, while the Atlantic sea surface remaining above it provided continuous unidirectional eastward flow of relatively fresh water into the Mediterranean, balancing evaporation. Still, we are unable to affirm whether there were sporadic outflows across the Mediterranean-Atlantic gateway during the middle to upper Messinian, which may be required to maintain salinity below evaporitic saturation (Roveri et al., 2014), as the primary impact would be deep scouring close to the strait (Siddall et al., 2004) later masked by Pliocene erosion (Fig. 4-4). We likewise find no positive indication of changes in seismic facies in the middle to upper Messinian unit within the seismic resolution of our dataset that could account for sporadic outflows in parts of the margins with a more conformable succession (Fig. 4-2). Further research is necessary to determine whether this period of apparently no MOW nor AMW plume activity is punctuated by shorter returns to two-way water-mass exchange; or whether salt was lost from the Mediterranean basin by other means, such as an earlier-than-anticipated onset of evaporite deposition in the deep Eastern Mediterranean basins.

Implications of the Late Miocene Mediterranean-Atlantic Gateway Restriction

The basal unconformity of the middle to late Messinian unit (~6.4 Ma) is linked to an onset of dominantly hemipelagic depositional environment. This seismic and lithologic change suggests absent or intermittent bottom currents without the influence of MOW through the Late Miocene paleo-gateways before the onset of MSC evaporite precipitation and deposition in the Mediterranean. The reduced MOW in the Gulf of Cádiz during the middle to late Messinian was probably due to the shallowing of the sill in the paleo-gateway by tectonic uplift (Krijgsman et al., 1999). Accordingly, the threshold depth allowed solely Atlantic inflow (Capella et al., 2019; Flecker et al., 2015) or intermittent outflow incapable

of significantly reworking sediments on the slope of the Gulf of Cádiz since at least 6.37 Ma, ~400 kyr preceding the onset of the MSC (Manzi et al., 2018). This scenario is consistent with a shift from paleo-MOW to paleo-Atlantic bottom waters in the Onshore Gharb basin between ~6.64 and 6.44 Ma, based on Neodymium (Nd) isotope values in the Bou Regreg valley succession in the Riffian corridor (Salé Briqueterie, Ain El Beida and Oued Akrech; Fig. 4-7; Ivanovic et al., 2013). Regional uplift and tectonism (Duggen et al., 2003) could also have driven formation of the turbidites observed at the base of the middle to upper Messinian unit, with turbidite channels scouring into the lower Messinian unit. The reduction of MOW we report at the ~6.4 Ma mark also coincides with a 400-kyr eccentricity minima of the orbital solution by Laskar et al. (2004) (Fig. 4-5) and supports a stepwise nature for the progressive restriction of the Mediterranean-Atlantic gateway, further consolidating the 400-kyr periodicity orbital forcing superimposed on a gradual tectonic trend as the mechanism behind gateway closure (Hilgen et al., 2007) and changes in the dominant depositional style. An astronomical link to the long eccentricity orbital forcing has been proposed for the evolution of stratigraphic events in this region leading up to the MSC (Roveri et al., 2014), namely the Tortonian salinity crisis (7.8–7.6 Ma) (Krijgsman et al., 2000), the stepwise restriction of Mediterranean-Atlantic connection (~7.2 and ~6.8 Ma) (Kouwenhoven et al., 2003), onset of MSC (5.97 Ma) (Manzi et al., 2018), and the "Messinian Gap" or MSC acme event (5.6–5.55 Ma) (Krijgsman et al., 1999). The gateway restriction, along with paleoceanographic changes, could explain the concurrent phylogenetic divergence of Mediterranean-New World monk seals around 6.3 Ma, similar to the effect of the Central American seaway closure on Caribbean-Hawaiian monk seal divergence (Scheel et al., 2014).

In the Mediterranean, the gateway restriction was also recorded progressively, leading up to the weakening of the MOW at ~6.4 Ma, firstly by a significant reduction of deep-water ventilation immediately after the Tortonian-Messinian boundary (7.15 Ma), followed by an intensification of bottom-water stagnation and water stratification (6.7 Ma; Blanc-Valleron et al., 2002; Kouwenhoven et al., 1999; 2003). These changes were accompanied by a lesser diversity of calcareous planktons (Sierro et al., 2003). Then, deposition of aplanktic levels related to more adverse conditions of restriction with

increased salinity (>50 g/L) took place since 6.4 Ma (Sierro et al., 2008). This period (6.45 – 6.29 Ma) is furthermore characterized by more negative and unstable $\delta^{18}O$ values in the Mediterranean, suggesting stronger dilution by continental waters, pointing to a severe isolation of the Mediterranean basin, which was no longer regulated by oceanic input but by climatic fluctuations (Blanc-Valleron et al., 2002). The widespread precipitation of authigenic calcite, dolomite and/or aragonite in the Mediterranean between 6.3 and 5.97 Ma, prior to the deposition of MSC evaporites, moreover indicates an increasingly restrictive and supersaturated environment (Blanc-Valleron et al., 2002; Sierro et al., 2003). A continuous but reduced surficial Atlantic inflow into the Mediterranean could contribute to varying salinity levels around the upper tolerance limit of foraminifera (50 g/L), but below the threshold of gypsum deposition (130 g/L; Flecker et al., 2015) in the Mediterranean marginal basins; meanwhile, the absence of outflow to the Atlantic requires salt being lost from the Mediterranean basin through other means, from the initiation of the transparent unit until the onset of MSC (~6.4 – 5.97 Ma). In the deeper basins, euxinic shales in the pre-MSC interval (Roveri et al., 2014) extending into the first stage of MSC (de Lange and Krijgsman, 2010) indicate anoxic and sulphidic bottom water conditions that could impede the precipitation of gypsum even where salinity was strongly enhanced. Reduced conditions in the deep basin would also explain the synchronous onset of marginal gypsum and basinal halite precipitation, reaching saturations of 130 and 350 g/L, respectively (Meilijson et al., 2018). Such a scenario still requires a sink of salt from the basin, however either via sporadic outbursts into the Atlantic too subtle for seismic reflection data to resolve or owing to an earlier-than-anticipated onset of salt deposition in the deep Mediterranean basins. Either hypothesis will need to be tested via new coring and research.

The transition from contouritic to hemipelagic sedimentation in the Miocene would give rise to changes in the Atlantic paleoceanographic regime (Fig. 4-6). A restricted Mediterranean-Atlantic connection and an absence or intermittence of MOW during the middle to late Messinian would have significantly reduced Atlantic water entrainment and halted formation of the AMW (Rogerson et al., 2012b). This would alter the strength, structure and possibly the position of the Azores Front (Ozgokmen et al., 2001) and

destabilize the AMOC (Ivanovic et al., 2014; Pérez-Asensio et al., 2012, Sierro et al., 2020). Assuming that the buoyancy export during the early Messinian was similar to that existing today, a loss of MOW would reduce the buoyancy loss within the North Atlantic by ~8.53 x 10^5 kg s^{-1}, which is a change of the same magnitude as that arising from Anthropocene Arctic sea ice loss (Liu et al., 2019). A unidirectional loss of salt into the Mediterranean via an inflow-without-outflow scenario at Gibraltar during the Messinian would also differ from a small net inflow of salt relative to the total inflow-outflow budget under the present two-way exchange scenario. This would likely result in anomalously low salinity in the adjacent Northeastern Atlantic, and possibly the weakest AMOC since the closure of the connection between the Mediterranean and the Indian Ocean during the middle Miocene (de la Vara et al., 2013). A revised astronomical age model for ODP Site 982 in the North Atlantic (Fig. 4-6; Drury et al., 2018), correlated to the Ain El Beida section in the Bou Regreg Valley (Fig. 4-6; van der Laan et al., 2005) indicates benthic excursions of δ^{18}O and δ^{13}C in the Atlantic intermediate water depths (500–1500 m; *sensu* Emery and Meincke, 1986) around ~6.4 Ma (Drury et al., 2018). The higher average δ^{18}O and δ^{13}C values suggest colder conditions (Drury et al., 2018) and could testify to the removal of warm and saline AMW and glacial shoaling of the NADW (Gebbie, 2014; Fig. 4-6b). This major paleoceanographic change is responsible for the enhanced subsurface and atmospheric cooling in the mid-latitudes of the Northern Hemisphere (Boulton et al., 2014; Ivanovic et al., 2014), which coincides with dynamic ice sheet expansion and strengthening of the cryosphere-carbon cycle coupling between 6.4 and 5.4 Ma (Drury et al., 2018; Herbert et al., 2016).

Conclusion

The widespread distribution of a predominantly hemipelagic middle to upper Messinian unit along the continental slope in the Gulf of Cádiz and the southern part of the West Iberian margin can be viewed as the sedimentary response to an absence or intermittence of intermediate circulation. This implies no continuous outflow of the Mediterranean-Atlantic exchange at least ~400 kyr preceding the MSC, simultaneous to

progressive gateway restriction, and correlates to AMOC weakening and North Atlantic cooling in the latest Miocene. An alternative interpretation is that the AMOC was severely reduced throughout this period, causing the MOW plume to settle at great depth. As this is not consistent with existing reconstructions of the Atlantic during the Late Miocene, we support the former scenario.

Either as a means of explaining the transparent unit via deep settling, or as a consequence of inflow-without-outflow causing major palaeoceanographic changes throughout the North Atlantic, the evolution of the Mediterranean at this time seems to be inextricably bound to the evolution of AMOC. One important outcome of this study is the recognition of the disadvantages of considering the two basins in isolation, and of the need to integrate conceptual models of Atlantic paleoceanography with Mediterranean geological models for the latest Miocene.

Acknowledgments and Data

References

Berggren, W.A. (1982). Role of Ocean Gateways in Climate Change. In: Climate in Earth History. *Studies in Geophysics*, 118-125. Washington D.C.: National Academy Press.

Bethoux, J. P., & Gentili, B. (1999). Functioning of the Mediterranean Sea: past and present changes related to freshwater input and climate changes. *Journal of Marine Systems, 20*, 33-47. doi:10.1016/S0924-7963(98)00069-4

Blanc-Valleron, M.-M., Pierre, C., Caulet, J. P., Caruso, A., Rouchy, J.-M., Cespuglio, G., Sprovieri, R., Pestrea, S., & Di Stefano, E. (2002). Sedimentary, stable isotope and micropaleontological records of paleoceanographic change in the Messinian Tripoli Formation (Sicily, Italy). *Palaeogeography, Palaeoclimatology, Palaeoecology 185,* 255-286. doi:10.1016/S0031-0182(02)00302-4

Boulton, C. A., Allison, L. C., & Lenton T. M. (2014). Early warning signals of Atlantic Meridional Overturning Circulation collapse in a fully coupled climate model. *Nature Communications 5*, 5752. doi:10.1038/ncomms6752

Bryden, L. H. (1993). Sill exchange to and from enclosed seas. In N. F. R. Delia Croce (Ed.), *Symposium Mediterranean Seas 2000*, Università di Genova, Santa Margherita Ligure, 23–27 September 1991 (pp. 17-41) Genova: Instituto Scienze Ambientali Marine.

Capella, W., Flecker, R., Hernández-Molina, F. J., Simon, D., Meijer, P. T., Rogerson, M., Sierro, F. J., & Krijgsman, W. (2019). Mediterranean isolation preconditioning the Earth System for late Miocene climate cooling. *Scientific Reports, 9*, 3795. doi:10.1038/s41598-019-40208-2

Capella, W., Hernández-Molina, F. J., Flecker, R., Hilgen, F. J., Hssain, M., Kouwenhoven, T. J., van Oorschot, M., Sierro, F. J., Stow, D. A. V., Trabucho-Alexandre, J., Tulbure, M. A., de Weger, W., Yousfi, M. Z., & Krijgsman, W. (2017). Sandy contourite drift in the late Miocene Rifian Corridor (Morocco): reconstruction of depositional environments in a foreland-basin seaway. *Sedimentary Geology, 355*, 31–57. doi:10.1016/j.sedgeo.2017.04.004

Culp, J., Strom, K., Parent, A., & Romans, B. W. (2020). Sorting of fine-grained sediment by currents: Testing the sortable silt hypothesis with laboratory experiments. *Earth Arxiv.* doi:10.31223/osf.io/xec2t [Accessed 31/12/2020].

de la Vara, A., Meijer, P. Th., & Wortel, M. J. R. (2013). Model study of the circulation of the Miocene Mediterranean Sea and Paratethys: closure of the Indian Gateway. *Climate of the Past Discussion, 9*, 4385-4424. doi:10.5194/cpd-9-4385-2013

de Lange, G. J., & Krijgsman, W. (2010). Messinian salinity crisis: A novel unifying shallow gypsum/deep dolomite formation mechanism. *Marine Geology, 275*, 273–277. doi:10.1016/j.margeo.2010.05.003

de Weger, W., Hernández-Molina, F. J., Flecker, R., Sierro, F. J., Chiarella, D., Krijgsman, W. & Manar, M. A. (2020). Late Miocene contourite channel system reveals intermittent overflow behavior. *Geology.* doi:10.1130/G47944.1

Drury, A. J., Westerhold, T., Hodell, D., & Röhl, U. (2018). Reinforcing the North Atlantic backbone: revision and extension of the composite splice at ODP Site 982. *Climate of the Past, 14*, 321-338. doi:10.5194/cp-14-321-2018

Ducassou, E., Fournier, L., Sierro, F. J., Alvarez Zarikian, C. A., Lofi, J., Flores, J. A., & Roque, C. (2016). Origin of the large Pliocene and Pleistocene debris flows on the Algarve margin. *Marine Geology, 377*, 58-76. doi:10.1016/j.margeo.2015.08.018

Duggen, S., Hoernle, K., van den Bogaard, P., Rüpke, L., & Morgan, J. P. (2003). Deep roots of the Messinian salinity crisis. *Nature, 422*, 602-606. doi:10.1038/nature01551

Emery, W. J., & Meincke, J. (1986). Global Water Masses: Summary and Review. *Oceanologica Acta, 9*, 383-391.

Flecker, R. & Ellam, R.M. (2006). Identifying Late Miocene episodes of connection and isolation in the Mediterranean–Paratethyan realm using Sr isotopes. *Sedimentary Geology 188-189,* 189-203. doi:10.1016/j.sedgeo.2006.03.005

Flecker, R., Krijgsman, W., Capella, W., de Castro Martíns, C., Dmitrieva, E., Mayser, J. P., Marzocchi, A., Modestou, S., Ochoa, D., Simon, D., Tulbure, M., van den Berg, B., van der Schee, M., de Lange, G., Ellam, R., Govers, R., Gutjahr, M., Hilgen, F. J., Kouwenhoven, T., Lofi, J., Meijer, P., Sierro, F. J., Bachiri, N., Barhoun, N., Chakor Alami, A., Chacon, B., Flores, J. A., Gregory, J., Howard, J., Lunt, D., Ochoa, M., Pancost, R., Vincent, S., & Zakaria Yousfi, M. (2015). Evolution of the Late Miocene

Mediterranean-Atlantic gateways and their impact on regional and global environmental change. *Earth-Science Reviews 150*, 365-392. doi:10.1016/j.earscirev.2015.08.007

Gebbie, G. (2014). How much did Glacial North Atlantic Water shoal? *Paleoceanography, 29*, 190-209. doi:10.1002/2013PA002557

Henrich R., & Hüneke, H. (2011). Hemipelagic Advection and Periplatform Sedimentation. In: H. Hüneke, & T. Mulder (Eds.), Deep-sea Sediments. *Developments in Sedimentology, 63*, 353-396. doi:10.1016/B978-0-444-53000-4.00005-6

Herbert, T. D., Lawrence, K. T., Tzanova, A., Peterson, L. C., Caballero-Gill, R., & Kelly, C.S. (2016). Late Miocene global cooling and the rise of modern ecosystems. *Nature Geoscience, 9*, 843–847. doi:10.1038/ngeo2813

Hernández-Molina, F. J., Llave, E., Preu, B., Ercilla, G., Fontan, A., Bruno, M., Serra, N., Gomiz, J. J., Brackenridge, R. E., Sierro, F. J., Stow, D. A. V., García, M., Juan, C., Sandoval, N., & Arnáiz, A. (2014). Contourite processes associated with the Mediterranean Outflow water after its exit from the Strait of Gibraltar: global and conceptual implications. *Geology, 42*, 227–230. doi:10.1130/G35083.1

Hernández-Molina, F. J., Sierro, F. J., Llave, E., Roque, C., Stow, D. A. V., Williams, T., Lofi, J., van der Schee, M., Arnáiz, A., Ledesma, S., Rosales, C., Rodríguez-Tovar, F. J., Pardo-Igúzquiza, E., & Brackenridge, R. E. (2016). Evolution of the gulf of Cádiz margin and southwest Portugal contourite depositional system: Tectonic, sedimentary and paleoceanographic implications from IODP expedition 339. *Marine Geology 377*, 7-39. doi:10.1016/j.margeo.2015.09.013

Hilgen, F. J., Krijgsman, W., Langereis, C. G., Lourens, L. J., Santarelli, A., & Zachariasse, W. J. (1995). Extending the astronomical (polarity) time scale into the Miocene. *Earth Planetary Science Letters 136*, 495-510. doi:10.1016/0012-821X(95)00207-S

Hilgen, F., Kuiper, K., Krijgsman, W., Snel, E., & van der Laan, E. (2007). Astronomical tuning as the basis for high resolution chronostratigraphy: the intricate history of the Messinian Salinity Crisis. *Stratigraphy 4*, 231-238.

Hodell, D. A., Curtis, J. H., Sierro, F. J., & Raymo, M. E., (2001). Correlation of late Miocene to early Pliocene sequences between the Mediterranean and North Atlantic. *Palaeoceanography 16*, 164–178. doi:10.1029/1999PA000487

Hüsing, S. K., Oms, O., Agustí, J., Garcés, M., Kouwenhoven, T. J., Krijgsman, W., & Zachariasse, W.-J. (2010). On the late Miocene closure of the Mediterranean–Atlantic gateway through the Guadix basin (southern Spain). *Palaeogeography, Palaeoclimatology, Palaeoecology 291*, 167–179. doi:10.1016/j.palaeo.2010.02.005.

Iaccarino, S. M., Cita, M. B., Gaboardi, S., & Gruppini, G. M. (1999). High-resolution biostratigraphy at the Miocene/Pliocene boundary in Holes 974B and 975B, western Mediterranean. *Proceedings of the Ocean Drilling Program, Scientific Results 161* (pp. 197–221). College Station, TX: Ocean Drilling Program. doi:10.2973/odp.proc.sr.161.247.1999

Ivanovic, R. F., Flecker, R., Gutjahr, M., & Valdesa, P. J. (2013). First Nd isotope record of Mediterranean–Atlantic water exchange through the Moroccan Rifian Corridor during the Messinian Salinity Crisis. *Earth Planetary Science Letters, 368*, 163-174. doi:10.1016/j.epsl.2013.03.010

Ivanovic, R. F., Valdes, P. J., Flecker, R., & Gutjahr, M. (2014). Modelling global-scale climate impacts of the late Miocene Messinian Salinity Crisis. *Climate of the Past, 10*, 607-622. doi:10.5194/cp-10-607-2014

Knutz, P.C. (2008). Paleoceanographic significance of contourite drifts. In: M. Rebesco & A. Camerlenghi (Eds.), Contourites. *Developments in Sedimentology, 60*, 511-535. Amsterdam: Elsevier.

Kouwenhoven, T. J., Seidenkrantz, M.-S. & van der Zwaana, G. J. (1999). Deep-water changes: the near-synchronous disappearance of a group of benthic foraminifera from the Late Miocene Mediterranean. *Palaeogeography, Palaeoclimatology, Palaeoecology 152,* 259-281. doi:10.1016/S0031-0182(99)00065-6

Kouwenhoven, T. J., Hilgen, F. J., & van der Zwaan, G. J. (2003). Late Tortonian-early Messinian stepwise disruption of the Mediterranean-Atlantic connections: constraints from benthic foraminiferal and geochemical data. *Palaeogeography Palaeoclimatology Palaeoecology, 198*, 303-319. doi:10.1016/S0031-0182(03)00472-3

Krijgsman, W., Capella, W., Simon, D., Hilgen, F. J., Kouwenhoven, T. J., Meijer, P. Th., Sierro, F. J., Tulbure, M. A., van den Berg, B. C. J., van der Schee, M., & Flecker, R. (2018). The Gibraltar Corridor: Watergate of the Messinian Salinity Crisis. *Marine Geology, 403*, 238-246. doi:10.1016/j.margeo.2018.06.008

Krijgsman, W., Gaboardi, S., Hilgen, F. J., Iaccarino, S., de Kaenel, E., & van der Laan, E. (2004). Revised astrochronology for the Ain el Beida section (Atlantic Morocco): No glacio-eustatic control for the onset of the Messinian Salinity Crisis. *Stratigraphy, 1***,** 87-101.

Krijgsman, W., Garcés, M., Agustí, J., Raffi, I., Taberner, C., & Zachariasse, W. J. (2000). The 'Tortonian salinity crisis' of the eastern Betics (Spain). *Earth Planetary Science Letters, 181*, 497-51. doi:10.1016/S0012-821X(00)00224-7

Krijgsman,W., Hilgen, F. J., Raffi, I., Sierro, F. J., & Wilson, D. S. (1999). Chronology, causes and progression of the Messinian salinity crisis. *Nature, 400*, 652–655. doi:10.1038/23231

Laskar, J., Robutel, P., Joutel, F., Gastineau, M, Correia, A. C. M., & Levrard., B. (2004). A long-term numerical solution for the insolation quantities of the Earth. *Astronomy and Astrophysics 428*, 261-285. doi:10.1051/0004-6361:20041335

Ledesma, S. (2000). Astrobiocronología y estratigrafía de alta resolución del Neógeno de la Cuenca del Guadalquivir-Golfo De Cádiz, (Doctoral dissertation). Retrieved from Grupo de Geociencias Oceánicas. (http://oceano.usal.es/wp-content/uploads/sites/30/2017/10/SantiagoLedesmaTesis.compressed-1.pdf). Salamanca: Universidad de Salamanca.

Liu, W., Fedorov, A., & Sévellec, F. (2019). The Mechanisms of the Atlantic Meridional Overturning Circulation Slowdown Induced by Arctic Sea Ice Decline. *Journal of Climate, 32*, 977-996. doi:10.1175/JCLI-D-18-0231.1

Liu, W., Fedorov, A., Xie, S.-P., & Hu, S. (2020). Climate impacts of a weakened Atlantic Meridional Overturning Circulation in a warming climate. *Science Advances, 6*, eaaz4876. doi:10.1126/sciadv.aaz4876

Llave, E., Schönfeld, J., Hernández-Molina, F. J., Mulder, T., Somoza, L., Díaz del Río, V., & Sánchez-Almazo, I. (2006). High-resolution stratigraphy of the Mediterranean outflow contourite system in the Gulf of Cadiz during the late Pleistocene: The impact

of Heinrich events. *Marine Geology*, *227*, 241 – 262. doi:10.1016/j.margeo.2005.11.015

Lopes, F. C., Cunha, P. P., & Le Gall, B. (2006). Cenozoic seismic stratigraphy and tectonic evolution of the Algarve margin (offshore Portugal, southwestern Iberian Peninsula). *Marine Geology, 231*, 1-36. doi:10.1016/j.margeo.2006.05.007

Lourens, L. J., Antonarakou, A., Hilgen, F. J., Van Hoof, A. A. M., Vergnaud-Grazzini, C., & Zachariasse, W. J. (1996). Evaluation of the Plio-Pleistocene astronomical timescale. *Paleoceanography, 11*, 391-413. doi:10.1029/96PA01125

Lourens, L. J., Hilgen, F. J., Shackleton, J., Laskar, J., & Wilson, J. (2004). The Neogene Period. In: F. Gradstein, J. Ogg, & A. Simth (Eds.), *A Geologic Time Scale*, 409–440. London: Cambridge University Press.

Maldonado, A., Somoza, L., & Pallarés, L., (1999). The Betic orogen and the Iberian-African boundary in the Gulf of Cádiz: geological evolution (central North Atlantic). *Marine Geology, 155*, 9-43. doi:10.1016/S0025-3227(98)00139-X

Manzi, V., Gennari, R., Lugli, S., Persico, D., Reghizzi, M., Roveri, M., Schreiber, B. C., Calvo, R., Gavrieli, I., & Gvirtzman, Z. (2018). The onset of the Messinian salinity crisis in the deep Eastern Mediterranean basin. *Terra Nova, 30*, 189-198. doi:10.1111/ter.12325

Martín, J. M., Braga, J. C. & Betzler, C. (2002). The Messinian Guadalhorce corridor: the last northern, Atlantic–Mediterranean gateway. *Terra Nova 13*, 418-424. doi:10.1046/j.1365-3121.2001.00376.x

Martín, J. M., Braga, J. C., Aguirre, J., & Puga-Bernabéu, Á. (2009). History and evolution of the North-Betic Strait (Prebetic Zone, Betic Cordillera): A narrow, early Tortonian, tidal-dominated, Atlantic-Mediterranean marine passage. *Sedimentary Geology, 216*, 80-90. doi:10.1016/j.sedgeo.2009.01.005

McCave, I. N., & Hall, I. R. (2006), Size sorting in marine muds: Processes, pitfalls, and prospects for paleoflow-speed proxies. *Geochemistry, Geophysics, Geosystems, 7*, Q10N05, doi:10.1029/2006GC001284.

McCave, I. N., Thornalley, D. J. R., & Hall, I. R. (2017). Relation of sortable silt grain-size to deep-sea current speeds: Calibration of the 'Mud Current Meter'. *Deep Sea*

Research Part I: Oceanographic Research Papers, 127, 1-12. doi:10.1016/j.dsr.2017.07.003

Medialdea, T., Vegas, R., Somoza, L., Vázquez, J. T., Maldonado, A., Díaz-del-Río, V., Maestro, A., Córdoba, D., & Fernández-Puga, M. C., (2004). Structure and evolution of the ''Olistostrome'' complex of the Gibraltar Arc in the Gulf of Cádiz (eastern Central Atlantic): evidence from two long seismic cross-sections. *Marine Geology 209*, 173-198. doi:10.1016/j.margeo.2004.05.029

Meijer, P. Th. & Krijgsman, W. (2005). A quantitative analysis of the desiccation and re-filling of the Mediterranean during the Messinian Salinity Crisis. *Earth and Planetary Science Letters 240*, 510 – 520. doi:10.1016/j.epsl.2005.09.029

Meilijson, A., Steinberg, J., Hilgen, F. J, Bialik, O. M., Waldmann, N. D., & Makovsky, Y. (2018). Deep-basin evidence resolves a 50-year-old debate and demonstrates synchronous onset of Messinian evaporite deposition in a non-desiccated Mediterranean. *Geology, 46*, 243–246. doi:10.1130/G39868.1

Millot, C., Candela, J., Fuda, J.-L., & Tber, Y. (2006). Large warming and salinification of the Mediterranean outflow due to changes in its composition. *Deep Sea Research Part I: Oceanographic Research Papers, 53*, 656-666. doi:10.1016/j.dsr.2005.12.017

O'Neill-Baringer, M., & Price, J. F. (1997). Mixing and spreading of the Mediterranean outflow. *Journal of Physical Oceanography, 27*, 1654-1677. doi:10.1175/1520-0485(1997)027<1654:MASOTM>2.0.CO;2

O'Neill-Baringer, M. & Price, J. F. (1999). A review of the physical oceanography of the Mediterranean outflow. *Marine Geology, 155*, 63-82. doi:10.1016/S0025-3227(98)00141-8

Ozgokmen, T. M., Chassignet, E. P., & Rooth, C. G. H. (2001). On the connection between the Mediterranean Outflow and the Azores current. *Journal of Physiscal Oceanograrphy, 31*, 461-480. doi:10.1175/1520-0485(2001)031<0461:OTCBTM>2.0.CO;2

Pérez-Asensio, J. N., Aguirre, J., Schmiedl, G., & Civis, J. (2012). Impact of restriction of the Atlantic-Mediterranean gateway on the Mediterranean Outflow Water and eastern Atlantic circulation during the Messinian. *Paleoceanography, 27*, PA3222. doi:10.1029/2012PA002309

Pérez-Asensio, J. N., Larrasoaña, J. C., Samankassou, E. Sierro, F. J., García Castellanos, D., Jiménez-Moreno, G., Salazar, Á., Salvany i Duran, J. M., Ledesma, S., Mata, M. P., Civis, J., & Mediavilla, C. (2018). Magnetobiochronology of Lower Pliocene marine sediments from the lower Guadalquivir basin: Insights into the tectonic evolution of the Strait of Gibraltar area. *Geological Society of America Bulletin, 130*, 1791-1808. doi:10.1130/B31892.1

Prather, B. E., Booth, J. R., Steffens, G. S., & Craig, P. A. (1998). Classification, Lithologic Calibration, and Stratigraphic Succession of Seismic Facies of Intraslope basins, Deep-Water Gulf of Mexico. *AAPG Bulletin 82*, 701–728. doi:10.1306/1D9BC5D9-172D-11D7-8645000102C1865D

Riaza, C., & Martínez del Olmo, W. (1996). Depositional model of the Guadalquivir – Gulf of Cádiz Tertiary basin. In P. F, Friend, & C. J. Dabrio (Eds), *Tertiary basins of Spain: The Stratigraphic Record of Crustal Kinematics* (pp. 330-338). Cambridge: Cambridge University Press. doi:10.1017/CBO9780511524851

Rodrigues, S. M. (2017). Seismostratigraphic model of the Sines Contourite Drift (SW Portuguese margin) – depositional evolution, structural control and paleoceanographic implications. (Master's thesis.) Retrieved from Repositório da Universidade de Lisboa. (http://hdl.handle.net/10451/27603). Lisbon: Universidade de Lisboa.

Rogerson, M., Bigg, G. R., Rohling, E., & Ramirez, J. (2012a). Vertical density gradient in the eastern North Atlantic during the last 30,000 years. *Climate Dynamics 39*, 589-598. doi:10.1007/s00382-011-1148-4

Rogerson, M., Rohling, E. J., Bigg, G. R., & Ramirez, J. (2012b). Palaeoceanography of the Atlantic-Mediterranean Exchange: Overview and first quantitative assessment of climatic forcing. *Reviews of Geophysics, 50*, RG2003. doi:10.1029/2011RG000376

Rogerson, M., Rohling, E. J., Weaver, P. P. E., & Murray, J. W. (2004). The Azores Front since the Last Glacial Maximum. *Earth and Planetary Science Letters, 222*, 779-789. doi:10.1016/j.epsl.2004.03.039

Rogerson, M., Rohling, E. J., Weaver, P. P. E., & Murray, J. W. (2005). Glacial to Interglacial Changes in the Settling Depth of the Mediterranean Outflow Plume. *Paleoceanography, 20*, PA3007. doi:10.1029/2004PA001106

Roque, C. (2007). Tectonostratigrafia Do Cenozóico Das Margens Continentais Sul E Sudoeste Portuguesas: Um Modelo De Correlação Sismostratigráfica. (Doctoral dissertation.) Retrieved from Repositório da Universidade de Lisboa. (http://hdl.handle.net/10451/1521). Lisbon: Universidade de Lisboa.

Roveri, M., Flecker, R., Krijgsman, W., Lofi, J., Lugli, S., Manzi, V., Sierro, F. J., Bertini, A., Camerlenghi, A., De Lange, G., Govers, R., Hilgen, F. J., Hübscher, C., Meijer, P. Th., & Stoica, M. (2014). The Messinian Salinity Crisis: Past and future of a great challenge for marine sciences. *Marine Geology, 352*, 25-58. doi:10.1016/j.margeo.2014.02.002

Sánchez-Leal, R. F., Bellanco, M. J., Fernández-Salas, L. M., García-Lafuente, J., Gasser-Rubinat, M., González-Pola, C., Hernández-Molina, F. J., Pelegrí, J. L., Peliz, A., Relvas, P., Roque, D., Ruiz-Villarreal, M., Sammartino, S., & Sánchez-Garrido, J. C. (2017). The Mediterranean Overflow in the Gulf of Cadiz: A rugged journey. *Science Advances, 3*, eaao0609. doi:10.1126/sciadv.aao0609

Scheel, D. M., Slater, G. J., Kolokotronis S. -O., Potter, C. W., Rotstein, D. S., Tsangaras, K., Greenwood A. D., & Helgen, K.M. (2014). Biogeography and taxonomy of extinct and endangered monk seals illuminated by ancient DNA and skull morphology. *ZooKeys, 409*, 1-33. doi:10.3897/zookeys.409.6244

Schönfeld, J., Zahn, R., & Abreu, L. (2003). Surface and deep water response to rapid climate changes at the Western Iberian Margin. *Global and Planetary Change*, *36*, 237 – 264. doi:10.1016/S0921-8181(02)00197-2

Scotese, C. R. (2014). Atlas of Neogene Paleogeographic Maps (Mollweide Projection). In: *PALEOMAP Atlas for ArcGIS, Volume 1, The Cenozoic* (Maps No. 1-7). Evanston, IL: PALEOMAP Project. doi:10.13140/2.1.4151.3922

Selli, R., (1960). Il Messiniano Mayer-Eymar 1867. Proposta di un neostratotipo. *Giornale di Geologia 28*, 1–33. In: Roveri, M., Flecker, R., Krijgsman, W., Lofi, J., Lugli, S., Manzi, V., Sierro, F. J., Bertini, A., Camerlenghi, A., De Lange, G., Govers, R., Hilgen, F. J., Hübscher, C., Meijer, P. Th., & Stoica, M. (2014). The Messinian Salinity Crisis: Past and future of a great challenge for marine sciences. *Marine Geology, 352*, 25-58. doi:10.1016/j.margeo.2014.02.002

Siddall, M., Pratt, L. J., Helfrich, K. R., & Giosan, L. (2004). Testing the physical oceanographic implications of the suggested sudden Black Sea infill 8400 years ago. *Paleoceanography, 19*, PA1024. doi:10.1029/2003PA000903

Sierro, F. J., Flores, J. A., Francés, G., Vazquez, A., Utrilla, R., Zamarreño, I., Erlenkeuser, H., & Barcena, M. A. (2003). Orbitally-controlled oscillations in planktic communities and cyclic changes in western Mediterranean hydrography during the Messinian. *Palaeogeography Palaeoclimatology Palaeoecology, 190*, 289-316. doi:10.1016/S0031-0182(02)00611-9

Sierro, F. J., González Delgado, J. A., Dabrio, C. J., Flores, J. A., & Civis, J., (1996). Late Neogene depositional sequences in the foreland basin of Guadalquivir (SW Spain). In P. F. Friend & C. J. Dabrio (Eds), *Tertiary basins of Spain: The Stratigraphic Record of Crustal Kinematics* (pp.339-345). Cambridge: Cambridge University Press. doi:10.1017/CBO9780511524851.048

Sierro, F. J., Hilgen, F. J., Krijgsman, W., & Flores, J. A. (2001). The Abad composite (SE Spain): A Mediterranean and global reference section for the Messinian. *Palaeogeograrphy Palaeoecology Palaeoclimatology, 168*, 141-169. doi:10.1016/S0031-0182(00)00253-4

Sierro F. J., Hodell, D. A., Andersen, N., Azibeiro, L., A., Jimenez-Espejo, F. J., Bahr, A., Flores, J. A., Ausin, B., Rogerson, M., Lozano-Luz, R., Lebreiro, S. M., & Hernandez-Molina, F. J. (2020). Mediterranean Overflow Over the Last 250 kyr: Freshwater Forcing From the Tropics to the Ice Sheets. *Paleoceanography and Paleoclimatology 35*. doi:10.1029/2020PA003931

Sierro, F. J., Ledesma, S., & Flores, J. A. (2008). Astrobiochronology of Late Neogene deposits near the Strait of Gibraltar (SW Spain): Implications for the tectonic control of the Messinian Salinity Crisis. In F. Briand (Ed.), *The Messinian Salinity Crisis from mega-deposits to microbiology - A consensus report: N° 33 in CIESM Workshop Monographs* (pp. 45-48). Monaco: CIESM Publisher.

Sierro, F. J., Ledesma, S., Flores, J. A., Torrescusa, S., & Martínez del Olmo, W. (2000). Sonic and gamma ray astrochronology: Cycle to cycle calibration of Atlantic climatic records to Mediterranean sapropels and astronomical oscillations. *Geology, 28*, 695-698. doi:10.1130/0091-7613(2000)28<695:SAGACT>2.0.CO;2

Simon, D., & Meijer, P. Th. (2015). Dimensions of the Atlantic–Mediterranean connection that caused the Messinian Salinity Crisis. *Marine Geology, 364*, 53-64. doi:10.1016/j.margeo.2015.02.004

Simon, D., & Meijer, P. Th. (2017). Salinity stratification of the Mediterranean Sea during the Messinian crisis: A first model analysis. *Earth and Planetary Science Letters, 479*, 366-376. doi:10.1016/j.epsl.2017.09.045

Steinthorsdottir, M., Coxall, H. K., De Boer, A. M., Huber, M., Barbolini, N., Bradshaw, C. D., Burls, N. J., Feakins, S. J., Gasson, E., Henderiks, J., Holbourn, A., Kiel, S., Kohn, M. J., Knorr, G., Kürschner, W. M., Lear, C. H., Liebrand, D., Lunt, D. J., Mörs, T., Pearson, P. N., Pound, M. J., Stoll, H., & Strömberg, C. A. E. (2020). The Miocene: the Future of the Past. *Paleoceanography and Paleoclimatology,* e2020PA004037.

Straume, E.O., Gaina, C., Medvedev, S., & Nisancioglu, K.H. (2020). Global Cenozoic Paleobathymetry with a focus on the Northern Hemisphere Oceanic Gateways. *Gondwana Research*, *86*, 126-143. doi:10.1016/j.gr.2020.05.011.

van der Laan, E., Gaboardi, S., Hilgen, F. J. & Lourens, L. J. (2005). Regional climate and glacial control on high-resolution oxygen isotope records from Ain El Beida (latest Miocene, NW Morocco): A cyclostratigraphic analysis in the depth and time domain. *Paleoceanography 20*, PA1001. doi:10.1029/2003PA000995

van der Laan, E., Snel, E., de Kaenel, E., Hilgen, F. J., & Krijgsman, W. (2006). No major deglaciation across the Miocene–Pliocene boundary: integrated stratigraphy and astronomical tuning of the Loulja sections (Bou Regreg area, NW Morocco). *Paleoceanography, 21*, 1–27. doi:10.1029/2005PA001193

van der Schee, M., Sierro, F., Jimenez-Espejo, F., Hernández-Molina, F., Flecker, R., Flores, J., Acton, G., Gutjahr, M., Grunert, P., García-Gallardo, A., & Andersen, N. (2016). Evidence of early bottom water current flow after the Messinian Salinity Crisis in the Gulf of Cádiz. *Marine Geology, 380*, 315-329. doi:10.1016/j.margeo.2016.04.005

Wüst, G. (1961). On the vertical circulation of the Mediterranean Sea. *Journal of Geophyical Research, 66*, 3261–3271. doi:10.1029/JZ066i010p03261.

Wynn R.B., Cronin B.T., Peakall J. (2007). Sinuous deep-water channels: Genesis, geometry and architecture. Marine and Petroleum Geology 24, 341–387. doi:10.1016/j.marpetgeo.2007.06.001

Yoshimura, T., Kuroda, J., Lugli, S., Tamenori, Y., Ogawa, N. O., Jiménez-Espejo, F. J., Isaji, Y., Roveri, M., Manzi, V., & Kawahata, H. (2016). An X-ray spectroscopic perspective on Messinian evaporite from Sicily: Sedimentary fabrics, element distributions, and chemical environments of S and Mg. *Geochemistry, Geophysics, Geosystems, 17*, 1383-1400.

Zickfeld, K., Eby, M., & Weaver, A. J. (2008). Carbon-cycle feedbacks of changes in the Atlantic meridional overturning circulation under future atmospheric CO2. *Global Biogeochemical Cycles, 22*, GB3024. doi:10.1029/2007GB003118

Supplementary Material

Figure 4-S1   Relationship between mixing coefficient Φ (Phi) and velocity.
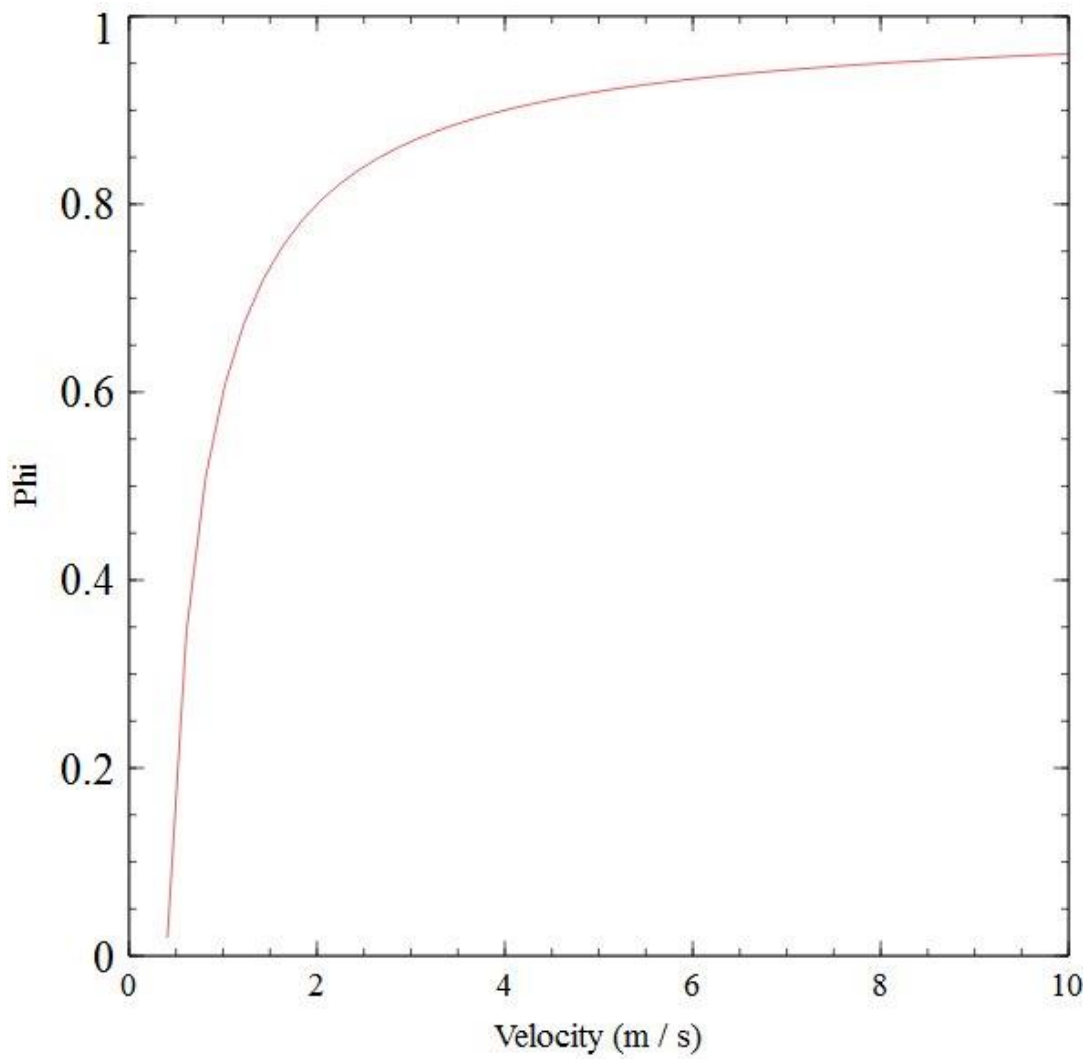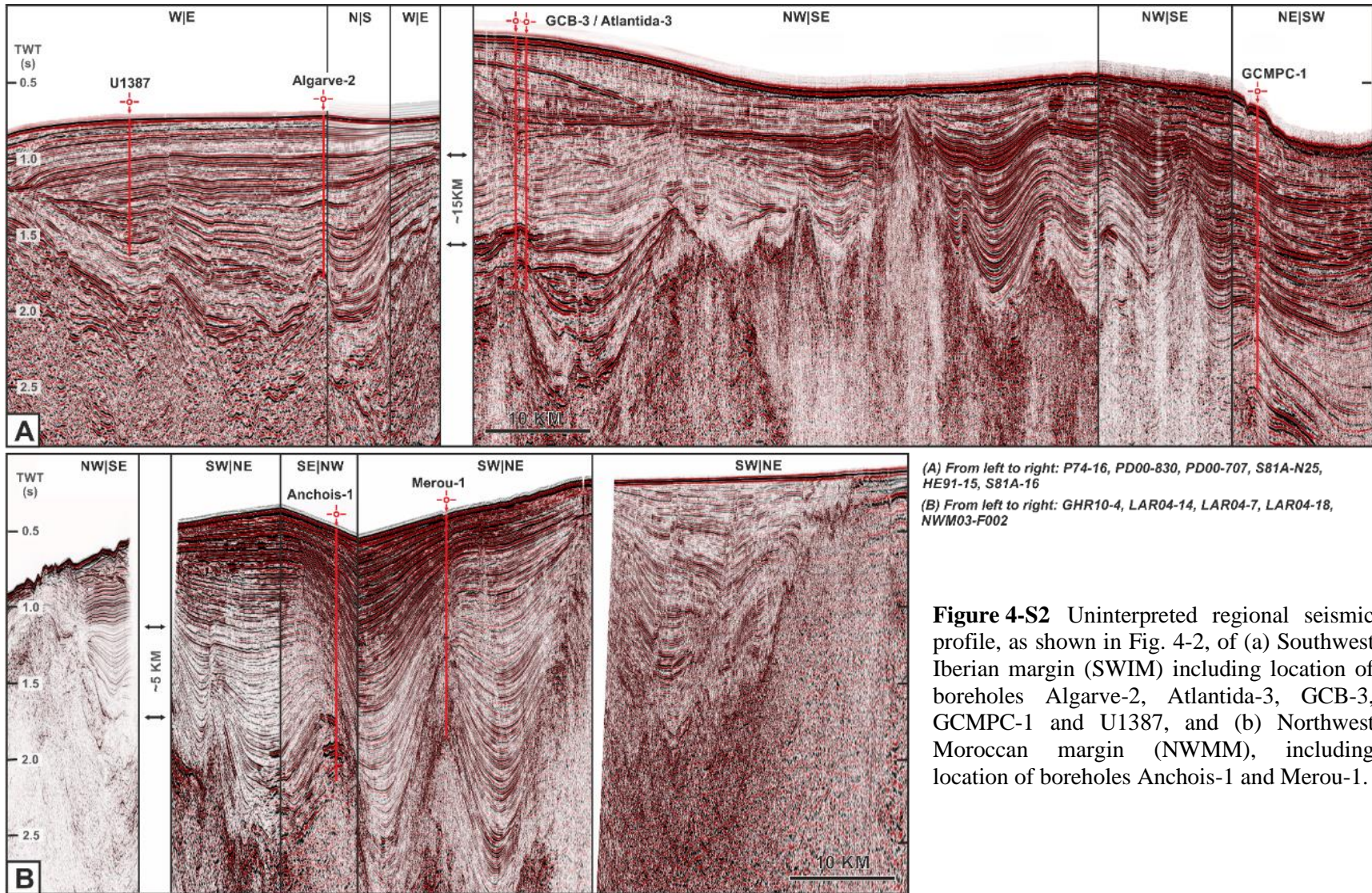
Figure 4-S2 Uninterpreted regional seismic profile, as shown in Fig. 4-2, of (a) Southwest Iberian margin (SWIM) including location of boreholes Algarve-2, Atlantida-3, GCB-3, GCMPC-1 and U1387, and (b) Northwest Moroccan margin (NWMM), including location of boreholes Anchois-1 and Merou-1.

(A) From left to right: P74-16, PD00-830, PD00-707, S81A-N25, HE91-15, S81A-16

(B) From left to right: GHR10-4, LAR04-14, LAR04-7, LAR04-18, NWM03-F002
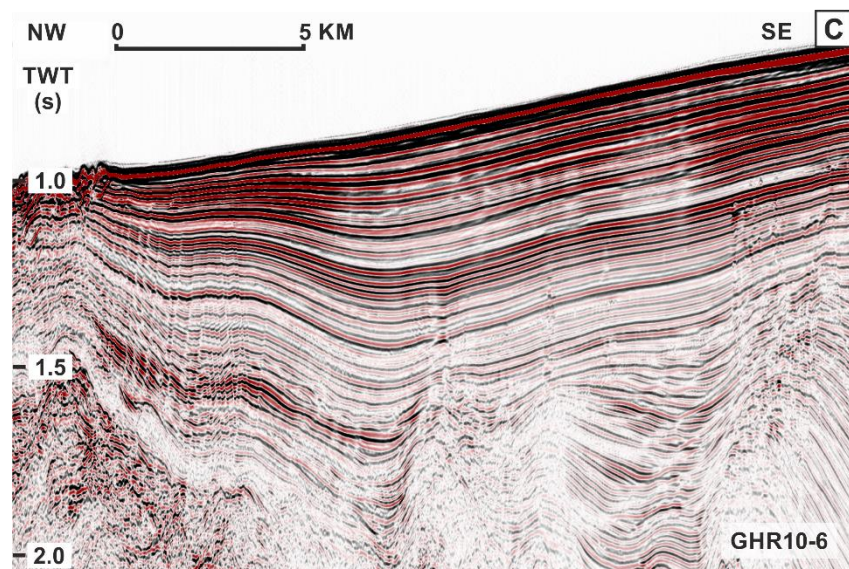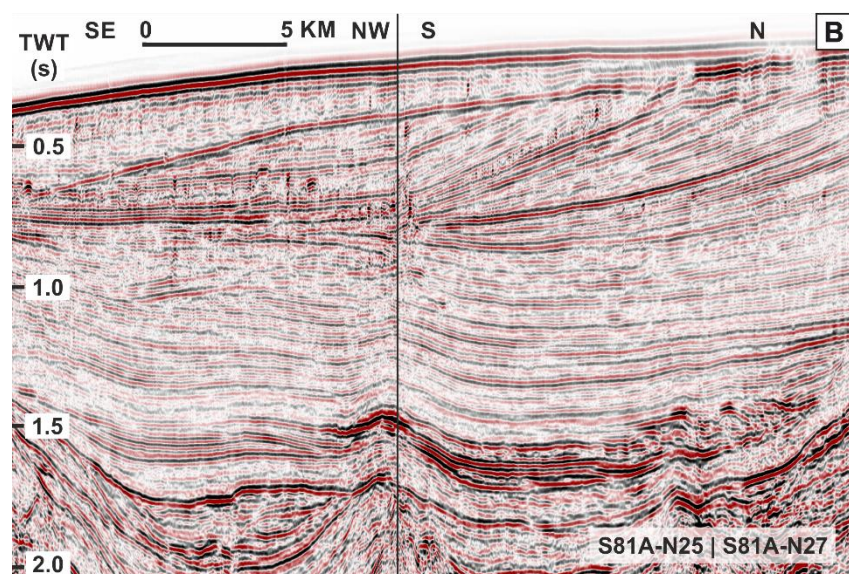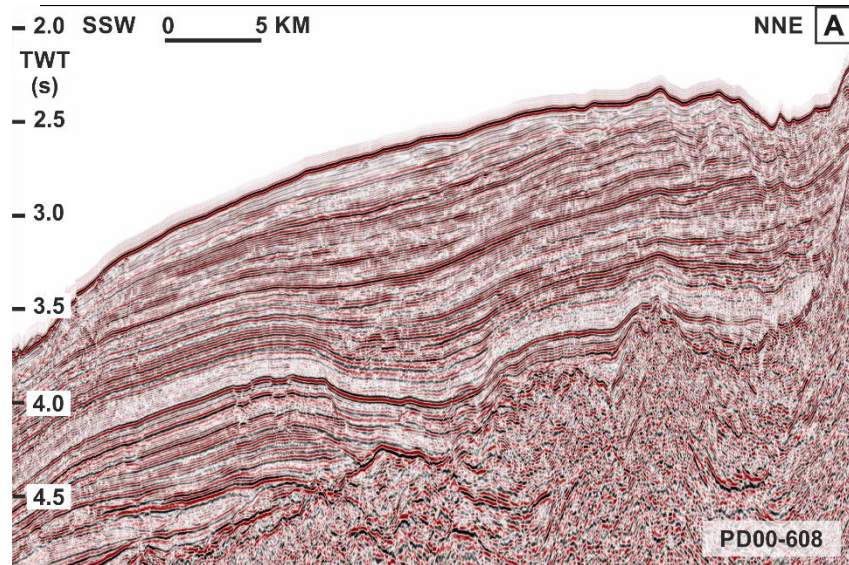
Figure 4-S3 Uninterpreted seismic profiles as shown in Fig. 4-3, across (a) southern West Iberian margin (WIM): PD00-608; (b) Southwest Iberian margin (SWIM): S81-N27 and S81-N25; and (c) Northwest Moroccan margin (NWMM): GHR10-6.

Planktonic foraminifera biohorizon / cyclo-stratigraphic correlation (*)	Age of event (Ma)	References	Borehole mean depth (mbsl)							
			Algarve-2 (10)	Anchois-1 (11)	Atlantida-3 (12)	Deep Thon-1 (11)	GCB-3 (12)	GCMPC-1 (13)	Merou-1 (11)	U1387 (14)
Measured Depth (MD) datum (KB/RT/SF)			*-15.24*	*-23.70*	*-13.70*	*-18.30*	*-9.50*	*-15.24*	*-18.30*	*558.40*
Seafloor	0		539.8	387.58	139.00	126.00	122.50	489.51	317.70	558.40
LO *G. puncticulata*	2.41	(1)					610.50			
LO *G. altispira*	3.17	(1)			856.30					
LO *Sphaeroidinellopsis*	3.19	(1)			856.30	556.70	765.50		981.70	
LO *G.margaritae*	3.85	(2)		1026.30	981.30			1220.76		1193.00
LaO/LCO *G.margaritae*	3.98	(1)			1021.30	636.70	848.00		1076.70	
FO *G. puncticulata*	4.52	(2)				646.70		1445.76	1116.70	1189.22
Influx *G. menardii*	5.31, 5.32	(1, 3)								1310.25
Influx sin. coiled *N. acostaensis*	5.30, 5.32	(1, 4)								1367.27
Miocene-Pliocene boundary*	**5.33**	**(5)**	**1442.76**	**1696.30**		**661.70**	**1270.50**	**1695.76**	**1176.70**	**1384.40**
FaO G. margaritae	5.80	(6)				996.70			1392.20	
FCO *G. margaritae*	6.05	(7)					1370.50			
FO *G. margaritae*	**6.31-6.35**	**(7)**		**2095.30**			**1375.50**	**1810.76**		
LRO *G. miotumida* (sin)	**6.31**	**(6)**			**1407.80**		**1375.50**	**1810.76**		
LaO *G. miotumida* (sin)	**6.35**	**(6)**				**1546.70**			**1777.70**	
Sin. to dx. coiling change *N. acostaensis*	**6.37**	**(2, 6)**			**1426.80**	**1546.70**	**1415.50**			
LO *G. menardii 5* (dx)	7.24	(8)			1676.30	1766.70	1690.50			
FCO *G. menardii 5* (dx)	7.35	(8)			1691.30		1705.50			
LCO *G. menardii 4* (sin)	7.51	(8)			1696.30		1710.50			
Basal Foredeep Unconformity (BFU)	~8.2	(9)			1746.30		1747.50			

References: (*1*) Lourens et al., 1996; (*2*) Lourens et al., 2004; (*3*) van der Laan et al., 2006; (*4*) Iaccarino et al., 1999; (*5*) Sierro et al., 2000; (*6*) Krijgsman et al., 2004; (*7*) Sierro et al., 2001; (*8*) Hilgen et al., 1995; (*9*) Maldonado et al., 1999; (*10*) Hernández-Molina et al., 2016; (*11*) Repsol S.A., 2013; (*12*) Ledesma, 2000; (*13*) Hernández-Molina et al., 2014; (*14*) van der Schee et al., 2016

Table 4-S1 Bio- and cyclo-stratigraphic dating using planktonic foraminifera biohorizon and astronomical forced climate cycle in boreholes: Algarve-2, Atlantida-3, GCB-3 (Golfo de Cádiz B-3), GCMPC-1 (Golfo de Cádiz Mar Profundo-1) and U1387, with age events corrected to mean depth in mbsl (meters below sea level). (Key: FCO; first common occurrence; FO – first occurrence; LaO – last abundant occurrence; LCO – last common occurrence; LO – last occurrence; LRO – last regular occurrence; dx – dextral; sin – sinistral; KB – 115elly bushing; RT – rotary table; SF – seafloor.

Chapter 5

Late Miocene Contourite Depositional System of the Gulf of Cádiz: The sedimentary signature of the paleo-Mediterranean Outflow Water

Zhi Lin Ng, F. Javier Hernández-Molina, Débora Duarte, Cristina Roque, Francisco J. Sierro, Estefanía Llave, M. Amine Manar, 2021. Late Miocene Contourite Depositional System of the Gulf of Cádiz: The sedimentary signature of the paleo-Mediterranean Outflow Water. Marine Geology 442, 106605. Doi:10.1016/j.margeo.2021.106605
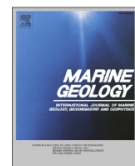
Late Miocene contourite depositional system of the Gulf of Cádiz: The sedimentary signature of the paleo-Mediterranean Outflow Water

Late Miocene Contourite Depositional System of the Gulf of Cádiz: The sedimentary signature of the paleo-Mediterranean Outflow Water

Zhi Lin Ng[1*], F. Javier Hernández-Molina[1], Débora Duarte[1,2], Cristina Roque[3,4], Francisco J. Sierro[5], Estefanía Llave[6], M. Amine Manar[7]

[1]Department of Earth Sciences, Royal Holloway University of London, Egham TW20 0EX, UK
[2]Instituto Português do Mar e da Atmosfera (IPMA), 1749-077 Lisboa, Portugal
[3]Estrutura de Missão para a Extensão da Plataforma Continental (EMEPC), 2770-047 Paço de Arcos, Portugal
[4]Instituto Dom Luiz (IDL), Faculdade de Ciência da Universidade de Lisboa, 1749-016 Lisboa, Portugal
[5]Departamento de Geología, Universidad de Salamanca, 37008 Salamanca, Spain
[6]Instituto Geológico y Minero de España (IGME), 28003 Madrid, Spain
[7]Office National des Hydrocarbures et des Mines (ONHYM), B.P. 99 Rabat, Morocco
*Corresponding author: Zhi Lin Ng (Zhi.Ng.2016@live.rhul.ac.uk)

Abstract

Late Miocene contourite deposits related to the paleo-Mediterranean Outflow Water (MOW) were identified in the Betic and Rifian corridors prior to the restriction of the Mediterranean-Atlantic gateway during the latest Miocene. In this study, we identified for the first time their downstream continuation in the Gulf of Cádiz through seismic stratigraphic analysis and the interpretation of contourite diagnostic features. The late Miocene contourite depositional system (CDS) consists of three stages (*initial-, growth-,* and *maintenance-drift)* which recorded the late Tortonian to early Messinian evolution from weak to vigorous bottom current flow in the Gulf of Cádiz prior to its cessation in the middle to late Messinian, represented by the *buried-drift* stage. Development of the CDS in the Gulf of Cádiz is coeval to a period when the continental margins were affected by regional deformation. Tectonism and diapirism, on top of sedimentary and climatic factors, exerted control on drift distribution and dimensions. However, dataset limitations hindered detailed analysis on the effect of deformation on CDS evolution. Overall, the long-term evolution of the late Miocene CDS across the Gulf of Cádiz towards the West Iberian margin suggests strengthening of paleo-MOW during the late Miocene which has significant impact on the North Atlantic Ocean circulation and the late Miocene global cooling trend.

Keywords: contourite depositional system, late Miocene, paleo-MOW, tectonic deformation, Gulf of Cádiz, North Atlantic

Introduction

Contourites provide valuable information for oceanographic and climatic changes of the past through the retainment of sedimentological, paleontological, and geochemical properties related to the temporal and spatial variability in ocean circulation patterns (Rebesco et al., 2014). One of the key diagnostic criteria of a contourite depositional system (CDS) is the identification of depositional and erosional features through the interpretation of morphological features and acoustic facies using seismic reflection data (e.g., Faugères et al., 1999; Nielsen et al., 2008; Rebesco et al., 2014). However, tectonic evolution of the continental margin and the degree of deformation imposed on original deposits throughout the geological history could complicate the identification of these features, particularly for ancient contourite records. Moreover, in active tectonic settings, syn-tectonic deformation also plays an important role in controlling the morphology and stacking pattern of contourite deposits (e.g., Reed et al., 1987; Bailey et al., 2021). It modifies the typical configuration of contourite drifts, making their identification difficult and thus remains as one of the less studied issues in contourite research.

The Gulf of Cádiz is home to one of the best-known examples of contourite depositional systems in the world, where its Pliocene and Quaternary sedimentary succession have been studied in detail, particularly during and after the International Ocean Drilling Program (IODP) Expedition 339 (Expedition 339 Scientists, 2012; Hernández-Molina et al., 2013; Stow et al., 2013). This Pliocene-Quaternary CDS evolved along the Southwest Iberian margin as a consequence of the Mediterranean Outflow Water (MOW) exiting through the Strait of Gibraltar (or Gibraltar gateway) from the early Pliocene to the present (Hernández-Molina et al., 2016). This configuration was established since the reopening of the Mediterranean-Atlantic exchange following the end of the Messinian Salinity Crisis (5.97–5.33 Ma) (Flecker et al., 2015; Manzi et al., 2018). Prior to the middle to late Messinian restriction of the Mediterranean basin (Ng et al. 2021), the exchange of water-mass between the Mediterranean and the Atlantic took place through the Betic and Rifian corridors (or gateways) during the late Tortonian to early Messinian (Krijgsman et al., 2018). This notion was substantiated through the identification of contourite deposits bearing the signature of the paleo-MOW, in the outcrops along the corridors onshore south of Spain and north of Morocco, respectively (Martin et al. 2009; Capella et al., 2017a; de Weger et al. 2020). However, the downstream continuation of this late Miocene CDS in the Gulf of Cádiz towards the West Iberian margin has yet to be

located. The ancient contourite deposits in the onshore Betic-Rif chain, including the foreland and intramontane basins (Martin et al., 2009; Capella et al., 2017a), are only able to give a glimpse of the bigger picture of the paleo-MOW evolution through fieldwork observation of small- to medium-scale features where permitted by outcrop exposure (Rebesco et al., 2014). Whereas, unearthing the subsurface system offshore in the Gulf of Cádiz with the use of seismic reflection data will provide an opportunity for the comprehension of its wider regional implications, including insights into the evolution of the paleo-MOW circulation after its exit from the Mediterranean and its influence on the North Atlantic paleoceanography and paleoclimate during the Tortonian to Messinian stages, where it is thought to have a significant contribution to the global climate cooling of the late Miocene (Capella et al., 2019).

The criteria for the recognition of the large scale CDS features have been established in the literature, generally for examples within undeformed modern passive continental margins (Faugères et al., 1999, Hernández-Molina et al., 2008). Howbeit, there is a lack of guidelines for the diagnosis of ancient contourites which require paleogeographic and tectonic reconstructions (Hüneke and Stow, 2008), especially for tectonically active margins such as the Southwest Iberian margin and the Northwest Moroccan margin (Gràcia et al., 2003; Vergés and Fernàndez, 2012). In the Gulf of Cádiz, tectonic deformation due to the Betic-Rif orogeny have largely disturbed stratifications and modified original depositional structures, making geometric reconstruction of contourite drift bodies very difficult. Regional scale tectonic deformations are responsible for the modifications of basin shape and the connectivity among basins or sub-basins (Verdicchio and Trincardi, 2008), by creating structural highs including fault bocks, anticlines, sills and or diapiric ridges, which has a significant impact on the bottom current circulation (Pellegrini et al., 2016; Duarte et al., 2020). With access to regional seismic reflection data integrated with borehole data in the study area, we could constrain the main tectonic evolution stages of the margin by implementing stratigraphic, structural and paleogeographic reconstructions. The main objectives of this contribution are a) to describe the characteristics and to analyse the distribution of the late Miocene CDS in the Gulf of Cádiz; b) to infer the evolution of the paleo-MOW circulation and the Mediterranean-Atlantic exchange from the characterization of the late Miocene CDS; and c) to evaluate the control factors for contourite deposition in an active continental margin. We also highlighted the implications and limitations for the interpretation of the identified late Miocene CDS.

Regional Setting

Geological framework

The Gulf of Cádiz is located in the Atlantic side of the Mediterranean-Atlantic exchange, off the Strait of Gibraltar (Fig. 5-1). It is surrounded by the Southwest Iberian margin and the Northwest Moroccan margin. Tectonically, the Gulf of Cádiz lies on the eastern convergent segment of the Azores Gibraltar Fracture Zone, the plate boundary which separates the Iberian part of the Eurasian plate and the Nubian part of the African plate (Vergés and Fernàndez, 2012). The continental convergence between Iberia and Africa since the Late Cretaceous led to the formation of the Betic-Rif orogenic system in the middle Miocene, collectively known as the Gibraltar Arc (*sensu* Flinch, 1993), which includes, besides the Betic and Rif chain, the Alboran back-arc and the Guadalquivir and Gharb foreland basins (Vergés and Fernàndez, 2012). An eastward-dipping subduction and westward rollback of a remnant Tethyan oceanic lithosphere saw the westward migration of the Gibraltar Arc from the early to middle Miocene, which developed the Gulf of Cádiz accretionary wedge (GCAW; *sensu* Duarte et al. 2011) (Fig. 5-1). Mantle flow dynamics related to the subducted slab caused surface uplift of the Gibraltar Arc to achieve isostatic equilibrium (Duggen et al., 2003; Civiero et al., 2020). Gravitational collapse of the overthrusted imbricated accretionary wedge produced radial emplacement of the chaotic allochthonous unit of the Gulf of Cádiz (AUGC; *sensu* Medialdea et al., 2004). It was emplaced westwards from the deformation front of the accretionary wedge (Fig. 5-1) towards the Horseshoe and Seine abyssal plains (Maldonado et al., 1999; Medialdea et al., 2004) until the late Tortonian (7–8 Ma; Gràcia et al., 2003). New wedges were successively emplaced advancing westward from the tectonic reactivation of the allochthonous unit as a result of NE-SW late Miocene thick-skinned compression (Medialdea et al., 2004), with coeval extensional collapse on the back (Maestro et al., 2003). In the Horseshoe Abyssal plain (Fig. 5-1), the chaotic unit is called the Horseshoe Gravitational Unit (*sensu* Iribarren et al., 2007), its tectonic and gravitational domains cannot be clearly differentiated. Overall, its gravitational-derived material is sourced from the AUGC, to the east, and the surrounding basement highs (Fig. 5-1) such as the Gorringe bank and the Coral Patch ridge (Torelli et al., 1997; Iribarren et al., 2007).

Figure 5-1 Geological map showing the main structural units of the Betic-Rif orogeny (AUGC: allochthonous unit of the Gulf of Cádiz; GCAW: Gulf of Cádiz accretionary wedge), tectonic features of the Gulf of Cádiz (AH: Albufeira high; CF: Cádiz fault; CPS: Coral Patch seamount; DS: Descobridores seamount GB: Guadalquivir bank; GEF: Gil Eanes fault; GF: Grandola fault; HAP: Horseshoe abyssal plain; HF: Horseshoe fault; HGU: Horseshoe Gravitational Unit; MPF: Marquês de Pombal fault; MPP: Marquês de Pombal plateau; PAS: Príncipe de Avis seamount; PDE: Pen Duick escarpment; PF, Portimão fault; PH: Portimão High: PSF: Pereira de Sousa fault; SAP: Seine abyssal plain; SMQF: São Marcos-Quarteira fault; SVF: São Vicente fault; TAP: Tagus abyssal plain), associated Neogene sedimentary basins (AlB: Alentejo basin; DAB: Deep Algarve basin; DB: Doñana basin; CB: Cádiz basin; OGB: Offshore Gharb basin; RdLB: Rincão do Lebre basin; SB: Sanlúcar basin) and sedimentary features (FC: Faro canyon; LC: Lagos canyon; PC: Portimão canyon; SC: Sagres canyon; SeC: Setúbal canyon; SVC: São Vicente canyon) (Adapted from Hernández-Molina et al., 2016).

In the central Gulf of Cádiz, this massively chaotic allochthonous unit is interbedded within the late Miocene sedimentary infill (Lopes et al., 2006; Duarte et al., 2020). The base of the late Miocene sequence is marked either by the top of the accretionary wedge (GCAW, Duarte et al., 2020) or allochthonous unit (Medialdea et al., 2004), or by the regional basal foredeep unconformity (BFU; *sensu* Maldonado et al., 1999). The top of the chaotic allochthonous unit is highly irregular due to post-emplacement mobilization of sediments by salt and shale tectonism, which forms the abundant diapiric ridges in the Gulf of Cádiz (Medialdea et al., 2009). The Gulf of Cádiz Neogene basins, including the Deep Algarve, Doñana, Sanlúcar, Cádiz and the Offshore Gharb basins (Fig. 5-1), are bounded or separated by these diapiric ridges or structural highs, which are formed by Neogene to recent halokinesis and half grabens of Mesozoic origin respectively (Ramos et al., 2017; Duarte et al., 2020). Both the Deep Algarve and Alentejo basins (in the southern West Iberian margin, Fig. 5-1) initially formed during the Mesozoic rifting related to the opening of the Tethys and North Atlantic respectively (Srivastava et al., 1990; Pereira and Alves 2013; Pereira et al., 2016; Terrinha et al., 2019a), and were since subjected to two major inversion tectonic phases linked to the Pyrenean and Betic-Rif orogenies, in the Paleogene and Miocene respectively (Terrinha et al., 2019b). The reactivation and inversion of older rift faults during the middle to late Miocene Betic paroxysm caused uplifting of the basement highs in the southern West Iberian margin (Fig. 5-1) (Torelli et al., 1997; Tortella et al., 1997; Zitellini et al., 2004; Pereira et al., 2011). At the southwest corner of the margins off the Cape of São Vicente, deep incisions of submarine canyons, such as the Portimão and São Vicente canyons (Fig. 5-1), dominated the slope. These canyons are also controlled by the steep rift-inherited faults since the onset of tectonic uplift (Terrinha et al., 2009, Pereira and Alves, 2013).

Paleoceanography and bottom current influence on sedimentation

The lithospheric uplift resulting from the compressional events in the Gibraltar Arc (Duggen et al., 2003) imposed major transformation of the Mediterranean-Atlantic water mass exchange pattern. It changed from a single wide connection until the middle Miocene into several narrow and shallow Betic and Rifian corridors in the late Miocene (Capella et al., 2019). This evolution saw the importance of the outflowing intermediate water mass from the Mediterranean into the Atlantic, known as paleo-Mediterranean Outflow Water (MOW), and the formation of the Atlantic Mediterranean Water (AMW; sensu Rogerson et al., 2012) by mixing with ambient Atlantic water in the corridors (Martin et al., 2009; de Weger et al., 2020)

and by the Guadalquivir and Gharb basins (Perez-Asensio et al. 2012; Capella et al., 2017a). Continuous uplifting of the Betif and Rif corridors raised the flow velocity of the paleo-MOW, and as a consequence sandy contourites were deposited (Capella et al., 2019) and eventually closed the Mediterranean-Atlantic exchange, leading to the restriction of paleo-MOW. Subsequently, Messinian Salinity Crisis evaporites were deposited in the Mediterranean, simultaneous to widespread deposition of hemipelagites in the Gulf of Cádiz (Flecker et al., 2015; Ng et al., 2021). The Guadalquivir and Gharb basins were thus reduced to marine embayment areas with the closure of the late Miocene gateways towards the east (Martin et al., 2009; Ivanovic et al., 2013). Following the reopening of the Mediterranean-Atlantic exchange through the Strait of Gibraltar, the Pliocene to Quaternary sedimentary evolution of the Gulf of Cádiz was dominated by bottom current circulation of the MOW and distribution of the resulting Pliocene-Quaternary contourite depositional system (CDS) along the Southwest Iberian margin (Hernández-Molina et al., 2016), the southern West Iberian margin (Rodrigues et al., 2020) and towards the North Iberian margin in the southern Bay of Biscay (Liu et al., 2020). The onset of the weak MOW since the end of the Messinian Salinity Crisis produced a regional unconformity across the Gulf of Cádiz and the West Iberian margin (van der Schee et al., 2016; Ng et al., 2021). The Miocene Pliocene boundary (MPB, 5.33 Ma; sensu Hernández-Molina et al., 2016) separates the Miocene.

The Pliocene Quaternary CDS has been studied in detail for the Southwest Iberian margin (Llave et al., 2011; Roque et al., 2012; Hernández-Molina et al., 2016) and southern West Iberian margin (Rodrigues et al., 2020). The evolution of the Gulf of Cádiz CDS in the Southwest Iberian margin was primarily influenced by tectonics, eustasy and climate, at varying temporal scales, and can be summarised into three stages: an initial-drift stage with weak MOW and large sheeted or mixed drift during the early Pliocene (5.33–3.2 Ma); a transitional-drift stage with MOW intensification, upslope migration and moat development from late Pliocene to early Quaternary (3.2–2 Ma); and a growth-drift stage involving further MOW strengthening with elongated mounded or sandy sheeted drifts from late Quaternary to the present (<2 Ma), separated by major hiatuses (Hernández-Molina et al., 2016). Furthermore, the relationship between sedimentary deposition and tectonic activity is reflected in the overlapping distribution of the morphosedimentary (Hernández-Molina et al., 2003) and tectonosedimentary domains (Duarte et al., 2020). Tectonic structures such as diapiric ridges and basement highs separated the Neogene basins in the Gulf of Cádiz and split up the MOW

pathways into two main cores: a warmer and less saline upper core (MU: 500–800 m; 13–14 °C and 35.7–37‰); and a colder and more saline lower core (ML: 800–1400 m; 10.5–11.5 °C and 36.5–37.5‰) (Ambar and Howe, 1979; Llave et al., 2007, García et al., 2009). The latter further splits into three branches: intermediate, principal, and southern (Louarn and Morin, 2011), as it descends across the middle slope northward, due to Coriolis deflection. Driven by density, the MOW sinks after flowing over the Camarinal Sill of the Strait of Gibraltar, mixing with the Atlantic ambient water (O'Neill-Baringer and Price, 1997; Sánchez-Leal et al., 2017) to form the AMW (Rogerson et al., 2012). It achieves neutral buoyancy as it reaches the Cape São Vicente and settles at a depth of ~1400 m above the North Atlantic Deep Water (NADW) (Hernández-Molina et al., 2016). In the southern West Iberian margin, the Sines contourite drift is deposited in the Alentejo basin coevally with the Gulf of Cadiz CDS. Yet the three-stage evolution differs slightly, starting with an initial stage of weak MOW and sheeted drift until the late Pliocene (5.33–2.5 Ma); followed by a growing stage of strengthening MOW and mounded drift from early to middle Quaternary (2.5–0.7 Ma); and ending with a maintenance stage from middle Pleistocene to present (<0.7 Ma), characterised by phases of MOW intensification with higher sedimentation rates, and a shift to a plastered drift stacking pattern (Rodrigues et al. 2020). At the Northwest Moroccan margin, a predominantly hemipelagic environment during the Pliocene is consistent with the absence of the MOW since the reopening of the Mediterranean-Atlantic connection through the Strait of Gibraltar. However, younger Quaternary contourite deposits with distinct evolutionary phases were identified around the Pen Duick escarpment (Fig. 5-1) (Vandorpe et al., 2014; Vancraeynest, 2015). These sediments were deposited under the recent influence of the Antarctic Intermediate Water (AAIW), with the absence of MOW in the southern part of the Gulf of Cadiz since the Pliocene (Vandorpe et al, 2014).

Methodology

Dataset

We compiled an integrated dataset of seismic reflection and borehole data from within the Gulf of Cádiz to the southern West Iberian margin (Fig. 5-2). The seismic data include two-dimensional (2D) multi-channel seismic reflection (MCS) profiles in time domain (TWT – two way travel time) from 8 surveys: GC-D, GHR10, HE91, LAR04, NWM03, P74, PD00, PDT00,

S81A, TASYO2000 (Fig. 5-2); as well as 2 three-dimensional (3D) post stack time migrated (PSTM) seismic surveys, including Calypso-1 and Calypso-2, acquired from industry or academic projects and cruises predominantly with an airgun array seismic source, processed to common depth point and stacked, and time migrated using standard procedures (Maldonado et al., 1999; Llave et al., 2011; Roque et al., 2012; Brackenridge et al., 2013; Hernández-Molina et al., 2016). Acquisition parameters for seismic surveys are available in Supplementary Material (Table 5-S1). The borehole data are from exploration wells including Algarve-2, Anchois-1, Atlantida-3, Deep Thon-1, Golfo de Cádiz B-3 (GCB-3), Golfo de Cádiz Mar Profundo C-1 (GCMPC-1), Merou-1, Neptuno-1, Neptuno-2; and the International Ocean Drilling Program Expedition 339 scientific sites (Expedition 339 Scientists, 2012; Hernández-Molina et al., 2013; Stow et al., 2013), including U1396, U1387, U1388, U1389, U1390, and U1391 (Fig. 5-2).
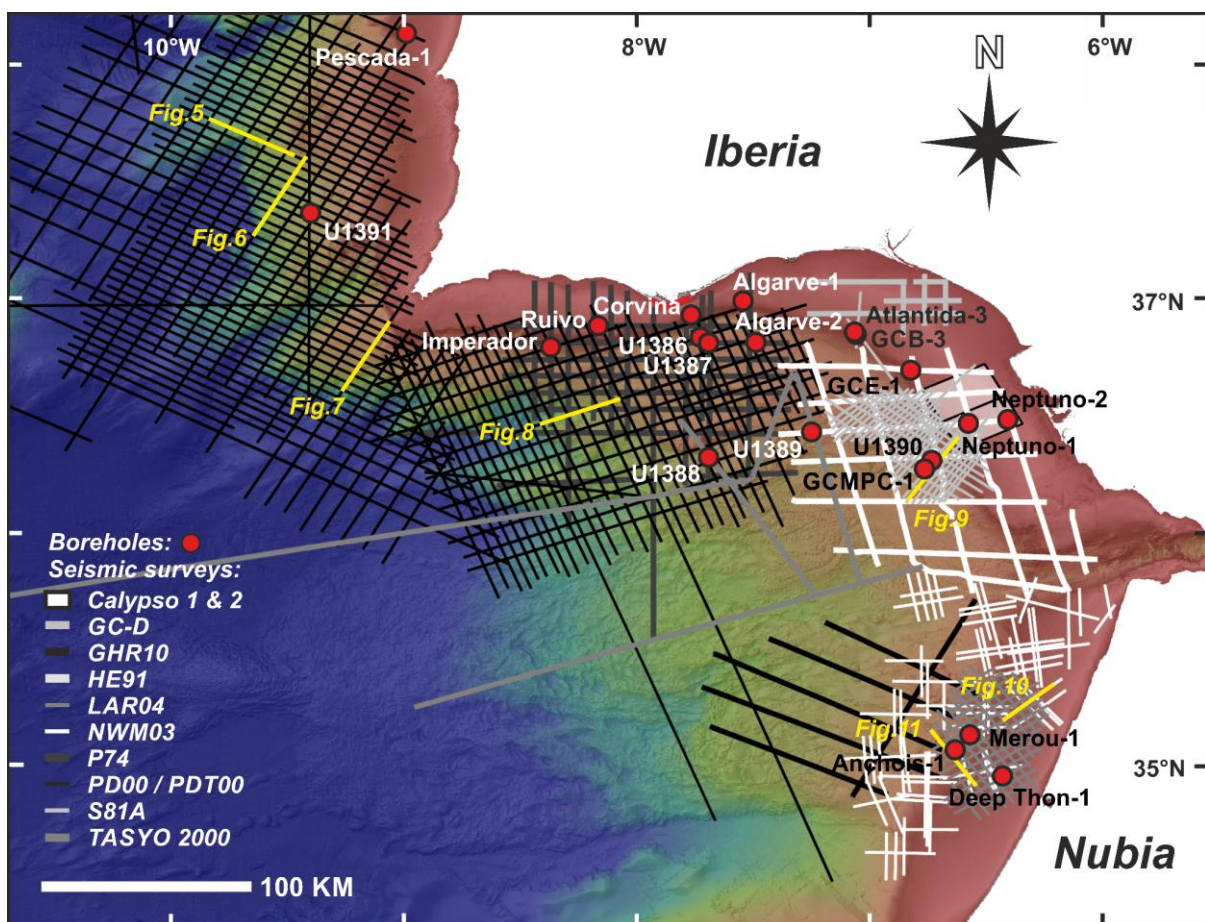
Figure 5-2   Map of the dataset (including seismic surveys, boreholes, and bathymetry).

Methods

We utilised an array of seismic attribute analyses involving signal processing and structural methods, in the order of structural smoothing with dip-guided wedge enhancement, Butterworth band-pass frequency filter (lower slope: 18 dB, 8 Hz; upper slope: 72 dB, 36 Hz), and the second derivative of the trace envelope, available at Schlumberger's Petrel E&P software platform to assist in the interpretation workflow by enhancing edges/faults and continuity of seismic events, removing noise, and identifying all reflecting interfaces within the seismic bandwidth. We then carried out the seismic stratigraphic analysis of the Gulf of Cádiz Neogene basins following Mitchum et al. (1977) in distinguishing seismostratigraphic units by seismic facies and boundaries, assigning geologic ages based on correlation with biostratigraphic information acquired from borehole data (summarised in Fig. 5-3). Afterwards, structure and isopach mapping of the major seismic discontinuities and their intervals was done to briefly reconstruct the regional paleogeography and to identify the distribution pattern of the seismic unit, respectively. The maps were generated using the Petrel E&P software with a grid increment of 50 m for both X and Y dimensions and surface operation smoothing parameters including: number of iterations – 3; filter width – 3.

The seismic interpretation was facilitated by diagnostic criteria for the recognition of contourites introduced by Faugères et al. (1999) and Nielsen et al. (2008), and the identification of depositional (drifts) and erosional (channels, furrows, moats, scours) features related to bottom current action (Hernández-Molina et al., 2008; García et al., 2009; Rebesco et al., 2014). The interpreted seismic features were compared in terms of their acoustic character and distribution against other deposits of other deep-water sedimentary process, e.g., gravity flow deposits including turbidites and mass transport deposits (MTDs) (Posamentier and Erskine, 1991; Stow and Smillie, 2020), and pelagites or hemipelagites. Interactions of multiple processes to produce mixed or hybrid deposits were taken into consideration, as reported for a modern example in the Southwest Iberian margin (Brackenridge et al., 2013; Teixeira et al., 2019; de Castro et al., 2020; Serra et al., 2020). Finally, we analysed these features to unravel the influence of the paleo-Mediterranean Outflow Water (MOW) on the sedimentary evolution of the middle slope of the Southwest Iberian, Northwest Moroccan, and the southern West Iberian margins, and compare them to modern and ancient analogues in the region (Llave et al., 2001; 2007; 2011; Roque et al., 2012; Hernández-Molina et al., 2016; Teixeira et al., 2019; de Weger et al., 2020; Mencaroni et al., 2020; Rodrigues et al., 2020). We also listed the limitations and suggestions for further study in Supplementary Material (Text S1).
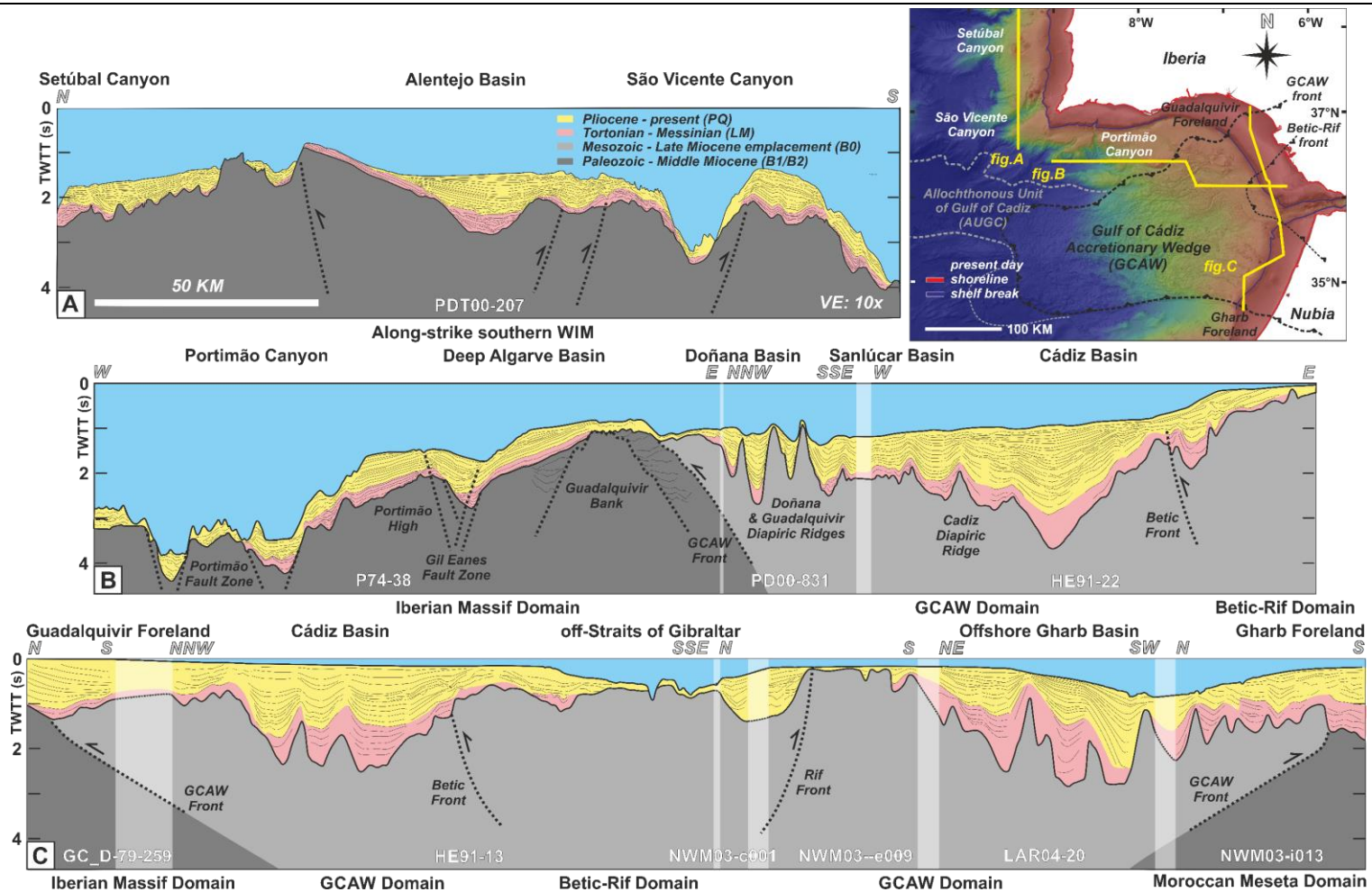
Figure 5-3 Regional profiles of the study area showing the distribution of the Neogene sedimentary basins (Alentejo basin, Cádiz basin, Deep Algarve basin, Doñana basin, Offshore Gharb basin, Sanlúcar basin), tectonic domains (Betic-Rif orogeny, Gulf of Cádiz accretionary wedge, Iberian Massif, Moroccan Meseta and West Iberian passive margin) and seismic units (PQ, LM and B): a. N-S southern West Iberian margin (WIM), b. W-E Gulf of Cádiz, c. N-S Gulf of Cádiz.

Nomenclature

The nomenclature adopted to describe the main seismic sequences, units, subunits, and discontinuities (Fig. 5-4) are adapted from previous studies (Maldonado et al., 1999; Lopes et al., 2006; Llave et al., 2011; Roque et al., 2012; Hernández-Molina et al., 2016; Rodrigues et al., 2020). They reflect the age of the intervals (e.g., PQ – Pliocene-Quaternary, LM – late Miocene). This study focuses on the late Miocene interval, previously identified as Units M2 and M1 of Maldonado et al. (1999) and Unit E of Lopes et al. (2006). The subunits (M3, M2 and M1) in this study were labelled according to their stratigraphic position from top to bottom. The Miocene-Pliocene boundary (MPB) and basal foredeep unconformity (BFU) were previously described in detail by Hernández-Molina et al. (2016) and Maldonado et al. (1999) respectively, whereas the allochthonous unit of the Gulf of Cádiz (AUGC) was described by Medialdea et al. (2004). Two new discontinuities were introduced in this study (Fig, 5-4), namely the intra-Messinian unconformity (IMU) and the intra-Tortonian unconformity (ITU). The ITU is differentiated from the BFU due to the contrast in genetic origin of their respective margins since the Miocene (inverted passive southern West Iberian margin versus foreland basin of the active Southwest Iberian margin).

The term contourites refers to "sediments deposited or substantially reworked by the persistent action of bottom currents", whereas bottom currents refer to "any persistent water current near the seafloor" (sensu Rebesco et al., 2014). A contourite drift is a "large accumulation of sediments by bottom currents", which are classed based on their variation in location, morphologies, size, sediment patterns, construction mechanisms and controls (Faugères and Stow, 2008; Hernández-Molina et al., 2008; Rebesco et al., 2014). Whereas a contourite depositional system (CDS) is referred to as "the association of various drifts and related erosional features", and could occur interbedded with other deep-water facies type, such as turbidites, pelagites and mass transport deposits (Hernández-Molina et al., 2008; Rebesco et al. 2014, de Castro et al., 2021).
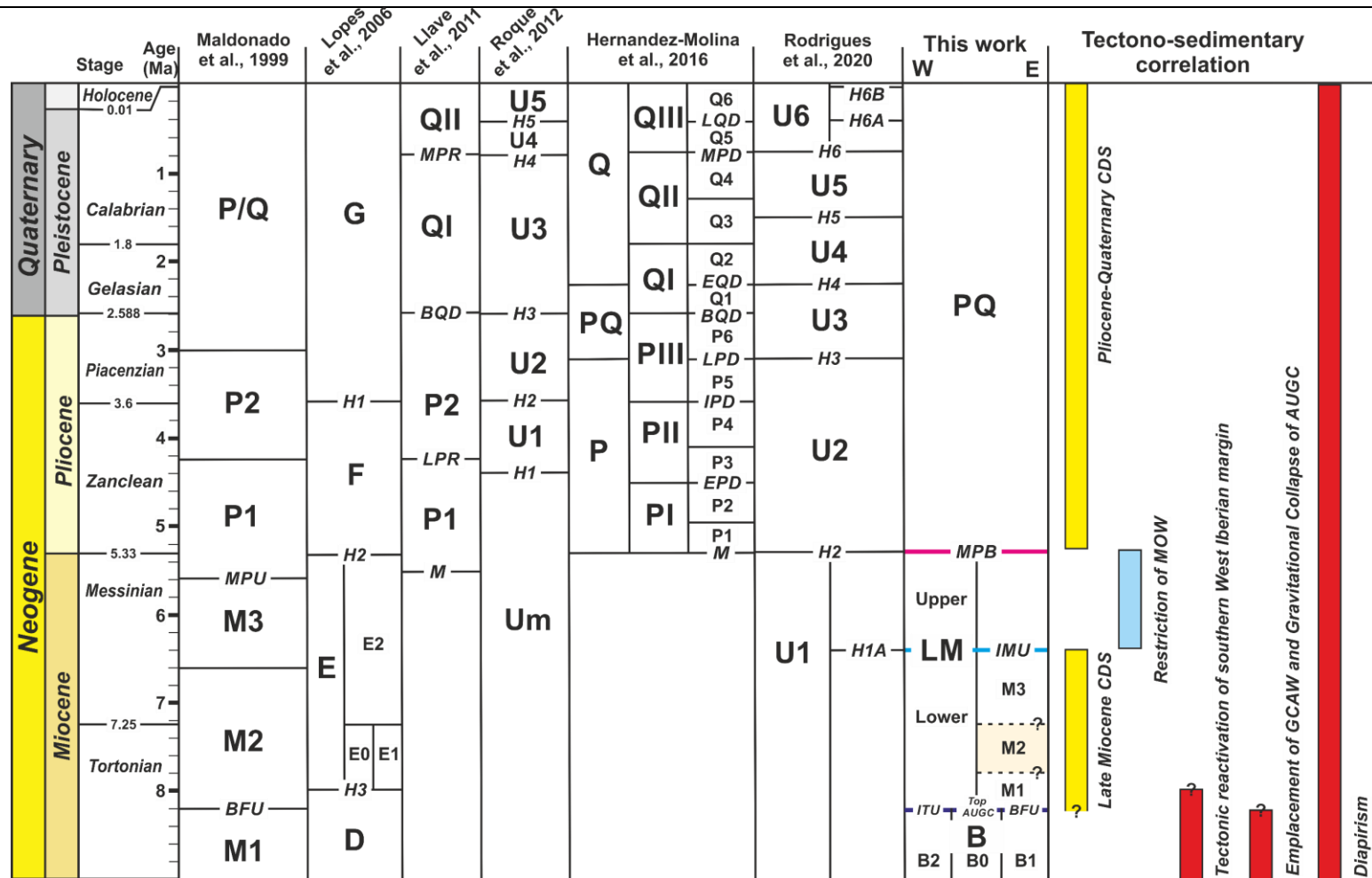
Figure 5-4 Stratigraphic correlation of the main sequences (PQ, LM, B), units (Upper and Lower LM) and sub-units (M1, M2 and M3) described in the present work, including stratigraphic correlations interpreted by previous authors and main tectonic and sedimentary events in the region (Abbreviation for discontinuities, BFU: basal foredeep unconformity; IMU: intra-Messinian unconformity; ITU; intra-Tortonian unconformity; MPB: Miocene-Pliocene boundary; Top AUGC: top allochthonous unit of the Gulf of Cádiz).

Results

Seismic analysis: units and boundaries

The study area is divided into three different sectors: a) the Neogene basin of the West Iberian margin, including the Alentejo basin (Fig. 5-3a); b) the Betic foreland basin in the northern and northwestern Gulf of Cádiz, which includes the Deep Algarve basin (Fig. 5-3b); and c) the wedge top basins in the central Gulf of Cádiz, taking in the Doñana, Sanlúcar, Cádiz and Offshore Gharb basins (Fig. 5-3c). We identified three main regional seismic sequences from seismic analysis of all three sectors, correlated to the biostratigraphic information from the borehole (from oldest to youngest): a) Pre-late Miocene, which is distinct for three sectors (B0, B1 and B2); b) Tortonian to Messinian (LM), divided into Upper and Lower LM unit; and c) Pliocene to present (PQ) (Figs. 5-3 and 5-4). Their descriptions are summarized in Table 5-1.

The distribution of the seismic sequence LM, shown in Figure 5-3 and 5-5, varies across the three different sectors, being thicker in the Cádiz and Offshore Gharb basin, averaging ~1 s TWT, and up to ~1.5–2s TWT in the central part of the Offshore Gharb basin. This unit can also be found sparsely distributed within the middle slope of the offshore Betic foreland basin and the southern West Iberian margin on flatter slopes or terraces, or within canyons and valleys; otherwise, it is only thinly draped over basement highs or truncated against the younger seismic unit PQ (Fig. 5-3). The presence (or absence) of the Lower LM unit is largely responsible for the variability of the distribution of seismic sequence LM across the different sectors, which can reach up to 0.5 s in the Betic foreland basin and the southern West Iberian margin, and over 1.0 s TWT in the Cádiz and Offshore Gharb wedge top basins (Fig. 5-5). The Lower LM unit is divided into sub-units of distinct seismic facies (Fig. 4). The basal surface of seismic sequence LM is represented by the combination of Top AUGC (allochthonous unit of the Gulf of Cádiz), BFU (basal foredeep unconformity) and ITU (intra-Tortonian unconformity) horizons in their respective sectors (Fig. 5-6b, 5-7 to 5-13). Above the basal surface, an older interval (sub-unit M1) of transparent or low- amplitude discontinuous to semi-continuous facies can be observed mainly in the offshore Betic foreland and wedge top basins of the Gulf of Cádiz above the BFU or Top AUGC (Figs. 5-10 to 5-13). Similar facies are interspersed in the southern West Iberian margin above the ITU, in the basin centre or towards the lower slope (Figs. 5-7 and 5-8). Above sub-unit M1, a second interval (sub-unit M2)

consists of two alternating high- to low-amplitude facies cycles, the lower section having a mounded geometry with continuous reflections and baselap or downlap terminations internally; it transitions into a top wavy to shingled or subparallel geometry for the upper section (Figs. 5-7 to 5-13). Sub-unit M2 directly overlies the ITU in some areas of the southern West Iberian Margin (Figs. 5-8 to 5-9). Towards the top of the seismic sequence LM, the younger interval (sub-unit M3) is truncated against the IMU (intra-Messinian unconformity) horizon. This sub-unit consists of bottom low amplitude semi-continuous to discontinuous facies transitioning upwards into top prominent high amplitude subparallel facies with wavy to sigmoidal reflections (Figs. 5-10, 5-12 to 5-13). Channelised features developed along the flank of the basin margin are normally associated with this phase (Figs. 5-11 to 5-13). The overall geometry of sub-unit M3 is usually not captured as the top section may be absent in the basin margin, with only the lower section truncated against the IMU (Figs. 5-10 to 5-12). Where observed, sub-unit consists of a similar cyclic facies trend with a low amplitude base transitioning upwards to a moderate- to high- amplitude top (Figs. 5-10 and 5-13). In the basin centre, this phase, represented by an elongated and lenticular or sheeted wedge at its top with an internal subparallel configuration with downlap and truncation, can be observed as relatively concordant with the overlying Upper LM unit (Fig. 5-13). The IMU horizon is marked by erosional truncation of the Lower LM unit (Figs. 5-7 to 5-13).

Seismic facies of the Lower LM unit

Figures 5-7 to 5-13 show some examples of seismic facies and geometries identified within the Lower LM unit. In the middle slope of the southern West Iberian margin, we identified a mounded geometry (~10 km long and ~0.3 s TWT thick, at ~2.5–2.8 s TWT) in the SW-NE oriented PD00-517 profile (Fig. 5-7) of the sub-unit M2 located on a flatter part of the slope on the western flank of a basement high (lower section of seismic sequence B2) protruding above the seafloor. A channelised feature (~1 km wide and 0.15 s TWT deep), also seen on the present-day seafloor, separates the mounded feature from the basement high. The internal configuration of the mounded feature consists of subparallel reflections with baselap terminations against sub-unit M1 or the ITU above seismic sequence B2, proximal to the valley-shaped feature, whereas more obvious downlap terminations are observed in the distal part of the mound. Towards the top part of the mound, a minor unconformity separates an upper high amplitude section from the lower moderate to low amplitude section. The crestal part of the mound is also affected by faulting. Underlying sub-unit M1 is sparsely distributed along
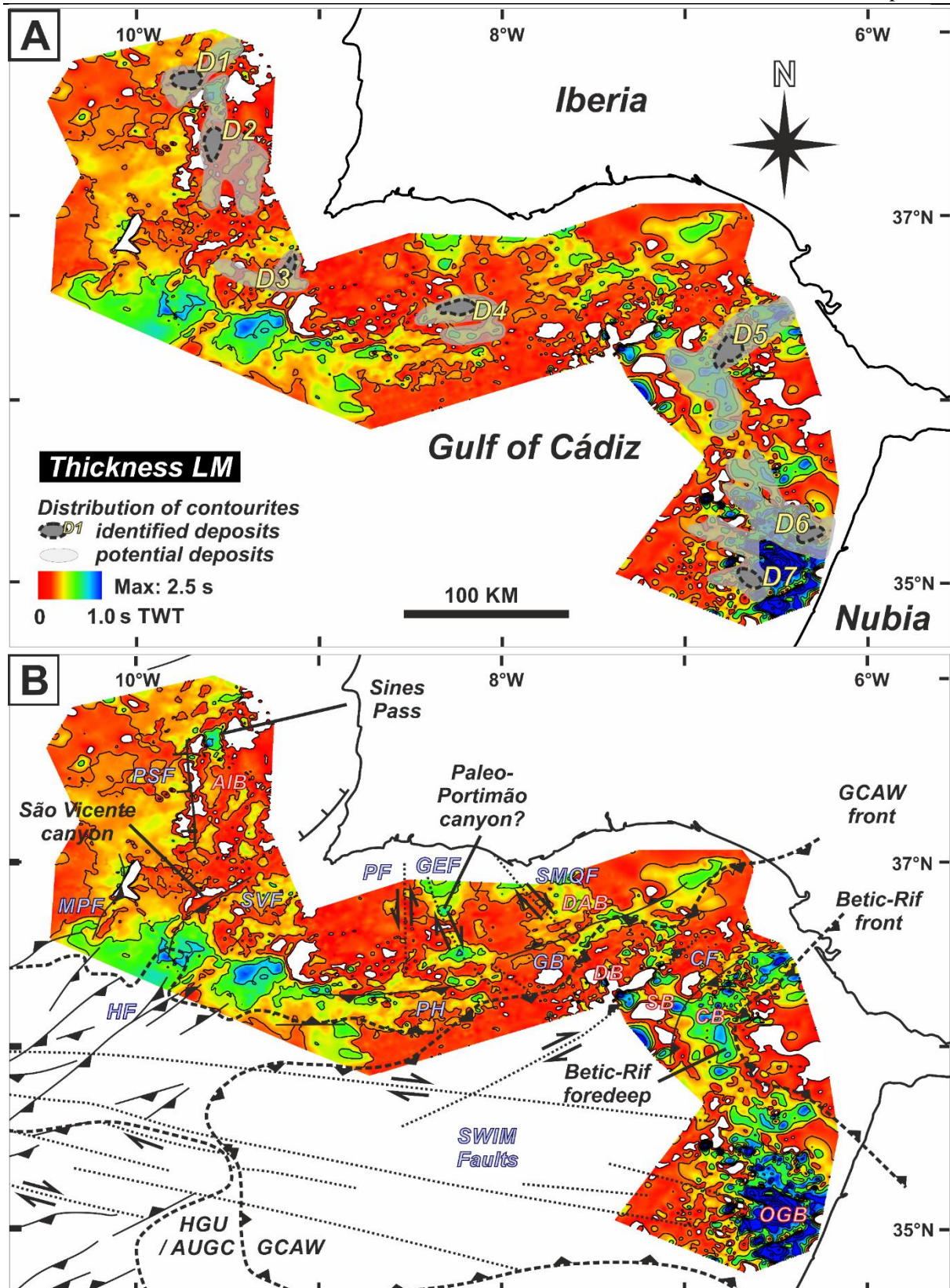
Figure 5-5 Thickness map of Unit LM showing (*a*) the distribution of contourite deposits (D1-D7), and (*b*) their relationship with tectonic and sedimentary features in the Gulf of Cádiz (Structural features adapted from Hernández-Molina et al., 2016; abbreviations given in Fig. 5-1).
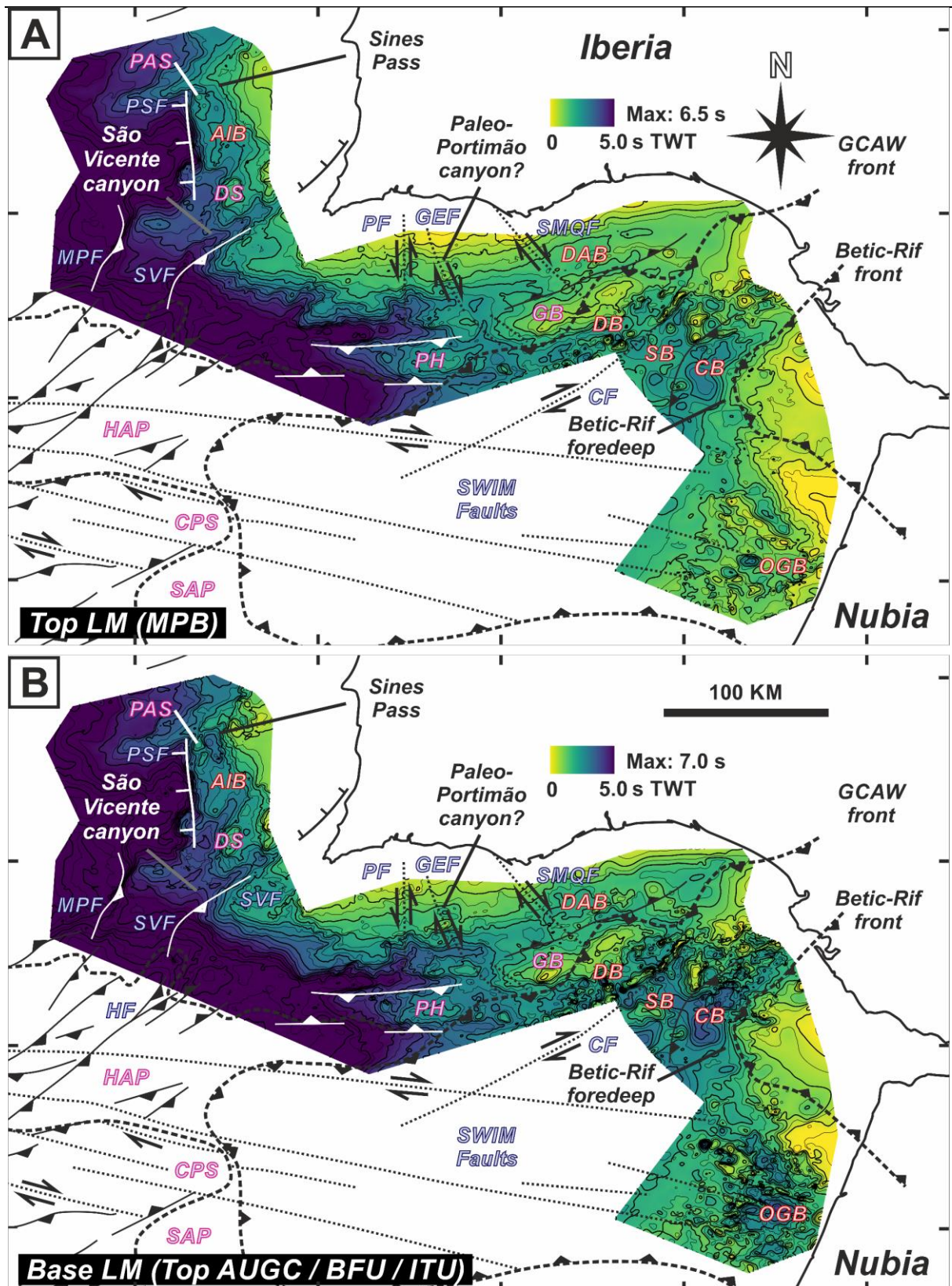
Figure 5-6   Structure maps and locations of key tectonic and sedimentary features in the Gulf of Cádiz: (***a***) Top LM (MPB), and (***b***) Base LM (combination of Top AUGC, BFU and ITU) (Structural features adapted from Hernández-Molina et al., 2016; abbreviations given in Fig. 5-1)

the distal part of the slope and truncates sub-unit M2, while overlying sub-unit M3 onlaps the northwestern side of the mounded geometry (Fig. 5-7). Below the ITU, a mounded geometry can also be identified within the uppermost interval of seismic sequence B2, which had developed against the flank of the basement high (Fig. 5-7). Development of channel features was furthermore observed within the tabular sub-units M2 and M3 on the eastern flank of the basement high within a valley. Towards the base of the valley, the younger sub-unit M2 is deposited conformably on top of sub-unit M1 (Fig. 5-7).
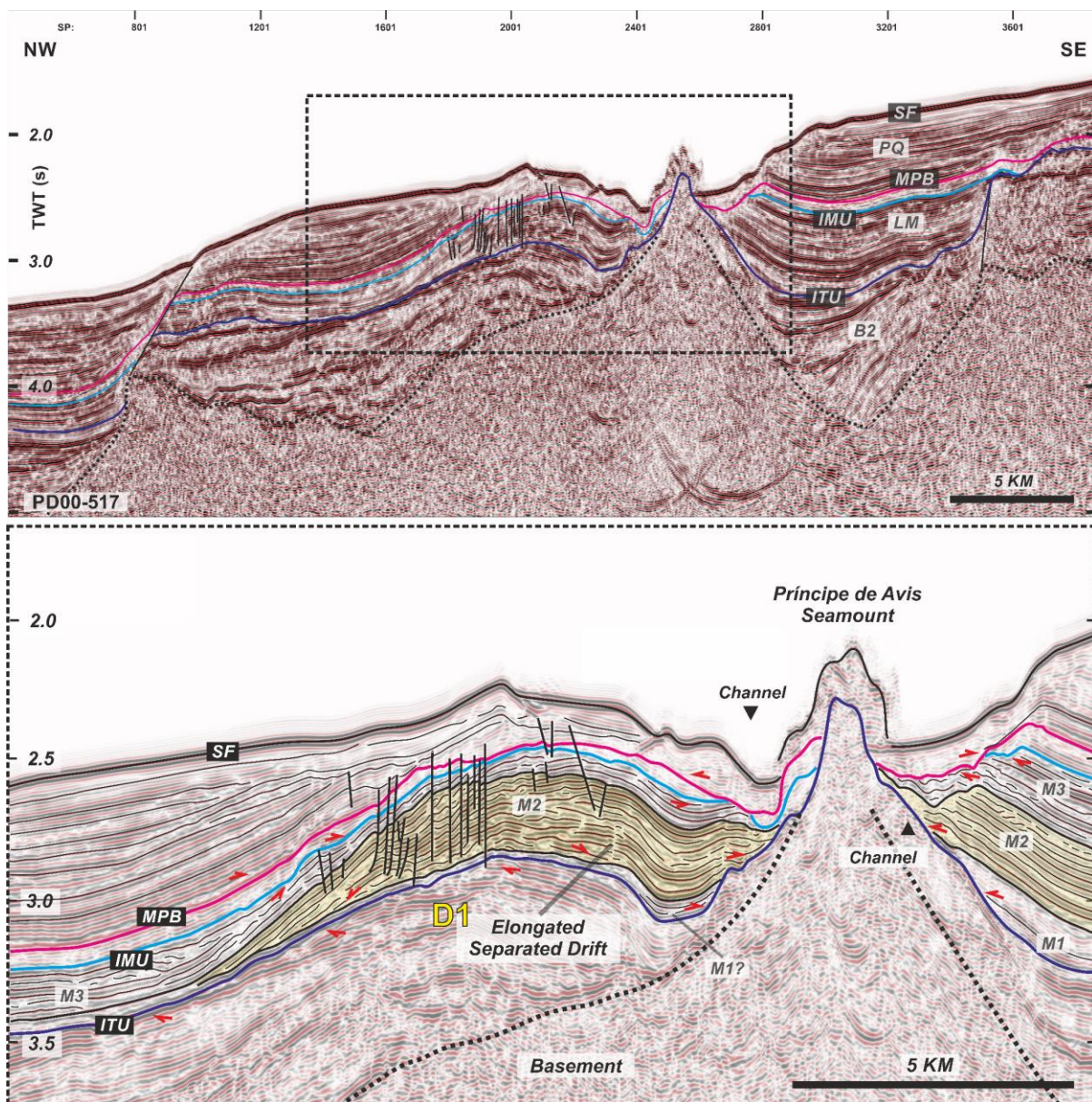
Figure 5-7   Seismic profile in the middle slope of southern West Iberian margin (PD00-517) showing an elongated separated drift (D1) associated with a contourite channel west of the Príncipe de Avis seamount (PAS). Profile location given in Fig. 5-2. Shown are major sequences (PQ, LM and B2), subunits of Lower LM (M3 and M2) and main boundaries or discontinuities (SF: seafloor; other abbreviations given in Fig. 5-4; red arrows: stratal terminations).

In profile PD00-610 (Fig. 5-8), located in the Alentejo basin, we observed an elongated feature (~30 km long and ~0.15 s TWT thick, at 2.5–2.7 s TWT) with downlap terminations in the basal part (sub-unit M2) of a thinner Lower LM unit onto the ITU horizon. We likewise identified a channelised feature (~1 km wide and ~0.15 s TWT deep, at ~2.6 s TWT) scoured into the basal seismic sequence B2 along the base of the upper slope located E-NE of the drift. This feature dented a relatively flat ITU horizon towards the SW. Towards the distal part of the slope (W-SW), before the break into the abyssal plain, the reflection pattern evolves into ~10 km high amplitude long wavy geometries; they are more prominent in the upper section of sub-unit M2, which is equivalent to the top part of the mound, whereas the basal part consists of an older sub-unit M1 with transparent to low-amplitude reflections (Fig. 5-8).

Around Cape São Vicente, we identified fan geometries in the lower slope or continental rise to the Horseshoe abyssal plain (HAP) connected to the São Vicente and Sagres canyons (Fig. 5-5). São Vicente canyon develops in a NE-SW orientation through both seismic units PQ and LM. The N-S development of the Sagres canyon is more prominent in the seismic sequence LM interval than PQ. In the middle slope, Sagres canyon develops along the flank of the basement high in the east, cutting into seismic sequence B2 (Fig. 5-9). On the western flank of Sagres canyon, we identified in seismic profiles PD00-602 and 602A (Fig. 5-9) a mounded feature of sub-unit M2 with downlap terminations onto the ITU, building out to the west up to ~5 km long (and 0.2 s TWT thick, at 2–2.2 s TWT), which is in asymmetry with the eastern flank. The erosive IMU cuts into the thalweg of the canyon and is filled by the Upper LM unit. Distally from this structure towards the southwest, the Lower LM unit transitions upwards into wavy geometry on the lower slope. This is followed by a truncation termination against the IMU in a section with erosion or an absence of the Lower LM unit distribution (at 2.6–3.0 s TWT) and deposition of a growth wedge further towards the lower slope (Fig. 5-9).

Towards the western section of the Betic foreland basin, the thickest Lower LM unit interval (up to ~0.6 s TWT thick, at 2.5–3.1 s TWT) was found within Faro canyon, a valley (~0.6 s TWT deep) located west of the Deep Algarve basin (Fig. 5-3b), which is observed in seismic profile PD00-707 (Fig. 5-10). The discordant relationship of the Lower LM and Upper LM units separated by the IMU make geometrical interpretation of the upper sub-unit M3 interval unclear. Still, its internal configuration can be observed as low-amplitude discontinuous facies transitioning upwards into high-amplitude subparallel facies. In the sub-
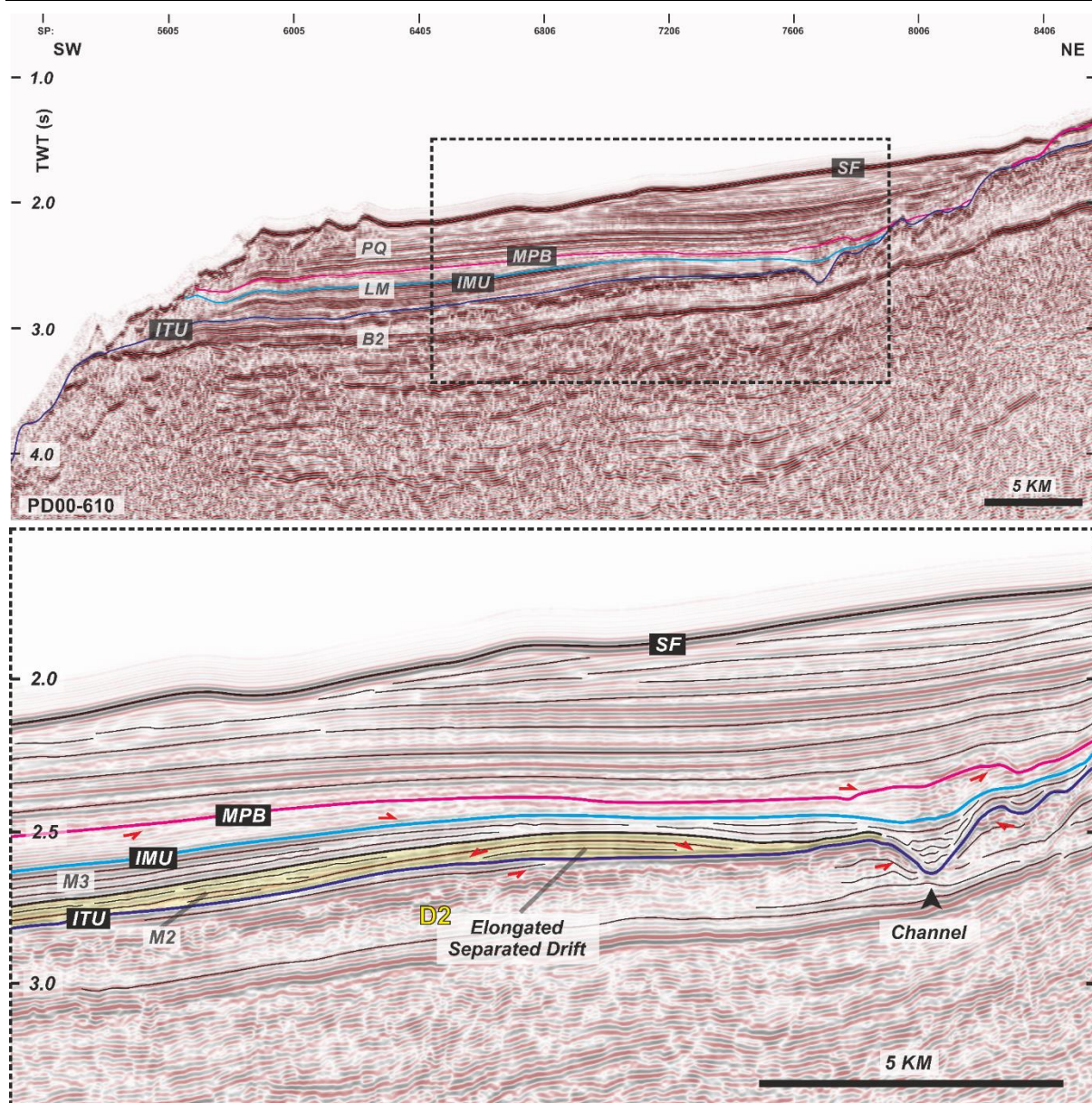
Figure 5-8   Seismic profile of Alentejo basin (AlB), southern West Iberian margin (PD00-610) showing an elongated separated drift (D2) west of a contourite channel. Profile location given in Fig. 5-2. Major sequences (PQ, LM and B2), subunits of Lower LM (M3 and M2) and the main boundaries or discontinuities (SF: seafloor; other abbreviations given in Fig. 5-4; red arrows: stratal terminations).

unit M2 interval, we similarly observed two cycles of alternating low- to high-amplitude reflection. The bottom (older) section has a mounded geometry, while the overlying (younger) section features a wavy geometry (Fig. 5-10). The internal configuration of the top cross-stratified wavy geometry (~1.5–2 km long and ~0.15 s TWT thick, at ~2.8 s TWT) consists of shingled facies with a concordant depositional western side and a truncated erosional eastern side. We also observed a channel feature (~1 km wide) to the west of this interval, flanking an intrusive structure. The mounded feature in the bottom section (~10 km long and ~0.25 s thick,

at ~2.8–3.1 s TWT) developed in an E-W direction. It correlates to a channel feature towards the eastern end of this section, with the underlying lower amplitude semi-continuous reflections (sub-unit M1) truncated against the channel. In contrast, sub-unit M1 below shows of an overall thin tabular to sheeted geometry (Fig. 5-10).
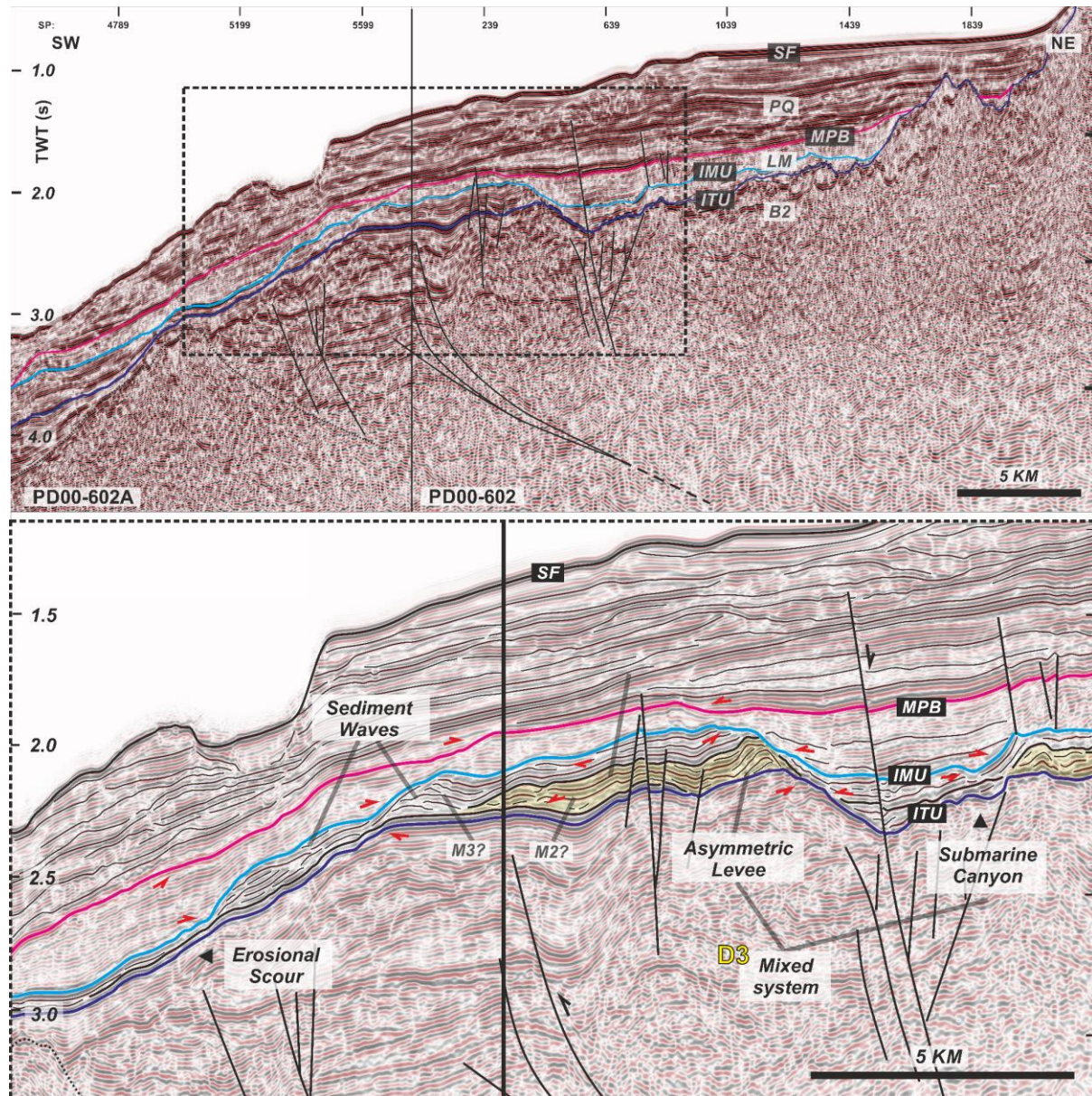
Figure 5-9 Seismic profile across Sagres canyon (SC), southern West Iberian margin (PD00-602 & PD00-602A) showing an asymmetric levee and the Sagres submarine canyon associated with a mixed system (D3), as well as sediment waves and erosional scour on the middle slope. Profile location given in Fig. 5-2. Major sequences (PQ, LM and B2), subunits of Lower LM (M3? and M2?) and the main boundaries or discontinuities (SF: seafloor; other abbreviations given in Fig. 5-4; red arrows: stratal terminations)

In the central Gulf of Cádiz, distribution of seismic sequence LM is concentrated along the front of the Betic and Rif chain of the Gibraltar Arc, mainly in the Cádiz and Offshore Gharb basins (Fig. 5-5). Here, the Lower LM unit is also truncated against the IMU, but with a very distinct change in seismic facies, in terms of continuity and amplitude, than a transparent unit in the Upper LM unit. As seen in seismic profile S81-N14 (Fig. 5-11) situated in the Cádiz basin, the distribution of the Lower LM unit is thicker at the footwall of a normal fault structure, albeit discordant against the overlying units/sub-units. Within the Lower LM unit, we identified a high amplitude interval (M2, at ~2.5–3 s TWT) with a lower section comprising multiple smaller channels cutting into an older interval of discordant to chaotic reflections (sub-unit M1) formed at the foot walls of thrust faults above a diapir, that were cut by a younger listric fault (at ~2.9–3 s TWT); and an upper section with a mounded feature (~4 km long and ~0.1 s TWT thick) associated with a channel that developed against the hanging wall of the fault. Seismic profile NWM03-F002 (Fig. 5-12) from the Offshore Gharb basin just off the Rifian front (Fig. 5-1), similarly identified a higher-amplitude interval (sub-unit M2) but shallower at 0.9 – 1.5 s TWT associated with a fault, above an interval of transparent to low-amplitude semi-continuous discordant to chaotic reflection facies (sub-unit M1). In turn, sub-unit M2 (~7 km long and ~0.4 s TWT thick) comprise two cycles of alternating low- to high- amplitude reflections. The lower section features a mounded geometry with a basal boundary having downlap terminations and a top boundary truncated against the upper section. The upper section is elongated and pinches out towards the southwest, with a transition from lower-amplitude with downlap terminations at the bottom, to higher-amplitude at the top. In both localities, we identified, above the high amplitude interval (sub-unit M2), a channel geometry (~1.5–2 km wide) associated with an upper (sub-unit M3) interval that developed along the front of a structural high (Fig. 5-11).

To the west of the Offshore Gharb basin, we identified a depocenter for seismic sequence LM in the deeper section of the basin (~3 s TWT deep), reaching up to ~1.3 s TWT in thickness, as seen in seismic profile LAR04-5 (Fig. 5-13). Here we note a concordance between the Upper and Lower LM units. The Lower LM unit has a sheeted geometry (~7 km long and ~0.6 s TWT thick) in the basin centre, correlated to a deep channel (~0.2 s TWT); and an erosional scar in the northern margin off a diapiric high, separating it from the Lower LM unit. The top interval (sub-unit M3) of this unit consists of lower amplitude reflections transitioned into prominent high-amplitude reflections with a wedge shape at the top (~0.2 s TWT thick), capped by the IMU. We also identified smaller channels (~0.5–1 km wide)

developed along the southern margin. The sub-unit M2 interval consist of a lower section with parallel facies having onlap or truncation terminations, respectively against the northern diapir or channel, that transitioned upwards into subparallel reflections with internal stratal terminations. Sub-unit M2 overlies a sub-unit M1 interval having transparent to low-amplitude semi-continuous discordant to chaotic facies.
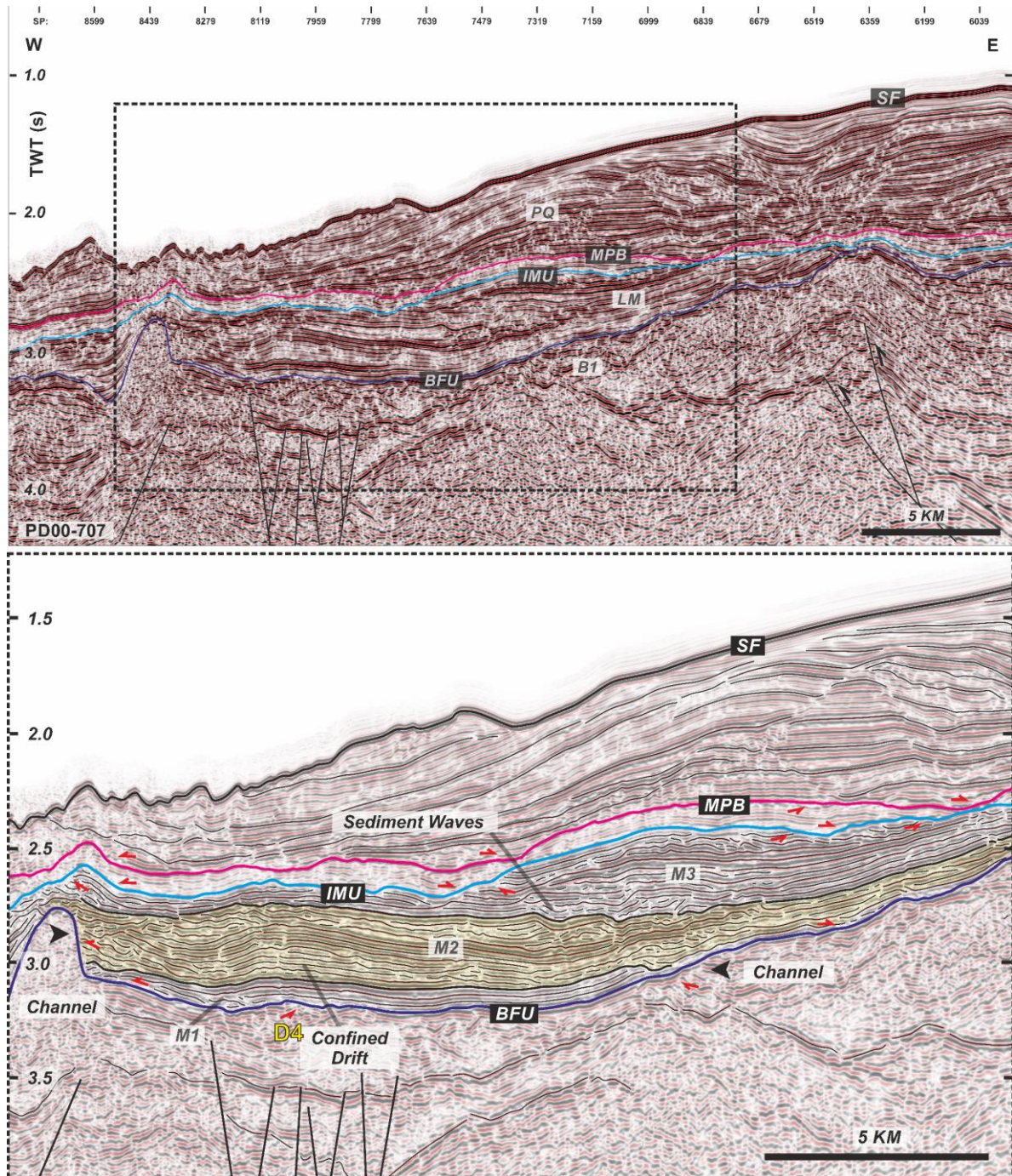
Figure 5-10 Seismic profile across Faro canyon (FC), Southwest Iberian margin (PD00-707) showing a mounded confined drift (D4) and sediment waves. Profile location given in Fig. 5-2. Major sequences (PQ, LM and B1), subunits of Lower LM (M3, M2 and M1) and main boundaries or discontinuities (SF: seafloor; other abbreviations given in Fig. 5-4; red arrows: stratal terminations).

Interpretation

Distribution of the late Miocene contourite depositional system

We interpret some of the larger seismic geometries identified within the Lower LM unit of the Gulf of Cádiz as large depositional, erosional, and mixed features related to a regional late Miocene contourite depositional system (CDS) (Figs. 5-5 and 5-14).

In the southern West Iberian reactivated passive margin, the mounded feature observed within sub-unit M2 (Fig. 5-7) is interpreted as an elongated separated drift (D1) associated with an adjacent NE-SW contourite channel (moat) that developed under a north-easterly bottom current direction (Figs. 5-5 and 5-14), flowing on the western flank of the Príncipes de Avis seamount (PAS; Figs. 5-1 and 5-7). This interpretation conforms to the classification of drifts and inferred bottom current flow pattern in the northern hemisphere put forth by Faugères et al., (1999). The morphology of upper sub-unit M3 is unclear, given the erosional IMU (intra-Messinian unconformity) at the top (Fig. 5-7). While sub-unit M3 onlaps on the western side of the M2 mounded drift, separated by an unconformity, the development of the channel along the flank of the seamount during the deposition of sub-unit M3 is more pronounced (Fig. 5-7). The mounded feature identified below the ITU (intra-Tortonian unconformity) in seismic sequence B2 is likewise viewed as an elongated separated drift, but older in age (Oligocene-Eocene to early middle Miocene?) separated by an erosional hiatus across the ITU, though its interpretation lies beyond the focus of this study (Fig. 5-7). On the eastern flank of the Príncipes de Avis seamount, contourite channels developed at the same time as the sub-unit M2 and M3 within the western margin of the Sines Pass valley, which acts as a depocenter during the deposition of the Lower LM unit (Figs. 5-5 to 5-7, 5-14). Within the Alentejo basin, we interpret the basal feature of sub-unit M2 (Fig. 5-8) as an elongated separated drift (D2) and a NW-SE contourite channel (moat) developing alongslope, located adjacent to the base of the upper slope, owing to a north-westerly bottom current direction (Fig. 5-5 and 5-14), following the drift classification, and inferred bottom current directions of Faugères et al. (1999). The drift transitions into sediment waves towards the distal part of a terrace on the middle slope. Towards the top, sub-unit M3 is separated from sub-unit M2 by an unconformity and is eroded by the IMU (Fig. 5-8).
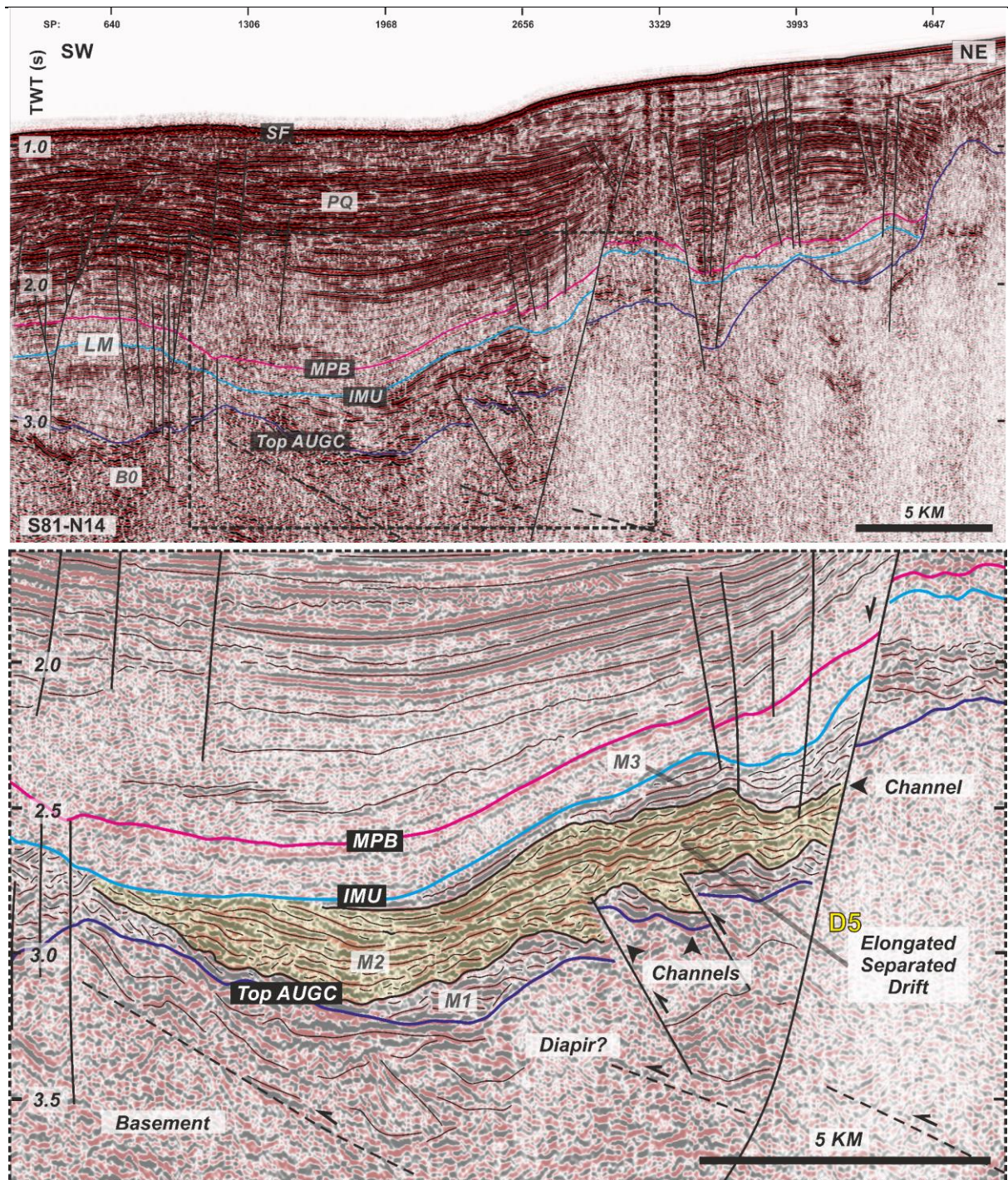
Figure 5-11 Seismic profile in Cádiz basin (CB), Southwest Iberian margin (S81-N14) showing a mounded drift (D5) west of a fault scarp. Profile location given in Fig. 5-2. Major sequences (PQ, LM and B0), subunits of Lower LM (M3, M2 and M1) and main boundaries or discontinuities (SF: seafloor; other abbreviations given in Fig. 5-4; red arrows: stratal terminations)

Further south off Cape São Vicente, we interpret the fan geometries connected to the São Vicente and Sagres canyons in the lower slope to continental rise as submarine fans (F1 & F2; Fig. 5-5), controlled by southward downslope depositional processes. On the middle slope region of this area (Fig. 5-9), the mounded deposits on the western flank of the Sagres canyon are interpreted as an asymmetric levee on the flanks of the Sagres canyon associated with the occurrence of a mixed or hybrid system (D3). This could happen as a result of short lateral diversion of the turbidity current by a westward flowing bottom current (Figs. 5-5 and 5-14), creating asymmetric levees as described by Menard (1955) and Miramontes et al. (2020); or further transport of sediment capture of the tail of the turbidity current by the bottom current to form the levee or drift body; or else winnowing or cleaning by the paleo-Mediterranean Outflow Water (MOW) to form bottom current reworked turbidite deposits within the channels (e.g. de Castro et al., 2020). The Sagres canyon became inactive in the middle to late Messinian, its development terminated by the IMU, and its thalweg filled by the Upper LM unit (Fig. 5-9). Further down the slope, the wavy geometry and erosional features that developed WNW-ESE alongslope are respectively interpreted as sediment waves and an erosional scour due to the westward flowing bottom current, bounded at the top by the IMU (Fig. 5-9). The features are thought to be deposited within sub-unit M2 overlying the ITU, while extensive erosion of the slope marked by the IMU could have removed sub-unit M3.

Towards the Southwest Iberian margin, the distribution of the contourite features is most prominent within the Faro canyon in the west, owing to its deeper local paleotopography in the late Miocene in comparison to the Deep Algarve basin, hence providing accommodation for the deposition of the Lower LM unit (Figs. 5-5 and 5-6b). We interpret the top wavy and bottom mounded features identified within Faro canyon for sub-unit M2 as the development of a confined drift (D4), according to the classification of Faugères et al. (1999), that transitioned upwards into sediment waves (Fig. 5-10). The drift deposition is confined within Faro canyon by the slope face in the east and a diapir in the west, resulting in the development of channels on either side of the drift because of a northerly bottom current direction (Fig. 5-10). Sub-unit M2 is capped by an unconformity, underlying sub-unit M3. At the top of the upper sub-unit M3, the high amplitude continuous reflections to the east at the top of the interval may indicate more pronounce bottom current activity towards Messinian times, although the erosion marked by the IMU impedes interpretation of the seismic geometry for this sub-unit (Fig. 5-10).
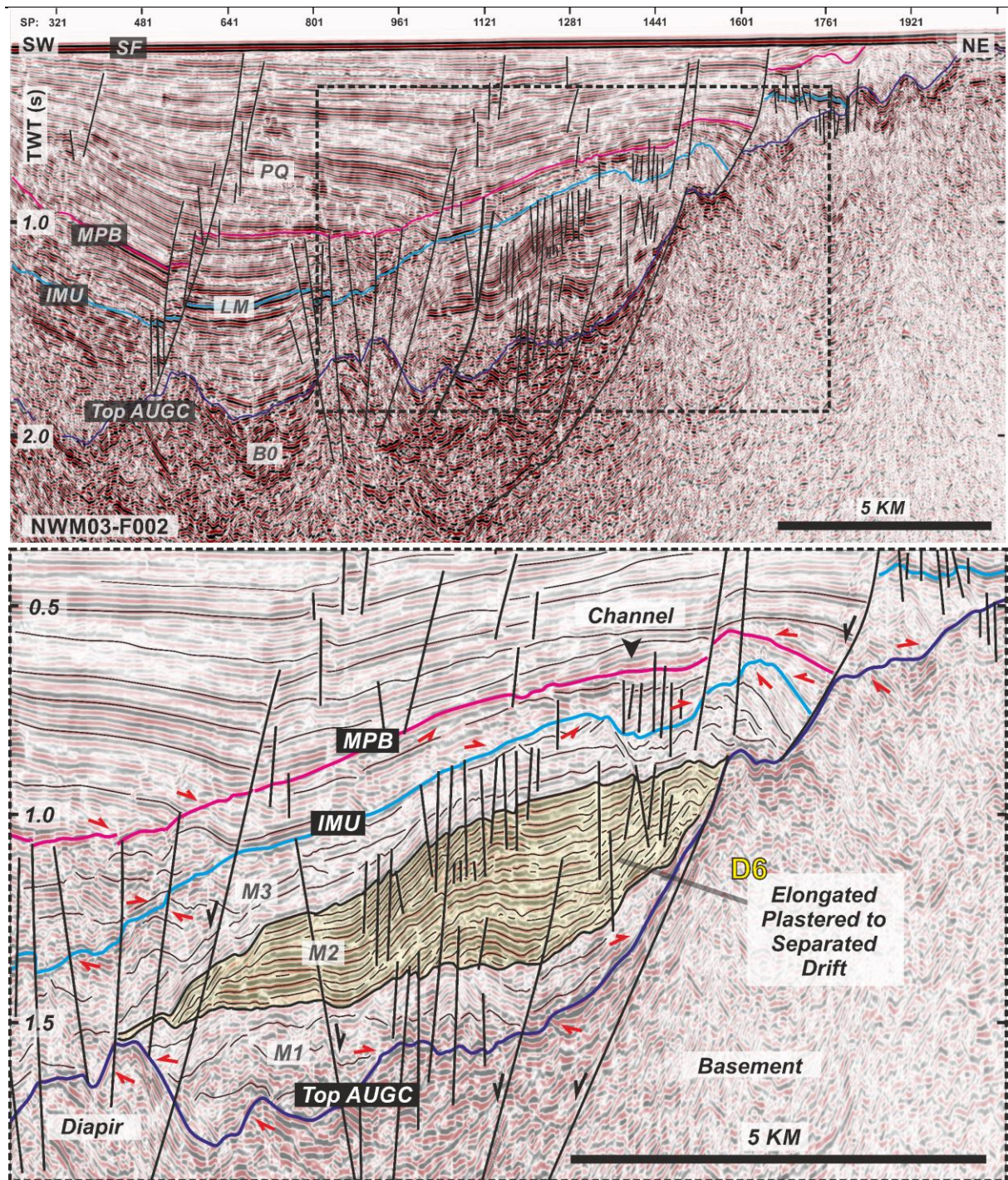
Figure 5-12 Seismic profile in eastern Offshore Gharb basin, Northwest Moroccan margin (NWM03-F002) showing a plastered to mounded drift (D6) west of a fault scarp. Profile location given in Fig. 5-2. Major sequences (PQ, LM and B0), subunits of Lower LM (M3, M2 and M1) and main boundaries or discontinuities (SF: seafloor; other abbreviations given in Fig. 5-4; red arrows: stratal terminations)

Meanwhile towards the central Gulf of Cádiz and above the wedge top basins, an elongated separated drift (D5) and an elongated plastered to separated drift (D6) are respectively interpreted for the mounded features with high amplitude reflections identified in sub-unit M2 for the Cádiz and Offshore Cádiz basins (Figs. 5-11 and 5-12), based on the classification of Faugères et al. (1999). The location of this contourite drift is associated with faults or structural highs, where bottom currents would be enhanced in a northward direction along the hanging wall or the flank of the high, located in the eastern margin of the basin (Figs. 5-5 and 5-14). In the Cádiz basin, we propose that contourite channels were formed by thrust faults linked to a decollement associated with the emplacement of the accretionary wedge (GCAW) but were later displaced by a listric fault caused by the gravitational collapse (Fig. 5-11). The local enhancement of bottom current could also be constrained by diapiric structures, which might have further strengthened current erosivity and its capacity in the scouring of channels. In turn, in the Offshore Gharb basin, drift deposition evolved from a basal separated drift to a plastered drift (D6) at the top of sub-unit M2, within accommodation caused by the normal listric fault (Fig. 5-12). This contourite drift is distinguished from pure growth strata features in extensional rollover systems (as in the upper LM and PQ units) given the mounded geometry of the deposits as well as the configuration of the reflection terminations against the fault scarp. Just above the sub-unit M2, sub-unit M3 shows a lower-amplitude reflection (Figs. 5-11 and 5-12), but it is partially eroded at its top, marked by the IMU. Contourite channels interpreted from the alongslope development of these channelised features of sub-unit M3 (Fig. 5-12) indicate a stronger influence of bottom currents towards the end of the Lower LM unit, albeit a transition to low-amplitude seismic facies at the lower part of sub-unit M3.

Towards the western part of the Offshore Gharb basin, a continuous section of the seismic sequence LM could be identified (Fig. 5-13). We interpret the succession as a confined drift (D7), again according to Faugères et al. (1999), associated with contourite channels in the northwest and southeast having a westward bottom current direction (Figs. 5-5 and 5-14). The drift is asymmetrical with a skew towards the main channel in the northwest. The erosion of the channel is less prominent for sub-unit M2 with an internal erosive surface and capped by a minor unconformity (Fig. 5-13), thus indicating a more spread-out bottom current affecting the depocenter. The erosional scouring created a deeper channel for sub-unit M3, associated with a wedge-shaped deposit at the top of the drift and channelisation in the SE margin, indicative of a more focused and enhanced bottom current. These features associated with drift D7 are

analogous to those of the late Quaternary contourite drift observed in the Doñana basin (Hernández-Molina et al., 2016).
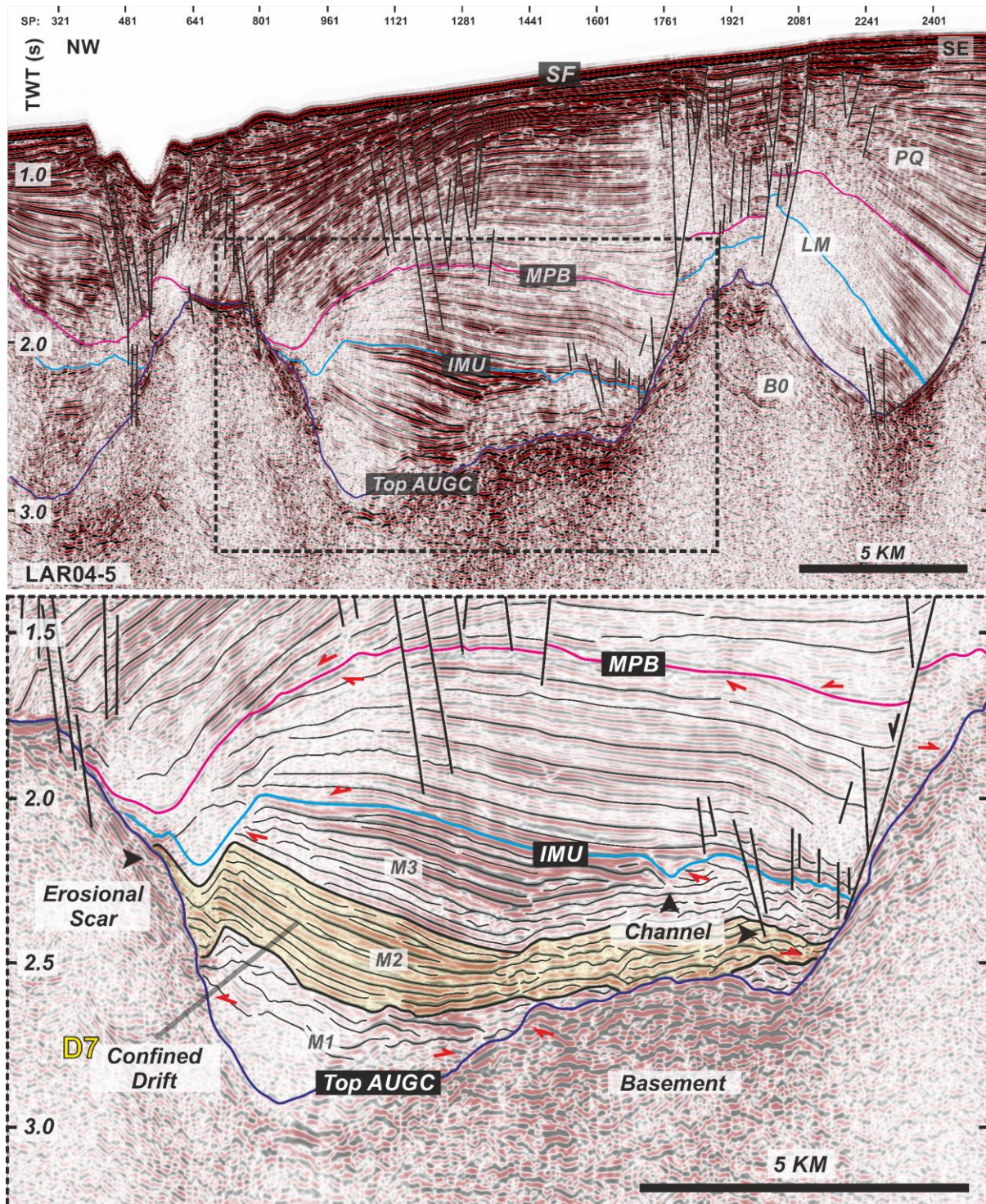
Figure 5-13 Seismic profile in western Offshore Gharb basin, Northwest Moroccan margin (LAR04-5) showing an asymmetric confined drift (D7) bounded by basement highs and flanked by erosional scar and channels. Profile location given in Fig. 5-2. Major sequences (PQ, LM and B0), subunits of Lower LM (M3, M2 and M1) and main boundaries or discontinuities (SF: seafloor; other abbreviations given in Fig. 5-4; red arrows: stratal terminations)

Discussion

Stratigraphic and chronologic framework

The seismic stratigraphy of the Gulf of Cádiz is summarised in Figure 5-4 and Table 5-1, and the seismic sequence LM is discussed in detail here. For the basal surface of the Lower LM unit, the basal foredeep unconformity (BFU) is documented as ~8 Ma (Maldonado et al., 1999), whereas the age for the intra-Tortonian unconformity (ITU) is speculative due to a lack of chronological information. We assume an age between ~7–8 Ma for the ITU, which correlates to the timing of final emplacement of the allochthonous units towards the northwest of the Gulf of Cadiz (Gràcia et al., 2003). This could have led to the thinner distribution or absence of the lowermost section of the Lower LM unit (sub-unit M1) to the northwest. The distribution of the upper Tortonian to lower Messinian Lower LM unit of the seismic sequence LM (~8–~6.4 Ma) is also dependent on the erosion and hiatus associated with the intra-Messinian unconformity (IMU, ~6.4 Ma; Ng et al., 2021) in different parts of the basin. Its deposition is controlled by the paleotopography of the underlying units, distinct in its respective sectors (seismic units B0, B1 and B2) (Fig. 5-6b; Table 5-1). Only a handful of boreholes are available for the correlation of the late Miocene succession. The GCMPC-1 well, located in the Cádiz basin (Fig. 5-2), penetrated the deep-marine Lower LM unit, but did not reach the allochthonous unit (AUGC) or the accretionary wedge (GCAW). The M1/M2 boundary correlates to fluctuations in the geophysical logs, with increases in spontaneous potential (SP) and gamma ray (GR), while the M2/M3 boundary correlates to a slight lithological change, the lower section becoming siltier and more fossiliferous, with occasional micritic or oolitic limestone beds and traces of coal. (Hernández-Molina et al., 2014). The wells Anchois-1, Deep Thon-1 and Merou-1 also penetrated the late Miocene succession in the Offshore Gharb basin. In the Deep Thon-1 and Merou-1 well, the Lower LM unit is dominated by distal turbidite channels, lobes, or basin plain deposits, possibly reworked by later turbidity currents and or bottom currents (Ng et al., 2021). Upwards, the IMU horizon (~6.4 Ma) correlates to biostratigraphic events such as the Last Regular Occurrence (LRO) of Globorotalia miotumida, replaced by the First Occurrence (FO) of Globorotalia margaritae, dated 6.31–6.35 Ma, identified within a section of light grey clays interspersed with silts and very fine unconsolidated sands at the base of the Upper LM unit (Hernández-Molina et al., 2014; Ng et al., 2021). Still, the magnitude of this erosional hiatus is not known, as high-resolution biostratigraphic data below this boundary are lacking. We therefore postulate an age of ~6.6–

6.4 Ma, inferred from the disappearance of paleo-Mediterranean Outflow Water (MOW) in the Onshore Gharb basin (Ivanovic et al., 2013). Above the Lower LM unit, the Upper LM unit is represented by the middle to upper Messinian unit of Ng et al. (2021) and the uppermost part of the U1 unit in Rodrigues et al. (2020). This unit correlates to a period dominated by pelagites or hemipelagites of the middle to late Messinian (~6.4 to 5.33 Ma; Ng et al., 2021). The background sediments are interrupted by gravity flow deposits, most prominently in the Deep Algarve and Offshore Gharb basins (Ng et al., 2020). Based on the Anchois-1 well, the Upper LM unit would consist of stacked channel storeys or complexes separated by thick hemipelagic drapes (Ng et al., 2021). Overall, seismic sequence LM reflects the late Miocene contourite depositional system.
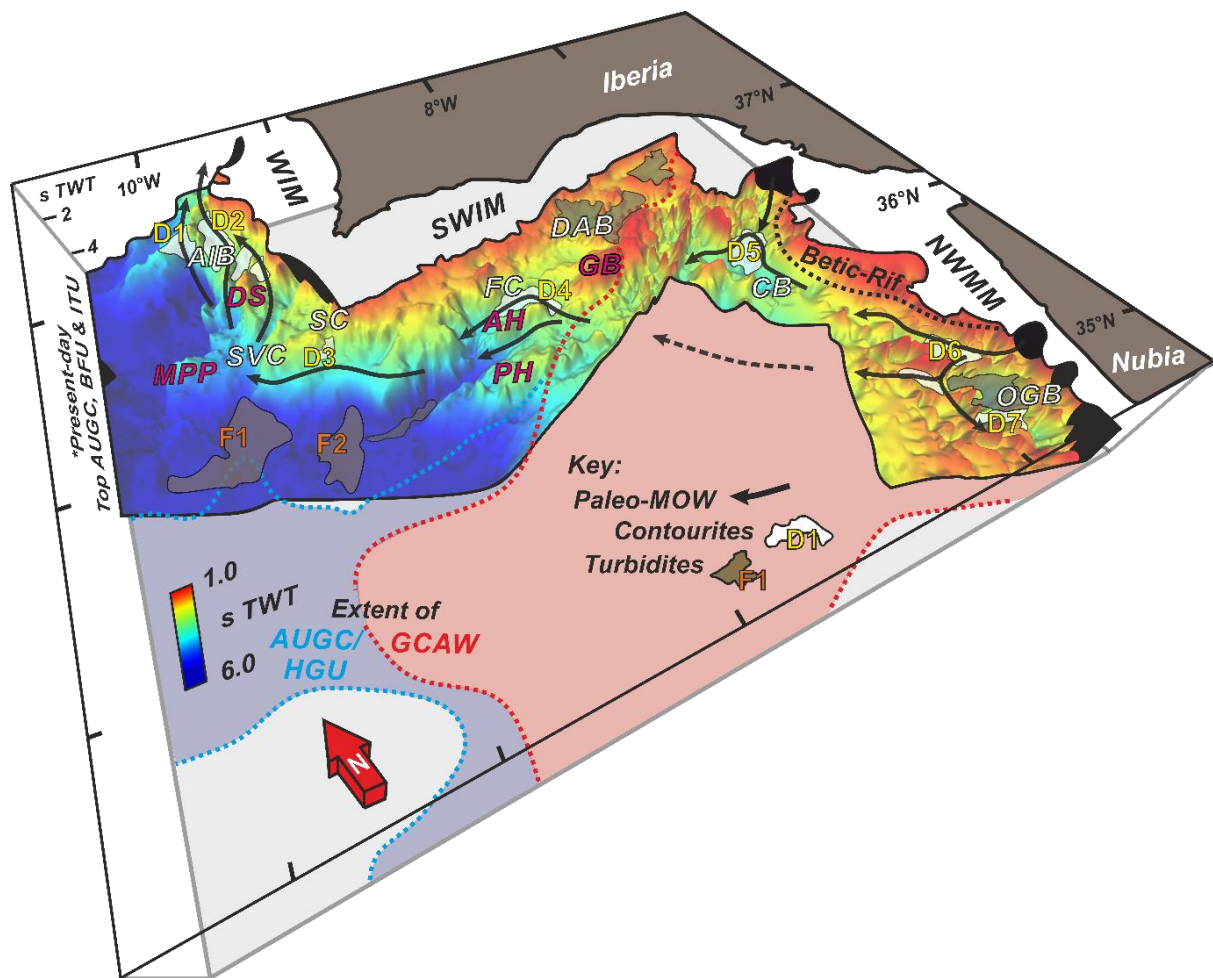
Figure 5-14 Schematic model for the relationship between contourite distribution (Fig. 5-5a, D1-D7) and potential pathway of the paleo-Mediterranean Outflow Water (MOW) for the late Miocene Gulf of Cádiz CDS, superposed on the Base LM structure map (Fig. 5-6b) loosely representing the paleobathymetry of the late Miocene. (NWMM: Northwest Moroccan margin, SWIM: Southwest Iberian margin, WIM: West Iberian margin; other abbreviations given in Fig. 5-1).

Seimostratigraphic unit		Top boundary	Seismic facies and description	Depositional setting and interpretation
Pre-late Miocene	B0 (Wedge top basin)	Top allochthonous unit of Gulf of Cadiz (AUGC)	Mega-chaotic seismic body affected by listric or thrust faulting	Allochthonous unit of the Gulf of Cadiz (AUGC; Medialdea et al., 2004; Irribarren et al., 2007)
	B1 (Betic foreland basin)	Basal foredeep unconformity (BFU)	Upper section of top-discordant high amplitude semi-continuous to chaotic reflections and lower section of homogenous chaotic reflections	Mesozoic to middle-late Miocene sedimentary succession and Paleozoic basement (Maldonado et al., 1999; Pereira et al., 2016)
	B2 (West Iberian margin)	Intra Tortonian unconformity (ITU)	Upper section of high amplitude discontinuous to wavy continuous reflections and lower section of chaotic reflections	
Tortonian – Messinian	Lower LM (~8.0–~6.4 Ma)	Intra Messinian unconformity (IMU)	See sections 4.1 and 4.2	Late Miocene contourite depositional system (This study)
	Upper LM (~6.4–5.33 Ma)	Miocene Pliocene boundary (MPB)	Transparent to low amplitude continuous reflections, except for Offshore Gharb basin, which consists of intervals of high amplitude reflections in between lower amplitude intervals.	Pelagites or hemipelagites, interrupted locally by turbidites (Ng et al., 2021)
Pliocene-present	PQ (5.33–0 Ma)	Seafloor	Erosional base with medium to high amplitude parallel to semi-parallel continuous reflections in the lowermost section, locally in areas relatively conformable within seismic resolution, having continuous low amplitude reflections in the lowermost section	Pliocene-Quaternary contourite depositional system (Llave et al., 2011; Roque et al., 2012; Hernandez-Molina et al., 2016)

Table 5-1   Summary of seismostratigraphic units and boundaries of the Gulf of Cádiz and southern West Iberian margin.

Evolution of the late Miocene contourite depositional system

The long-term evolution of the late Miocene contourite depositional system (CDS) can be divided into three stages (initial-, growth-, and maintenance-drift) based on the morphology of the contourite features identified, followed by a final (buried-drift) stage representing the cessation of the system.

Initial-drift stage

At the base of the Lower LM unit, the predominantly transparent to low amplitude semi-continuous sub-unit M1 is interpreted as the initial-drift stage of the late Miocene CDS, which is marked by the onset of paleo-Mediterranean Outflow Water (MOW) during the late Tortonian above the BFU (~8 Ma). The sheeted to tabular distribution of sub-unit M1 in Faro Canyon (Fig. 5-10) and the Sines Pass in the southern West Iberian margin (Fig. 5-7) may have been originated by weak bottom current prior to the deposition of the more pronounced contourite features in sub-unit M2. This stage is comparable to the early Pliocene weak MOW phase observed for seismic sequence PQ, or Pliocene-Quaternary CDS (Hernández-Molina et al., 2016). The deposition of sub-unit M1 could also be synchronous with the emplacement of new imbricate wedges in the Gharb-Saiss basin, also known as the Prerifian Nappe [sensu Levy and Tilloy, 1962; as the equivalent to the allochthonous unit of the Gulf of Cádiz (AUGC) in the Rifian corridor (Flinch, 1993)], from ~8.4 to 7.8 Ma, just before the onset of contourite deposition in the Rifian Corridor (Capella et al., 2017b; de Weger et al., 2020). This is supported by the presence of deformed sub-unit M1 in the wedge top basins in the central Gulf of Cádiz above the Top AUGC (Figs. 5-11 to 5-13). The emplacement of the accretionary wedge and the gravitational collapse in the wedge top basins (Medialdea et al., 2004) prior to during this stage created the bathymetric control and accommodation for the evolution of the late Miocene CDS. The southern West-Iberian margin is likewise affected by the tectonic reactivation caused by an inversion of rift-related faults that uplifted the margin (Zitellini et al., 2004; Pereira et al., 2011). The sparse distribution of sub-unit M1 following the Miocene hiatus, represented by the ITU horizon in the Alentejo basin, corroborates this hypothesis.

Growth-drift stage

The growth-drift stage is represented by the sub-unit M2 interval, which consist of well-defined contourite drifts throughout the Gulf of Cádiz continental margins. More pronounced

erosional and depositional features of the late Miocene contourite depositional system, such as mounded drifts and contourite channels, first developed after the onset of sub-unit M2 (Figs. 5-7 to 5-13). This represents an increase in the paleo-MOW velocity as it flows towards the Gulf of Cádiz, the outflow evolving into an overflow setting as suggested by Capella et al. (2019). Meanwhile, tectonic activity extending into the latest Tortonian (7–8 Ma; Gràcia et al., 2003) in the wedge top basins would have continued to create accommodation for drift growth. The base of sub-unit M2 is coeval with the onset of the sandy contourites succession described for the Rifian Corridor, which began between 7.8 Ma until 7.25 Ma during a period of relative tectonic quiescence (Capella et al., 2017a; de Weger et al., 2020). The boundary between sub-unit M2 and the overlying sub-unit M3 is marked by a minor unconformity and a shift from the high-amplitude top M2 interval to a low-amplitude bottom M3 interval. This could be attributed to an abrupt weakening or a change in pathway of the paleo-MOW and may further be related to a regional-scale event for the external wedges of the Gibraltar Arc during the Tortonian to Messinian (Abbassi et al., 2020). In the Rifian corridor onshore Morocco, a compressional tectonic event dated 7.25 Ma (Tortonian-Messinian boundary), linked to the transition from a thin- to thick-skinned tectonic regime for the Betic-Rif orogeny, is identified as the termination of a contourite depositional sequence in the Saiss basin (Capella et al., 2017b; de Weger et al., 2020); younger contourite deposits (~6.4–7.25 Ma) are also identified in the Onshore Gharb basin (Capella et al., 2017a). This event might have been responsible for the transition at the M2/M3 boundary. The Tortonian-Messinian boundary is moreover regarded as the initiation of the stepwise restriction of the Mediterranean-Atlantic exchange in the framework of a changing Mediterranean deep-water environment (Flecker et al., 2015).

Maintenance-drift stage

Sub-unit M3 is sparsely distributed from the Gulf of Cádiz to the southern West Iberian margin, due to an erosional phase post-deposition marked by the IMU during the early to middle Messinian (~6.4 Ma; sensu Ng et al., 2021). Sub-unit M3 transition upwards from low-amplitude reflections to very high-amplitude reflections, where deeply erosive alongslope contourite channels can be identified until the IMU (Figs. 5-8 and 5-12 to 5-13). In addition, contourite drift morphologies are observed only in the upper part of the sub-unit, being most obvious in the Offshore Gharb basin (Fig. 5-13). The evolution in the channel geometry and the change in drift morphology from subunit M2 to M3 in the western part of the Offshore Gharb would indicate an overall strengthening of the paleo-MOW. This is in agreement with

the evolution of late Miocene CDS in the Rifian Corridor, where the paleo-MOW overflow is enhanced before its cessation (Capella et al., 2019). Therefore, we interpret sub-unit M3 as the maintenance-drift stage of the late Miocene CDS, similar to the present-day setting of the Pliocene-Quaternary CDS (Hernández-Molina et al., 2016).

Buried-drift stage

Subunit M3 is capped by the IMU, a tectonic episode witnessing the margin-wide erosion of the upper parts of subunit M3, plus a hiatus that lasted from ~6.6–6.4 Ma. The Upper LM unit is interpreted as the buried-drift stage, following the cessation of the paleo-MOW from ~6.4 Ma onwards, owing to the restriction of water exchange between the Mediterranean and the Atlantic due to uplift caused by the Betic-Rif orogeny, as well as the closure of the Betic and Rifian gateways (Krijgsman et al., 2018). This meant a switch from a contouritic to a predominantly pelagic or hemipelagic environment from the middle-late Messinian until the end of the Miocene (Ng et al., 2021). This stage is characterised by the inactivity of the contourite channels and their eventual and filling up by pelagic settling, along with the fossilization of the remaining drift deposits which were unaffected by the IMU erosional unconformity. In the Offshore Gharb basin, the presence of thick hemipelagic drapes in between the turbiditic channel storeys or complexes further corroborates an absence of bottom currents at this time (Ng et al., 2021).

Control factors

The evolution of the late Miocene contourite depositional system (CDS) is controlled by the interplay between tectonic, sedimentary, and climatic forces.

Deformation from tectonism and diapirism

During the late Miocene, the formation of the elongated wedge top basins, such as the Cádiz and offshore Gharb basins, created relatively deeper passages for the paleo-MOW through the central part of the Gulf of Cádiz, that is, in comparison to the foredeep basins at the front of the Southwest Iberian and Northwest Moroccan margins (Figs. 5-3 and 5-5). The tectonic transformation of the Mediterranean-Atlantic gateways would have led to an increase in salinity and density for the outflowing paleo-MOW through the Betic and Rifian corridors (Capella et al., 2019), and sinking towards the deeper wedge top basins, driven by the density, and mixing with ambient water before reaching neutral buoyancy west of the Doñana basin. In

the initial-drift stage, the distribution of the highly deformed sub-unit M1 in the wedge top basins of the Gulf of Cádiz reflected the complex syn-tectonic depositional processes during this period (Figs. 5-12 to 5-13). Gravitational collapse and AUGC development, in addition to diapirism, disrupted and controlled the synchronous deposition of the sub-unit M1. At the southern West Iberian margin, continuous uplift due to tectonic inversion up to the late Tortonian could have led to erosion and an intersperse distribution or lack of preservation of the initial-drift stage (Figs. 5-7 and 5-8). The occurrence of larger and more mounded drift morphologies pertaining to the growth- and maintenance-drift phases in sub-units M2 and M3 would also be a result of morphotectonic activity exerting control on the confinement of bottom current pathways. The dimensions of the drift geometries within the central Gulf of Cádiz wedge top basins for the late Miocene are relatively small (<7 km in width) when compared to drifts in the southern West Iberian margin (10-30 km wide) or the Deep Algarve basin Pliocene-Quaternary drifts (40-50 km wide; Hernández-Molina et al., 2016). The smaller late Miocene drifts reflect how the effects of bathymetric irregularities caused by tectonism and diapirism during this period conditioned both drift morphologies and distributions. As a result of the tectonic processes, basement highs, fault scarps and diapiric structures (salt domes, salt walls) acted as obstacles that locally enhanced bottom current flow and formed erosional features (channels, scours) or deposited mounded drifts with coarser sediments, controlling and confining the distribution of the late Miocene CDS from the Gulf of Cádiz to the southern West Iberian margin (Figs. 5-10 to 5-13). The effects of these bathymetric features in enhancing MOW have also been documented in the Pliocene-Quaternary CDS (Sánchez-Leal et al., 2017; Duarte et al., 2020).

Interplay of turbidity and bottom currents

Deposition of the late Miocene CDS was also controlled by the interaction of alongslope and downslope sedimentary processes. Gravitational deposits over the continental margins were reworked by the paleo-MOW flowing across the Gulf of Cádiz during the late Miocene. Examples of downslope processes during this period include the turbiditic systems within the Deep Algarve and Offshore Gharb basins (Figs. 5-3b and c; Ng et al. 2021), and the formation of the Sagres and São Vicente submarine canyons in the southern West Iberian margin (Figs. 5-3 and 5-5). Reworking of these gravity flow deposits by the paleo-MOW bottom currents would have produced mixed or hybrid systems (Mulder et al., 2008, Rodriguez et al., 2021). Yet, a paleo-Portimão submarine canyon (Figs. 5-5 and 5-6) controlled by the Gil

Eanes fault zone (GEF; sensu Duarte et al. 2020) could have supplied sediments for drift development in Faro canyon. In the offshore Gharb basin, the presence of bottom-currents could rework the dominantly turbiditic environment, giving rise to bottom-current reworked sands and contourite drifts (Shanmugam, 2008). Recent research in the Gulf of Cádiz underlines the complexity of the relationship between the two processes: MOW bottom currents and gravity flows (mass transport and turbidity currents), in the context of the Pliocene-Quaternary CDS (Brackenridge et al., 2013; de Castro et al., 2020; 2021; Mencaroni et al., 2020; Mestdagh et al., 2020; Serra et al., 2020). The interaction of different sedimentary processes in the deposition of contourite drift is well demonstrated in the analyses of core, log, and seismic scales for the Pliocene to Quaternary interval (Brackenridge et al., 2013; de Castro et al., 2021; Mestdagh et al., 2020); the influence of the MOW on the São Vicente submarine canyon has also been documented (Mencaroni et al., 2020; Serra et al., 2020).

Orbital and millennial variability

Some examples of the late Miocene drift features evoke cyclicities previously identified for the Pliocene-Quaternary CDS (Llave et al., 2001; Hernández-Molina et al., 2016; Figs. 5-10 and 5-13). These cyclic seismic facies trend with a transparent base, parallel reflectors of moderate-to-high amplitude top and capped by a continuous high-amplitude erosional surface are here interpreted as a coarsening-upward sequence linking MOW variability with orbital cycles (Hernández-Molina et al., 2016). The sub-unit scale cyclicity could be influenced by the Milankovitch precession cycles modulated by eccentricity cycles, which are thought to have an influence on sea-level variation, sediment supply, and bottom current activity, according to seismic and sequence stratigraphic analysis of the Pliocene-Quaternary CDS in the Gulf of Cádiz (Hernández-Molina et al., 2016; Mestdagh et al., 2019). The termination of the late Miocene CDS also took place coevally to both tectonic and sedimentary changes influenced by orbital cycles. This margin-wide erosive event coupled with increasing turbidite deposition, and the subsequent pelagic environment across the Gulf of Cádiz, marked the weakening and eventual cessation of paleo-MOW driven by the uplifting and shallowing of the sills within the Betic and Rifian corridors (Krijgsman et al., 1999; Ng et al., 2021). The event is furthermore linked to the stepwise restriction of the Mediterranean-Atlantic connection, which is imprinted on long-term eccentricity orbital cycles (Hilgen et al., 2007; Ng et al., 2021). Variations in MOW strength are also observed at the smaller precessional to millennial scale (Llave et al., 2006; de Castro et al., 2020; Sierro et al., 2020). High-amplitude facies are represented by

coarser-grained sediments, deposited during precession maxima or Greenland stadials, where enhancement of the MOW would be a result of aridity and increased buoyancy loss in the eastern Mediterranean (Sierro et al., 2020). During Heinrich stadials, increasing strength and a deepening of the MOW towards the lower core, along with decreasing MOW strength in the upper core, would entail freshening of the Atlantic and increased density contrast with the MOW (Llave et al., 2006; Sierro et al., 2020). Such climatic-induced effects can also be seen in the intermittent behaviour of the paleo-MOW as it controls the deposition of late Miocene contourites in the Rifian corridor (de Weger et al., 2020).

Figure 5-15 (*Top*) Seismic profile in western Onshore Gharb basin, subsurface of the Haricha section (85-LK-28), showing the distribution of the Lower LM subunits (M3, M2 and M1), main boundaries and discontinuities, and the presence of elongated separated drifts associated with the late Miocene contourite depositional system in the Rifian corridor. Seismic interpretation adapted from Capella et al. (2017). (T/M boundary: Tortonian-Messinian boundary, other abbreviations available in Fig. 5-4); (*Bottom*) Simplified geological map of the Rifian corridor showing the location of seismic profile 85-LK-28 and sedimentary sections of the Rifian corridor late Miocene CDS, and the paleo-MOW pathway (adapted from Capella et al., 2017) (Location of section indicated in Fig. 5-1).

Implications of the late Miocene contourite depositional system

The long-term evolution of drift morphologies of the late Miocene contourite depositional system (CDS) shows similarities with other modern examples around the Iberian margin, such as the Gulf of Cadiz Pliocene-Quaternary CDS in the Southwest Iberian margin (Hernández-Molina et al., 2016); the Sines drift in the West Iberian margin (Rodrigues et al., 2020); and the Le Danois CDS in the Northern Iberian margin (Liu et al., 2020). These modern examples developed as a result of Pliocene to present-day setting of the Mediterranean Outflow Water (MOW) (Llave et al., 2019), where they reflect its evolution towards a denser and more restricted setting across the Strait of Gibraltar (Hernández-Molina et al., 2016). Similarly, the development of the late Miocene contourite depositional system acts as an imprint upon the paleo-MOW circulation in the Gulf of Cádiz towards the southern West Iberian margin, where its different stages (initial-, growth- and maintenance-drift) trace the increasing density contrast between the Mediterranean and Atlantic throughout the late Miocene. The narrowing and subsequent closure of the Betic and Rifian corridors since the late Miocene led to the evolution of the paleo-MOW into an overflow setting with a more saline and denser water mass (Capella et al., 2019). Ultimately, the outflow was reduced or halted (Ng et al., 2021), followed by the partial isolation of the Mediterranean Sea and the precipitation of the Messinian Salinity Crisis evaporites during the late Messinian (Flecker et al., 2015). This transformation from an outflow to an overflow setting is also evident for the coeval deposition of contourites in the Rifian corridor (Capella et al., 2017a, de Weger et al., 2020). The late Miocene CDS, likewise identified by Capella et al. (2017a), is seen in the seismic profile subsurface of the Haricha section, at the eastern margin of the onshore Gharb basin by the exit of the Rifian corridor. Here, elongated separated drifts are interpreted for subunits M2 and M3 (growth- and maintenance-drift stage), while subunit M1 with its sheeted and tabular geometry, points to the initial-drift stage (Fig. 5-15).

The presence of the late Miocene CDS in the Gulf of Cádiz occurred during a period of tectonic deformation as a consequence of the ongoing progressive restriction of the Mediterranean-Atlantic gateway during the Tortonian to Messinian stages (Capella et al., 2017b) due to convergence of the Iberian and African plates leading to the uplift of the Gibraltar Arc (Duggen et al., 2003; Civiero et al., 2020). In contrast to other contourite systems, in this case tectonism and diapirism exerted greater control over the distribution and dimension of the deposits. The contourite drifts identified in the wedge top basins in the central Gulf of Cádiz

(Figs. 5-11 to 5-13, 5-14) are concentrated in areas confined by structural highs or fault scarps that developed synchronously, through the emplacement of the accretionary wedge and the gravitational collapse during the middle to late Miocene (Medialdea et al., 2004; Gràcia et al., 2003). Drifts in the southern West Iberian margin though, are located on the flank of structural highs (Figs. 5-7 to 5-8, 5-14) resulting from the tectonic inversion and reactivation of rift-related faults and margin uplift (Zitellini et al., 2004; Pereira et al., 2011). Bathymetric features such as these would have locally accelerated bottom current flow (Sánchez-Leal et al., 2017; Duarte et al., 2020). The smaller dimensions of these drift deposits would also be restricted by the availability of accommodation. In the setting of the onshore Gharb basin, the late Miocene contourite drift subsurface of the Haricha section (Fig. 5-15), identified by Capella et al. (2017a), is deposited in similar settings, the deposits being locally bounded by structural highs created by emplacement of the Rif Nappe, as seen in both the seismic cross section and the geological map (Fig. 5-15). The overall preservation of contourite drift deposits would have been adversely affected in continental margins undergoing deformation processes such as uplift, where deposits of older stages are susceptible to widespread erosion by younger and more vigorous bottom currents. Distinguishment of the late Miocene CDS may serve as a good analogue for drift discrimination in other tectonically active settings.

The late Miocene CDS also provide insights as to the climatic and oceanographic history from the Tortonian to the Messinian. A weaker outflow of the paleo-MOW across a wide Mediterranean-Atlantic gateway might have existed during the middle- to early-late Miocene (Capella et al., 2019), prior to deposition of the initial-drift stage, yet no evidence of such was preserved due to the tectonic activity and deformation in the Gulf of Cádiz towards the southern West Iberian margin. This outflow setting would have generated a distinctive water mass in the Atlantic and influenced the North Atlantic paleoceanography. The onset of the overflow setting of the paleo-MOW exchange during the late Miocene would have increased entrainment of ambient Atlantic water to form the paleo-Atlantic Mediterranean Water (AMW; Rogerson et al., 2012) and flowed towards the North Atlantic. This would have had a significant impact on the ocean circulation in the North Atlantic. The late Miocene Mediterranean overflow most likely helped to sustain the formation of the North Atlantic Deep Water (NADW) (Rogerson et al., 2012) and the Atlantic Meridional Overturning Circulation (AMOC) (Rogerson et al., 2006; Ivanovic et al., 2013). Capella et al. (2019) similarly suggested that overflow conditions could have favoured ocean-atmospheric carbon dioxide (CO_2) decoupling by initiating an ocean pump for CO_2 transport. Such a scenario would have

meant surface water cooling and carbon sequestration in the deep ocean (Capella et al., 2019), and contributed to the late Miocene global cooling trend (Herbert et al., 2016; Capella et al., 2019), hence the northern hemisphere Messinian ice ages (van der Laan et al., 2012).

Conclusion

A late Miocene contourite depositional system (CDS) in the Neogene basins across the middle slope of the Gulf of Cádiz was recognised through the documentation of drift deposits and erosional features which act as clues to the paleoceanographic imprints of bottom water circulation during the late Miocene. Here, we describe for the first time the occurrence of regional contourite features after the main emplacement of the accretionary wedge (GCAW) or allochthonous unit (AUGC) during the late Tortonian, prior to the disconnection of the Mediterranean-Atlantic exchange in the middle to late Messinian (~6.4 Ma). This supports the influence of paleo-Mediterranean Outflow Water (MOW) water mass in locally controlling the morphology and sedimentary stacking pattern on the middle continental slope of the Gulf of Cádiz and towards the southern West Iberian margin, downstream of the Betic and Rifian corridors. Seismic stratigraphic analysis served to identify the four stages related to the evolution of the late Miocene CDS, based on external morphological expressions and internal reflection configurations, namely the initial-drift stage (subunit M1), the growth-drift stage (sub-unit M2), the maintenance-drift stage (sub-unit M3), and the buried-drift stage (Upper LM unit). They record the weak to vigorous long-term evolution of the bottom current velocity and its subsequent halt in relation to the synchronous restriction of the Mediterranean-Atlantic gateway. The distribution and preservation of these contourite drifts are favoured by local syn- and post-depositional tectonic deformation. Locally, sediments within these drift deposits are supplied by downslope gravitational systems, whereas regional uplifting processes affects sediment erosion and accommodation, thereby contributing to the evolution of the overall drift morphology.

However, certain limitations of the seismic and borehole data impede a more detailed description of the sedimentary evolution of the CDS. Acquisition of 3D and reprocessing of 2D seismic data with a refined interpretation workflow, as well as the obtainment of sedimentological information from boreholes in the study area, would be necessary to unravel, with higher confidence, the role of bottom currents in controlling the sedimentary stacking

patterns, and their interaction with other deep-water processes in depositing the late Miocene CDS. Proxies for climatic and tectonic changes are also vital to explain their effects on the local and regional scale. The upcoming IMMAGE amphibious (IODP 895 and ICDP) drilling project (Investigating Miocene Mediterranean-Atlantic Gateway Exchange: http://immage.icdp-online.org) will be able to provide the data to better understand the late Miocene CDS of the Gulf of Cádiz. Notwithstanding, this work marks a crucial step towards understanding the long-term evolution of the late Miocene Mediterranean-Atlantic exchange and the effect of the paleo-MOW evolution on ocean circulation in the North Atlantic, as well as its impact on late Miocene global climate cooling. The seismic analysis of the late Miocene CDS in the Gulf of Cádiz could also serve as an analogue for recognising highly deformed contourite deposits in the subsurface of other tectonically active continental margins.

Acknowledgments

References

Abbassi, A., Cipollari, P., Zaghloul, M. N., Cosentino, D., 2020. The Rif Chain (Northern Morocco) in the Late Tortonian-Early Messinian Tectonics of the Western Mediterranean Orogenic Belt: Evidence from the Tanger-Al Manzla Wedge-Top Basin. Tectonics, 39, e2020TC006164. doi:10.1029/2020TC006164

Ambar, I., Howe, M.R., 1979. Observations of the Mediterranean outflow-II. The deep circulation in the vicinity of the Gulf of Cadiz. Deep-Sea Research, 26A, 555-568. doi:10.1016/0198-0149(79)90096-7

Bailey, W.S., McArthur, A.D., McCaffrey, W.D., 2021. Distribution of contourite drifts on convergent margins: Examples from the Hikurangi subduction margin of New Zealand. Sedimentology, 68, 294-323. doi:10.1111/sed.12779

Brackenridge, R., Hernández-Molina, F.J., Stow, D.A.V., Llave, E., 2013. A Pliocene mixed contourite-turbidite system offshore the Algarve Margin, Gulf of Cadiz: Seismic response, margin evolution and reservoir implications. Marine and Petroleum Geology, 46, 36-50. doi:10.1016/j.marpetgeo.2013.05.015

Capella, W., Flecker, R., Hernández-Molina, F.J., Simon, D., Meijer, P.T., Rogerson, M., Sierro, F.J., Krijgsman, W., 2019. Mediterranean isolation preconditioning the Earth System for late Miocene climate cooling. Scientific Reports, 9, 3795. doi:10.1038/s41598-019-40208-2

Capella, W., Hernández-Molina, F.J., Flecker, R., Hilgen, F.J., Hssain, M., Kouwenhoven, T.J., van Oorschot, M., Sierro, F.J., Stow, D.A.V., Trabucho-Alexandre, J., Tulbure, M.A., de Weger, W., Yousfi, M.Z., Krijgsman, W., 2017a. Sandy contourite drift in the late Miocene Rifian Corridor (Morocco): reconstruction of depositional environments in a foreland-basin seaway. Sedimentary Geology, 355, 31–57. doi:10.1016/j.sedgeo.2017.04.004

Capella, W., Matenco, L., Dmitrieva, E., Roest, W.M., Hessels, S., Hssain, M., Chakor-Alami, A., Sierro, F.J., and Krijgsman, W., 2017b. Thick-skinned tectonics closing the Rifian Corridor. Tectonophysics, 710, 249–265. doi:10.1016/j.tecto.2016.09.028

Civiero, C., Custódio, S., Duarte, J.C., Mendes, V.B., Faccenna, C., 2020. Dynamics of the Gibraltar Arc System: A Complex Interaction Between Plate Convergence, Slab Pull, and Mantle Flow. Journal of Geophysical Research: Solid Earth, 125, e2019JB018873. doi:10.1029/2019JB018873

de Castro, S., Hernández-Molina, F.J., de Weger, W., Jiménez-Espejo, F.J., Rodríguez-Tovar, F.J., Mena, A., Llave, E., Sierro, F.J., 2021. Contourite characterization and its discrimination from other deep-water deposits in the Gulf of Cadiz contourite depositional system. Sedimentology. doi:10.1111/sed.12813

de Castro, S., Hernández-Molina, F.J., Rodríguez-Tovar, F.J., Llave, E., Ng, Z.L., Nishida, N., Mena, A., 2020. Contourites and bottom current reworked sands: Bed facies model and implications. Marine Geology, 428, 106267. doi:10.1016/j.margeo.2020.106267

de Weger, W., Hernández-Molina, F.J., Flecker, R., Sierro, F.J., Chiarella, D., Krijgsman, W., Manar, M.A., 2020. late Miocene contourite channel system reveals intermittent overflow behavior. Geology. doi:10.1130/G47944.1

Duarte, D., Roque, C., Hernández-Molina, F.J., Ng, Z.L., Magalhães, V.H., Llave, E., Sierro, F.J., 2020. Tectonic domains of the Betic Foreland System, SW Iberian Margin: Implications for the Gulf of Cadiz Contourite System. EGU General Assembly 2020, Online, 4-8 May 2020, EGU2020-1033. doi:10.5194/egusphere-egu2020-1033

Duarte, J.C., Rosas, F.M., Terrinha, P., Gutscher, M.-A., Malavieille, J., Silva, S., Matias, L., 2011. Thrust–wrench interference tectonics in the Gulf of Cadiz (Africa–Iberia plate boundary in the North-East Atlantic): insights from analog models. Marine Geology, 289, 135-149. doi:10.1016/j.margeo.2011.09.014

Duggen, S., Hoernle, K., van den Bogaard, P., Rüpke, L., Morgan, J.P., 2003. Deep roots of the Messinian salinity crisis. Nature, 422, 602-606. doi:10.1038/nature01553

Expedition 339 Scientists, 2012. Mediterranean outflow: environmental significance of the Mediterranean Outflow Water and its global implications. IODP Preliminary Report, 339. doi:10.2204/iodp.pr.339.2012

Faugères, J.-C., Stow, D.A.V., 2008. Continental drifts: nature, evolution, and controls. In: Rebesco, M., Camerlenghi, A. (Eds.), Contourites. Developments in Sedimentology, 60. Elsevier, Amsterdam, pp. 259–288.

Faugères, J.-C., Stow, D.A.V., Imbert, P., Viana. A., 1999. Seismic features diagnostic of contourite drifts. Marine Geology, 162, 1-38. doi:10.1016/S0025-3227(99)00068-7

Flecker, R., Krijgsman, W., Capella, W., de Castro Martíns, C., Dmitrieva, E., Mayser, J.P., Marzocchi, A., Modestou, S., Ochoa, D., Simon, D., Tulbure, M., van den Berg, B., van der Schee, M., de Lange, G., Ellam, R., Govers, R., Gutjahr, M., Hilgen, F.J., Kouwenhoven, T., Lofi, J., Meijer, P., Sierro, F.J., Bachiri, N., Barhoun, N., Chakor Alami, A., Chacon, B., Flores, J.A., Gregory, J., Howard, J., Lunt, D., Ochoa, M., Pancost,

R., Vincent, S., Zakaria Yousfi, M., 2015. Evolution of the late Miocene Mediterranean-Atlantic gateways and their impact on regional and global environmental change. Earth-Science Reviews, 150, 365-392. doi:10.1016/j.earscirev.2015.08.007

Flinch, J.F., 1993. Tectonic evolution of the Gibraltar Arc. Ph.D. Thesis. Rice University, Houston. doi:10.13140/RG.2.1.3898.6085

García, M., Hernández-Molina, F.J., Llave, E., Stow, D.A.V., León, R., Fernández-Puga, M.C., Díaz del Río, V., Somoza, L., 2009. Contourite erosive features caused by the Mediterranean Outflow Water in the Gulf of Cadiz: Quaternary tectonic and oceanographic implications. Marine Geology, 257, 24–40. doi:10.1016/j.margeo.2008.10.009

Gràcia, E., Dañobeitia, J., Vergés, J., Bartolomé, R., 2003. Crustal architecture and tectonic evolution of the Gulf of Cadiz (SW Iberian margin) at the convergence of the Eurasian and African plates. Tectonics, 22, 1033. doi:10.1029/2001TC901045

Herbert, T. D., Lawrence, K.T., Tzanova, A., Peterson, L.C., Caballero-Gill, R., Kelly, C.S., 2016. Late Miocene global cooling and the rise of modern ecosystems. Nature Geoscience 9, 843-847. doi:10.1038/ngeo2813

Hernández-Molina, F.J., Llave, E., Somoza, L., Fernández-Puga, M.C., Maestro, A., León, R., Barnolas, A., Medialdea, T., García, M., Vázquez, J.T., Díaz del Río, V., Fernández-Salas, L.M., Lobo, F., Alveirinho Dias, J.M., Rodero, J., Gardner, J., 2003. Looking for clues to paleoceanographic imprints: a diagnosis of the gulf of Cadiz contourite depositional systems. Geology, 31, 19–22. doi:10.1130/0091-7613(2003)031<0019:LFCTPI>2.0.CO;2

Hernández-Molina, F.J., Sierro, F.J., Llave, E., Roque, C., Stow, D.A.V., Williams, T., Lofi, J., van der Schee, M., Arnáiz, A., Ledesma, S., Rosales, C., Rodríguez-Tovar, F.J., Pardo-Igúzquiza, E., Brackenridge, R.E., 2016. Evolution of the gulf of Cádiz margin and southwest Portugal contourite depositional system: Tectonic, sedimentary and paleoceanographic implications from IODP expedition 339. Marine Geology, 377, 7-39. doi:10.1016/j.margeo.2015.09.013

Hernández-Molina, F.J., Stow, D.A.V., Llave, E., 2008. Continental slope contourites. In: Rebesco, M., Camerlenghi, A. (Eds.), Contourites. Developments in Sedimentology, 60. Elsevier, Amsterdam, pp. 379–408.

Hernández-Molina, F.J., Stow, D., Alvarez-Zarikian, C., and Expedition IODP 339 Scientists, 2013. IODP Expedition 339 in the Gulf of Cadiz and off West Iberia: decoding the

environmental significance of the Mediterranean outflow water and its global influence. Sci. Drill., 16:1–11. doi:10.5194/sd-16-1-2013

Hilgen, F., Kuiper, K., Krijgsman, W., Snel, E., & van der Laan, E., 2007. Astronomical tuning as the basis for high resolution chronostratigraphy: the intricate history of the Messinian Salinity Crisis. Stratigraphy, 4, 231-238.

Hüneke, H., Hernández-Molina, F.J., Rodríguez-Tovar, F.J., Llave, E., Chiarella, D., Mena, A., Stow, D.A.V., 2020. Diagnostic criteria using microfacies for calcareous contourites, turbidites and pelagites in the Eocene–Miocene slope succession, southern Cyprus. Sedimentology. doi:10.1111/sed.12792

Hüneke, H., Stow, D.A.V., 2008. Identification of ancient contourites: problems and palaeoceanographic significance. In: Rebesco, M., Camerlenghi, A. (Eds.), Contourites. Developments in Sedimentology, 60. Elsevier, Amsterdam, pp. 323–344.

Iribarren, L., Vergés, J., Camurri, F., Fullea, J., Fernàndez, M. 2007. The structure of the Atlantic–Mediterranean transition zone from the Alboran Sea to the Horseshoe Abyssal Plain (Iberia–Africa plate boundary). Marine Geology, 243, 97–119. doi:10.1016/j.margeo.2007.05.011

Ivanovic, R.F., Flecker, R., Gutjahr, M., Valdesa, P.J., 2013. First Nd isotope record of Mediterranean–Atlantic water exchange through the Moroccan Rifian Corridor during the Messinian Salinity Crisis. Earth Planetary Science Letters, 368, 163-174. doi:10.1016/j.epsl.2013.03.010

Krijgsman, W., Capella, W., Simon, D., Hilgen, F.J., Kouwenhoven, T.J., Meijer, P.Th., Sierro, F.J., Tulbure, M.A., van den Berg, B.C.J., van der Schee, M., Flecker, R., 2018. The Gibraltar Corridor: Watergate of the Messinian Salinity Crisis. Marine Geology, 403, 238-246. doi:10.1016/j.margeo.2018.06.008

Krijgsman, W., Hilgen, F. J., Raffi, I., Sierro, F. J., Wilson, D. S., 1999. Chronology causes and progression of the Messinian salinity crisis. Nature, 400, 652–655. doi:10.1038/23231

Levy, R.G., Tilloy, R., 1962. Maroc Septentrional (Chaine du Rif), partie B. Livret-Guide des excursions A31 et C31. Congres Geologique International, XIX session, Alger. pp. 8-65. In: Capella, W., Matenco, L., Dmitrieva, E., Roest, W.M., Hessels, S., Hssain, M., Chakor-Alami, A., Sierro, F.J., and Krijgsman, W., 2017b, Thick-skinned tectonics closing the Rifian Corridor: Tectonophysics, 710, 249–265. doi:10.1016/ j.tecto.2016.09.028

Liu, S., Hernández-Molina, F.J., Ercilla, G., Van Rooij, D., 2020. Sedimentary evolution of the Le Danois contourite drift systems (southern Bay of Biscay, NE Atlantic): A

reconstruction of the Atlantic Mediterranean Water circulation since the Pliocene. Marine Geology, 427, 106217. doi:10.1016/j.margeo.2020.106217

Llave, E., Hernández-Molina, F.J., García, M., Ercilla, G., Roque, C., Juan, C., Mena, A., Preu, B., Van Rooij, D., Rebesco, M., Brackenridge, R., Jané, G., Gómez-Ballesteros, M., Stow, D., 2019. Contourites along the Iberian continental margins: conceptual and economic implications. Geological Society London Special Publications, 476, 403-436. doi:10.1144/SP476-2017-46

Llave, E., Hernández-Molina, F.J., Somoza, L., Díaz del Río, V., Stow, D.A.V., Maestro, A., Alveirinho Dias, J.M., 2001. Seismic stacking pattern of the Faro-Albufeira contourite system (Gulf of Cadiz): A Quaternary record of paleoceanographic and tectonic influences. Marine Geophysical Research, 22, 475–496. doi:10.1023/A:1016355801344

Llave, E., Hernández-Molina, F.J., Somoza, L., Stow, D.A.V., Díaz del Río, V., 2007. Quaternary evolution of the contourite depositional system in the Gulf of Cadiz. In: Viana, A.R., Rebesco, M. (Eds.), Economic and Palaeoceanographic Significance of Contourite Deposits. Geological Society London Special Publication, 276, 49-79. doi:10.1144/GSL.SP.2007.276.01.03

Llave, E., Matias, H., Hernández-Molina, F.J., Ercilla, G., Stow, D.A.V., Medialdea, T., 2011. Pliocene–Quaternary contourites along the northern gulf of Cadiz margin: sedimentary stacking pattern and regional distribution. Geo-Marine Letters, 31, 377–390. doi:10.1007/s00367-011-0241-3

Llave, E., Schönfeld, J., Hernández-Molina, F.J., Mulder, T., Somoza, L., Del Río, V.D., Sánchez-Almazo, I., 2006. High-resolution stratigraphy of the Mediterranean outflow contourite system in the Gulf of Cadiz during the late Pleistocene: The impact of Heinrich events. Marine Geology, 227, 241–262. https://doi .org/10.1016/ j.margeo.2005.11.015

Lopes, F. C., Cunha, P. P., & Le Gall, B., 2006. Cenozoic seismic stratigraphy and tectonic evolution of the Algarve margin (offshore Portugal, southwestern Iberian Peninsula). Marine Geology, 231, 1-36. doi:10.1016/j.margeo.2006.05.007

Louarn, E., Morin, P., 2011. Antarctic intermediate water influence on Mediterranean sea water outflow. Deep-Sea Research I Oceanography Research Papers, 58, 932–942, doi:10.1016/j.dsr.2011.05.009

Maestro, A., Somoza, L., Medialdea, T., Talbot, C.J., Lowrie, A., Vázquez, J.T. and Díaz-del-Río, V., 2003. Large-scale slope failure involving Triassic and Middle Miocene salt and

shale in the Gulf of Cádiz (Atlantic Iberian Margin). Terra Nova, 15, 380-391. doi:10.1046/j.1365-3121.2003.00513.x

Maldonado, A., Somoza, L., Pallarés, L., 1999. The Betic orogen and the Iberian-African boundary in the Gulf of Cádiz: geological evolution (central North Atlantic). Marine Geology, 155, 9-43. doi:10.1016/S0025-3227(98)00139-X

Manzi, V., Gennari, R., Lugli, S., Persico, D., Reghizzi, M., Roveri, M., Schreiber, B.C., Calvo, R., Gavrieli, I., Gvirtzman, Z., 2018. The onset of the Messinian salinity crisis in the deep Eastern Mediterranean basin. Terra Nova, 30, 189-198. doi:10.1111/ter.12325

Martín, J.M., Braga, J.C., Aguirre, J., Puga-Bernabéu, Á., 2009. History and evolution of the North-Betic Strait (Prebetic Zone, Betic Cordillera): A narrow, Early Tortonian, tidal-dominated, Atlantic-Mediterranean marine passage. Sedimentary Geology, 216, 80-90. doi:10.1016/j.sedgeo.2009.01.005

Martínez-Loriente, S., Gràcia, E., Bartolome, R., Sallarès, V., Connors, C., Perea, H., Lo Iacono, C., Klaeschen, D., Terrinha, P., Dañobeitia, J.J., Zitellini, N., 2013. Active deformation in old oceanic lithosphere and significance for earthquake hazard: Seismic imaging of the Coral Patch Ridge area and neighboring abyssal plains (SW Iberian Margin). Geochemistry, Geophysics, Geosystems, 14, 2206-2231. doi:10.1002/ggge.20173

Medialdea, T., Vegas, R., Somoza, L., Vázquez, J.T., Maldonado, A., Díaz-del-Río, V., Maestro, A., Córdoba, D., and Fernández-Puga, M.C., 2004. Structure and evolution of the ''Olistostrome'' complex of the Gibraltar Arc in the Gulf of Cádiz (eastern Central Atlantic): evidence from two long seismic cross-sections. Marine Geology, 209, 173-198. doi:10.1016/j.margeo.2004.05.029

Medialdea, T., Somoza, L., Pinheiro, L.M., Fernández-Puga, M.C., Vázquez, J.T., León, R., Ivanov, M.K., Magalhaes, V., Díaz-del-Río, V., Vegas, R., 2009. Tectonics and mud volcano development in the Gulf of Cádiz. Marine Geology, 261, 48–63. doi:10.1016/j.margeo.2008.10.007

Menard, H.W., 1955. Deformation of the northeastern Pacific basin and the west coast of North America. Geological Society of America Bulletin, 66, 1149-1198. doi:10.1130/0016-7606(1955)66[1149:DOTNPB]2.0.CO;2

Mencaroni, D., Urgeles, R., Ford, J., Llopart, J., Sánchez Serra, C., Calahorrano, A., Brito, P., Lo Iacono, C., Bartolomè, R., Gràcia, E., Rebesco, M., Camerlenghi, A., Bellwald, B., 2020. How deep does sand deposits in the Alentejo basin (Gulf of Cadiz) reach? Evaluating

slope stability from bottom-current activities through time. EGU General Assembly 2020, 4-8 May 2020, EGU2020-18904. doi:10.5194/egusphere-egu2020-18904

Mestdagh, T., Lobo, F.J., Llave, E., Hernández-Molina, F.J., Van Rooij, D., 2019. Review of the late Quaternary stratigraphy of the northern Gulf of Cadiz continental margin: new insights into controlling factors and global implications. Earth Science Reviews, 198, 102944. doi.org/10.1016/j.earscirev.2019.102944

Mestdagh, T., Lobo, F.J., Llave, E., Hernández-Molina, F.J., García Ledesma, A., Puga-Bernabéu, Á., Fernández-Salas, L.-M., Rooij, D.V., 2020. Late Quaternary multi-genetic processes and products on the northern Gulf of Cadiz upper continental slope (SW Iberian Peninsula). Marine Geology, 427, 106214. doi:10.1016/j.margeo.2020.106214

Miramontes, E., Eggenhuisen, J.T., Jacinto, R.S., Poneti, G., Pohl, F., Normandeau, A., Campbell, D.C., Hernández-Molina, F.J., 2020. Channel-levee evolution in combined contour current-turbidity current flows from flume-tank experiments. Geology, 48, 353-357. doi:10.1130/G47111.1

Mitchum, R.M. Jr., Vail, P.R., Sangree, J.B., 1977. Seismic stratigraphy and global changes of sea level; Part 6, Stratigraphic interpretation of seismic reflection patterns in depositional sequences. In: Payton, C.E. (Ed.), Seismic stratigraphy – applications to hydrocarbon exploration. American Association of Petroleum Geologists (AAPG) Memoir, 26, 117-133.

Mulder, T., Faugères, J.-C., Gonthier, E., Rebesco, M., Camerlenghi, A., 2008. Mixed turbidite-contourite systems. In: Rebesco, M., Camerlenghi, A. (Eds.), Contourites. Developments in Sedimentology, 60. Elsevier, Amsterdam, pp. 435–456. doi:10.1016/S0070-4571(08)10021-8

Ng, Z.L., Hernández-Molina, F.J., Duarte, D., Sierro, F.J., Ledesma, S., Rogerson, M., Llave, E., Roque, C., Manar, M.A., 2021. Latest Miocene restriction of the Mediterranean Outflow Water: a perspective from the Gulf of Cádiz. Geo-Marine Letters, 41, 23. doi.org/10.1007/s00367-021-00693-9

Nielsen, T., Knutz, P.C., Kuijpers, A., 2008. Seismic Expression of Contourite Depositional Systems. In: Rebesco, M., Camerlenghi, A. (Eds.), Contourites. Developments in Sedimentology, 60. Elsevier, Amsterdam, pp. 301–321.

O'Neill-Baringer, M., Price, J.F., 1997. Mixing and spreading of the Mediterranean outflow. Journal of Physical Oceanography, 27, 1654-1677. doi:10.1175/1520-0485(1997)027<1654:MASOTM>2.0.CO;2

Pellegrini, C., Maselli, V., Trincardi, F., 2016. Pliocene–Quaternary contourite depositional system along the south-western Adriatic margin: changes in sedimentary stacking pattern and associated bottom currents. Geo-Marine Letters, 36, 67-79. doi:10.1007/s00367-015-0424-4

Pereira, R., Alves, T.M., 2013. Crustal deformation and submarine canyon incision in a Meso-Cenozoic first-order transfer zone (SW Iberia, North Atlantic Ocean). Tectonophysics, 601, 148-162. doi:10.1016/j.tecto.2013.05.007

Pereira, R., Alves, T.M., Cartwright, J., 2011. Post-rift compression on the SW Iberian margin (eastern North Atlantic): a case for prolonged inversion in the ocean–continent transition zone. Journal of the Geological Society, 168, 1249-1263. doi:10.1144/0016-76492010-151

Pereira, R., Alves, T.M., Mata, J., 2016. Alternating crustal architecture in West Iberia: a review of its significance in the context of NE Atlantic rifting. Journal of the Geological Society, 174, 522-540. doi:10.1144/jgs2016-050

Pérez-Asensio, J.N., Aguirre, J., Schmiedl, G., Civis, J., 2012. Impact of restriction of the Atlantic-Mediterranean gateway on the Mediterranean Outflow Water and eastern Atlantic circulation during the Messinian. Paleoceanography, 27, PA3222. doi:10.1029/2012PA002309

Posamentier H.W., Erskine R.D., 1991. Seismic Expression and Recognition Criteria of Ancient Submarine Fans. In: Weimer P., Link M.H. (Eds.) Seismic Facies and Sedimentary Processes of Submarine Fans and Turbidite Systems. Frontiers in Sedimentary Geology. Springer, New York. pp. 197-222. doi:10.1007/978-1-4684-8276-8_10

Ramos, A., Fernández, O., Muñoz, J.A., Terrinha, P., 2017. Impact of basin structure and evaporite distribution on salt tectonics in the Algarve Basin, Southwest Iberian margin. Marine and Petroleum Geology, 88, 961–984. doi:10.1016/j.marpetgeo.2017.09.028

Rebesco, M., Hernández-Molina, F.J., Van Rooij, D., Wåhlin, A., 2014. Contourites and associated sediments controlled by deep-water circulation processes: State-of-the-art and future considerations. Marine Geology, 352, 111-154. doi:10.1016/j.margeo.2014.03.011

Reed, D.L., Meyer, A.W., Silver, E.A., Prasetyo, H., 1987. Contourite sedimentation in an intracratonic forearc system: eastern Sunda Arc, Indonesia. Marine Geology, 76, 223-241. doi:10.1016/0025-3227(87)90031-4

Rodrigues, S., Roque, C., Hernández-Molina, F.J., Llave, E., Terrinha, P., 2020. The Sines Contourite Depositional System along the SW Portuguese Margin: onset, evolution, and conceptual implications. Marine Geology, 106357. doi:10.1016/j.margeo.2020.106357

Rodrigues, S., Hernández-Molina, F.J., Kirby, A., 2021. A Late Cretaceous mixed (turbidite-contourite) system along the Argentine Margin: Paleoceanographic and conceptual implications. Marine and Petroleum Geology, 104768. doi:10.1016/j.marpetgeo.2020.104768

Rogerson, M., Rohling, E. J., Weaver, P. P. E, 2006. Promotion of meridional overturning by Mediterranean derived salt during the last deglaciation. Paleoceanography, 21, PA4101, doi:10.1029/2006PA001306.

Rogerson, M., Rohling, E.J., Bigg, G.R., Ramirez, J., 2012. Palaeoceanography of the Atlantic-Mediterranean Exchange: Overview and first quantitative assessment of climatic forcing. Reviews of Geophysics, 50, RG2003. doi:10.1029/2011RG000376

Roque, C., Duarte, H., Terrinha, P., Valadares, V., Noiva, J., Cachão, M., Ferreira, J., Legoinha, P., Zitellini, N., 2012. Pliocene and Quaternary depositional model of the Algarve margin contourite drifts (gulf of Cadiz, SW Iberia): seismic architecture, tectonic control and paleoceanographic insights. Marine Geology, 303–306, 42–62. doi:10.1016/j.margeo.2011.11.001

Sánchez-Leal, R.F., Bellanco, M.J., Fernández-Salas, L.M., García-Lafuente, J., Gasser-Rubinat, M., González-Pola, C., Hernández-Molina, F.J., Pelegrí, J.L., Peliz, A., Relvas, P., Roque, D., Ruiz-Villarreal, M., Sammartino, S., Sánchez-Garrido, J.C., 2017. The Mediterranean Overflow in the Gulf of Cadiz: A rugged journey. Science Advances, 3, eaao0609. doi:10.1126/sciadv.aao0609

Serra, C.S., Martínez-Loriente, S., Gràcia, E., Urgeles, R., Vizcaino, A., Perea, H., Bartolome, R., Pallàs, R., Lo Iacono, C., Diez, S., Dañobeitia, J., Terrinha, P., Zitellini, N., 2020. Tectonic evolution, geomorphology, and influence of bottom currents along a large submarine canyon system: The São Vicente Canyon (SW Iberian margin). Marine Geology, 426, 106219. doi:10.1016/j.margeo.2020.106219

Shanmugam, G., 2008. Deep-water bottom currents and their deposits. In: Rebesco, M., Camerlenghi, A. (Eds.), Contourites. Developments in Sedimentology, 60. Elsevier, Amsterdam, pp. 59–81.

Sierro, F.J., Hodell, D.A., Andersen, N., Azibeiro, L.A., Jimenez-Espejo, F.J., Bahr, A., Flores, J.A., Ausin, B., Rogerson, M., Lozano-Luz, R., Lebreiro, S.M., Hernández-Molina, F.J.,

2020. Mediterranean overflow over the last 250 kyr: Freshwater forcing from the tropics to the ice sheets. Paleoceanography and Paleoclimatology, 35, e2020PA003931. doi:10.1029/2020PA003931

Srivastava, S.P., Schouten, H., Roest, W.R., Klitgord, K.D., Kovacs, L.C., Verhoef, J. & Macnab, R. 1990. Iberian plate kinematics: a jumping plate boundary between Eurasia and Africa. Nature, 344, 756–759. doi:10.1038/344756a0

Stow, D.A.V., Hernández-Molina, F.J., Alvarez Zarikian, C.A., the Expedition 339 Scientists, 2013. Proceedings IODP, 339. Integrated Ocean Drilling Program Management International, Tokyo. doi:10.2204/iodp.proc.339.2013

Stow, D.A.V., Smillie, Z., 2020. Distinguishing between Deep-Water Sediment Facies: Turbidites, Contourites and Hemipelagites. Geosciences, 10, 68. doi:10.3390/geosciences10020068

Teixeira, M., Terrinha, P., Roque, C., Rosa, M., Ercilla, G., Casas, D., 2019. Interaction of alongslope and downslope processes in the Alentejo Margin (SW Iberia) – Implications on slope stability. Marine Geology, 410, 88-108. doi:10.1016/j.margeo.2018.12.011

Terrinha, P., Kullberg, J.C., Neres, M., Alves, T., Ramos, A., Ribeiro, C., Mata, J., Pinheiro, L., Afilhado, A., Matias, L., Luís, J., Muñoz, J.A., Fernández, Ó., 2019a. Rifting of the Southwest and West Iberia Continental Margins. In. Quesada, C., Oliveira, J.T. (Eds.), The Geology of Iberia: A Geodynamic Approach. Regional Geology Reviews. Springer, Cham. pp. 251-283. doi:10.1007/978-3-030-11295-0_6

Terrinha, P., Matias, L., Vicente, J., Duarte, J., Luíse, J., Pinheiro L., Lourenço, N., Diez, S., Rosas, F., Magalhães, V., Valadaresa, V., Zitellini, N., Roque, C., Mendes Víctor, L., MATESPRO Team, 2009. Strain partitioning and morphotectonics at the Iberia-Africa plate boundary from multibeam and seismic reflection data. Marine Geology, 267, 156-174. doi:10.1016/j.margeo.2009.09.012

Terrinha, P., Ramos, A., Neres, M., Valadares, V., Duarte, J., Martínez-Loriente, S., Silva, S., Mata J., Kullberg, J.C., Casas-Sainz, A., Matias, L., Fernández, Ó., Muñoz, J.A., Ribeiro, C., Font, E., Neves, C., Roque, C., Rosas, F., Pinheiro, L., Bartolomé, R., Sallarès, V., Magalhães, V., Medialdea, T., Somoza, L., Gràcia, E., Hensen, C., Gutscher, M.-A., Ribeiro, A., Zitellini, N., 2019b. The Alpine Orogeny in the West and Southwest Iberia Margins. In: Quesada C., Oliveira J. (Eds.) The Geology of Iberia: A Geodynamic Approach. Regional Geology Reviews. Springer, Cham. pp. 487-505. doi:10.1007/978-3-030-11295-0_11

Torelli, L., Sartori, R., Zitellini, N., 1997. The giant chaotic body in the Atlantic Ocean off Gibraltar: new results from a deep seismic reflection survey. Marine and Petroleum Geology, 14, 125-134. doi:10.1016/S0264-8172(96)00060-8

Tortella, D., Torne, M., Pérez-Estáun, A., 1997. Geodynamic Evolution of the Eastern Segment of the Azores-Gibraltar Zone: The Gorringe Bank and the Gulf of Cadiz Region. Marine Geophysical Researches 19, 211–230. doi:10.1023/A:1004258510797

van der Laan, E., Hilgen, F.J., Lourens, L.J., de Kaenel, E., Gaboardi, S., Iaccarino, S., 2012. Astronomical forcing of Northwest African climate and glacial history during the late Messinian (6.5-5.5 Ma). Palaeogeography Palaeoclimatology Palaeoecology, 313, 107-126. doi:10.1016/j.palaeo.2011.10.013

van der Schee, M., Sierro, F., Jimenez-Espejo, F., Hernández-Molina, F., Flecker, R., Flores, J., Acton, G., Gutjahr, M., Grunert, P., García-Gallardo, A., Andersen, N., 2016. Evidence of early bottom water current flow after the Messinian Salinity Crisis in the Gulf of Cádiz. Marine Geology, 380, 315-329. doi:10.1016/j.margeo.2016.04.005

Vancraeynest, F. 2015. Contourite depositional systems in the El Arraiche area, Moroccan Atlantic margin. Master's dissertation, Universiteit Gent. https://lib.ugent.be/fulltxt/RUG01/002/213/957/RUG01-002213957_2015_0001_AC.pdf

Vandorpe, T., Van Rooij, D., de Haas, H., 2014. Stratigraphy and paleoceanography of a topography-controlled contourite drift in the Pen Duick area, southern Gulf of Cádiz. Marine Geology, 349, 136-151. doi:10.1016/j.margeo.2014.01.007

Verdicchio, G., Trincardi, F., 2008. Shallow-water Contourites. In: Rebesco, M., Camerlenghi, A. (Eds.), Contourites. Developments in Sedimentology, 60. Elsevier, Amsterdam, pp. 409–433.

Vergés, J., Fernàndez, M., 2012. Tethys–Atlantic interaction along the Iberia–Africa plate boundary: The Betic–Rif orogenic system: Tectonophysics, 579, 144-172. doi:10.1016/j.tecto.2012.08.032.

Zitellini, N., Rovere, M., Terrinha, P., Chierici, F., Matias, L., Bigsets Team, 2004. Neogene Through Quaternary Tectonic Reactivation of SW Iberian Passive Margin. Pure and Applied Geophysics, 161, 565–587. doi:10.1007/s00024-003-2463-4

Supplementary Material

Table 5-S1 Acquisition parameters of the 2D seismic surveys used in this study: GC-D, GHR-10, HE91, LAR04, NWM03, P74, PD00 / PDT00, S81A, TASYO 2000 (TWT – two-way travel time).

Dataset (*Survey*)	Operator / *Institution*	Contractor / *Research Vessel*	Year	No. of Lines	Streamer Length	Source	Shotpoint Interval	Channels	Recording Length	Sample Rate (Resample)	Line Orientation & Spacing	Reference
GC-d	Repsol	-	-	7	-	Airgun	-	-	4 s TWT	2 ms	N-S, E-W	Hernández-Molina et al. (2016)
GHR10 (*Gharb*)	Repsol	PGS	2010	6	-	Airgun	18.75 m	408	6 s TWT	2 ms	NNW-SSE, ENE-WSW	-
HE91	*IGME*	*R/V Hesperides*	1980s	14	-	Airgun	-	-	4 s TWT	4 ms	NNW-SSE, E-W	Maldonado et al. (1999)
LAR04	Repsol	Fugro-Geoteam	2004	30	4.5 km	Airgun	25 m	360	6 s TWT	4 ms	NE-SW: 4 km, NW-SE: 4km	-
NWM03	Skidmore	Fugro-Geoteam	2000	71	6 km	Airgun	25 m	480	7 s TWT	4 ms	-	-
P74	Chevron	-	1970s	19	2.35 km	Airgun	50 m	48	6 s TWT	4 ms	N-S: 6-14 km, E-W: 8-11 km	Roque et al. (2012)
PD00 / PDT00	TGS	*R/V Zephyr 1*	2000	58	6 km	Airgun	25-30 m	240-480	12 s TWT	2 ms (4 ms)	NNW-SSE: 4 km, ENE-WSW: 8 km	Llave et al. (2011)
S81A	Repsol	-	2003	41	-	Airgun	-	-	7 s TWT	4 ms	NE-SW, NW-SE	Hernández-Molina et al. (2016)
TASYO 2000	*IGME*	*R/V Hesperides*	2000	14	2.5 km	TOPAS	50 m	96	10 s TWT	2 ms (4 ms)	ENE-WSW, NE-SW, NW-SE	Medialdea et al. (2004)

Text 5-S1   Limitations and suggestions for further study

The interpretation of the late Miocene contourite depositional system (CDS) of the Gulf of Cádiz is based on 2D multi-channel seismic (MCS) surveys correlated to limited borehole information. The identification of CDS through its morphological features and acoustic facies using seismic reflection data is dependent on the quality and resolution of the available seismic data, in respect to their line spacing and coverage, vertical and horizontal resolution, acquisition noise, and processing artefacts, in revealing or obscuring true reflection events.

The compilation of the seismic dataset did not include high-resolution seismic data from high-frequency sparker or airgun source surveys available in the study area (Llave et al., 2011; Brackenridge et al., 2013; Hernández-Molina et al, 2016, among others). This is due to lack of depth penetration for these surveys (<1000 m) to record the distribution of the late Miocene interval. However, the lower frequency airgun-sourced multichannel seismic profiles could only capture the longer-term sedimentary changes and larger-scale sediment bodies, with its lower average vertical resolution of 15 – 30 m (Llave et al., 2011; Roque et al., 2012) and decreasing horizontal resolution (>60 m) due to the increasing Fresnel zone with depth. Also, the wide line-spacing for the 2D seismic surveys (min: 4 km; Table 5-S1) did not permit the accurate representation of detailed seismic morphologies through surface mapping. Moreover, the increase in seismic artefacts with depth due to inadequate processing techniques for the deeper section of the seismic profiles also hinder the interpretation of the late Miocene interval. In contrast to the analysis of the modern CDS in the Gulf of Cádiz, the availability of a more robust dataset, such as the high-resolution sparker-sourced seismic, a high-resolution bathymetric compilation, continuous well logs and detailed core descriptions from borehole drilling, and a refined age model including bio- and cyclo-stratigraphic framework enabled a comprehensive analysis of the Pliocene-Quaternary sedimentary succession (see Llave et al., 2006; Stow et al., 2013; Hernández-Molina et al. 2016 for review). Examples of the workflow include the identification of erosional and depositional features of a CDS on bathymetric maps and their relationship with interpreted morphologies on seismic profiles, the distinguishment of sedimentary trends through high-resolution ties to well log, core and seismic data, correlation of seismic sub-units to sequence stratigraphy and sea-level variation, and the precise age assignment of sedimentary interval, all of which are impossible for the analysis of the ancient late Miocene interval with the available dataset.

This study also relies heavily on modern and ancient analogue studies, such as the Pliocene-Quaternary Gulf of Cádiz CDS and the outcrop-based late Miocene contourites of the Riffian corridor (Capella et al., 2017; de Weger et al., 2020), instead of sedimentary information from in-situ drilling. This is due to the lack of detail description within industry boreholes that penetrated the late Miocene interval as they were not primary targets (e.g., Corvina, Imperador, Ruivo, Neptuno-1, Neptuno-2). While we could draw similarities with the two systems, the conditions to which these deposits were formed may not represent that of the late Miocene CDS in the Gulf of Cádiz. For example, we would expect more proximal facies for the late Miocene contourites in the Riffian corridor in comparison to the Gulf of Cádiz as it is located closer to the sill of the late Miocene gateway. Whereas the current velocity of the Mediterranean Outflow Water (MOW) in controlling the evolution of the Pliocene-Quaternary CDS may have been more (or less) vigorous in comparison to the late Miocene due to the formation of the Strait of Gibraltar during the late Messinian to early Pliocene. Moreover, the tectonic and diapiric effects on this system are varied for their respective localities and time period. The tectonic deformation during the late Miocene could have changed the morphologies of the drift deposits and their paleodepths.

Therefore, we suggest that future works include reprocessing of the existing 2D seismic survey and or the acquisition of 3D seismic data to have a better coverage for a more rigorous interpretation and mapping of the contourite features and their distribution. We also recommend the reinterpretation or drilling of a continuous section targeting the contourite body to acquire sedimentological information to document and describe in detail the sedimentary facies and the evolution of the late Miocene CDS with regards to the paleo-MOW oceanography and to better understand the link between the control factors (tectonic, sedimentary, climatic) and the drift deposits. The upcoming IMMAGE amphibious (IODP 895 and ICDP) drilling project (Investigating Miocene Mediterranean-Atlantic Gateway Exchange: http://immage.icdp-online.org) aims to drill the late Miocene sedimentary record in this region, where its potential results will be crucial in investigating the hypotheses presented from this work in order to better understand the paleo-MOW variability and its implications. On top of that, backstripping analysis technique of the sedimentary sequence could provide a better understanding on the effects of the tectonic driving forces, such as basin subsidence or uplift, on the deviation from the original depositional position of the late Miocene CDS along the continental margins.

Chapter 6

Late Miocene evolution of the eastern Deep Algarve basin: interaction of bottom currents and gravitational processes in a foredeep setting

Zhi Lin Ng, F. Javier Hernández-Molina, Santiago Ledesma, Francisco J. Sierro, Débora Duarte, Estefanía Llave, Cristina Roque, Álvaro Arnáiz. 2021. Late Miocene evolution of the eastern Deep Algarve basin: interaction of bottom currents and gravitational processes in a foredeep setting.

Late Miocene evolution of the eastern Deep Algarve basin: interaction of bottom currents and gravitational processes in a foredeep setting

Zhi Lin Ng[1*], F. Javier Hernández-Molina[1], Santiago Ledesma[2], Francisco J. Sierro[3], Débora Duarte[1,4], Estefanía Llave[5], Cristina Roque[6,7], Álvaro Arnáiz[8]

[1]Dept. Earth Sciences, Royal Holloway University of London, Egham TW20 0EX, UK
[2]Naturgy Energy Group S.A., 28033 Madrid, Spain
[3]Departamento de Geología, Universidad de Salamanca, 37008 Salamanca, Spain
[4]Instituto Português do Mar e da Atmosfera (IPMA), 1749-077 Lisboa, Portugal
[5]Instituto Geológico y Minero de España (IGME), 28003 Madrid, Spain
[6]Estrutura de Missão para a Extensão da Plataforma Continental (EMEPC), 2770-047 Paço de Arcos, Portugal
[7]Instituto Dom Luiz (IDL), Faculdade de Ciência da Universidade de Lisboa, 1749-016 Lisboa, Portugal
[8]Repsol S.A., 28045 Madrid, Spain
[*]*Corresponding author:* Zhi Lin Ng (Zhi.Ng.2016@live.rhul.ac.uk)

Abstract

Foreland basins are normally dominated by turbidite deposits in the early stages of their evolution. In this work, we show evidences of bottom current influence in the Algarve basin, which evolved as a foredeep basin of the Betic-Rif orogeny, during which the paleo-Mediterranean Outflow Water (MOW) was active through the Betic and Rifian corridors. Seismic interpretation identified four stages of sedimentary evolution (Stages I-IV) in the eastern domain of the Deep Algarve basin. Stages I and II correspond to the Late Miocene contourite depositional system during the late Tortonian to early Messinian, interrupted by the emplacement of the allochthonous unit of the Gulf of Cádiz. Bottom currents reworked the initial turbiditic sediments in the eastern Deep Algarve basin, as the downstream continuation of the Guadalquivir sands turbidite system, forming contourite drifts prior to the severe weakening or cessation of the paleo-MOW around mid-Messinian. Stages III and IV represent the evolution of the turbidite system with a lack of bottom current influence, through the downstream translation and lateral migration of meandering submarine channels, and their subsequent abandonment, during the late Messinian. The Tortonian to Messinian evolution of bottom current is modulated by the water-mass exchange between the Mediterranean and the Atlantic due to the shallowing of sill and subsequent restriction of the paleo-MOW through the Betic and Rifian gateways around ~6.4 Ma. Tectonic and glacioeustatic changes exerted control over both the turbidite and contourite depositional systems, where tectonic pulses of about 400-kyr dictated their large-scale morphosedimentary evolution and interactions.

Keywords: Deep-marine sedimentation, bottom currents, gravitational processes, paleo-Mediterranean Outflow Water, Late Miocene, Deep Algarve basin

Introduction

The Late Miocene evolution of the Gulf of Cádiz consists of a complex interaction between tectonic, sedimentary, and oceanographic processes. Recent discovery of a Late Miocene contourite depositional system in the Gulf of Cádiz has led to the belief that the paleo-Mediterranean Outflow Water (MOW) had a major influence on the evolution of the Southwest Iberian margin since at least late Tortonian until early Messinian (Ng et al., 2021a). Synchronously, the Deep Algarve basin has undergone tectono-morphological changes with the formation of salt structures as a consequence of halokinesis (Lopes et al., 2006; Matias et al., 2011; Duarte et al., 2019), while its sedimentary infill was dominated by turbiditic systems sourced from onshore Algarve as well as the Guadalquivir basin (Riaza and Martínez del Olmo, 1996; Sierro et al., 1996; Ledesma, 2000). The deposition of turbidites likely reflects the initial phase of a foreland basin following thrusting (Riaza and Martínez del Olmo, 1996; Hernández-Molina et al., 2016). The Deep Algarve basin is separated from the rest of the Gulf of Cádiz by a series of structural highs (Hernández-Molina et al., 2016; Duarte et al. 2020). This raises the question of whether the Deep Algarve basin could have been isolated from the circulation of the paleo-MOW prevalent in the Gulf of Cádiz during this time. A detailed seismic analysis of the Late Miocene sedimentary succession of the Deep Algarve basin could unveil the interaction between the two deep marine processes – gravity flows and bottom currents.

Turbidites are sediments deposited by turbidity currents or flows that are delivered downslope to the deep marine realm through submarine channels as conduits and accumulate as submarine lobes in basin floor fans at the base of the continental slope (Barnes & Normark, 1985; Piper & Normark, 2001). Submarine channels are known to have unique migration styles (Peakall et al., 2000; Wynn et al., 2007), although bearing some similarities in their morphologies to fluvial systems (Damuth et al., 1983). The migration of submarine channels, which include the expansion and downstream translation of meander bends, and the vertical movements by incision and aggradation, dictate the stratigraphic architecture of these systems (Sylvester et al., 2011; Jobe et al., 2016). As turbidity currents follow the steepest descent across the continental slope, they can be confined, diverted, deflected, or blocked by complex seafloor topography caused by tectonic deformation (Clark and Cartwright, 2009; 2011; Covault et al., 2019). These structures, such as basement highs and salt diapirs, create accommodation with the formation of intraslope basins or terraces (Prather et al., 1998; Prather, 2003) and localize pathways of submarine channels (Gee & Gawthorpe, 2006), modifying their

depositional architecture (Cumberpatch et al., 2021). These confinements also lead to the development of ponded, perched, or transient turbiditic submarine lobes within the intraslope basins (Prather, 2003; Marchès et al., 2010; Gamberi and Rovere, 2011), where their infilling are counterbalanced by erosion and bypass to achieve slope equilibrium (Prather, 2003).

Bottom currents, on the other hand, are alongslope flows which are responsible for the deposition of contourites (Rebesco et al., 2014), interstratified with other deep-water facies (de Castro et al., 2021; de Weger et al., 2021). The thick accumulations of contourite deposits are called "drifts", which forms alongside their associated erosional features, as "channels" (McCave and Tucholke, 1986; Faugères and Stow, 2008; Hernández-Molina et al., 2008). Bottom currents could erode as well as rework sediments on the seafloor to form mixed deposits with distinguishable diagnostic criteria, such as reworked turbidites, or bottom current reworked sands (Shanmugam et al., 1993; de Castro et al., 2020). While mixed systems develop depending on the influence of their respective processes (e.g., bottom and turbidity currents or mass-wasting processes), only the characteristics of the dominant process are preserved, while masking the true nature of their interactions (Creaser et al., 2017). The sedimentary characteristics and architecture of mixed systems, such as bottom current affected channel complexes (Gong et al. 2013; 2018; Fonnesu et al., 2020; Fuhrmann et al., 2020; Miramontes et al., 2020) and mixed/hybrid drifts (Creaser et al., 2017; Rodrigues et al., 2021), are dependent on the mechanism and circumstance of interplay between gravity flows and bottom currents, such as tractional reworking versus lateral deflection and suspension fall-out of sediments (Sansom, 2018), and passive, phased or synchronous interactions of these currents (Miramontes et al., 2021).

The interactions between these processes have been widely reported for passive margin settings (e.g., Creaser et al., 2017; Miramontes et al., 2021; Rodrigues et al., 2021), whereas gravitational processes are considered as the dominant component within active margin settings, such as the turbiditic infill with the early stages of foreland basin evolution (e.g., Bayliss and Pickering, 2015; Butler et al., 2020). Can these tectonically active basins also be affected by bottom current processes? The main aim of this work is to decode the possibility of paleo-MOW influence on the deposition of the Late Miocene turbidite system during the initial phase of the peripheral foreland basin based on seismic stratigraphic analysis in the eastern domain of the Deep Algarve basin (Fig. 1). The stratigraphic architecture of the Late Miocene interval is characterised, which includes the distal section of the Guadalquivir sands turbidite system, using 3D seismic-reflection data, to distinguish the influence of bottom

currents in the evolution of the eastern domain of the Deep Algarve basin. Also, the interplay of both the turbidite and contourite systems, as well as their control factors, regional and conceptual implications, are evaluated and discussed.
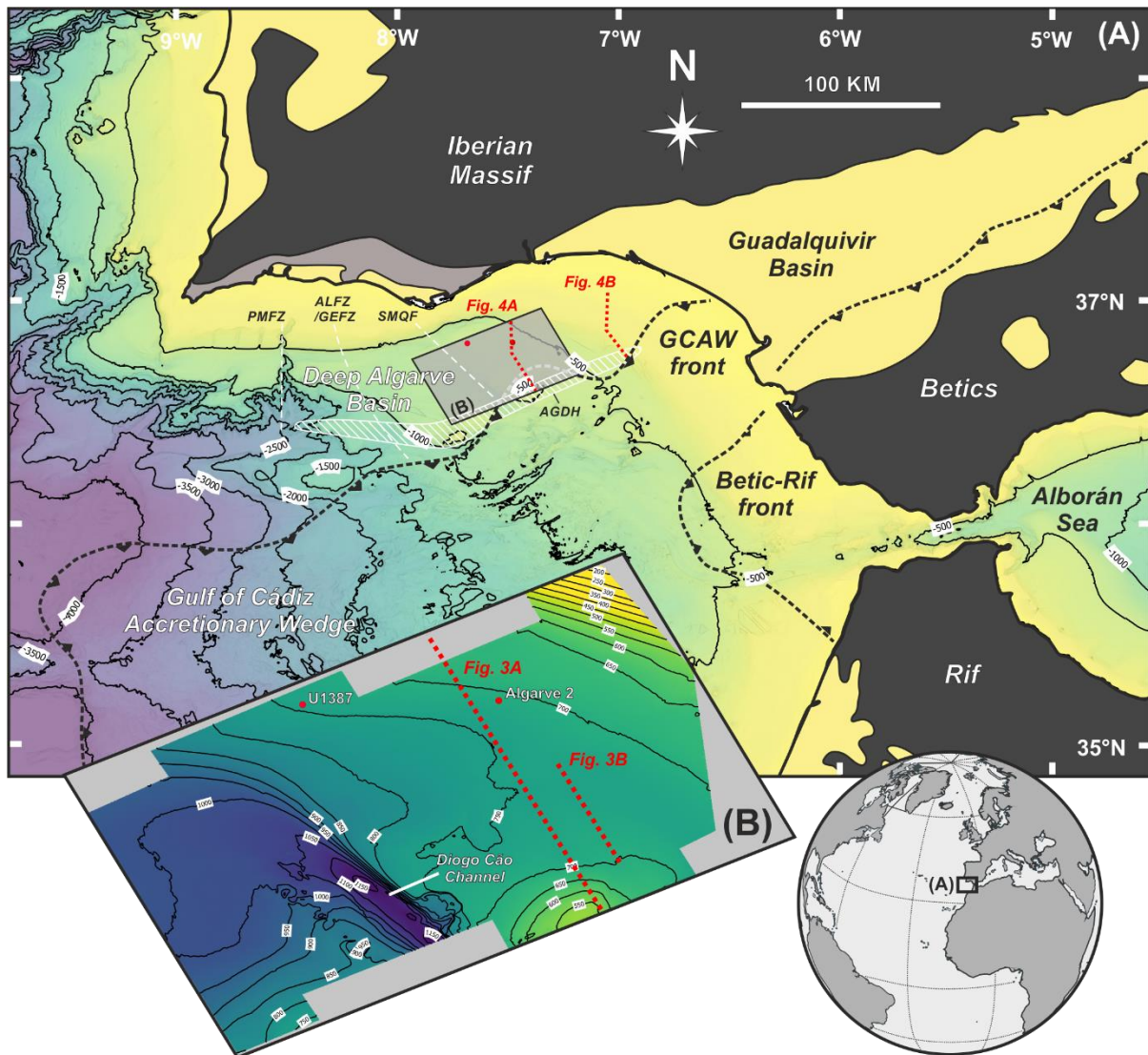
Figure 6-1 **(A)** Study area in the Gulf of Cádiz. Gray rectangle indicates location of the Algarve-2012 3D seismic reflection survey in B. Modified from Ng et al. (2021a). **(B)** Seafloor of the study area. Red dots indicate location of boreholes (Algarve-2 and U1387); red dotted lines indicate location of cross sections in Figures 3 and 4 (Abbreviations – AGDH: Albufeira-Guadalquivir-Doñana High; ALFZ: Albufeira fault zone; GEFZ: Gil Eanes fault zone; PMFZ: Portimão-Monchique fault zone; SMQF: São Marcos-Quarteira fault zone),

Geological setting

The Deep Algarve basin is located in the northern part of the Gulf of Cádiz, as the offshore extension of the onshore Algarve and Guadalquivir basins, which has a westward dipping axial gradient (Fig. 6-1). It is bounded by the continental slope and the onshore basins to the north and northeast (Lopes et al., 2006); and the Albufeira-Guadalquivir-Doñana basement high (AGDH), which include the Albufeira high and the Guadalquivir bank, to the south (Duarte et al. 2020). The Algarve basin is divided into the eastern and western domains, separated by the Albufeira (ALFZ; Lopes et al., 2006) or Gil Eanes fault zone (GEFZ; Duarte et al., 2020) (Fig. 6-1). In the eastern domain, the basin is divided into central eastern and far eastern subdomains by the São Marcos-Quarteira fault zone (SMQF); whereas the western domain is also split into two by the Portimão-Monchique fault zone (PMFZ, Lopes et al., 2006) (Fig. 6-1). The Algarve basin was initially formed during the Mesozoic rifting related to the opening of the Tethys Ocean (Srivastava et al., 1990). It evolved during the Cenozoic from both the reactivation of Hercynian basement (thick-skinned deformation) and the synchronous extensions and imbricate thrusts above the Triassic and Jurassic evaporites as a décollement (thin-skinned deformation), in relation to the Pyrenean and Betic-Rif orogenies (Lopes et al., 2006; Terrinha et al., 2019). Since the Late Cretaceous, the geodynamic evolution of the Gulf of Cádiz was controlled by the convergence of the Eurasian and African plates and the westward migration of the Alboran domain, which led to the formation of the Gibraltar arc (Vergés and Fernàndez, 2012). Eastward dipping subduction of the Tethyan oceanic lithosphere under the Gibraltar arc saw the development of the Gulf of Cádiz accretionary wedge (GCAW) during the Early to Middle Miocene (Gutscher et al., 2002; Iribarren et al., 2007; Duarte et al., 2011) as the outermost structure of the Betic–Rif orogenic system (Ramos et al., 2020). It was followed by the radial emplacement of a chaotic giant olistostrome, also known as the allochthonous unit of the Gulf of Cádiz (AUGC), until the Late Miocene due to gravitational collapse of the overthrusted GCAW (Torelli et al., 1997; Gràcia et al., 2003; Medialdea et al., 2004). This setting led to the development of a foreland basin system, which consisted of the Algarve foredeep basin, and the Doñana, Sanlúcar and Cádiz basins (Hernández-Molina et al., 2016; Duarte et al., 2020). Halokinesis processes also persisted from the Late Cretaceous until present, which generated both salt structures and salt-withdrawal sub-basins (Lopes et al., 2006; Matias et al., 2011; Duarte et al., 2020).

Based on previous works on the sedimentary evolution of the Deep Algarve basin (e.g., Riaza and Martínez del Olmo, 1996; Lopes et al., 2006; Maldonado et al., 1999), the Late Miocene interval is generally divided into three seismostratigraphic units (Fig. 6-2). The basal allochthonous wedge (Medialdea et al. 2004) was emplaced by north-to-westward thrusts, up till the late Tortonian (Gràcia et al., 2003). The AUGC acts as the foundation for the wedge-top basins in the Gulf of Cádiz, which pinches out in the southern edge of the Algarve foredeep basin, where the Guadalquivir Bank acted as a barrier to its progression (Ramos et al., 2017), and interfingers with the basin fill obscuring older Late Miocene deposits (Lopes et al., 2006). North of the AUGC, the lower boundary of the Late Miocene interval consists of a widespread erosional unconformity, known as the basal foredeep unconformity (BFU, Maldonado et al., 1999), formed by the middle Tortonian Betic compression (Lopes et al., 2006). Above the BFU, the older syn-olistostromic upper Tortonian to lower Messinian unit, equivalent to the Bética group (Riaza and Martínez del Olmo, 1996), consists of the Guadalquivir sands interbedded within hemipelagites deposits. The younger post-olistostromic upper Messinian unit, equivalent to the Andalucía and Marismas Group (Riaza and Martínez del Olmo, 1996), consists of hemipelagites draping over the AUGC and basal slope fan complexes representing the Guadiana sands which are derived from the northern Gulf of Cádiz margin (Lopes et al., 2006; Maldonado et al., 1999). However, Ledesma (2000) argued for the Guadiana sands within the Gulf of Cádiz as the natural continuation of the Guadalquivir sands turbidites of the lower Guadalquivir. The Guadalquivir sands turbidite system consists of seven complete episodes which originated from the northeast where they prograde southwestwards in the axis of the Guadalquivir basin into the Gulf of Cádiz, linked to pulses in tectonic elevation during the Messinian (Suárez et al. 1989; Sierro et al., 1996; Ledesma, 2000). The lateral northward migration of these turbiditic lobes was conditioned by regional tectonics, including the uplift from the Betic orogeny and the emplacement of the AUGC (Ledesma, 2000). According to Ledesma (2000), the first turbidite episodes (Gv-1 and Gv-2) started in the upper Guadalquivir basin since the Tortonian-Messinian boundary (7.24 Ma), and only reached the lower Guadalquivir basin to the Gulf of Cádiz region from the fifth until the seventh episodes (Gv-5 to Gv-7) between 6.72 to 5.5 Ma (Fig. 6-2). Onshore Algarve, the Late Miocene stratigraphy consist of an older lower to upper Tortonian "Fine sands and sandstones" unit and overlain by younger upper Tortonian to Messinian Cacela Formation, which consists dominantly of silts and marls (Fig. 6-2, Antunes et al., 1997; Pais et al., 2000).

Figure 6-2 Stratigraphic correlation of the seismic units (U1-U6) and boundaries (D1-D7) described in the present work, with previous authors in the Deep Algarve, onshore Algarve, and Guadalquivir basins (Abbreviations for stratigraphic discontinuities - BFU: basal foredeep unconformity; IMU: intra-Messinian unconformity; LMU; Late Miocene unconformity; MPB: Miocene-Pliocene boundary; MPU: Miocene-Pliocene unconformity).

Paleoceanographic setting

At present, the Gulf of Cádiz is connected to the Mediterranean in the east through the Strait of Gibraltar and opens up into the Atlantic towards the west. During the Late Miocene, the paleoceanography of the Gulf of Cádiz is dictated by the evolution of the Mediterranean-Atlantic water-mass exchange (Krijgsman et al., 2018; Ng et al., 2021b), which consists of the inflow of Atlantic water into the Mediterranean at the surface, and a reverse outflow of intermediate water-mass, known as the paleo-MOW. This exchange was active through a single wide connection in the middle Miocene, but gradually transformed into several narrow and shallow gateways in the late Miocene (Capella et al., 2019), collectively known as the Mediterranean-Atlantic gateways, due to lithospheric uplift resulting from compressional events in the Gibraltar arc (Duggen et al., 2003). During the Tortonian to Messinian period, the paleo-MOW would have exited the Mediterranean through the Betic and Rifian corridors, and the Strait of Gibraltar (Krijgsman et al., 2018), being modified to the Atlantic Mediterranean Water (AMW) by mixing with ambient Atlantic water (O'Neill Baringer and Price, 1999; Rogerson et al., 2012). The paleo-MOW is responsible for the deposition of sandy contourite deposits in the Betic and Rifian corridors (Martín et al., 2009; Capella et al., 2017a; de Weger et al., 2020; 2021), as well as the Late Miocene contourite depositional system (CDS) of the Gulf of Cádiz (Ng et al., 2021a). Continuous uplifting of the Betic and Rifian corridors eventually led to their closure, which restricted the paleo-MOW (~6.4 Ma) and shut off the Mediterranean-Atlantic water-mass exchange (Flecker et al., 2015; Ng et al., 2021b). This gave rise to an isolated Mediterranean and subsequent deposition of evaporites, as well as the conversion of the Guadalquivir and Gharb basins into marine embayment areas (Martín et al., 2009; Ivanovic et al., 2013). The reopening of the Mediterranean-Atlantic water-mass exchange through the Strait of Gibraltar since the Miocene-Pliocene boundary (MPB, 5.33 Ma) established the recirculation of the MOW, resulting in the distribution of the Pliocene-Quaternary CDS in the Gulf of Cádiz (Hernández-Molina et al., 2003, 2016; van der Schee et al., 2016). The Late Miocene CDS in the Gulf of Cádiz margin is similar in its long-term evolution with its Pliocene-Quaternary counterpart, with a three-stage (*initial-, transitional-, and growth-drift*) strengthening of bottom current influence (Hernández-Molina et al., 2016; Ng et al., 2021a), due to the enhancement of paleo-MOW from continuous uplifting and shallowing of the gateway sills (de Weger et al., 2020). Like the present-day setting, bifurcation of the paleo-MOW into two main cores (Hernández-Molina et al., 2014; de Weger et al., 2020) resulted of partial mixing of intermediate and deep Mediterranean waters, and further split into

multiple core and branches by bathymetric irregularities as it descends into the Gulf of Cádiz (Ng et al., 2021a; Duarte et al., 2020) driven by density and Coriolis deflection (de Weger et al., 2020).

Material and Method

A detailed seismic stratigraphic analysis has been executed using the Algarve-2012 three-dimensional (3D) narrow azimuth post-stack time migrated (PSTM) processed seismic reflection survey, located in the eastern domain of the Deep Algarve basin, in water depths roughly between 500 and 1000 m (Fig. 6-1). The 3D seismic volume, with an area of 1,500 km^2, was acquired by the Repsol S.A./Partex Oil and Gas consortium aboard the R/V Polarcus Naila in 2012. Acquisition and processing details are available in Supplementary Material (Tables 6-S1, 6-S2 and 6-S3). The seismic data was complemented by borehole data, which consist of an exploration well - Algarve-2, and an International Ocean Drilling Program Expedition 339 scientific site - U1387. Using the Schlumberger's Petrel E&P software platform, the root mean square (RMS) amplitude and coherence (variance) volume attributes were generated to assist in the seismic stratigraphic analysis workflow. Seven regional horizons for the Late Miocene interval were interpreted and mapped as major seismic stratigraphic discontinuities based on the distinguishment of stratigraphic units by their seismic facies and boundaries (Figs. 6-3 and 6-4). The identified Late Miocene seismic units were compared to seismostratigraphic studies of Maldonado et al. (1999), Lopes et al. (2006) and Ramos et al., (2017) (Fig. 6-2), while their chronology is correlated to regional borehole data (Fig. 6-4), from Ledesma (2000) and Ng et al. (2021b). Seismic (interval) attributes (e.g., RMS amplitude and variance) were extracted from their respective volumes to highlight the sedimentary depositional systems and to enhance structural and stratigraphic discontinuities respectively (Fig. 6-5). The interpreted seismic features are evaluated through their acoustic character and distribution for deposits of deep-water sedimentary process, such as gravity flow deposits including turbidites and mass transport deposits (MTDs), contourites, and pelagites or hemipelagites adapting the standard nomenclature for these deposits from the literature (Posamentier and Erskine, 1991; Faugères et al., 1999; Rebesco et al., 2014; Stow and Smillie, 2020).
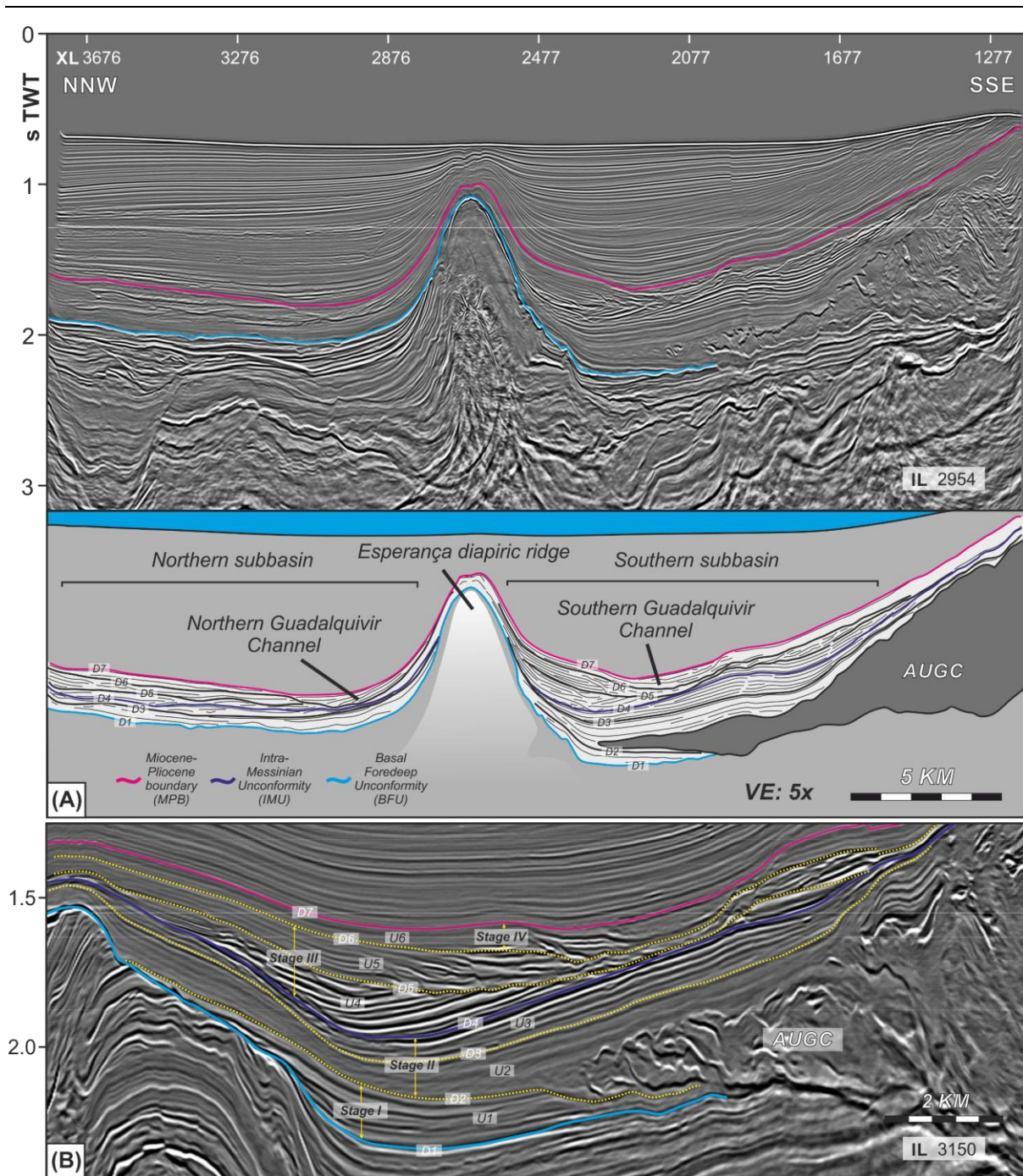
Figure 6-3 **(A)** Representative seismic reflection profile (IL 2954) across the study area (top) and their interpreted unit boundaries (D1-D7) (bottom). Profile locations are given in Figure 6-1(B). **(B)** Enlarged cross-section profile (IL 3150) across the southern sub-basin and interpreted seismic units (U1-U6) and evolutionary stages (I-IV).
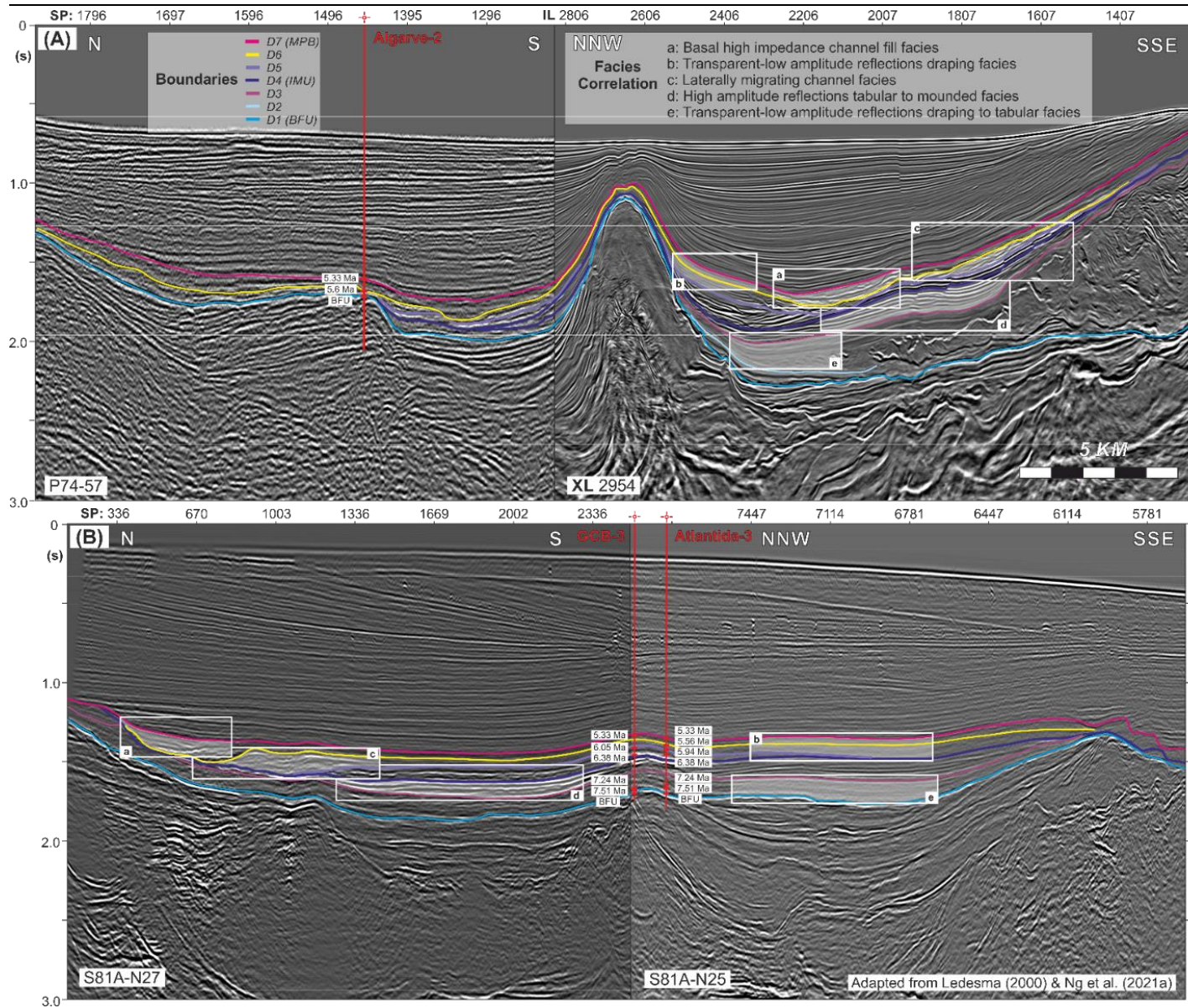
Figure 6-4 Borehole and facies correlation between **(A)** eastern and **(B)** far eastern Deep Algarve basin. Location given in Figure 1(A).

Results

Seismic analysis

Seven stratigraphic discontinuities were mapped across the seismic survey. The seismic character of the discontinuities and the seismic facies of seismic units are described from the base of the subsurface section (D1) to the top (D7) (Figs. 6-3 and 6-5). Surface mapping (isobath) of the horizons shows the presence of three sub-basins: the northern and southern sub-basins, separated by a central diapiric ridge, and the western sub-basin (Figs. 6-3 and 6-5). The northern sub-basin is bounded by the Southwest Iberian margin in the north, while the southern sub-basin is bounded in the south by the AUGC (allochthonous unit of the Gulf of Cádiz). The central diapiric ridge consists of a series of detached structural highs interrupted by gaps, which terminated in the west adjacent to the western sub-basin (Fig. 6-5).

The stratigraphic discontinuity D1 represents the base of the studied stratigraphic interval, which is characterised by high-amplitude seismic reflection truncating underlying high-amplitude package at mild to steep angles (Figs. 6-3 and 6-6). Seismic unit U1, which consists of a package of low-amplitude transitioning upwards into high-amplitude continuous seismic reflections, with parallel to wavy geometries, downlaps onto D1 and onlaps onto structural highs, such as the central diapiric ridge, in the southern sub-basin, (Figs. 6-3 and 6-6). Whereas in the northern sub-basin, U1 can only be observed in its western section, complemented by the distribution of a NW-SE elongated flattened strip with high-amplitude reflections, as shown in the RMS amplitude extraction for U1 (between D1 and D2) (Figs. 6-5a and 6-7). Distribution of the seismic unit U1 is also concentrated (100-200 ms TWT) in the northeastern section of the southern sub-basin (Fig. 6-5a). However, the thickest accumulation (>150 ms TWT) with high-amplitude reflections of U1 resides in the western sub-basin (Fig. 6-5a). This thick distribution of U1 is associated with an NNW-SSE oriented channelised indentation in its northern margin, where mounded high amplitude reflections can be seen on its western flank (Fig. 6-7). U1 has an overall sheeted geometry in the southern sub-basin, where reflections are more parallel in the centre of the sub-basins, and wavy towards their northern margins (Fig. 6-6), whereas it consists of small mounded geometry patches in the north and western sub-basins (Fig. 6-7). Small channel-like geometries are also observed in the western sub-basin within the cross-sections as well as RMS amplitude extraction maps for internal horizons 1 and 2, where they are seen to migrate northwards (Fig. 6-7).
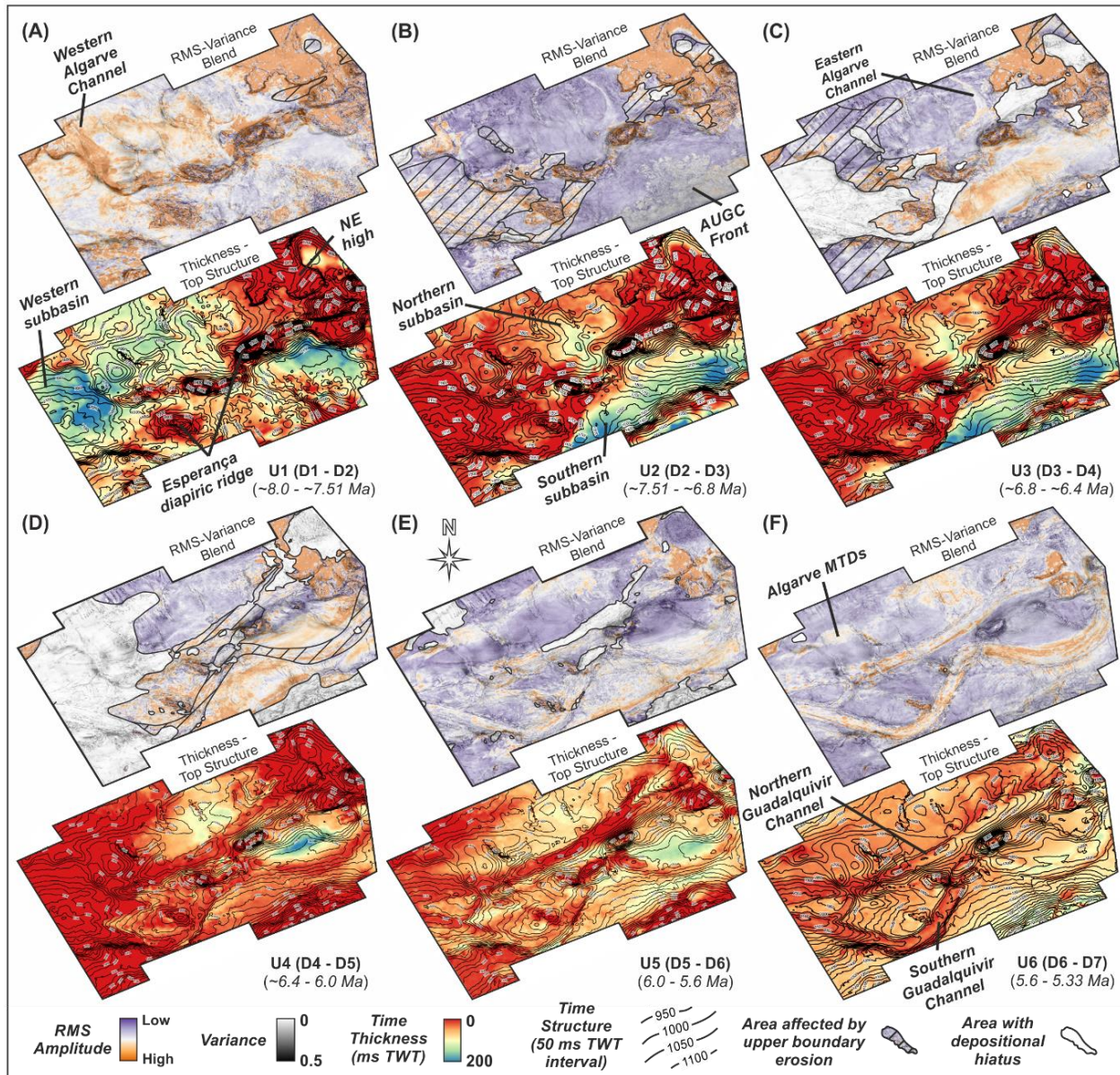
Figure 6-5 RMS amplitude and variance attributes blend, and time top structure and time thickness maps for the units U1 to U6 and respective boundaries D1 to D7 – **(A)** U1: D1 to D2, **(B)** U2: D2 to D3, **(C)** U3: D3 to D4, **(D)** U4: D4 to D5, **(E)** U5: D5 to D6, and **(F)** U6: D6 to D7.

Overlying U1, the stratigraphic discontinuity D2 consists of a high-amplitude horizon that truncates U1 and acts as a boundary of distinct amplitude contrast with seismic unit U2. Seismic unit U2 consists of a transparent to low-amplitude continuous seismic reflections package, which onlaps D2 and structural highs in the southern sub-basin, and interfingers with the chaotic AUGC (Figs. 6-3 and 6-6). In the eastern section of the northern sub-basin, U2 is deposited above D1 (Fig. 6-3). The thickness distribution of U2 is mainly focused along the southern sub-basin and within a N-S oriented depression in the centre of the northern sub-basin aligned with a gap in the central diapiric ridge (Fig. 6-5b). An RMS amplitude extraction for U2 (between D2 and D3) shows a uniform distribution of low-amplitude reflections across both the northern and southern sub-basins, whereas the variance attribute map shows the extend of the AUGC front covering half of the southern sub-basin (Fig. 6-5b). At the front of the AUGC, U2 has a wedge geometry, while it transitions upwards into sheet geometry as it covers over the chaotic unit (Fig. 6-6).
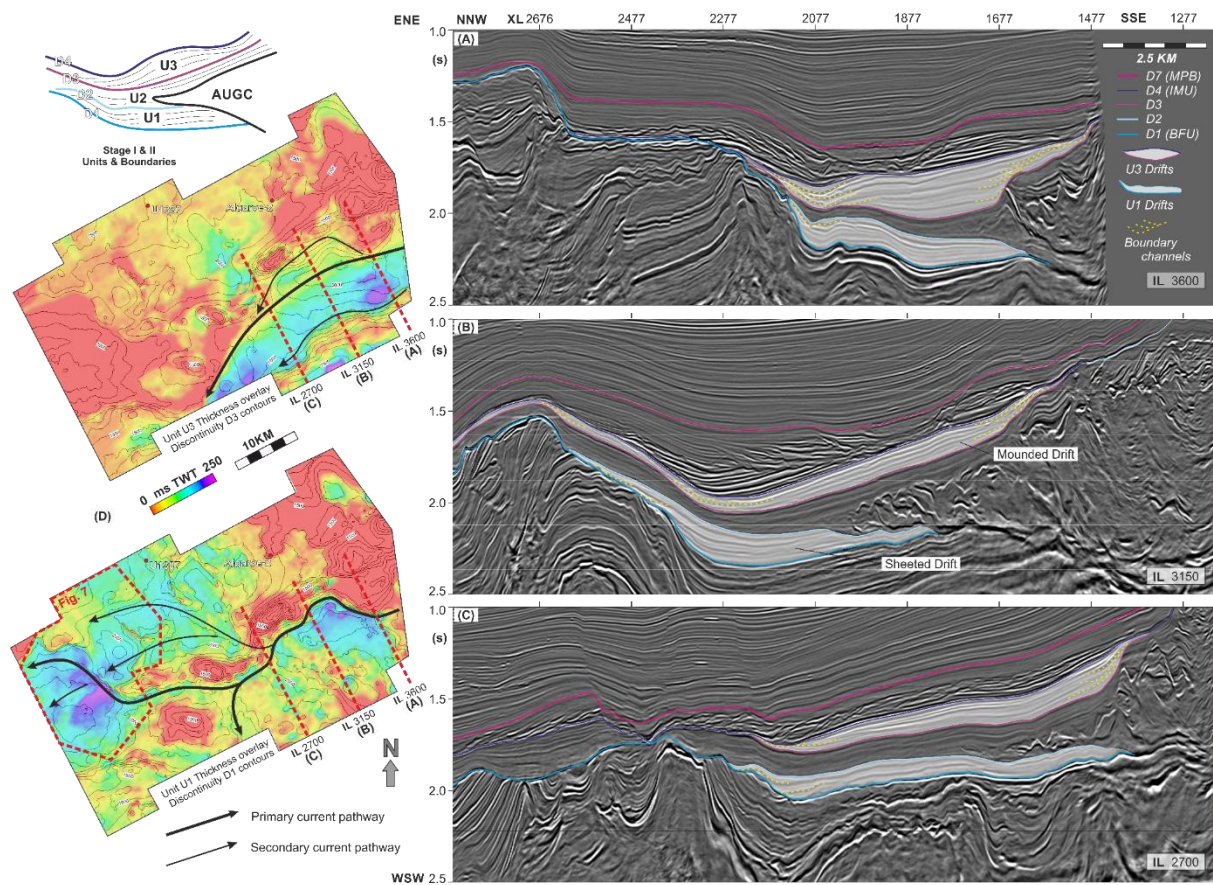
Figure 6-6 Distribution of Stage I and II (Unit U1, U2 & U3) deposits in the southern sub-basin of the Deep Algarve basin and their relationship with bottom currents, illustrated using seismic profiles **(A)** IL 3600, **(B)** IL 3150 and **(C)** 2700 from the Algarve-2012 3D seismic survey, and **(D)** thickness maps of Unit U1 and U3.

Stratigraphic discontinuity D3 separates the low-amplitude seismic reflections of U2 from seismic unit U3 above, which is characterised by a high-amplitude package. The overlying U3 has large mounded geometries in the southern sub-basin with several smaller crests (Fig. 6-6), capped by stratigraphic discontinuity D4 (Fig. 6-3). Seismic reflections within these mounded geometries pinch out and downlaps onto D3 away from the basin centres towards the margins of the southern sub-basin (Fig. 6-3). Thickness mapping of U3 shows similarity in its distribution with the underlying U2 where its depocentre lies within the centre of the southern sub-basin (Figs. 6-5b and 6-c), slightly thicker in places not underlain by the AUGC (Fig. 6-6). The RMS amplitude extraction for U3 (between D3 and D4) consists of an ENE-WSW oriented band of high-amplitude reflections across the southern sub-basin (Fig. 6-5c). This high-amplitude reflection band is flanked by low-amplitude reflection strips in its boundary (Fig. 6-5c), which can be correlated to an updip development of channelised features adjacent to both margins in the seismic section (Fig. 6-6). In the eastern section of the northern sub-basin, an arcuate channel pattern with a NW-SE orientation that bends westwards as it reaches the central diapiric ridge can also be observed, while the N-S oriented depression in the centre of the northern sub-basin remains with low-amplitude reflections (Fig. 6-5c).

The stratigraphic discontinuity D4 represents an erosional unconformity in the southern sub-basin, which separates the lower U3 of parallel to mounded geometries, from an upper seismic unit U4 which is composed of parallel to channelised geometries (Figs. 6-3, 6-6 and 6-8). D4 is also observed as a prominent erosional surface for the western sub-basin and the area east of the NE basement high (Fig. 6-5c). The high-amplitude channelised seismic reflections of U4 in the southern sub-basin are truncated by the concave-up shaped stratigraphic discontinuity D5 and are interspersed outside this central channel geometry (Fig. 6-3). These channelised features are also observed in the northern sub-basin (Fig. 6-3), where an E-W oriented channel develops along its southern margin, cutting through the NE basement high. Whereas similar to the interval between U3, an erosional surface can also be observed in the north-eastern region between the basement highs, but slightly more northerly than that of the underlying interval (Fig. 6-5d). Thickness mapping of U4 (between D4 and D5) indicate thicker distribution in the northern margin of the southern sub-basin (150-200 ms TWT), as well as spread out within the central region of the northern sub-basin (Fig. 6-5d). On top of that, an RMS amplitude extraction of U4 shows distribution of high-amplitude reflections across the entirety of the southern sub-basin, cut by the meandering channel geometry of D5 (Fig. 6-5d).
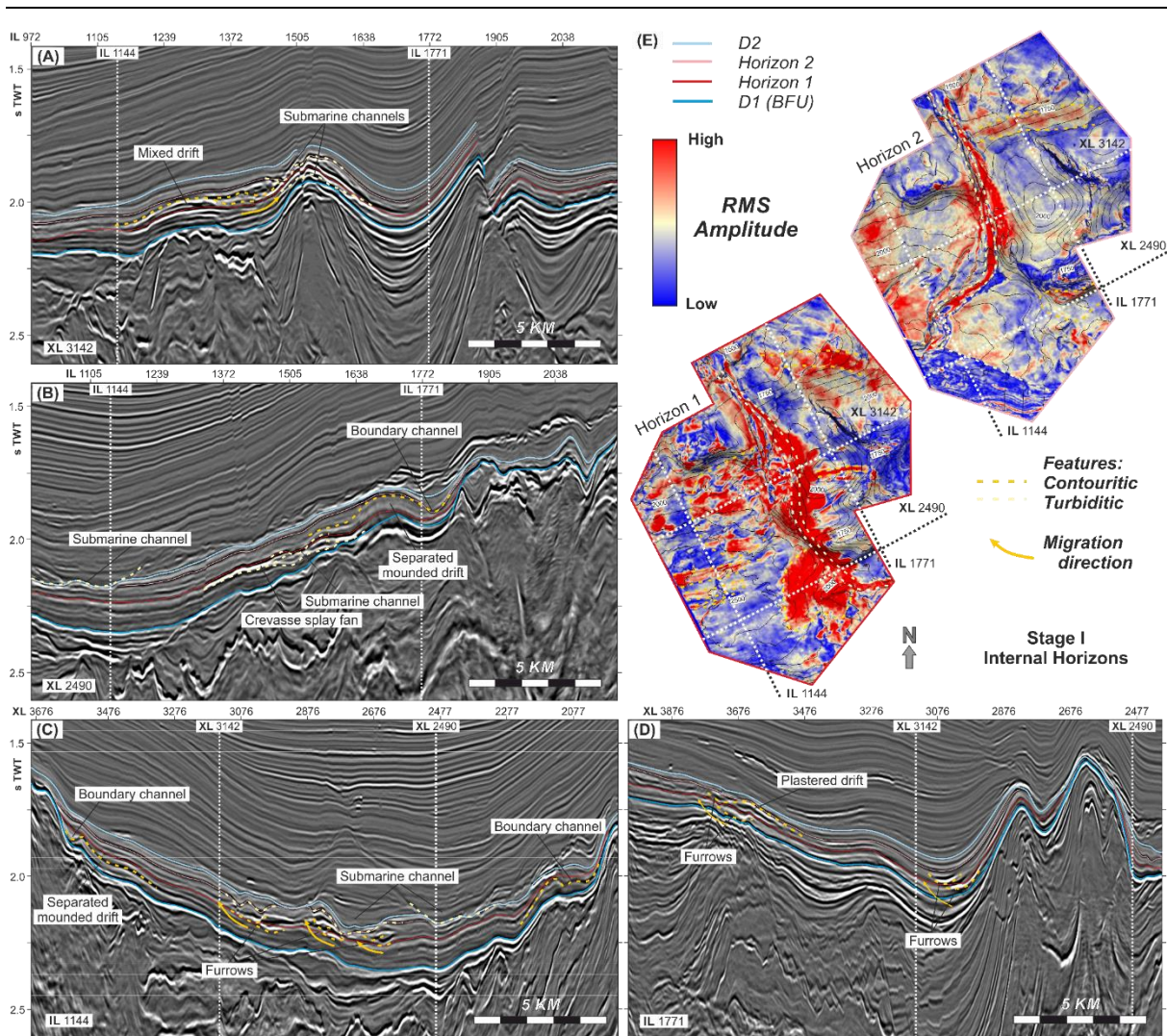
Figure 6-7 Evidence of turbidity and bottom current influence during Stage I (Unit U1) with the identification of erosional and depositional feature related to contourite depositional systems, illustrated using seismic profiles **(A)** XL 3142, **(B)** XL 2490, **(C)** IL 1144, **(D)** IL 1771, from the Algarve-2012 3D seismic survey, and **(E)** RMS amplitude extraction of internal horizons 1 and 2 of Unit U1. Location given in Figure 6-6(D).

Stratigraphic discontinuity D5 represents the base of seismic unit U5. The erosional hiatus in the western sub-basin observed for D4 also extends upwards to D5 (Fig. 6-3). U5 consists of high-amplitude with an overall oblique with internally wavy seismic reflections, which are stacked laterally in alternating orientations – respectively towards the northern or southern margins, within the southern sub-basin (Figs. 6-3 and 6-8). These oblique geometries are also represented in the variance attribute map as edges arranged in overlapping bends (Fig. 6-5e), which are indicative of channel boundaries and their lateral migration (Fig. 6-8). In plan-view, these features are observed as the downstream translation of meandering channel geometries (Fig. 6-8). Based on the RMS amplitude extraction of U5 (between D5 and D6),

the channels are confined within the width of the southern sub-basin (Fig. 6-5e). In the northern sub-basin, the E-W channel continues to develop along the southern margin; while at the base of the northern margin, patches of high-amplitude reflections can be observed in the RMS amplitude attribute map and can be correlated to small, detached channels seen further up on the slope in the variance attribute maps (Fig. 6-5e). These channels may have developed earlier in U4, but the associated high-amplitude reflection patches cannot be identified due to the erosional unconformity of D5 (Fig. 6-5d).

Stratigraphic discontinuity D6 is dominantly conformable and forms the base of the uppermost seismic unit U6 (Fig. 6-3). In the basin centre, D6 shows a channelised geometry truncating the underlying U5 (Figs. 6-3, 6-5f and 6-8). U6 consists of transparent to low amplitude seismic reflections which are observed to be away from a prominent high-amplitude basal channelised feature in the centre of the southern sub-basin, while chaotic to discontinuous low-amplitude seismic reflections are present within the central channel, capped by low amplitude continuous seismic reflections (Fig. 6-3). While in the northern sub-basin, the channel in its southern margin migrates laterally towards the north, slightly further away from the central diapiric ridge, and filled by transparent seismic facies (Fig. 6-3). RMS amplitude extractions of U6 (between D6 and D7) also show the distribution of high amplitude response for the base of the channels in both the northern and southern sub-basins, as well as high-amplitude patches at the base of the northern margin which are similarly observed for U5, while low-amplitude response dominated the rest of the basin (Fig. 6-5f). Finally, the top of this seismic unit is capped by the stratigraphic discontinuity D7, represented by a high-amplitude continuous seismic horizon. D7 marks the change in seismic facies from transparent to low-amplitude seismic reflections below, to high-amplitude parallel seismic reflections above (Figs. 6-3 and 6-6).

Interpretation

Bottom current features

The bottom current features identified in the eastern Deep Algarve basin for the studied interval are associated with the Late Miocene contourite depositional system. The sheeted geometry in seismic unit U1 within the southern sub-basin is interpreted as a sheeted drift (Figs. 6-6 and 6-9a), similar to those identified in the Rockall Trough by Stoker et al. (1998). Those

small mounded patches in the northern and western sub-basins are respectively interpreted as plastered and separated mounded drifts (Figs 6-7 and 6-9a), following the classification of Rebesco et al. (2014). The morphology for the plastered drift is comparable to examples previously described by van Rooij et al. (2010) on the Cantabrian slope, while the separated mounded drifts are comparable to examples in the Iberian margin (Llave et al., 2020). In the western sub-basin, the northward migrating channel-like features are interpreted as furrows, with present-day analogue in the Mozambique Channel described by Miramontes et al. (2021) (Fig. 6-7). The large mounded geometry identified in the seismic unit U3 (Fig. 6-6), within the southern sub-basin is interpreted as confined mounded drift with their associated boundary channels, based on the classification of Rebesco et al. (2014), They are analogous to the Sumba drift contourite system previously interpreted by Reed et al. (1987) in the eastern Sunda Arc, where the drifts were also developed in an active margin setting within a confining slope. The development of the U3 mounded drift terminated at the end of the U3, represented by stratigraphic discontinuity D4 (Fig. 6-6).

Gravitational features

The NNW-SSE oriented channel feature of seismic unit U1 in the northern margin of the western sub-basin (Figs. 6-5a and 6-7) and the NW-SE oriented arcuate channel of seismic unit U3 in the eastern section of the northern sub-basin (Figs. 6-5, b and c) are both interpreted as submarine channels of a turbidite system originating from the Algarve margin, hereinafter identified respectively as the Western Algarve and Eastern Algarve channels (Fig. 6-5). In the western sub-basin, the Western Algarve submarine channel evolves into submarine lobes and crevasse splays in the basin centre and migrates westward due to uplifting of the central diapiric ridge (Duarte et al., 2019). In the southern sub-basin, development of turbidite features occurred since the termination of contourite deposition, represented by stratigraphic discontinuity D4. The seismic features in seismic units U4 to U6 are associated as the downstream continuation of the Guadalquivir sands turbidite system previously identified by Suárez et al. (1989), Sierro et al. (1996), and Ledesma (2000). The turbidite system is interpreted to be prograding down the axial slope of the Algarve foredeep basin, starting with channelised submarine lobe facies for U4, transitioning into submarine channel facies in U5. The evolution of the submarine channel through lateral migration and downstream translation were observed for U5 and U6, analogous to the development of the Congo turbidite channel described by Babonneau et al. (2010). The Guadalquivir sands turbidite system terminated

prior to the stratigraphic discontinuity D7 and were since dominated by background hemipelagic deposition (Ng et al., 2021b). Coeval to the deposition of U5 and U6, high-amplitude patches identified in the northern margin of the northern sub-basin (Figs. 6-5e and 6-f) were interpreted as mass transport deposits (MTDs).
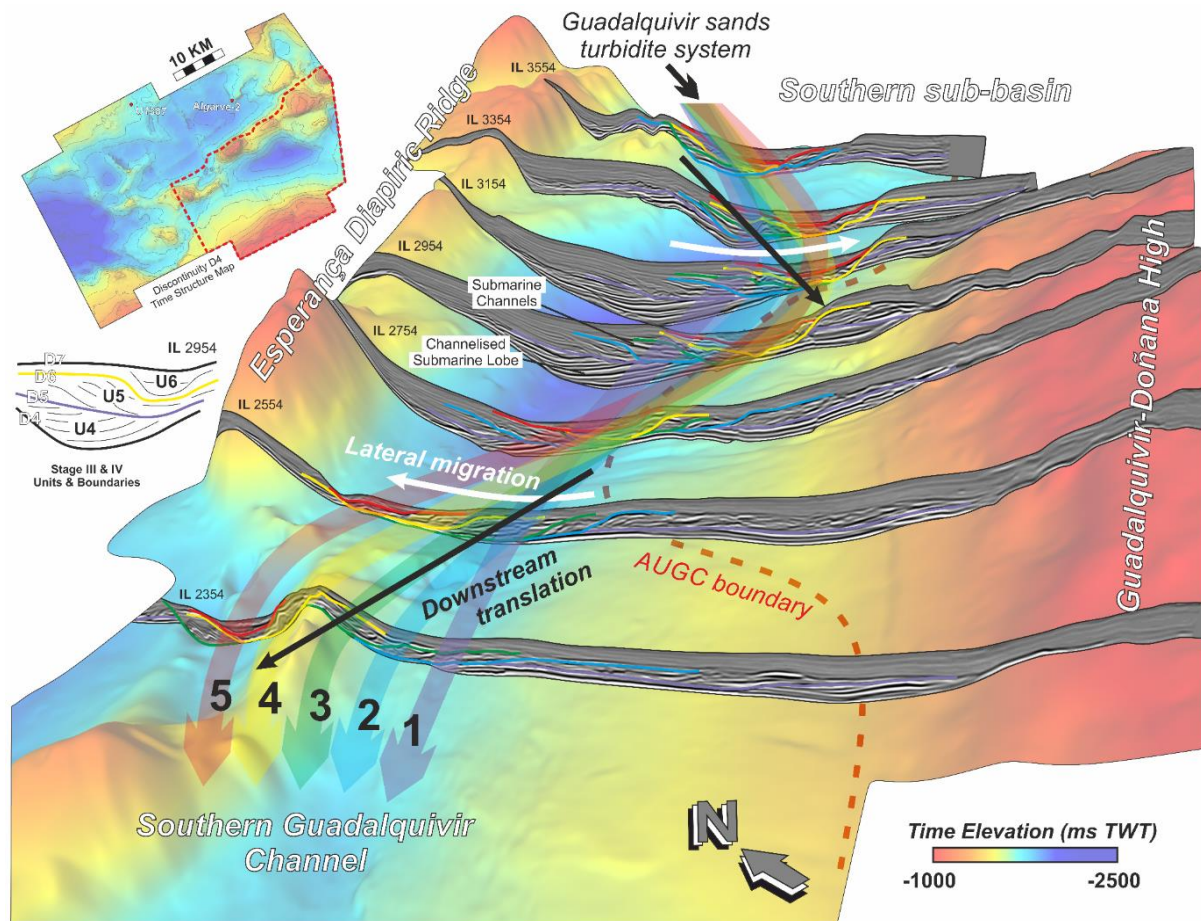
Figure 6-8   Evolution of the Guadalquivir Sands turbidite system (1 to 5) in the southern sub-basin of the Deep Algarve basin during Stage III and IV (Unit U4, U5 & U6), illustrated using seismic profiles IL 2354, 2554, 2754, 2954, 3154, 3354, and 3554 from the Algarve-2012 3D seismic survey (Abbreviation – AUGC: allochthonous unit of the Gulf of Cádiz).

Mixed (turbidite-contourite) features

Interaction of contouritic and turbiditic processes was interpreted from the presence of mixed features in the eastern Deep Algarve basin. The presence of asymmetric levees and the distribution of high-amplitude seismic reflections located west-to-northwest of the Western Algarve submarine channel in seismic unit U1 (Fig. 7) indicate a mixed drift, or "drift-mound" as previously described by Fonnesu et al. (2020). The asymmetric nature of the channel-levees

is due to the synchronous interaction of the turbidity flow down the submarine channel with a westward bottom current (Miramontes et al., 2021). This feature also has similar characteristics to the Late Miocene Sagres canyon mixed system previously described by Ng et al. (2021b). In seismic unit U3, the development of the mounded drift in the southern sub-basin may have also been influenced by turbiditic processes, where sediment supply originating from the Guadalquivir sands turbidite system would have supported the drift buildup. Albeit the seismic facies only corresponded to the characteristics of contourites as its dominant process (Fig. 6-6).

Discussion

Stratigraphic evolution and chronology

The seismic stratigraphy of the studied Late Miocene sequence is summarized into four main stages, illustrated in Figure 6-9. Seismic facies correlation with the far eastern Algarve to lower Guadalquivir area shows similarities in their characteristics and stratigraphy (Fig. 6-4), and thus we used regionally available chronologic information (Ledesma, 2000; Ng et al., 2021b) as an approximation for the eastern Deep Algarve basin.

Stage I (8.0-7.51 Ma)

The first stage consists of seismic unit U1, with its onset represented by the stratigraphic discontinuity D1, which constitutes the basal foredeep unconformity (BFU; Maldonado et al., 1999; Lopes et al., 2006; Duarte et al., 2020). This horizon represents a key regional unconformity, associated to a period of intense shortening and erosion during the Miocene (Ramos et al., 2017). It marks the transition of the Algarve basin from part of a rifted passive margin to a foredeep basin with its subsequent flexural subsidence in response to the Betic-Rif orogeny (Maldonado et al., 1999; Ramos et al., 2017; Duarte et al., 2020). Regional approximation for a late Tortonian age of 8-8.2 Ma was given in Maldonado et al. (1999) and Ledesma et al. (2000) for this horizon. Overall, Stage I reflects the initial period after the regional hiatus, which is characterised by a deep-marine setting affected by bottom currents (Figs. 6-6, 6-7 and 6-9a). During this stage, the central diapiric ridge, also known as the Esperança diapiric ridge (Duarte et al., 2019), would have already formed as a salt anticline sourced from the Esperança allochthonous salt nappe (Matias et al., 2011; Ramos et al., 2017),

while not as well developed compared to its present-day structure. It would have divided the eastern Algarve foredeep basin into the two sub-basins since the middle to late Tortonian. Locally, bottom currents would have originated from the east-to-southeast, most likely the Guadalquivir and Cádiz basins where the paleo-MOW were active during this period (Ng et al., 2021b). The bottom current would have flowed along the northern margin of the southern sub-basin forming sheeted drifts before reaching a submarine water gap in the Esperança diapiric ridge (Fig. 6-6). This gap acted as a gateway sill allowing bottom currents to flow across the Esperança diapiric ridge into the northern sub-basin, analogous to the present-day Diogo Cão deep (García et al., 2016). This would have increased the velocity of bottom currents by focussing its flow as it passes through the gap and moves towards the northern margin of the northern sub-basin or diverted southwest along the Esperança diapiric ridge (Figs. 6-6, 6-7 and 6-9a). The enhanced bottom current was able to rework sediments on terraces and channels, and deposit contourites as plastered or separated mounded drifts along the northern margin of the western sub-basin (Figs. 6-7 and 6-9a).

In the western sub-basin, presence of bottom currents could have advected fine-grained sediments away from the turbidity current within the Western Algarve channel to form mixed drifts and may also be vigorous enough after flowing through to form northward-migrating channels or furrows by scouring the seabed (Figs. 6-7 and 6-9a). The end of Stage I, represented by stratigraphic discontinuity D2, marks the emplacement of the AUGC in the Algarve basin, which is thought to have occurred regionally circa 7.51 Ma (Fig. 6-6, Ledesma, 2000; Capella et al., 2017b). The radial emplacement of the AUGC, which occurred after the development of the GCAW up till the Tortonian-Messinian boundary (Maldonado et al., 1999; Ledesma, 2000; Medialdea et al., 2004), locally affected the southern margin of the Algarve foredeep basin (Fig. 6-9b). The northward movement of AUGC would have isolated this basin from other wedge-top basins in the southeast (Duarte et al., 2020) and disrupted bottom current flow by diverting its pathway. This is further supported by the clear contrast in seismic facies between Stage I and the lower parts of Stage II in the eastern domain (Figs. 6-3 and 6-6). Whereas in the far eastern domain, Stage I equivalent deposits are not present, and the BFU is overlain directly by Stage II equivalent deposits (Fig. 6-4).

Stage II (7.51-6.4 Ma)

The second stage consists of the seismic units U2 and U3. It is characterised initially by a period lacking bottom currents features, following emplacement of the AUGC in the south;

followed by contourite drift deposition in a confined setting (Figs. 6-6 and 6-9b). The transition across the Tortonian-Messinian boundary from transparent to low-amplitude sheeted seismic facies in U2 (7.51-6.8 Ma), and further into moderate to high-amplitude mounded seismic facies in U3 during the early Messinian (6.8-6.4 Ma), depicted an intensification of bottom current influence during drift construction in the southern sub-basin, as well as in other areas in the Gulf of Cádiz towards west of Portugal (Ng et al., 2021). This gradual strengthening in amplitude could also be explained by coarsening of grain size input into the contourite system. That being said, Stage II developed simultaneously with the second to fifth episodes (Gv-2 to Gv-5) (starting at 7.24, 7.1 and 6.8 Ma) of the Guadalquivir sands turbidite system during the early Messinian (Fig. 6-2, Suárez et al. 1989, Sierro et al., 1996; Ledesma, 2000). This turbidite system originates from the lower Guadalquivir basin and prograde towards the Gulf of Cádiz, where it reached the Algarve basin since the fifth episode (Gv-5, 6.8 Ma onwards).

The progression from a more distal basin plain facies towards more proximal lobe facies of the Guadalquivir sands turbidite system could have supplied the sediment for contourite drift evolution through bottom current reworking of sediments and winnowing of suspended particles. During this period, the northeast of the study area consists of a basement high, which restricted turbidite flows into the northern sub-basin; and diverted them into the southern sub-basin (Fig. 6-9b). Coevally, the development of the Esperança diapiric ridge into a salt wall would have occurred, consistent with a major halokinesis during the late Tortonian to Messinian (Lopes et al., 2006; Duarte et al., 2019), which limited the flow of bottom currents within a confined southern sub-basin, closed off by the AUGC in the south. Albeit the submarine water gap in the Esperança diapiric ridge could have allowed the suspended part of the flow to overspill into the northern sub-basin, while the traction part of the flow is constrained within the southern sub-basin (Fig. 6-9b). During this stage, the development of the Eastern Algarve submarine channel would have also supplied sediments into the northern sub-basin, likewise confined by the Esperança diapiric ridge (Fig. 6-9b). The end of Stage II, represented by stratigraphic discontinuity D4, is equivalent to the intra-Messinian unconformity (IMU), interpreted with a middle Messinian age at approximately 6.4 Ma (Figs. 6-3 and 6-6, Ng et al., 2021a, b). This horizon marks a regional unconformity which represents a hiatus coeval to the severe weakening or cessation of the paleo-MOW through the Mediterranean-Atlantic gateways, which weakened or halted bottom current activities in the Gulf of Cádiz from the middle to late Messinian (Stages III and IV, Ng et al., 2021a).
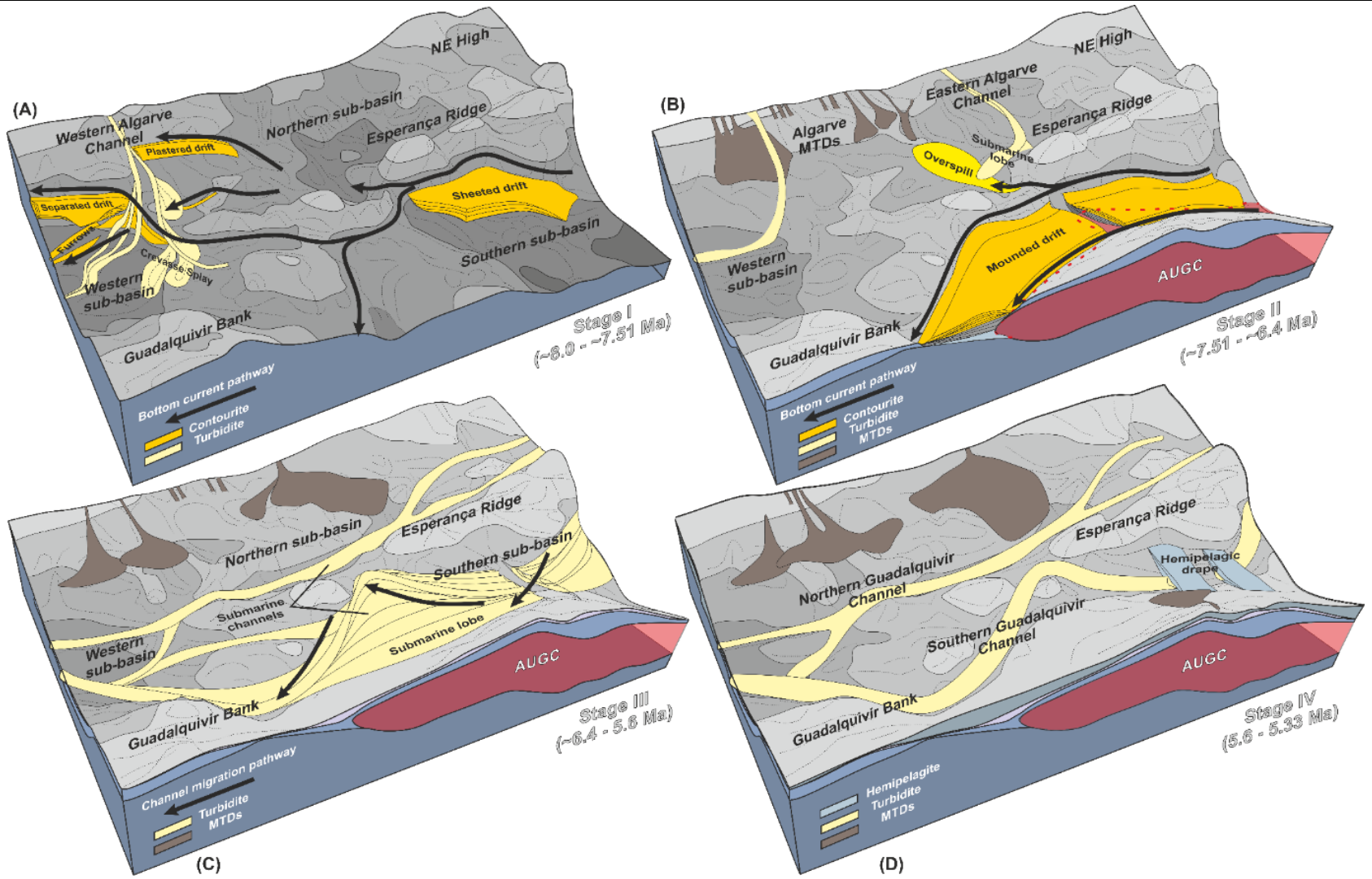
Figure 6-9   Schematic 4-stage evolutionary block model of the eastern Deep Algarve basin, with **(A)** Stage I (Unit U1), **(B)** Stage II (Unit U2 and U3), **(C)** Stage III (Unit U4 and U5), and **(D)** Stage IV (Unit U6).

Stage III (6.4-5.6 Ma)

The third stage consists of the seismic units U4 and U5 and is characterised by the submarine channel-lobe transition of a turbidite system (Fig. 6-8). In the southern sub-basin, this stage started initially with the channelised lobe facies of U4 during the middle Messinian (6.4-6.0 Ma), followed by the meandering channel-levee facies of the Southern Guadalquivir channel of U5 eroding into the older episodes during the late Messinian (Fig. 6-8, 6.0-5.5 Ma). The evolution of the U5 channels is defined by the incision, migration, and aggradation of an initially relatively straight channel (Sylvester et al., 2011), followed by development of meandering bends and their downstream translation, which are recognized as lateral migration of channel thalweg in the cross-sections (Fig. 6-8 and 6-9c, Babonneau et al., 2010). The incision of the channels became more intense towards the western sub-basin, where it eroded into Stage II deposits. This could be due to the confinement of turbidite channels and the restriction of downstream translation of their meandering bends due to structural obstacles related to the Esperança diapiric ridge (Clark and Cartwright 2009; 2011), which diverted and stabilized the channel pathway and intensified scouring of the turbidite flow (Fig. 6-9c). Overall, they represent the distal section of the final two episodes of the Guadalquivir sands turbidite system during the middle to late Messinian, where the sixth and seventh episode (Gv-6 & Gv-7) prograde basinward while gradually migrating northwards in the far east of the Algarve basin as the basin fills up (Figs. 6-2 and 6-4, Ledesma, 2000).

In the eastern domain, the turbiditic flows managed to overcome the structural obstacles by eroding into the northeastern basement high forming the Northern Guadalquivir channel flanking the southern margin of the northern sub-basin (Fig. 6-9c). This channel also appears relatively straight in comparison to its southern counterpart (Figs. 6-3 and 6-9c) due to the northern margin slope profile and the localized subsidence from the influence of the salt tectonics which draw the channel pathway towards the lower topography (Gee & Gawthorpe, 2006; Oluboyo et al., 2014). Coevally, the small channels formed on the Algarve margin, would have supplied the sediments to deposit mass transport deposits (MTDs) at the base of the slope (Fig. 6-9c). The end of this stage, represented by the stratigraphic discontinuity D6, correlates to the Algarve-2 borehole with an age of 5.6 Ma (Figs. 6-3 and 6-4). This unconformity could be related to the coeval glacial periods associated with the "Messinian Gap" event of desiccation and erosion in the Mediterranean marginal basins (5.6-5.55 Ma, Hsü et al., 1973; Lofi et al., 2011; Cosentino et al., 2013) which was triggered by glacio-eustatic sea-level fall

in response to the expansion of Antarctic ice sheets circa 6 Ma (Hodell et al., 2001; Ohneiser et al. 2015).

Stage IV (5.6-5.33 Ma)

The final stage corresponds to seismic unit U6, which represents the channel abandonment phase of the southern sub-basin in the latest Messinian (Figs. 6-8 and 6-9d). During this phase, the southern sub-basin consisted of a remnant meandering Southern Guadalquivir channel filled with basal lag deposits and capped by hemipelagites which are spread uniformly across the sub-basin. The development of the underlying meandering channel system was immaturely cut short and filled by hemipelagic deposits (Figs. 6-8 and 6-9d). In the northern sub-basin, the Northern Guadalquivir channel ran subparallel to the Esperança diapiric ridge, partially confined laterally by topography (Oluboyo et al., 2014; Clark and Cartwright, 2009; 2011). The channel gradually migrated northwards away from the Esperança diapiric ridge initially by eroding into older deposits and filled by coarser sediments, as the Esperança diapiric ridge continues to grow through salt diapirism (Duarte et al., 2019; Cumberpatch et al., 2021). Channel migration eventually stopped, and the northern sub-basin was subjected to hemipelagic deposition, similar to the southern sub-basin (Fig. 6-3). This change in sedimentary environment is probably due to the rise in sea level following the glacial periods of the "Messinian Gap" (Cosentino et al., 2013) and tectonic quiescence which also saw the refilling of the Mediterranean Sea. A 5.33 Ma age is assigned to the end of Stage IV, supported by chronologic information from the Algarve-2 and U1387 borehole (Fig. 6-2). Stratigraphic discontinuity D7, which is interpreted as the Miocene-Pliocene boundary (MPB, 5.33 Ma, Hernández-Molina et al., 2016), represents the lithological transition from a hemipelagic to a contouritic environment with the inception of weak MOW (van der Schee et al., 2016), The presence of MOW for the Pliocene indicates the reconnection of the Atlantic and the Mediterranean at the end of the Messinian Salinity Crisis (Flecker et al., 2015).

Deep-marine sedimentary systems, control factors and implications

The Late Miocene development of the eastern domain of the Deep Algarve basin is controlled mainly by the two dominant deep marine sedimentary processes: gravity flows and bottom currents.

Guadalquivir sands turbidite system

The evolution of the turbidite sedimentary system in the eastern domain corresponds to the distal section of the Guadalquivir sands turbidite system, downstream of the far eastern domain and the lower Guadalquivir. Seven episodes were identified in the Guadalquivir sands turbidite system (Gv-1 to Gv-7), which started in the upper Guadalquivir with the first two episodes at 7.24 Ma and prograde downstream from east to west along the axis of the basin, where sediments are also fed by its northern and southern margins (Suárez et al. 1989; Sierro et al., 1996; Ledesma, 2000). This axial turbidite system only reached the Algarve basin since its fifth episode (6.8 Ma onwards, Gv-5 to Gv-7, or U3 to U5), where in the far eastern to central eastern domains they continue to prograde downstream, developing the more distal lobe facies during late Stage II (U3, 6.8-6.4 Ma), followed by the channelised lobe facies in the early Stage III (U4, 6.4-6.0 Ma), and finally the more proximal channel-levee facies during late Stage III (U5, 6.0-5.6 Ma), which terminated in the earliest Stage IV (slightly after 5.6 Ma) (Fig. 6-8). The Southern Guadalquivir submarine channel initiated as a relatively straight channel in the early Messinian and developed its meanders through downstream translation and lateral migration (Babonneau et al., 2010; Sylvester et al., 2011) during the middle to late Messinian, albeit in a topographically confined basin (Covault et al., 2019). However, the developed meandering channel was abandoned following its final incision in the latest Messinian (Fig. 6-8).

Prior to the middle of Stage II (>6.8 Ma), sediments from the Guadalquivir sands turbidite system did not reach the Algarve basin, as the depocentre of the submarine lobes were located further upstream in the Guadalquivir valley (Ledesma, 2000). Thus, the basin was dominated by fine-grained pelagic or hemipelagic settings during the late Tortonian to earliest Messinian, however transverse turbidite systems originating from the adjacent Algarve margin in the north, such as the Western and Eastern Algarve channels (Figs. 6-5 and 6-7), has contributed sediments which could lead to deposition of confined or ponded turbidites in the northern and western sub-basins (Fig. 6-9, a and c, Prather, 2003; Patacci et al., 2015). These turbidite systems were not able to feed the southern sub-basins due to the Esperança diapiric ridge acting as a structural obstacle greater in height than the flow thickness, deflecting the pathways of turbidity currents (Patacci et al., 2015) westwards down the main axial gradient of the Algarve basin.

The evolution of the turbiditic system was influenced by two controlling factors, tectonics and eustasy. The development of the long and narrow Guadalquivir foreland to the Algarve foredeep basin was driven by Betic-Rif orogeny during the late Tortonian, where flexural subsidence due to thrust loading of the Betic Cordillera and emplacement of the GCAW caused rapid deepening of the basin (Garcia-Castellanos et al., 2002; Vergés and Fernàndez, 2012), creating accommodation for sediment deposition in a deep-marine setting (Sierro et al., 1996; Ledesma, 2000). The tectonic evolution of the Betic Cordillera and the Gibraltar arc, together with the northern paleo-margin of the Iberian Massif, confined the axial turbidite system of the Guadalquivir sands to prograde downslope of the foreland basin (Suárez et al, 1989), which are since progressively deposited in the Algarve basin. The deposition of the Guadalquivir sands is partially analogous to the Numidian sands turbidite system in the southern Apennines and the Morillo system in the Ainsa Basin of the Spanish Pyrenees, although these systems are instead confined within the wedge- or thrust-top section of the Hyblean-Apulian (Butler et al., 2020) and Pyrenean (Bayliss and Pickering, 2015) foreland basins respectively. Deformation and diapirism, which were prevalent during the late Tortonian to Messinian, created structures which acted as obstacles and diverted the pathways of the turbidity currents (Duarte et al., 2019). The progradational changes in the depositional facies of the Guadalquivir sands turbidite system, from lobe to channelised lobe to channel-levees, occurred in a roughly 400-kyr cycle (Fig. 6-9). These turbidite facies transition were probably affected by tectonic pulsing superimposed on the long-term eccentricity orbital forcing linked to the orogenic uplift of the Gibraltar arc, which led to the gradual emergence of the Betic Cordillera upstream of the Guadalquivir valley (Krijgsman et al., 1999; Braga et al., 2003). Similar controls were observed for the Eocene turbidites of the Ainsa basin, related to the Pyrenean orogeny, where the ~400-kyr Milankovitch eccentricity frequency regulated the sediment supply and growth of the channelised submarine fans (Pickering and Bayliss, 2009). Although the turbidite system generally prograde westwards from the Guadalquivir towards the Algarve foredeep basin, the internal configurations of the turbidites were also affected by the glacio-eustatic sea-level variations during the late Tortonian to Messinian (Sierro et al., 1996), where a series of transgressive-regressive cycles ending with prominent unconformities were interpreted for the turbidite units (Riaza and Martínez del Olmo, 1996). Towards the latest Messinian, retrogradation of the turbidite system caused by the rising sea levels following the glacial periods of the "Messinian Gap" (Cosentino et al., 2013) would have led to the abandonment of submarine channels (Ledesma, 2000).

Late Miocene contourite depositional system

The evolution of the contourite depositional system in the eastern domain of the Deep Algarve basin consists of two main periods: Stage I and mid-to-late Stage II, which are dependent on the evolution of the paleo-MOW through both the Betic and Rifian corridors. Erosional and depositional bottom current features identified in the upper Tortonian, such as sheeted, plastered and separated mounded drifts, and contourite channels and furrows (Stage I: 8.0-7.51 Ma), would have occurred prior to the emplacement of the AUGC in the Algarve basin (Ledesma, 2000). This stage corresponded to when the Betic corridor was still an active Mediterranean-Atlantic gateway with a two-way water-mass exchange (Krijgsman et al., 2018). Weak bottom currents from the paleo-MOW circulation along the margin during this period may also be responsible for conditioning the deposition of turbidites in the Western Algarve channel, where they are sufficient in strength to deflect suspended sediments from the turbidity currents to form asymmetric levees and mixed drifts (Sansom, 2018; Miramontes et al., 2020) as previously observed in the Late Miocene Sagres canyon (Ng et al., 2021b), as well as developing furrows and channels by scouring the seabed (Fig. 6-9a). Development of these drifts, as well as the separated mounded drifts in the western sub-basins, could have been related to shallowing of the North Betic and Guadix straits prior to their closure circa 7.8 Ma (Betzler et al., 2006; Hüsing et al., 2010), which would have limited paleo-MOW circulation through the remaining connections of the Betic corridor (Krijgsman et al., 2018). The emplacement of the AUGC, which occurred circa 7.51 Ma and lasted until the Tortonian-Messinian boundary (7.24 Ma) (Ledesma, 2000) acted as a barrier for bottom current circulation flowing into the eastern Deep Algarve basin by limiting its southern boundary and confined the foredeep basin to hemipelagic sedimentation. Tectonic uplift also led to the closure of the Guadalhorce strait and the Granada basin prior to 7.51 Ma (van der Schee et al., 2018) and 7.24 Ma (Corbi et al., 2012) respectively, which completely restricted paleo-MOW circulation through the Betic corridor by the end of late Tortonian (Krijgsman et al., 2018), and superseded by the evolution of the Guadalquivir sands turbidite system (Ledesma, 2000). Coevally in the Rifian corridor, tectonic emplacement of the Prerifian ridges accretionary wedge circa 7.51 Ma (Capella et al., 2017b) also saw the relocation of contourite sedimentation and deposition from the north (7.8-7.51 Ma) to the south (7.51-7.25 Ma) of the accretionary wedge (Capella et al., 2017a; de Weger et al., 2020, 2021), whereas their termination (7.25 Ma) was linked to the transition from thin- to thick-skinned compressional tectonic regime for the Betic-Rif orogeny (Capella et al., 2017b).

Following a period of bottom current inactivity in the eastern Deep Algarve basin (7.51-7.24 Ma), bottom currents began to influence the southern sub-basin again since the early Messinian (mid-to-late Stage II: 7.24-6.4 Ma), which could be attributed to the regional-scale compression event around the Tortonian-Messinian boundary (Capella et al., 2017b). The arrival of the turbidite system into the Gulf of Cádiz contributed coarser sediments to drift building, suggested by the increase in seismic amplitude response during Stage II (upper U2 to U3). The transition from sheeted to confined mounded drift towards the IMU was also due to the strengthening of the paleo-MOW from the shallowing of the Rifian corridor prior to its severe weakening (Ng et al., 2021b). During this period, boundary channels began to form in the southern sub-basin, as the core of bottom currents flow along the basin margins, reworking and depositing sediments in the basin centre. The mounded drift was formed from the boundary currents within the southern sub-basin with a confining slope (Fig. 6-9b), which restricted circulation within this narrow passage serving as corridors for accelerated bottom currents (Reed et al., 1987). Contourite deposition was terminated since ~6.4 Ma, as paleo-MOW circulation through the Mediterranean-Atlantic gateways were severely restricted (Ng et al., 2021a). Regionally, the Gulf of Cádiz reverted to a hemipelagic dominant environment, while the Algarve foredeep basin was still affected by the Guadalquivir sands turbidite system until the "Messinian Gap" event.

Similar to the turbidite system, the Late Miocene contourite depositional system was also controlled by the tectonics, on top of sedimentary and climate forces (Ng et al., 2021b). Tectonic drivers were largely responsible for the evolution of the Betic and Rifian corridors (Flecker et al., 2015; Capella et al., 2017b; Spakman et al., 2018), which in turn controls the paleo-MOW circulation in the Gulf of Cádiz, dictating the distribution and major changes, including onset and termination, of the contourite depositional system, as well as the stepwise restriction of the Mediterranean (Ng et al., 2021a; b). These events were imprinted on the long-term eccentricity orbital cycles (Hilgen et al., 2007; Ng et al., 2021a). Tectonics were also responsible for triggering gravitational flows, such as the Guadalquivir sand and Algarve channels turbidite systems, and possibly the Algarve MTDs, which acts as local sediment source for the contourite system (Fig. 6-9b). The uplift and shallowing of the sills within the Betic and Rifian corridors would have strengthened the paleo-MOW prior to its weakening at ~7.51 Ma and ~6.4 Ma respectively (Krijgsman et al., 1999; Capella et al., 2019; Ng et al., 2021a), and are reflected in the cyclic seismic facies with an upward increasing amplitude trend for the contourite intervals (Stage I and II). These cyclicities are related to a coarsening-upward

sequence linking paleo-MOW variability with Milankovitch precession cycles modulated by eccentricity cycles, as previously correlated for the Pliocene-Quaternary contourite depositional system, which is thought to have an influence on sea-level variation, sediment supply and bottom current activity (Llave et al., 2001; Hernández-Molina et al., 2016; Mestdagh et al., 2019; Sierro et al., 2020). These climatic-induced effects are also observed in the intermittent behaviour of the paleo-MOW during the deposition of late Miocene contourites in the Rifian corridor (de Weger et al., 2020).

Conclusion

The seismostratigraphic evolution of the eastern domain of the Deep Algarve basin consists of the interaction of gravitational and bottom current processes associated to the Late Miocene contourite depositional system of the Gulf of Cádiz and the Guadalquivir sands turbidite system. Their evolution is related to the initial infilling of a foreland basin synchronous to the closure of adjacent oceanic gateways. The contourite system dominated the first half of the Late Miocene stratigraphy, where it reflected the shallowing of the sill and subsequent restriction of the paleo-MOW through the Mediterranean-Atlantic gateways. The influence of the paleo-MOW on contourite deposition in the Gulf of Cádiz lasted until circa 6.4 Ma following severe weakening or cessation of paleo-MOW through the Rifian corridor, whereas sedimentary changes in the Deep Algarve basin between 7.51 Ma and 7.24 Ma, could be related to the weakening of paleo-MOW through the Betic corridor. Since the Tortonian-Messinian boundary, the Guadalquivir sands turbidite system was initiated in the Guadalquivir foreland basin but had only reached the Gulf of Cádiz since 6.8 Ma. In the Algarve foredeep basin, turbiditic sediments transported from the lower Guadalquivir were reworked by bottom currents sourced from the paleo-MOW which emerged from the Rifian corridor until ~6.4 Ma. Both the turbidite and contourite depositional systems were subjected to the influence of tectonic and orbital forcing, which had an impact on climate and eustasy. Tectonic pulses of about 400-kyr dictated the large-scale morphosedimentary evolution and the interaction between these sedimentary systems.

Acknowledgements

References

Antunes, M.T., Elderield, H., Legoinha, P., Pais, J., 1997. The Neogene of Algarve. Field trip guide - Excursão 2 (Portuguese Part). In: González-Delgado, J.A., Sierro, F.J., Pais, J. (Eds), 2nd congress of Regional Committee on Atlantic Neogene Stratigraphy (RCANS), Universidad de Salamanca, Salamanca. pp 37–55.

Babonneau, N., Savoye, B., Cremer, M., Bez, M., 2010. Sedimentary Architecture in Meanders of a Submarine Channel: Detailed Study of the Present Congo Turbidite Channel (Zaiango Project). Journal of Sedimentary Research **80**, 852–866. doi:10.2110/jsr.2010.078.

Barnes, N.E., Normark, W.R., 1985. Diagnostic parameters for comparing modern submarine fans and ancient turbidite systems. In: Bouma, A.H., Normark, W.R., Barnes, N.E. (Eds.), Submarine Fans and Related Turbidite Systems. Springer-Verlag, New York. pp. 13–14.

Bayliss, N.J., Pickering, K.T., 2015. Deep-marine structurally confined channelised sandy fans: Middle Eocene Morillo System, Ainsa Basin, Spanish Pyrenees. Earth-Science Reviews **144**, 82-106. doi:10.1016/j.earscirev.2014.11.014.

Betzler, C., Braga, J.C., Martín, J.M., Sánchez-Almazo, I.M., Lindhorst, S., 2006. Closure of a seaway: Stratigraphic record and facies (Guadix basin, Southern Spain). International Journal of Earth Sciences **95**, 903– 910. doi:10.1007/s00531-006-0073-y.

Braga, J.C., Martín, J.M., Quesada, C., 2003. Patterns and average rates of late Neogene– Recent uplift of the Betic Cordillera, SE Spain. Geomorphology **50**, 3-26. doi:10.1016/S0169-555X(02)00205-2.

Butler, R.W.H., Pinter, P.R., Maniscalco, R., Hartley, A.J., 2020. Deep-water sand-fairway mapping as a tool for tectonic restoration: decoding Miocene central Mediterranean palaeogeography using the Numidian turbidites of southern Italy. Journal of the Geological Society **177**, 766-783. doi:10.1144/jgs2020-008.

Capella, W., Flecker, R., Hernández-Molina, F.J., Simon, D., Meijer, P.T., Rogerson, M., Sierro, F.J., Krijgsman, W., 2019. Mediterranean isolation preconditioning the Earth System for late Miocene climate cooling. Scientific Reports **9**, 3795. doi:10.1038/s41598-019-40208-2.

Capella, W., Hernández-Molina, F.J., Flecker, R., Hilgen, F.J., Hssain, M., Kouwenhoven, T.J., van Oorschot, M., Sierro, F.J., Stow, D.A.V., Trabucho-Alexandre, J., Tulbure, M.A., de Weger, W., Yousfi, M.Z., Krijgsman, W., 2017a. Sandy contourite drift in the late Miocene Rifian Corridor (Morocco): reconstruction of depositional environments in a

foreland-basin seaway. Sedimentary Geology **355**, 31–57. doi:10.1016/j.sedgeo.2017.04.004.

Capella, W., Matenco, L., Dmitrieva, E., Roest, W.M., Hessels, S., Hssain, M., Chakor-Alami, A., Sierro, F.J., Krijgsman, W., 2017b. Thick-skinned tectonics closing the Rifian Corridor. Tectonophysics **710**, 249–265. doi:10.1016/j.tecto.2016.09.028.

Clark, I.R., Cartwright, J.A., 2009. Interactions between submarine channel systems and deformation in deepwater fold belts: Examples from the Levant Basin, Eastern Mediterranean Sea. Marine and Petroleum Geology **26**, 1465–1482. doi:10.1016/j.marpetgeo.2009.05.004.

Clark, I.R., Cartwright, J.A., 2011. Key controls on submarine channel development in structurally active settings. Marine and Petroleum Geology **28**, 1333-1349. doi:10.1016/j.marpetgeo.2011.02.001.

Corbí, H., Lancis, C., García-García, F., Pina, J.A., Soria, J.M., Tent-Manclús, J.E., Viseras, C., 2012. Updating the marine biostratigraphy of the Granada Basin (central Betic Cordillera). Insight for the Late Miocene palaeogeographic evolution of the Atlantic – Mediterranean seaway. Geobios **45**, 249– 263. doi:10.1016/j.geobios.2011.10.006.

Cosentino, D., Buchwaldt, R., Sampalmieri, G., Iadanza, A., Cipollari, P., Schildgen, T.F., Hinnov, L.A., Ramezani, J., Bowring, S.A., 2013. Refining the Mediterranean "Messinian gap" with high-precision U-Pb zircon geochronology, central and northern Italy. Geology **41**, 323–326. doi:10.1130/G33820.1.

Covault, J.A., Sylvester, Z., Hudec, M.R., Ceyhan, C., Dunlap, D., 2020. Submarine channels 'swept' downstream after bend cutoff in salt basins. The Depositional Record **6**, 259-272. doi:10.1002/dep2.75.

Creaser, A., Hernández-Molina, F.J., Badalini, G., Thompson, P., Walker, R., Soto, M., Conti, B., 2017. A Late Cretaceous mixed (turbidite-contourite) system along the Uruguayan Margin: Sedimentary and palaeoceanographic implications., Marine Geology **390**, 234-253. doi:10.1016/j.margeo.2017.07.004.

Cumberpatch, Z.A., Kane, I.A., Soutter, E.L., Hodgson, D.M., Jackson, C.A-L., Kilhams, B.A., Poprawski, Y., 2021. Interactions between deep-water gravity flows and active salt tectonics. Journal of Sedimentary Research **91**, 34–65. doi:10.2110/jsr.2020.047.

Damuth, J.E., Kolla, V., Flood, R.D., Kowsmann, R.O., Monteiro, M.C., Gorini, M.A., Palma, J.J.C., Belderson, R.H., 1983, Distributary channel meandering and bifurcation patterns on the Amazon deep-sea fan as revealed by long-range side-scan sonar (GLORIA). Geology **11**, 94– 98. doi:10.1130/0091-7613(1983)11<94:DCMABP>2.0.CO;2.

de Castro, S., Hernández-Molina, F.J., de Weger, W., Jiménez-Espejo, F.J., Rodríguez-Tovar, F.J., Mena, A., Llave, E., Sierro, F.J., 2021. Contourite characterization and its discrimination from other deep-water deposits in the Gulf of Cádiz contourite depositional system. Sedimentology. doi:10.1111/sed.12813.

de Castro, S., Hernández-Molina, F.J., Rodríguez-Tovar, F.J., Llave, E., Ng, Z.L., Nishida, N., Mena, A., 2020. Contourites and bottom current reworked sands: Bed facies model and implications. Marine Geology **428**, 106267. doi:10.1016/j.margeo.2020.106267.

de Weger, W., Hernández-Molina, F.J., Flecker, R., Sierro, F.J., Chiarella, D., Krijgsman, W., Manar, M.A., 2020. Late Miocene contourite channel system reveals intermittent overflow behavior. Geology **48,** 1194–1199. doi:10.1130/G47944.1.

de Weger, W., Hernández-Molina, F.J., Miguez-Salas, O., de Castro, S., Bruno, M., Chiarella, D., Sierro, F.J., Blackbourn, G., Manar, M.A., 2021. Contourite depositional system after the exit of a strait: Case study from the late Miocene South Rifian Corridor, Morocco. Sedimentology. doi:10.1111/sed.12882.

Duarte, D., Magalhães, V.H., Roque, C., Hernández-Molina, F.J., Ng Z.L., Ledesma, S., Sierro, F.J., 2019. The Esperança Diapiric Ridge: Late Miocene-Quaternary compressional reactivation of a Salt Nappe in the Eastern Deep Algarve Basin, SW Iberian Margin. Salt Tectonics: Understanding Rocks that Flow. The Geological Society, Burlington House, London, 29-31 October 2019.https://researchgate.net/publication/337568030_The _Esperanca_Diapiric_Ridge_Late_Miocene_Quaternary_compressional_reactivation_of _a_Salt_Nappe_in_the_Eastern_Deep_Algarve_Basin_SW_Iberian_Margin.

Duarte, D., Roque, C., Hernández-Molina, F.J., Ng, Z.L., Magalhães, V.H., Llave, E., Sierro, F.J., 2020. Tectonic domains of the Betic Foreland System, SW Iberian margin: Implications for the Gulf of Cádiz Contourite System. EGU General Assembly 2020, Online, 4-8 May 2020. doi:10.5194/egusphere-egu2020-1033.

Duarte, J.C., Rosas, F.M., Terrinha, P., Gutscher, M.-A., Malavieille, J., Silva, S., Matias, L., 2011. Thrust–wrench interference tectonics in the Gulf of Cádiz (Africa–Iberia plate boundary in the North-East Atlantic): insights from analog models. Marine Geology **289**, 135–149. doi:10.1016/j.margeo.2011.09.014.

Duarte, J.C., Rosas, F.M., Terrinha, P., Gutscher, M.-A., Malavieille, J., Silva, S., Matias, L., 2011. Thrust–wrench interference tectonics in the Gulf of Cádiz (Africa–Iberia plate boundary in the North-East Atlantic): insights from analog models. Marine Geology **289**, 135–149. doi:10.1016/j.margeo.2011.09.014.

Duggen, S., Hoernle, K., van den Bogaard, P., Rüpke, L., Morgan, J.P., 2003. Deep roots of the Messinian salinity crisis. Nature **422**, 602–606. doi:10.1038/nature01553.

Faugères, J.-C., Stow, D.A.V., 2008. Continental drifts: Nature, evolution, and controls. In: Rebesco, M., Camerlenghi, A. (Eds.), Contourites. Developments in Sedimentology, **60**. Elsevier, Amsterdam, pp. 259–288.

Faugères, J.-C., Stow, D.A.V., Imbert, P., Viana, A., 1999. Seismic features diagnostic of contourite drifts. Marine Geology **162**, 1–38. doi:10.1016/S0025-3227(99)00068-7.

Flecker, R., Krijgsman, W., Capella, W., de Castro Martíns, C., Dmitrieva, E., Mayser, J.P., Marzocchi, A., Modestou, S., Ochoa, D., Simon, D., Tulbure, M., van den Berg, B., van der Schee, M., de Lange, G., Ellam, R., Govers, R., Gutjahr, M., Hilgen, F.J., Kouwenhoven, T., Lofi, J., Meijer, P., Sierro, F.J., Bachiri, N., Barhoun, N., Chakor Alami, A., Chacon, B., Flores, J.A., Gregory, J., Howard, J., Lunt, D., Ochoa, M., Pancost, R., Vincent, S., Zakaria Yousfi, M., 2015. Evolution of the late Miocene Mediterranean-Atlantic gateways and their impact on regional and global environmental change. Earth Science Reviews **150**, 365–392. doi:10.1016/j.earscirev.2015.08.007.

Fonnesu, M., Palermo, D., Galbiati, M., Marchesini, M., Bonamini, E., Bendias, D., 2020. A new world-class deep-water play-type, deposited by the syndepositional interaction of turbidity flows and bottom currents: The giant Eocene Coral Field in northern Mozambique. Marine and Petroleum Geology **111**, 179–201. doi:10.1016/j.marpetgeo.2019.07.047.

Fuhrmann, A., Kane, I.A., Clare, M.A., Ferguson, R.A., Schomacker, E., Bonamini, E., Contreras, F.A., 2020. Hybrid turbidite-drift channel complexes: An integrated multiscale model. Geology **48**, 562–568. doi:10.1130/G47179.1.

Gamberi, F., Rovere, M., 2011. Architecture of a modern transient slope fan (Villafranca fan, Gioia basin–Southeastern Tyrrhenian Sea). Sedimentary Geology **236**, 211-225. doi:10.1016/j.sedgeo.2011.01.007.

García, M., Hernández-Molina, F.J., Alonso, B., Vázquez, J.T., Ercilla, G., Llave, E., Casas, D., 2016. Erosive sub-circular depressions on the Guadalquivir Bank (Gulf of Cádiz): Interaction between bottom current, mass-wasting, and tectonic processes. Marine Geology **378,** 5-19. doi:10.1016/j.margeo.2015.10.004.

Garcia-Castellanos, D., Fernàndez, M., Torne, M., 2002. Modelling the evolution of the Guadalquivir foreland basin (southern Spain). Tectonics **21**, 1018. doi:10.1029/2001TC001339.

Gee, M.J.R., Gawthorpe, R.L., 2006. Submarine channels controlled by salt tectonics: Examples from 3D seismic data offshore Angola. Marine and Petroleum Geology **23**, 443–458. doi:10.1016/j.marpetgeo.2006.01.002.

Gong, C., Wang, Y., Rebesco, M., Salon, S., Steel, R.J., 2018. How do turbidity flows interact with contour currents in unidirectionally migrating deep-water channels? Geology, **46**, 551–554. doi:10.1130/G40204.1.

Gong, C., Wang, Y., Zhu, W., Li, W., Xu, Q., 2013. Upper Miocene to Quaternary unidirectionally migrating deep-water channels in the Pearl River Mouth Basin, northern South China Sea. AAPG Bulletin **97**, 285–308. doi:10.1306/07121211159.

Gràcia, E., Dañobeitia, J., Vergés, J., Bartolomé, R., 2003. Crustal architecture and tectonic evolution of the Gulf of Cádiz (SW Iberian margin) at the convergence of the Eurasian and African plates. Tectonics **22**, 1033. doi:10.1029/2001TC901045.

Gutscher, M.-A., J. Malod, J.-P. Rehault, I. Contrucci, F. Klingelhoefer, L. Mendes-Victor, and W. Spakman (2002), Evidence for active subduction beneath Gibraltar. Geology **30**, 1071. doi:10.1130/0091-7613(2002)030<1071:EFASBG>2.0.CO;2.

Hernández-Molina, F.J., Llave, E., Somoza, L., Fernández-Puga, M.C., Maestro, A., León, R., Medialdea, T., Barnolas, A., García, M., Díaz del Río, V., Fernández-Salas, L.M., Vázquez, J.T., Lobo, F., Alveirinho Dias, J.M., Rodero, J., Gardner, J., 2003. Looking for clues to paleoceanographic imprints: A diagnosis of the Gulf of Cádiz contourite depositional systems. Geology **31**, 19-22. doi:10.1130/0091-7613(2003)031<0019:LFCTPI>2.0.CO;2.

Hernández-Molina, F.J., Llave, E., Preu, B., Ercilla, G., Fontan, A., Bruno, M., Serra, N., Gomiz, J.J., Brackenridge, R.E., Sierro, F.J., Stow, D.A.V., García, M., Juan, C., Sandoval, N., Arnaiz, A., 2014. Contourite processes associated with the Mediterranean Outflow Water after its exit from the Strait of Gibraltar: Global and conceptual implications. Geology **42**, 227–230. doi:10.1130/G35083.1.

Hernández-Molina, F.J., Sierro, F.J., Llave, E., Roque, C., Stow, D.A.V., Williams, T., Lofi, J., van der Schee, M., Arnáiz, A., Ledesma, S., Rosales, C., Rodríguez-Tovar, F.J., Pardo-Igúzquiza, E., Brackenridge, R.E., 2016. Evolution of the gulf of Cádiz margin and Southwest Portugal contourite depositional system: Tectonic, sedimentary and paleoceanographic implications from IODP expedition 339. Marine Geology **377**, 7–39. doi:10.1016/j.margeo.2015.09.013.

Hernández-Molina, F.J., Stow, D.A.V., Llave, E., 2008. Continental slope contourites. In: Rebesco, M., Camerlenghi, A. (Eds.), Contourites. Developments in Sedimentology, **60**. Elsevier, Amsterdam, pp. 379–408.

Hilgen, F., Kuiper, K., Krijgsman, W., Snel, E., van der Laan, E., 2007. Astronomical tuning as the basis for high resolution chronostratigraphy: the intricate history of the Messinian Salinity Crisis. Stratigraphy **4**, 231-238.

Hodell, D.A., Curtis, J.H., Sierro, F.J., and Raymo, M.E., 2001. Correlation of Late Miocene to Early Pliocene sequences between the Mediterranean and North Atlantic. Paleoceanography, **16**, 164– 178. doi:10.1029/1999PA000487.

Hsü, K.J., Ryan, W.B., Cita, M.B., 1973. Late Miocene desiccation of the Mediterranean. Nature **242**, 240-244. doi:10.1038/242240a0.

Hüsing, S. K., Oms, O., Agustí, J., Garcés, M., Kouwenhoven, T.J., Krijgsman, W., Zachariasse, W.J., 2010. On the late Miocene closure of the Mediterranean-Atlantic gateway through the Guadix Basin (Southern Spain). Palaeogeography Palaeoclimatology, Palaeoecology **291**, 167– 179. doi:10.1016/j.palaeo.2010.02.005.

Iribarren, L., Vergés, J., Camurri, F., Fullea, J., Fernàndez, M., 2007. The structure of the Atlantic–Mediterranean transition zone from the Alboran Sea to the Horseshoe Abyssal Plain (Iberia–Africa plate boundary). Marine Geology **243**, 97–119. doi:10.1016/j.margeo.2007.05.011.

Ivanovic, R.F., Flecker, R., Gutjahr, M., Valdesa, P.J., 2013. First Nd isotope record of Mediterranean–Atlantic water exchange through the Moroccan Rifian Corridor during the Messinian Salinity Crisis. Earth Planetary Science Letters **368**, 163–174. doi:10.1016/j.epsl.2013.03.010.

Jobe, Z.R., Howes, N.C., Auchter, N.C., 2016. Comparing submarine and fluvial channel kinematics: Implications for stratigraphic architecture. Geology **44**, 931– 934. doi:10.1130/G38158.1.

Krijgsman, W., Capella, W., Simon, D., Hilgen, F.J., Kouwenhoven, T.J., Meijer, P.Th., Sierro, F.J., Tulbure, M.A., van den Berg, B.C.J., van der Schee, M., Flecker, R., 2018. The Gibraltar Corridor: Watergate of the Messinian Salinity Crisis. Marine Geology **403**, 238–246. doi:10.1016/j.margeo.2018.06.008.

Krijgsman, W., Hilgen, F.J., Raffi, I., Sierro, F.J., Wilson, D.S., 1999. Chronology causes and progression of the Messinian salinity crisis. Nature **400**, 652-655. doi:10.1038/23231.

Ledesma, S.M., 2000. Astrobiocronología y estratigrafía de alta resolución del Neógeno de la Cuenca del Guadalquivir-Golfo de Cádiz. PhD thesis, Universidad de Salamanca, Salamanca, 464 pp.

Llave, E., Hernández-Molina, F.J., Somoza, L., Díaz-del-Río, V., Stow, D.A.V., Maestro, A., Alveirinho Dias, J.M., 2001. Seismic stacking pattern of the Faro-Albufeira contourite system (gulf of Cádiz): a Quaternary record of paleoceanographic and tectonic influences. Marine Geophysical Researches **22**, 487-508. doi:10.1023/A:1016355801344.

Lofi, J., Sage, F., Déverchère, J., Loncke, L., Maillard, A., Gaullier, V., Thinon, I., Gillet, H., Guennoc, P., Gorini, C., 2011. Refining our knowledge of the Messinian salinity crisis records in the offshore domain through multi-site seismic analysis. Bulletin de la Société Géologique de France **182**, 163-180. doi:10.2113/gssgfbull.182.2.163.

Lopes, F.C., Cunha, P.P., Le Gall, B., 2006. Cenozoic seismic stratigraphy and tectonic evolution of the Algarve margin (offshore Portugal, southwestern Iberian Peninsula). Marine Geology **231**, 1–36. doi:10.1016/j.margeo.2006.05.007.

Maldonado, A., Somoza, L., Pallarés, L., 1999. The Betic orogen and the Iberian-African boundary in the Gulf of Cádiz: geological evolution (Central North Atlantic). Marine Geology **155**, 9–43. doi:10.1016/S0025-3227(98)00139-X.

Marchès, E., Mulder, T., Gonthier, E., Cremer, M., Hanquiez, V., Garlan, T., Lecroart, P., 2010. Perched lobe formation in the Gulf of Cádiz: Interactions between gravity processes and contour currents (Algarve Margin, Southern Portugal). Sedimentary Geology **229**, 81-94. doi:10.1016/j.sedgeo.2009.03.008.

Martín, J.M., Braga, J.C., Aguirre, J., Puga-Bernabéu, Á., 2009. History and evolution of the North-Betic Strait (Prebetic Zone, Betic Cordillera): a narrow, early Tortonian, tidal-dominated, Atlantic-Mediterranean marine passage. Sedimentary Geology **216**, 80–90. doi:10.1016/j.sedgeo.2009.01.005.

Matias, H., Kress, P., Terrinha, P., Mohriak, W., Menezes, P.T.L., Matias, L., Santos, F., Sandnes, F., 2011. Salt tectonics in the western Gulf of Cádiz, southwest Iberia. AAPG Bulletin **95**, 1667–1698. doi:10.1306/01271110032.

McCave, I.N., Tucholke, B.E., 1986. Deep current-controlled sedimentation in the western North Atlantic. In: Vogt, P.R., Tucholke, B.E., (Eds), The Western North Atlantic Region. Geology of North America. Decade of North American Geology. Geological Society of America, Boulder. pp. 451-468. doi:10.1130/DNAG-GNA-M.451.

Medialdea, T., Vegas, R., Somoza, L., Vázquez, J.T., Maldonado, A., Díaz-del-Río, V., Maestro, A., Córdoba, D., Fernández-Puga, M.C., 2004. Structure and evolution of the

"Olistostrome" complex of the Gibraltar Arc in the Gulf of Cádiz (eastern Central Atlantic): evidence from two long seismic cross-sections. Marine Geology **209**, 173–198. doi:10.1016/j.margeo.2004.05.029.

Mestdagh, T., Lobo, F.J., Llave, E., Hernández-Molina, F.J., Van Rooij, D., 2019. Review of the late Quaternary stratigraphy of the northern Gulf of Cádiz continental margin: new insights into controlling factors and global implications. Earth-Science Reviews **198,** 102944. doi:10.1016/j.earscirev.2019.102944.

Miramontes, E., Eggenhuisen, J.T., Jacinto, R.S., Poneti, G., Pohl, F., Normandeau, A., Campbell, D.C., Hernández-Molina, F.J., 2020. Channel-levee evolution in combined contour current-turbidity current flows from flume-tank experiments. Geology **48**, 353–357. doi:10.1130/G47111.1.

Miramontes, E., Thiéblemont, A., Babonneau, N., Penven, P., Raisson, F., Droz, L., Jorry, S.J., Fierens, R., Counts, J.W., Wilckens, H., Cattaneo, A., Jouet, G., 2021. Contourite and mixed turbidite-contourite systems in the Mozambique Channel (SW Indian Ocean): Link between geometry, sediment characteristics and modelled bottom currents. Marine Geology **437**, 106502. doi:10.1016/j.margeo.2021.106502.

Ng, Z.L., Hernández-Molina, F.J., Duarte, D., Roque, C., Sierro, F.J., Llave, E., Manar, M.A., 2021a. Late Miocene contourite depositional system of the Gulf of Cádiz: The sedimentary signature of the paleo-Mediterranean Outflow Water. Marine Geology **442**, 106605. doi:10.1016/j.margeo.2021.106605.

Ng, Z.L., Hernández-Molina, F.J., Duarte, D., Sierro, F.J., Ledesma, S., Rogerson, M., Llave, E., Roque, C., Manar, M.A., 2021b. Latest Miocene restriction of the Mediterranean Outflow Water: a perspective from the Gulf of Cádiz. Geo-Marine Letters **41**, 23. doi:10.1007/s00367-021-00693-9.

O'Neill-Baringer, M., Price, J.F., 1999. A review of the physical oceanography of the Mediterranean outflow. Marine Geology **155**, 63–82. doi:10.1016/S0025-3227(98)00141-8.

Ohneiser, C., Florindo, F., Stocchi, P., Roberts, A.P., DeConto, R.M., Pollard, D., 2015. Antarctic glacio-eustatic contributions to late Miocene Mediterranean desiccation and reflooding. Nature Communications **6**, 8765. doi:10.1038/ncomms9765.

Oluboyo, A.P., Gawthorpe, R.L., Bakke, K., Hadler-Jacobsen, F., 2014. Salt tectonic controls on deep-water turbidite depositional systems: Miocene, southwestern Lower Congo Basin, offshore Angola. Basin Research **26**, 597–620. doi:10.1111/bre.12051.

Pais, J., Legoinha, P., Elderfield, H., Sousa, L., Estevens, M., 2000. The Neogene of Algarve (Portugal). Ciências de Terra (UNL) **14**, 277–288.

Pamela S., 2018. Hybrid turbidite–contourite systems of the Tanzanian margin. Petroleum Geoscience **24**, 258–276. doi:10.1144/petgeo2018-044.

Patacci, M., Haughton, P.D.W., Mccaffrey, W.D., 2015. Flow Behavior of Ponded Turbidity Currents. Journal of Sedimentary Research **85**, 885–902. doi:10.2110/jsr.2015.59.

Peakall, J., McCaffrey, B., Kneller, B., 2000. A process model for the evolution, morphology, and architecture of sinuous submarine channels. Journal of Sedimentary Research **70**, 434–448. doi:10.1306/2DC4091C-0E47-11D7-8643000102C1865D.

Pickering, K.T., Bayliss, N.J., 2009. Deconvolving tectono-climatic signals in deep-marine siliciclastics, Eocene Ainsa basin, Spanish Pyrenees: Seesaw tectonics versus eustasy. Geology **37**, 203–206. doi:10.1130/G25261A.1.

Piper, D.J., Normark, W.R., 2001. Sandy fans-from Amazon to Hueneme and beyond. AAPG Bulletin **85**, 1407– 1438. doi:10.1306/8626CACD-173B-11D7-8645000102C1865D.

Posamentier, H.W., Erskine R.D., 1991. Seismic Expression and Recognition Criteria of Ancient Submarine Fans. In: Weimer P., Link M.H. (Eds), Seismic Facies and Sedimentary Processes of Submarine Fans and Turbidite Systems. Frontiers in Sedimentary Geology. Springer, New York. doi:10.1007/978-1-4684-8276-8_10

Prather, B.E., 2003. Controls on reservoir distribution, architecture, and stratigraphic trapping in slope settings. Marine and Petroleum Geology **20**, 529-545. doi:10.1016/j.marpetgeo.2003.03.009.

Prather, B.E., Booth, J.R., Steffens, G.S., Craig, P.A., 1998. Classification, lithologic calibration, and stratigraphic succession of seismic facies of intraslope basins, deep-water Gulf of Mexico. AAPG Bulletin **82**. doi:10.1306/1D9BC5D9-172D-11D7-8645000102C1865D.

Ramos, A., Fernández, O., Muñoz, J.A., Terrinha, P., 2017. Impact of basin structure and evaporite distribution on salt tectonics in the Algarve Basin, Southwest Iberian margin. Marine and Petroleum Geology **88**, 961–984. doi:10.1016/j.marpetgeo.2017.09.028.

Ramos, A., Fernández, O., Terrinha, P., Muñoz J.A., Arnaiz, Á., 2020. Paleogeographic evolution of a segmented oblique passive margin: the case of the SW Iberian margin. International Journal of Earth Science (Geologische Rundschau) **109**, 1871–1895. doi:10.1007/s00531-020-01878-w.

Rebesco, M., Hernández-Molina, F.J., Van Rooij, D., Wåhlin, A., 2014. Contourites and associated sediments controlled by deep-water circulation processes: State-of-the-art and future considerations. Marine Geology **352**, 111–154. doi:10.1016/j.margeo.2014.03.011.

Reed, D.L., Meyer, A.W., Silver, E.A., Prasetyo, H., 1987. Contourite sedimentation in an intraoceanic forearc system: eastern Sunda Arc, Indonesia. Marine Geology **76**, 223-241. http://doi.org/10.1016/0025-3227(87)90031-4.

Riaza, C., Martínez del Olmo, W., 1996. Depositional model of the Guadalquivir–Gulf of Cádiz Tertiary basin. In: Friend, P.F., Dabrio, C.J. (Eds.), Tertiary Basins of Spain. The Stratigraphic Record of Crustal Kinematics. World and Regional Geology, **6**. Cambridge University Press, Cambridge. pp. 330–338

Rodrigues, S., Hernández-Molina, F.J., Kirby, A., 2021. A late cretaceous mixed (turbidite-contourite) system along the Argentine margin: Paleoceanographic and conceptual implications. Marine and Petroleum Geology **123**, 104768. doi:10.1016/j.marpetgeo.2020.104768.

Rogerson, M., Rohling, E.J., Bigg, G.R., Ramirez, J., 2012. Palaeoceanography of the Atlantic-Mediterranean Exchange: Overview and first quantitative assessment of climatic forcing. Reviews of Geophysics **50**, RG2003. doi:10.1029/2011RG000376.

Shanmugam, G., Spalding, T.D., Rofheart, D. H., 1993. Traction structures in deep-marine, bottom-current-reworked sands in the Pliocene and Pleistocene, Gulf of Mexico. Geology **21**, 929–932. doi:10.1130/0091-7613(1993)021<0929:TSIDMB>2.3.CO;2.

Sierro, F.J., González-Delgado, J.A., Dabrio, C.J., Flores, J.A., Civis, J., 1996. Late Neogene depositional sequences in the foreland basin of Guadalquivir (SW Spain). In: Friend, P.F., Dabrio, C.J. (Eds.), Tertiary Basins of Spain. The Stratigraphic Record of Crustal Kinematics. World and Regional Geology **6**. Cambridge University Press, Cambridge. pp. 339–345

Sierro, F.J., Hodell, D.A., Andersen, N., Azibeiro, L.A., Jimenez-Espejo, F.J., Bahr, A., Flores, J.A., Ausin, B., Rogerson, M., Lozano-Luz, R., Lebreiro, S.M., Hernández- Molina, F.J., 2020. Mediterranean overflow over the last 250 kyr: Freshwater forcing from the tropics to the ice sheets. Paleoceanography and Paleoclimatology **35**, e2020PA003931. doi:10.1029/2020PA003931.

Spakman, W., Chertova, M.V., van den Berg, A., van Hinsbergen, D.J., 2018. Puzzling features of western Mediterranean tectonics explained by slab dragging. Nature Geoscience **11**, 211– 216. doi:10.1038/s41561-018-0066-z.

Srivastava, S.P., Schouten, H., Roest, W.R., Klitgord, K.D., Kovacs, L.C., Verhoef, J., Macnab, R., 1990. Iberian plate kinematics: a jumping plate boundary between Eurasia and Africa. Nature **344**, 756–759. doi:10.1038/344756a0.

Stoker, M.S., Akhurst, M.C, Howe, J.A., Stow, D.A.V., 1998. Sediment drifts and contourites on the continental margin off northwest Britain. Sedimentary Geology **115**, 33-51. doi:10.1016/S0037-0738(97)00086-9.

Stow, D.A.V., Smillie, Z., 2020. Distinguishing between Deep-Water Sediment Facies: Turbidites, Contourites and Hemipelagites. Geosciences **10**, 68. doi:10.3390/geosciences10020068.

Suárez, J., Martínez del Olmo, W., Serrano, A., Leret Verdú, G. (1989). Estructura del sistema turbidítico de la formación arenas del Guadalquivir, Neógeno del valle del Guadalquivir. In: Libro homenaje a Rafael Soler, Asociación de Geólogos y Geofísicos Españoles del Petróleo, Madrid. pp.123-132.

Sylvester, Z., Pirmez, C., Cantelli, A., 2011. A model of submarine channel-levee evolution based on channel trajectories: Implications for stratigraphic architecture. Marine and Petroleum Geology **28**, 716– 727. doi:10.1016/j.marpetgeo.2010.05.012.

Terrinha, P., Ramos, A., Neres, M., Valadares, V., Duarte, J., Martínez-Loriente, S., Silva, S., Mata, J., Kullberg, J.C., Casas-Sainz, A., Matias, L., Fernández, Ó., Muñoz, J.A., Ribeiro, C., Font, E., Neves, C., Roque, C., Rosas, F., Pinheiro, L., Bartolomé, R., Sallarès, V., Magalhães, V., Medialdea, T., Somoza, L., Gràcia, E., Hensen, C., Gutscher, M.-A., Ribeiro, A., Zitellini, N., 2019. The Alpine Orogeny in the West and Southwest Iberia margins. In: Quesada, C., Oliveira, J. (Eds.), The Geology of Iberia: A Geodynamic Approach. Regional Geology Reviews. Springer, Cham, pp. 487–505. doi:10.1007/978-3-030-11295-0_11.

Torelli, L., Sartori, R., Zitellini, N., 1997. The giant chaotic body in the Atlantic Ocean off Gibraltar: new results from a deep seismic reflection survey. Marine and Petroleum Geology **14**, 125–134. doi:10.1016/S0264-8172(96)00060-8.

van der Schee, M., Sierro, F., Jimenez-Espejo, F., Hernández-Molina, F., Flecker, R., Flores, J., Acton, G., Gutjahr, M., Grunert, P., García-Gallardo, A., Andersen, N., 2016. Evidence of early bottom water current flow after the Messinian Salinity Crisis in the Gulf of Cádiz. Marine Geology **380**, 315–329. doi:10.1016/j.margeo.2016.04.005.

van der Schee, M., van den Berg, B.C.J., Capella, W., Simon, D., Sierro, F.J., Krijgsman, W., 2018. New age constraints on the western Betic intramontane basins: A late Tortonian closure of the Guadalhorce Corridor? Terra Nova **30**, 325-332. doi:10.1111/ter.12347

Van Rooij, D., Iglesias, J., Hernández-Molina, F.J., Ercilla, G., Gomez-Ballesteros, M., Casas, D., Llave, E., De Hauwere, A., Garcia-Gil, S., Acosta, J., Henriet, J.-P., 2010. The Le Danois Contourite Depositional System: Interactions between the Mediterranean Outflow Water and the upper Cantabrian slope (North Iberian margin). Marine Geology **274**, 1-20. doi:10.1016/j.margeo.2010.03.001.

Vergés, J., Fernàndez, M., 2012. Tethys–Atlantic Interaction along the Iberia–Africa Plate Boundary: The Betic–Rif Orogenic System. Tectonophysics **579**, 144–172. doi:10.1016/j.tecto.2012.08.032.

Wynn, R.B., Cronin, B.T., Peakall, J., 2007. Sinuous deep-water channels: Genesis, geometry, and architecture. Marine and Petroleum Geology **24**, 341– 387. doi:10.1016/j.marpetgeo.2007.06.001.

Supplementary Material

Table 6-S1 Input data of the Algarve-2012 3D seismic reflection survey

Key information	Description
Input surface (sqkm)	1,500
Input domain	Time
Input collection	CMP and shots gather
Input stage	Pre-processed
Number of offsets	Plans
Azimuth	Narrow Azimuth
Sampling interval (ms)	4
Record length (ms)	7000
Time of the first sample (ms)	0
Datum (m)	0
Grid (Density)	25 x 37.5
Input offset plans split description	100 ‑ 8000, I250
Pre ‑ processing shop	Repsol/CGG Dedicated Processing Center, Madrid
Total number of traces	
Media type	3592E Tapes
Media density	500GB
Sample format	IBM 32-bit floating point
Data format	SEGY
Time Seismic Data Limits	**Value**
In-line first	486
In-line last	2021
In-line spacing (m)	25
In-line increment	1
Cross-line first	589
Cross-line last	2038
Cross-line spacing (m)	37.5
Cross-line increment	1

Table 6-S2 Acquisition information of the Algarve-2012 3D seismic reflection survey

Data was acquired Narrow Azimuth with the boat and cable configuration below.	
General	
Parameter Wildrose	**Description**
Project	Algarve
Location	Offshore Portugal
Area	Algarve
Date shot	28 February 2012 – 18 April 2012
Type of survey	3D Narrow Azimuth
Acquisition company	Polarcus (Naila Vessel)
Number of streamers	10
Number of channels per streamer	(Total)
Nominal fold	108
Shot point interval (m)	37.5 (Flip/Flop)
Source depth (m)	7
Streamer length (m)	8100
Cable depth (m)	9
Group interval (m)	12.5
Recording sample rate (ms)	2
Record length (s)	7
Projection	
Parameter	**Description**
Survey datum	ED50
Spheroid	INTL 1924
Projection	UTM
Central Meridian	9 DEG W
UTM zone	29N
False northing	0
False easting	500000
Semi major axis	6378388.000
Inverse flattening	297.0000000
Latitude of origin	0 DEG N
Scale factor	0.9996

Table 6-S3 Processing details of the Algarve-2012 3D seismic reflection survey

PSTM Processing Flow	
(Time dataset was processed in 2012 by Repsol/CGG Dedicated Processing Centre)	
1.	Reformat from SEGD
2.	Delay correction ‑ 200 ms
3.	Seismic navigation merge
4.	T2 amplitude corrections
5.	Low cut filter 3 Hz/18 dB
6.	Designature
7.	Swell noise attenuation
8.	Trace edit
9.	Linear noise attenuation
10.	FK de ‑ aliazing
11.	Trace drop (one receiver over 2)
12.	Tidal statics corrections
13.	2D SRME
14.	3D SRME
15.	Velocity picking 2000 m x 2000 m
16.	HR Radon de ‑ multiple
17.	3D interpolation and regularization 25 m x 37.5 m
18.	Bin grid
19.	Inverse T2 amplitude corrections
20.	Phase only deabsorption Q83
21.	Gun and cable statics 10 ms down
22.	SEGY output
*Polarity: Increase in pressure is a positive number	

Chapter 7

Discussion and Critical Evaluation

7.1   What are the main contributions of this project?

The contributions of this research project are the definition of the sedimentary stacking pattern of the Tortonian to Messinian interval in the Gulf of Cádiz, and for the first time the characterisation of an ancient contourite depositional system in the tectonically active Southwest Iberian and Northwest Moroccan margins within the aforementioned sedimentary and stratigraphic evolution, through the identification of bottom current depositional and erosional features. In addition, the regional correlation of the identified contourite deposits and their respective evolutionary stages with those coeval onshore in the Betic and Rifian corridors, to understand the basin evolution and eventual restriction of the Mediterranean-Atlantic gateways which led to the Messinian salinity crisis. The synthesis of the results, including a quantitative modelling of the Mediterranean-Atlantic water-mass exchange, allowed for the determination of the paleoceanographic conditions leading up to gateway restriction and its implications on Late Miocene climate.

7.2   What happened in the Gulf of Cádiz during the Late Miocene?

The upper part of the Late Miocene evolution of the continental slopes surrounding the Gulf of Cádiz, including the Southwest Iberian and Northwest Moroccan margins, spans between 8.2 Ma to 5.33 Ma (Maldonado et al., 1999), with its lower boundary consisting of the regional basal foredeep unconformity (BFU) and its upper boundary representing the Miocene-Pliocene boundary (MPB). During the Late Miocene, syn-tectonic deformation and halokinetic processes were prevalent within the Gulf of Cádiz (Duarte et al., 2020). These processes, within the context of the Betic-Rif orogeny, were responsible for the formation of parallel ridges with a NE-SW orientation, which partitioned an originally large passive margin Algarve basin into the Neogene basins.

Since the late Tortonian to the present, the sedimentary depocentres in the Gulf of Cádiz are concentrated in the Neogene basins, which consist of the Deep Algarve, Doñana, Sanlúcar, Cádiz and Offshore Gharb basin. In the Deep Algarve foredeep basin, the BFU acts as its base, following flexural subsidence due to loading of the Gibraltar Arc formed from the Betic-Rif orogeny (Ramos et al., 2017). Whereas in the Doñana, Sanlúcar, Cádiz and Offshore Gharb wedge-top basins, the base is represented by the allochthonous unit of the Gulf of Cádiz (AUGC) or the Gulf of Cádiz accretionary wedge

(GCAW) (Duarte et al., 2020). During the late Tortonian to the early Messinian, the Late Miocene contourite depositional system dominated the Gulf of Cádiz towards the West Iberian margin. Generally, the Late Miocene contourite depositional system consists of three stages (initial-, growth-, and maintenance-drift), which recorded the evolution of the bottom current circulation originating from the paleo-Mediterranean Outflow Water (MOW) exiting the Mediterranean-Atlantic gateways. The evolution of the Late Miocene contourite depositional system through the distinct stages represented the transition from weak to vigorous bottom current flow prior to its cessation at ~6.4 Ma, which is represented by the buried-drift stage. In the Deep Algarve foredeep basin, the evolution of the Late Miocene contourite depositional system is distinct to the wedge-top basins, where contourite deposition is divided into two distinct stages (stages I and II), separated by the emplacement of the Gulf of Cádiz allochthonous unit. Contourite deposits in the earlier stage was thought to be dominantly influenced by paleo-Mediterranean Outflow Water originating from the Betic corridor, which lasted until its closure between 7.51 to 7.24 Ma, prior to the Tortonian-Messinian boundary (TMB). The latter stage began right after and lasted until ~6.4 Ma, where development of contourite drifts was controlled by the gradual increase of bottom current influence originating from the Rifian corridor.

Following restriction of paleo-Mediterranean Outflow Water through the Mediterranean-Atlantic gateways, the Gulf of Cádiz was dominated by a period of quiescence in which background hemipelagic settling were the dominant sedimentary process (between ~6.4 and 5.33 Ma). Locally in the Deep Algarve foredeep and Offshore Gharb wedge-top basins, turbiditic processes originating from the Guadalquivir and Gharb basins respectively, as well as from nearby structural highs, interrupted background sedimentation. Development of submarine channels and lobes were prominent within these basins, being most proximal to the Guadalquivir and Gharb foreland basins, which became embayment and the main source of sediment supply following uplift caused by the Betic and Rif orogeny (Iribarren et al., 2009). Abandonment of the turbidite system (~5.6-5.55 Ma?) was probably due to sea-level rise following the "Messinian Gap" event during the latest Messinian, simultaneous to the Messinian salinity crisis (Cosentino et al., 2013). The Doñana, Sanlúcar and Cádiz basins remained undisturbed and were by only affected by hemipelagic deposition throughout the middle to late Messinian, until the reconnection of the Mediterranean-Atlantic gateway through the Strait of Gibraltar and the reinstating the Mediterranean Outflow Water.

7.3   How did the Late Miocene contourite depositional system evolve?

The evolution of the Late Miocene contourite depositional system is described in Chapter 6. Conceptually, the long-term changes of the contourite depositional system consists of the initial-, growth- and maintenance-drift stages, followed by the buried-drift stage after its termination. The evolution of the distinct stages of the Late Miocene contourite depositional system is controlled by the influence of bottom current originating from the paleo-Mediterranean Outflow Water, linked to the evolution of the Mediterranean-Atlantic gateways (Figs. 7-1 and 7-2).

The initial-drift stage (~8.2-7.8 Ma) represents the onset of bottom current influence along the margin. Across the Gulf of Cádiz, including the Southwest Iberian and Northwest Moroccan margins, and towards the West Iberian margin, this stage is represented by sheeted drifts, with tabular drift geometries of transparent to low-amplitude seismic facies. Locally, such as the northern and western sub-basins of the Deep Algarve foredeep basin, plastered to separated mounded drifts and erosional features including channels and furrows can form due to increase in flow velocity after passing through structural obstacles, such as submarine water gaps and sills. The initial-drift stage is linked to the presence of weak bottom current flow during the late Tortonian with the creation of both the Betic and Rifian corridors after the formation of the Gibraltar arc (Capella et al., 2019). This coeval regional compressional event culminated in the emplacement of the imbricate wedge, or allochthonous unit of the Gulf of Cádiz, at the front of the Gibraltar arc (de Weger et al., 2020). During this period, the Betic and Rifian corridors were deep straits connecting the Mediterranean and Atlantic, with an anti-estuarine circulation consisting of a surficial Atlantic inflow and the bottom paleo-Mediterranean Outflow Water. The paleo-Mediterranean Outflow Water could also have been active prior to the formation of the Gibraltar arc, when a wider seaway connected the Atlantic and the Neotethys (Capella et al., 2019), but removed by the regional erosional event following the Betic-Rif orogeny represented by the basal foredeep unconformity, as observed in the Deep Algarve foredeep basin. Whereas the emplacement of the allochthonous unit would have deformed and incorporated the pre-Late Miocene sediments within the wedge-top basins.

The growth-drift stage (7.8-7.2 Ma) represents the development of contourite drift coeval to the transition of the paleo-Mediterranean Outflow Water from an outflow towards an overflow setting through the Betic and Rifian corridors (Capella et al., 2019).

The overflow is generated from restriction of the gateways following progressive uplifting in the Betic and Rif domain of the Gibraltar arc during the latest Tortonian (Capella et al., 2017a, de Weger et al., 2020). In the Gulf of Cádiz, this stage is represented by a temporal change in drift geometries from sheeted to mounded drifts alongside their associated contourite moats or channels, with a transition from low- to high-amplitude seismic facies capped by an unconformity. This evolution can also be observed in seismic scale within the Gharb basin and the West Iberian margin, as well as in correlatable outcrop analogues within the Saiss basin (Capella et al., 2017a; de Weger et al., 2021). In the Deep Algarve foredeep basin, there is a contrasting change in the seismic facies indicating a hemipelagic dominant environment directly after the final emplacement of the allochthonous unit at its front, which is thought to last from 7.51 to 7.25 Ma in age (Ledesma, 2000). This change is possibly related to the restriction of paleo-Mediterranean Outflow Water through the Betic corridor and its eventual closure due to the uplift and exhumation of the Betics (Krijgsman et al., 2018). Coevally, the presence of structural highs in the southern margin of the Deep Algarve foredeep basin, including the allochthonous unit of the Gulf of Cádiz, the Guadalquivir bank basement high – a remnant horst structure originating from the Mesozoic extensional phase (García et al., 2016), as well as salt walls and diapirs, would have restricted bottom currents originating from the Rifian corridor.

The maintenance-drift stage (7.2-6.4 Ma) represents the final stages of the drift evolution in an overall strengthening of the paleo-Mediterranean Outflow Water, prior to its cessation. This phase developed following the readjustment of the regional compressional tectonic regime from a thin-skinned to thick-skinned deformation for the Gibraltar Arc, and uplift around the Tortonian-Messinian boundary, related to final stages of orogenic collision (Capella et al., 2017b). The tectonic readjustment also saw sediment contributions from gravitational currents into the Gulf of Cádiz, including the Guadalquivir sands turbidite system. In the Gulf of Cádiz, the development of contourite drifts were sparsely distributed compared to the growth-drift stage but were linked to deeply erosive contourite channels or moats. The changes in channel and drift geometries in the Offshore Gharb basin suggest an enhancement of outflowing paleo-Mediterranean Outflow Water velocity due to the increasing salinity and density contrast across the gateway (Capella et al., 2019). As the accommodation in the wedge-top basins were filled with drift deposits of previous stages, dense bottom currents are able flow over structural obstacles into the Deep Algarve foredeep basin, including salt walls and diapirs, the

Guadalquivir bank basement highs, and the front of the Gulf of Cádiz allochthonous unit. At the end of this stage, continuous tectonic uplift closed the Rifian Corridor during middle Messinian (Krijgsman et al., 2018), which saw a margin-wide erosion and a hiatus towards the end of this stage, represented by the intra-Messinian unconformity (IMU). Following the termination of the paleo-Mediterranean Outflow Water and Late Miocene contourite depositional system, the Gulf of Cádiz switch to a predominantly pelagic or hemipelagic environment until the latest Messinian, coeval to the Messinian salinity crisis in the Mediterranean. This period represents the buried-drift stage with the fossilization of the Late Miocene contourite depositional system unaffected by the intra-Messinian erosional unconformity.
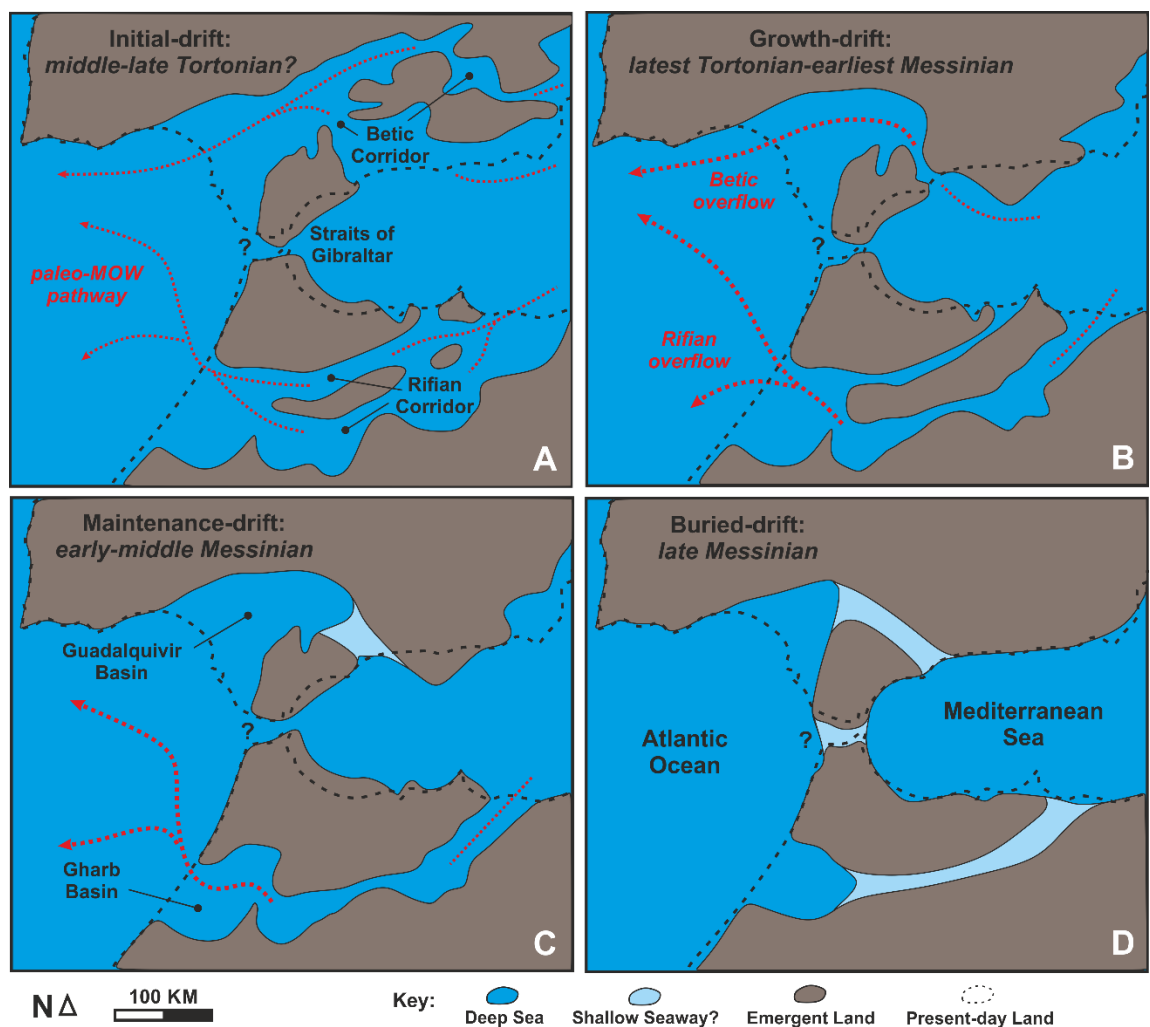
Figure 7-1 The distinct stages of the Late Miocene contourite depositional system correlated to the paleogeography of Mediterranean-Atlantic gateways: **(A)** Initial-drift stage during the middle to late Tortonian; **(B)** Growth-drift stage during the latest Tortonian to earliest Messinian; **(C)** Maintenance-drift stage during the early to middle Messinian; and **(D)** Buried-drift stage during the late Messinian (adapted from Martín et al., 2009).

7.4 How does the Late Miocene contourite depositional system compare to other systems?

The Late Miocene contourite depositional system of the Gulf of Cádiz is the predecessor of the Pliocene-Quaternary contourite depositional system, where both systems are controlled by the Mediterranean-Atlantic gateway evolution and water-mass exchange, separated by a period of restriction during the latest Miocene (Flecker et al., 2015, Krijgsman et al., 2018). In comparison, the evolution of the Pliocene-Quaternary contourite depositional system of the Gulf of Cádiz also consists of the two main stages, with a middle transitional-drift stage separating the initial- and growth-drift stages (Hernández-Molina et al., 2016), but with the absence of a buried-drift stage due to its ongoing nature of the contourite depositional system evolution. The evolution of the Pliocene-Quaternary contourite depositional system of the Gulf of Cádiz is also coeval to the Sines contourite depositional system which had developed on the southern West Iberian margin as its distal continuation. The Sines contourite depositional system is more similar in its evolution compared to the Late Miocene contourite depositional system of the Gulf of Cádiz, where both these contourite depositional systems started with an initial-drift stage of tabular drift geometries, followed by a growth-drift stage with a change towards mounded drift geometries and development of moats and channels, and ended with the maintenance-drift stage with a change in drift architecture with an absence of tectonic influence (Rodrigues et al., 2020). However, the maintenance-drift stage for the Late Miocene contourite depositional system in the Gulf of Cádiz varies from the Sines contourite depositional system in the proximal parts of the system in relation to the Rifian corridor (including the Onshore and Offshore Gharb basins, which consists of mounded drifts with deeper moat and channel development, analogous to the final growth-drift stage of the Gulf of Cádiz Pliocene-Quaternary contourite depositional system (Hernández-Molina et al., 2006; Llave et al., 2007). Also, the Late Miocene contourite depositional system has a shorter growth-drift stage (0.6 Myr) compared to the Sines contourite depositional system (1.8 Myr). This is probably due to the difference of intensity in the tectonic influence on drift evolution (Rodrigues et al., 2020) for both systems in their respective time periods, while the reconfiguration of the sill connecting the Mediterranean-Atlantic gateways would also have impacted the dynamics of the ocean circulation (de Weger et al., 2020).
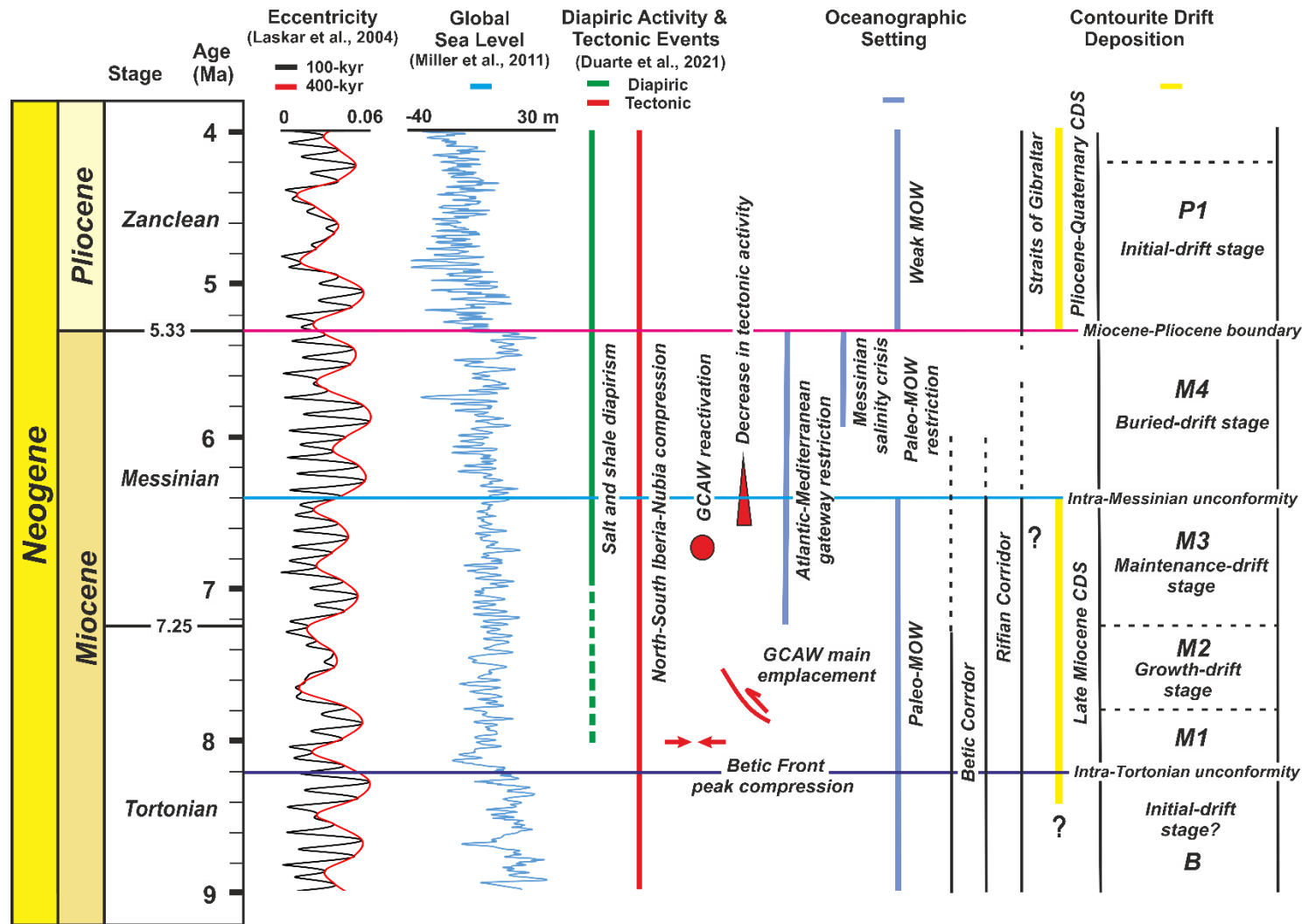
Figure 7-2 The evolution of the Late Miocene contourite depositional system correlated to the eccentricity orbital cycle (Laskar et al., 2004); global sea level (Miller et al., 2011); diapiric activity and tectonic events (Duarte et al., 2021); and oceanographic changes during the late Tortonian to late Messinian.

In other margins, development of contourite depositional systems also varies slightly in its long-tern evolutionary stages. These contourite depositional systems mainly consists of three stages, which include the onset, drift growth and burial stages. These include examples across the world, such as the Argentine basin contourite depositional system (Hernández-Molina et al., 2009; Creaser et al., 2017; Kirby et al., 2021a, b) and Le Danois contourite depositional system in the Bay of Biscay (van Rooij et al., 2010; Liu et al., 2020). As the evolution of these contourite depositional systems occurred at longer time periods (up to >10 Myr), the growth-drift stages are normally comprised of intervals which included the development of mounded drifts prior to their burial, above the tabular sheeted drifts of the onset- or initial-drift stage. Whereas in some areas, the evolution of contourite depositional systems would also contain the same four stages with the inclusion of the maintenance-drift stage, such as the Pacific margin contourite depositional system of the Antarctica Peninsula (Rebesco et al., 2002) and the Mozambique channel contourite depositional system (Thiéblemont et al., 2020). The maintenance-drift nomenclature is not well defined but were generally used where a change in drift development had occurred albeit with continuing growth (Thiéblemont et al., 2020). The maintenance-drift stage has been applied for periods with a weakening of tectonic influence or a reduction of water-mass circulation following the growth-drift stage, (Thiéblemont et al., 2020; Rodrigues et al., 2020). Albeit, apart from the subtle differences between the example defined in the literature, all these contourite depositional systems consists of a long-term trend of bottom current variation from weak to vigorous flows, prior to their burial by hemipelagic deposits.

Therefore, the late phase of the Late Miocene contourite depositional system evolution of the Gulf of Cádiz could have incorporated both the growth-drift and maintenance-drift stages respectively in the proximal and distal parts. In the Onshore and Offshore Gharb basins, the development of mounded drift morphologies with deep moats or channels in the third stage could have represented a continuing growth-drift stage instead of a transition to the maintenance-drift stage, similar to the Pliocene-Quaternary contourite depositional system of the Gulf of Cádiz. This is probably related to the proximity of these localities to the shallowing of the sills - Camarinal and Taza-Guercif respectively (Hernández-Molina et al., 2016; de Weger et al., 2020), and the intensification of the outflowing water-mass through the Mediterranean-Atlantic gateways in response to tectonic uplifting of the Betic-Rif orogen (Capella et al., 2019). Whereas in the southwest Iberian to southern West Iberian margin, drifts were less

developed, and their deposits were sparsely distributed. This could have occurred due to the lack of sediment supply from a reduction of tectonic influence in these distal parts from the switch from thin- to thick-skinned tectonic regime for the Betic-Rif orogen (Capella et al., 2017b; de Weger et al., 2020), similar in its effect as the maintenance-drift stage of the Sines drift (Rodrigues et al., 2020). It could also be explained by an erosional hiatus prior to the buried-drift stage.

All in all, the long-term evolution of a margin wide contourite depositional system, such as the Late Miocene contourite depositional system of the Gulf of Cádiz and their Pliocene-Quaternary counterparts, could vary spatially as well as temporally due to their various controlling factors. One such variability can be observed in the Pliocene-Quaternary contourite depositional system since the mid-Pleistocene revolution, which saw higher climatic fluctuations in its later stages of its evolution (Llave et al., 2011). In addition, accelerated cooling at the mid- to high-latitude regions during the Messinian leading to northern hemisphere glaciation resulted in approximately modern conditions, which shifted the world to a strong equator-pole temperature gradients from an equable climate (Herbert et al., 2016). This justifies the comparison between the ancient Late Miocene and modern Pliocene-Quaternary systems. This is also application to warmer conditions in the Tortonian and Pliocene before and after the Late Miocene global cooling, respectively.

7.5   What are the controlling factors for the contourite deposition?

The long-term evolution of the Late Miocene contourite depositional system is described in section 7.3, which were largely controlled by the tectonic forces, which resulted in the shallowing of the sills and final closure of adjacent oceanic gateways and corridors. The development of the contourite depositional system is coeval to a period of regional deformation for the continental margins surrounding the Gulf of Cádiz, where it exerted control on paleo-Mediterranean Outflow Water activity through either the Betic, Rifian or Gibraltar gateways, and confined bottom current pathways within the Neogene basins (Fig. 7-2). In this active margin setting, the tectonic and diapiric processes governed the accommodation of the Neogene basins, and drift distribution within the bathymetric irregularities. These bathymetric features are also able to enhance bottom currents locally (Sánchez-Leal et al., 2017; Duarte et al., 2020), leading to accumulation

of drift geometries with smaller dimensions compared to those identified in passive margins.

Overall, the Late Miocene contourite depositional system was deposited at least across a period of 1.8 Myr (>8.2-6.4 Ma), where the contourite drift evolution were also controlled by cyclicities with a 400-800 kyr period (Fig. 7-2). However, paleo-Mediterranean Outflow Water influence could have started earlier in the Middle Miocene, as proposed by Capella et al. (2019), but were not preserved due to the deformation induced by the Betic-Rif orogeny. The effect of tectonic activity is also clear for the Pliocene-Quaternary contourite depositional system in the Gulf of Cádiz, where tectonic pulses every 800-900 kyr and 2.0-2.5 Myr control drift evolution since the latest Miocene (Hernández-Molina et al., 2016). During the upper part of the Late Miocene, the changes in the dominant depositional style across the main units of the contourite depositional system stages and its termination are controlled by a 400-kyr stepwise restriction of the Mediterranean-Atlantic gateways, which is believed to be the mechanism behind their closure (Hilgen et al., 2007). This periodicity in the stratigraphic events of the region is astronomically linked to the long-term eccentricity orbital forcing superimposed on a gradual tectonic trend, which are responsible for the intermittent sediment supply to the contourite systems across the margin.

A shorter scale cyclic seismic facies trend with a base of transparent reflectors to a top with moderate-to-high amplitude parallel reflectors, capped by a continuous high-amplitude erosional surface can also be observed as the dominant depositional architecture for the contourite drifts. This trend has been previously identified for the Pliocene-Quaternary contourite depositional system (Llave et al., 2001, 2006; Hernández-Molina et al., 2016; Lofi et al., 2016). This sub-unit short-term evolution of the drifts are influenced by precession cycles modulated by the long-term eccentricity cycles, which has an impact on the control factors of drift evolution, such as eustasy, sediment supply, and bottom current activity (Fig. 7-2, Llave et al., 2001; Hernández-Molina et al., 2016). In the Pliocene-Quaternary examples of the Gulf of Cádiz, these cyclicities are also interpreted as coarsening-upward sequences linked to Mediterranean Outflow Water variability with smaller precessional to millennial scale orbital cycles (Llave et al., 2006; de Castro et al., 2020; Mestdagh et al., 2020; Sierro et al., 2020). The high-amplitude facies within the cycles are represented by coarser-grained sediments deposited during precession maxima or Greenland stadials, correlated to Mediterranean Outflow Water

enhancement as a result of aridity and increased buoyancy loss in the Mediterranean, vice versa (Sierro et al., 2020; de Castro et al., 2021a).

As the paleo-Mediterranean Outflow Water were split into two main cores analogous to the present-day setting through the Strait of Gibraltar (Hernández-Molina et al, 2016; de Weger et al., 2020), climatic-induced changes in the precessional to millennial scale could also lead to contrasting effects in the upper and lower core. Using the Pliocene-Quaternary contourite depositional system as an example, deepening of Mediterranean Outflow Water and an increasing strength towards lower core, along with decreasing strength in the upper core were observed during Heinrich stadials (Llave et al., 2006; Sierro et al., 2020). This led to the intermittent behaviour of the paleo-Mediterranean Outflow Water observed in the Late Miocene contourites of the Rifian corridor (de Weger et al., 2020). However, it is unknown how the variations between the two cores affect the evolution of the Late Miocene contourite depositional system in the Gulf of Cádiz.

7.6 How does the interaction of deep marine processes impact each other?

During the upper part of the Late Miocene, the Gulf of Cádiz was influenced by the interaction of alongslope and downslope sedimentary processes, which masked the background settling of pelagic or hemipelagic sediments. Across the continental margins, bottom currents processes originating from the paleo-Mediterranean Outflow Water dictated the depositional characteristics by reworking sediments along the slope, where they can reach velocities over 1 ms-1 (de Castro et al., 2020), as seen from examples for the Quaternary. This was evident with the identification of erosional and depositional features related to the Late Miocene contourite depositional system across the Neogene basins of the Gulf of Cádiz towards the Southwest Iberian margin. The presence of these contourite features, such as drifts, channels, furrows, etc., lasted until the cessation of the paleo-Mediterranean Outflow Water in the middle Messinian due to the stepwise restriction of the Mediterranean-Atlantic gateways. Thereafter until the end of the Miocene, hemipelagic deposition dominated the continental slopes of the Gulf of Cádiz, simultaneous to the restriction of the water-mass exchange which led to the Messinian

salinity crisis. This period of quiescence led to the deposition of the upper Messinian transparent unit across the margins.

Locally, downslope gravitational processes were more prominent, such as the Guadalquivir sands turbidite system in the Deep Algarve foredeep basin, and other turbidite and mass transport deposit systems observed along the Algarve margin, such as the West and East Algarve channels, and the paleo-Portimão, Sagres and Sao Vicente canyons, as well as within the offshore Gharb basin. The gravity flow deposits were triggered by tectonic processes related to the Betic-Rif orogeny modulated by long-term eccentricity orbital forcing, which occurred with a periodicity of roughly 400-kyr. Prior to the restriction of the paleo-Mediterranean Outflow Water, these episodic gravity flow deposits were reworked by bottom currents to produce mixed or hybrid systems (*sensu* Fonnesu et al., 2020; Fuhrmann et al., 2020), where they provided the intermittent sediment supply to support drift growth and development. The complexity of the relationship between the Mediterranean Outflow Water and gravity flow processes were underlined within recent research for the Pliocene-Quaternary (e.g., Brackenridge et al., 2013; Hernández-Molina et al., 2016; de Castro et al., 2020; 2021a; Serra et al., 2020; Mestdagh et al., 2020; Mencaroni et al., 2021). Following the closure of the Mediterranean-Atlantic gateways, turbidite depositional systems were able to develop without the influence of bottom currents, forming submarine lobes and channels within the intraslope basins.

7.7 What are the implications of the Late Miocene evolution of the contourite system?

The identification of the Late Miocene contourite depositional system provided many conceptual scientific implications, including the understanding of the bottom current depositional processes and products within tectonically active settings, as well as a notable example for the evolution of a closing oceanic gateway. Other than the theoretical aspects of contourite studies, these study outcomes also provided insights in the global or regional understanding for the upper part of the Late Miocene, such as the Tortonian to Messinian paleoceanography and paleoclimate, especially for the North Atlantic. On a more local scale, they are also relevant on the economic front, such as their applications in hydrocarbon exploration and carbon sequestration.

The description of the Late Miocene contourite depositional system provided a rare example for the recognition of ancient contourite systems within an active tectonic setting. Although they show many similarities with their passive margin counterparts (Faugères et al. 1999; Rebesco et al., 2014; Rodrigues et al., 2020), such as the development of distinct stages of a contourite depositional system (initial-, growth- and or maintenance-, and buried-drift); they also have distinct traits which are unique to tectonically active settings, such as drift distribution, dimensions, geometries, and their preservation potential. The different stages of the contourite depositional system represented the increasing density contrast between the Mediterranean and the Atlantic during the Tortonian and Messinian, due to the progressive stepwise restriction of the connection, following tectonic deformation related to the uplift of the Gibraltar Arc following the convergence of the Iberian and African plates (Duggen et al., 2003a; Civiero et al., 2020). This narrowing and subsequent closure of the Betic and Rifian corridors led to transformation of the paleo-Mediterranean Outflow Water from an outflow setting towards an overflow setting with a more saline and denser water mass (Capella et al., 2019), and eventual halting of the paleo- Mediterranean Outflow Water following partial isolation of the Mediterranean coeval to the precipitation of the Messinian salinity crisis evaporites (Flecker et al., 2015).

The evolution of the Late Miocene contourite depositional system provided insights into the oceanographic and climatic history from the Tortonian to Messinian period. The development of the Late Miocene contourite depositional system acts as an imprint of the paleo-Mediterranean Outflow Water circulation as it exits the Mediterranean through the Betic and Rifian (Martín et al., 2009; Capella et al., 2017a; de Weger et al., 2020), and flows through the Gulf of Cádiz, including the Southwest Iberian and Northwest Moroccan margins, subsequently towards the southern West Iberian margin as a distinctive water mass. While a weaker paleo-Mediterranean Outflow Water across a wide Mediterranean-Atlantic gateway might have existed during the Middle to early-Late Miocene (Capella et al., 2019), the onset of an overflow paleo-Mediterranean Outflow Water would have increased entrainment of ambient Atlantic water to form the paleo-Atlantic Mediterranean Water (AMW; Rogerson et al., 2012) and flowed towards the North Atlantic and influenced its paleoceanography. Similarly, the modern Pliocene to present-day setting of the Mediterranean Outflow Water influenced the depositional architecture of sediments along the Southwest Iberian margin (Hernández-Molina et al., 2016; Llave et al., 2020; Liu et al., 2020; Rodrigues et al., 2020), where their evolution

reflects a more saline and denser Mediterranean Outflow Water towards a more restricted setting across the Strait of Gibraltar (Hernández-Molina et al., 2016). Using modern day analogues, the Late Miocene paleo-Mediterranean Outflow Water overflow would have had a significant impact on the ocean circulation in the North Atlantic and would have helped in sustaining the formation of the North Atlantic Deep Water (NADW) (Rogerson et al., 2012) and the Atlantic Meridional Overturning Circulation (AMOC) (Rogerson et al., 2006; Ivanovic et al., 2014). These conditions would also have favoured ocean-atmospheric carbon dioxide (CO_2) decoupling by initiating an ocean pump for carbon dioxide transport, surface water cooling and carbon sequestration in the deep ocean (Capella et al., 2019), and contributed to the Late Miocene global cooling trend (Herbert et al., 2016; Capella et al., 2019), hence the northern hemisphere Messinian ice ages (van der Laan et al., 2012).

In an economic perspective, the Late Miocene contourite depositional system is also an ideal petroleum play for hydrocarbon exploration (Riaza and Martínez del Olmo, 1996; Mojonero and Martinez del Olmo, 2001; Matias et al., 2011). Petrophysical studies on sandy deposits of the Late Miocene contourite system in the Rifian corridor show exceptional petrophysical characteristics with high porosity and permeability values (de Weger et al., 2021), making them suitable candidates as petroleum reservoirs. These results were reinforced by similar studies for the coarse-grained contourite deposits in contourite channels, terraces, and at the exits of straits or gateways (Viana, 2001; Hernández-Molina et al., 2018; de Castro et al., 2021b), where these well-sorted sandy sheets can stretch out to over 1000s of km^2 in area with considerable thicknesses (Viana and Rebesco, 2007; Viana, 2008; Shanmugam, 2012). However, the extensiveness and effectiveness of these systems are not well understood for contourite systems in tectonically active margins, where sediments reworked and transported by bottom currents are restricted by structural obstacles. However, the constraints imposed on these systems could be beneficial for hydrocarbon prospectivity as these tectonic structures can act as traps for a petroleum system. In the Gulf of Cádiz, Matias et al. (2011) demonstrated the presence of trap structures produced by salt diapirism and deformation in the Algarve basin, where they also act migrating pathways for hydrocarbon sourced from the Mesozoic (Fernandes et al., 2013). On the other hand, the drift or levee part of the contourite system, which consists primarily of the fine-grained silts and muds, can serve as an effective seal in a petroleum system (Bailey et al., 2021). For the Late Miocene contourite depositional system, the presence of the upper Messinian transparent unit could

also provide a regional sealing component across the Gulf of Cádiz. Adjacent to the Gulf of Cádiz, the Guadalquivir foreland basin is a well-known petroleum province, with at least 20 biogenic gas fields in the Messinian and early Pliocene sediments (Mojonero and Martinez del Olmo, 2001). In the Deep Algarve basin, Stocker (2021) identified direct hydrocarbon indicators (DHI) for the Messinian interval, such as phase reversals, dim and bright spots, pockmarks, and gas chimneys. These were supported by the interpretations of Matias et al. (2011), which argued for the presence of fluid migration associated to halokinesis in the region through the presence of direct hydrocarbon indicators, including gas chimneys and pockmarks features, as well as seismic amplitude anomaly in the overburden of salt structures.

These systems are also viable candidates for carbon sequestration where these ancient contourite deposits are located deeper than 800 mbsf, as the carbon dioxide must be injected below this depth as a supercritical fluid (800-900 kg m-3) for safe storage and to be economically viable (Pereira et al., 2021). As the reservoir characteristics and subsurface architecture required for carbon capture and storage (CCS) strongly resemble those required for petroleum reservoirs, the Late Miocene contourite depositional system of the Gulf of Cádiz is an ideal prospect as potential carbon capture and storage reservoirs. The presence of an effective sealing and trapping mechanism of the Late Miocene contourite depositional system adds on to the suitability of the system for carbon capture and storage. Pereira et al. (2021) and Stocker (2021) discussed the risks associated to carbon capture and storage activity in the Deep Algarve basin, where ongoing tectonic activity and seismicity, borderline critical depth, and the resistance of the local community would be its most critical issue and would require further studies to understand its consequences.

7.8   How does the paleoceanographic evolution impact the existing views of the Mediterranean-Atlantic gateway exchange during the latest Miocene?

The paleoceanographic changes during the Messinian were supported by quantitative representations of the Mediterranean-Atlantic gateway exchange, as seen in Chapter 4. As the Atlantic respond to variations in gateway configuration through changes to the density and volume of the Mediterranean Outflow Water and the reconstruction of

gateway dimensions and exchange patterns (Flecker et al., 2015), their possible outcome were considered and eliminated through the hypothetico-deductive method by limiting the variables set by the results observed in the sedimentary changes of the Gulf of Cádiz during the latest Miocene. As the Late Miocene contourite depositional system acts as an imprint of the paleo-Mediterranean Outflow Water circulation, the absence of these sedimentary deposits during the middle to late Messinian would have suggested a discontinuation of the overflow and the formation of the paleo-Atlantic Mediterranean Water through the entrainment of ambient Atlantic water and restriction of the paleo-Mediterranean-Atlantic gateways.

The current understanding for the Late Miocene Mediterranean-Atlantic exchange were established mainly from observations within the Mediterranean domain or the Betic and Rifian corridors. Using box models to establish water conservation of the exchange, previous workers (Krijgsman and Meijer; 2008; Topper et al, 2011) suggested that the Mediterranean Outflow Water must have continued during the first stage of the Messinian salinity crisis to maintain the saturation state for gypsum precipitation. Whereas the base-level drawdown during the second stage of the Messinian salinity crisis would have led to the restriction of the Mediterranean Outflow Water, reducing salt export to the Atlantic which led to the deposition of halite. In both stages, Atlantic inflow would have continued to constantly supply the ions required for gypsum and halite formation. However, the qualitative findings from the sedimentary changes in the Atlantic domain, together with the quantitative assessment of the paleoceanographic exchange through the gateways, contradict the notion and indicated that the Mediterranean Outflow Water had weakened prior to the Messinian salinity crisis. This was supported by new findings in the deep basinal Mediterranean where halite precipitation occurred synchronous to the marginal gypsum deposits (Meilijson et al., 2018), thus invalidating previous assumptions that relied on limited data. Therefore, it is essential that the stratigraphic model for Messinian salinity crisis is revised to incorporate recent advances.

Nevertheless, the quantitative representations used to model the paleoceanographic conditions using the results and observations from the Gulf of Cadiz constitute a simplification of the Mediterranean-Atlantic gateway exchange system. These representation encompassed the key variables affecting the dynamics of the exchange, howbeit in a one-dimensional nature which emulates the present-day physical configuration of the water-mass exchange through the Strait of Gibraltar. One of the main assumptions for the formulation of the exchange is the two-layer system, with the

Mediterranean Outflow Water as a single component, which omits the consideration of its source water composition, consisting of both the Mediterranean Intermediate and Dense Water (MIW and MDW; Rogerson et al, 2012). Changes in their respective properties in a three-layer system would have an effect on the buoyancy flux of the Atlantic-Mediterranean exchange, especially during the latest Miocene where stratification of the Mediterranean would have led to a dense brine bottom water. In fact, Millot (2009) recognised four components that make up the Mediterranean Outer Water today, namely the Winter Intermediate Water (WIW), Levantine Intermediate Water (LIW), Tyrrhenian Dense Water (TDW) and Western Mediterranean Deep Water (WMDW), from top to bottom. Other than that, it is also not possible to completely disregard the possibility of a change in the gateway position and pathway of Mediterranean Outflow Water beyond the seismic data utilised in the evaluation. Therefore, with new information, including seismic and drilling data onshore and offshore surrounding the Gulf of Cádiz, as well as novel discoveries in the Mediterranean, more scenarios can be eliminated in order to reconstruct the actualities of the exchange during the latest Miocene.

7.9   What are the main limitations of this project?

These studies were based on a collection of seismic reflection surveys and borehole data within the Gulf of Cádiz, across the Southwest Iberian and Northwest Moroccan margins. As previously mentioned in Chapter 5, the identification of Late Miocene contourite depositional system, through their seismic facies and geometries, depended on the quality and resolution of the available seismic data. The overall resolution and quality of the seismic data relied on their line spacing and coverage, vertical and horizontal resolution, acquisition noise, and processing artefacts. In comparison, seismic stratigraphic analysis of the modern Pliocene-Quaternary contourite depositional system in the Gulf of Cádiz was carried out with the availability of a robust dataset, including high-resolution sparker-sourced seismic, high-resolution bathymetric compilation, continuous well logs and detailed core descriptions, and refined age model through bio- and cyclo-stratigraphic framework (Llave et al., 2001; 2006; Stow et al., 2013; Hernández-Molina et al. 2016). This allowed an elaborate workflow which included the correlation of erosional and depositional features on bathymetric maps and

seismic profiles, distinguishment of sedimentary trends using log and core data, and precise age assignment of sedimentary interval.

In contrast for the Late Miocene interval, only the 2D multi-channel seismic (MCS) surveys and a handful of 3D seismic volumes can be utilised for the seismic stratigraphic analysis of the Late Miocene contourite depositional system, out of the many seismic surveys available within the collection. This is due to the lack of depth penetration during acquisition (<1000 mbsl) of the high-resolution seismic data from high frequency sparker and airgun source surveys in the region to record the Tortonian and Messinian interval. On top of that, the lower frequency airgun-sourced multichannel seismic profiles have lower vertical (15 – 50 m) and horizontal (>60 m) resolution due to the increase in the Fresnel zone with depth. This also affected the processing stages of the seismic data, as inadequate processing techniques for the deeper section increased the presence of seismic artefacts. The lack of detailed description and interpretation in industry boreholes which penetrated the Tortonian and Messinian interval, but which were not primary targets, also did not help in the seismic stratigraphic analysis of the Late Miocene contourite depositional system. As the available 3D seismic volumes only cover a small area within the Gulf of Cádiz, the studies rely heavily on the 2D multi-channel seismic surveys to locate the distribution of the Tortonian and Messinian interval. The wide line-spacing (>4 km) of the survey lack accuracy in the interpretation of seismic bodies or morphologies through surface mapping. This limitation was especially significant in the analysis on the effect of deformation on sedimentary evolution, as the continuity of tectonic structures were not accurately represented within the gaps. However, the available seismic dataset still enabled for the first time the identification of the ancient contourite depositional system albeit only a more regional characterisation of the system.

On top of that, this study also relied heavily on comparative studies with modern and ancient analogues, such as the Pliocene-Quaternary Gulf of Cádiz contourite depositional system and the outcrop-based Late Miocene contourites of the Rifian corridor (Capella et al., 2017; de Weger et al., 2020), instead of sedimentary information from in-situ drilling. The available industry boreholes which penetrated the Late Miocene interval generally lacked detail description as they were not primary targets (e.g., Corvina, Imperador, Ruivo, Neptuno-1, Neptuno-2), whereas the remaining ones are sparsely distributed across the Gulf of Cádiz (Anchois-1, Deep Thon-1, Merou-1, GCB-1, GCE-1, GCMPC-1) which provided a glimpse into the sedimentary facies of the Late Miocene contourite depositional system of the Gulf of Cádiz. Therefore, it is not possible to be

conclusive in the conditions in which the Late Miocene contourite depositional system was formed and can only be suggested through comparisons with analogues. Future research in the area, such as the proposed Integrated Ocean Discovery Program - IODP 771 and IMMAGE amphibious (IODP 895 and ICDP) drilling projects, will be able to provide the necessary data essential for better understanding of the chronology, facies, and their associations, as well as changes within the sedimentary depositional systems linked to paleocirculation, paleoclimate and tectonic variations.

Chapter 8
Conclusion

8.1 Epilogue

The Late Miocene continental slope evolution in the Gulf of Cádiz, which includes the Southwest Iberian and Northwest Moroccan continental margins, consists of a deep-marine environment with the presence of pelagic/hemipelagic, contourite and turbidite depositional system, identified through the characterisation of the sedimentary and stratigraphic changes of Tortonian to Messinian interval. The contourite and turbidite deposits are primarily recognised in the Neogene basins across the middle slope of the Gulf of Cádiz. Regionally, the Late Miocene contourite depositional system was identified through documentation of depositional and erosional features related to bottom current activity in the Gulf of Cádiz. This contourite depositional system acts as clues to the Late Miocene paleoceanographic imprint of the paleo-Mediterranean Outflow Water at the exit of a closing Mediterranean-Atlantic gateway.

The occurrence of these regional contourite features is mainly limited to the period before and after the main emplacement of the accretionary wedge or allochthonous unit during the Tortonian. Based on seismic stratigraphic analysis, the Late Miocene contourite depositional system consists of four evolutionary stages throughout the Tortonian to Messinian, identified through their external morphological expressions and internal reflection configurations. They are namely the initial-drift, growth-drift, maintenance-drift, and buried-drift stages. These different stages of the contourite depositional system record the long-term evolution of the paleo-Mediterranean Outflow Water, from weak to vigorous bottom current velocity, prior to the weakening or halting of the water-mass exchange through the progressively restricting Mediterranean-Atlantic gateway during the latest Miocene. The widespread distribution of a predominantly hemipelagic unit along the continental slope in the Gulf of Cádiz following the cessation of the Late Miocene contourite depositional system also represents the sedimentary response to an absence or intermittence of the paleo-Mediterranean Outflow Water circulation, ~400 kyr preceding the Messinian salinity crisis. The cessation of the paleo-Mediterranean Outflow Water in the latest Miocene correlates to period of Atlantic Meridional Overturning Circulation weakening and North Atlantic cooling.

Overall, the Late Miocene sedimentary evolution of the Gulf of Cádiz is subjected to the influence of tectonic and orbital forcing, where tectonic pulses with a 400-kyr period dictated the large-scale morphosedimentary characteristics. In this tectonically active margin, while the paleo-Mediterranean Outflow Water water mass locally

controlled the morphology and sedimentary stacking pattern on the continental slopes across the Gulf of Cádiz, their distribution and preservation were influenced by deformation, where regional uplifting processes affects sediment erosion and accommodation. Locally, sediments within the contourite drift deposits are supplied by downslope gravitational systems, which can also produce mixed or hybrid systems.

8.2   Future Works

The work carried out within this study was based on seismic and borehole data with limited resolution, as explained in section 7.9. A variety of scientific projects were proposed for the acquisition of seismic and sedimentological data with better coverage and detail, as well as other relevant proxies, to be able to carry out refined interpretation workflow. One of these key projects are the upcoming International Ocean Discovery Program - IODP 771 and IMMAGE amphibious (IODP 895 and ICDP) (Investigating Miocene Mediterranean-Atlantic Gateway Exchange: http://immage.icdp-online.org) drilling projects.

With the availability of a more diversified and detailed dataset, further studies on the sedimentary evolution of the Late Miocene contourite depositional system will be able to unravel the paleoceanographic change during the Late Miocene and the evolution of the Gulf of Cádiz continental slope, as well as the Mediterranean-Atlantic gateway, which include:

1. The shorter-term evolution within the different stages of the Late Miocene contourite depositional system through the correlation between seismic and sedimentary facies to understand the temporal and spatial changes in a proximal versus distal setting of contourite systems relative to the exit of a strait or gateway, correlating it to the onshore analogues such as the Late Miocene Rifian corridor contourite channel system.

2. Small-scale sedimentary changes through the transition from the Late Miocene contourite depositional system to the middle to upper Messinian transparent unit to characterise the nature of the restriction of the Mediterranean-Atlantic exchange and bottom current circulation in the Gulf of Cádiz and the North Atlantic, as well as its impact on late Miocene climate.

3. Further detailed study of the Late Miocene deposits on the present-day upper slope to onshore region of the Southwest Iberian margin and the Guadalquivir basin, to identify and characterise Late Miocene contourite depositional system under the influence of paleo-Mediterranean Outflow Water originating from the Betic corridor during the Tortonian, and its gateway evolution.

4. Correlation with the tectonostratigraphic evolution, including tectonic pulsing, to understand the effect of structural features arising from tectonic deformation or diapirism on the sedimentary evolution of the Late Miocene contourite depositional system as well as other deep marine deposits, to propose diagnostic criteria for contourite deposits in tectonically active margins elsewhere.

Bibliography

Allen, J.R.L., 1985, Loose-boundary hydraulics and fluid mechanics: selected advances since 1961. Sedimentology: Recent Developments and Applied Aspects, *in* Brenchley, P.J. and Williams, P.J. eds., Sedimentology: Recent Developments and Applied Aspects, published for the Geological Society, Oxford, Blackwell Scientific Publications, p. 7–28.

Alves, T.M., Gawthorpe, R.L., Hunt, D.W., and Monteiro, J.H., 2003, Cenozoic tectono-sedimentary evolution of the western Iberian margin: Marine Geology, v. 195, p. 75–108, doi:10.1016/S0025-3227(02)00683-7.

Ambar, I., and Howe, M.R., 1979, Observations of the Mediterranean outflow—I mixing in the Mediterranean outflow: Deep Sea Research Part A. Oceanographic Research Papers, v. 26, p. 535–554, doi:10.1016/0198-0149(79)90095-5.

Ambar, I., Serra, N., Brogueira, M.J., Cabeçadas, G., Abrantes, F., Freitas, P., Gonçalves, C., and Gonzalez, N., 2002, Physical, chemical, and sedimentological aspects of the Mediterranean outflow off Iberia: Deep Sea Research Part II: Topical Studies in Oceanography, v. 49, p. 4163–4177, doi:10.1016/S0967-0645(02)00148-0.

Antunes, M.T., Bizon, G., Nascimento, A., and Pais, J., 1981, Nouvelles données sur la datation des dépôts miocènes de l'Algarve (Portugal), et l'évolution géologique regionale: Ciências da Terra (UNL), v. 6, p. 153–168.

Argus, D.F., Gordon, R.G., DeMets, C., and Stein, S., 1989, Closure of the Africa-Eurasia-North America Plate motion circuit and tectonics of the Gloria Fault: Journal of Geophysical Research, v. 94, p. 5585, doi:10.1029/JB094iB05p05585.

Bailey, W.S., McArthur, A.D., and McCaffrey, W.D., 2021, Distribution of contourite drifts on convergent margins: Examples from the Hikurangi subduction margin of New Zealand: Sedimentology, v. 68, p. 294–323, doi:10.1111/sed.12779.

Berástegui, X., Banks, C.J., Puig, C., Taberner, C., Waltham, D., and Fernàndez, M., 1998, Lateral diapiric emplacement of Triassic evaporites at the southern margin of the Guadalquivir Basin, Spain: Geological Society, London, Special Publications, v. 134, p. 49–68, doi:10.1144/GSL.SP.1998.134.01.04.

Betzler, C., Braga, J.C., Martín, J.M., Sánchez-Almazo, I.M., and Lindhorst, S., 2006, Closure of a seaway: stratigraphic record and facies (Guadix basin, Southern Spain): International Journal of Earth Sciences, v. 95, p. 903–910, doi:10.1007/s00531-006-0073-y.

Bouma, A.H., 1962, Sedimentology of some Flysch deposits; a graphic approach to facies interpretation. Amsterdam, Elsevier, 168 p.

Brackenridge, R.E., Hernández-Molina, F.J., Stow, D.A.V., and Llave, E., 2013, A Pliocene mixed contourite–turbidite system offshore the Algarve Margin, Gulf of Cadiz: Seismic response, margin evolution and reservoir implications: Marine and Petroleum Geology, v. 46, p. 36–50, doi:10.1016/j.marpetgeo.2013.05.015.

Buiter, S.J.H., 2000, Surface deformation resulting from subduction and slab detachment: PhD Thesis. Utrecht University, Utrecht, 134 p.

Buitrago, J., García, C., Cajebread-Brow, J., Jiménez, A.Y., and Martínez del Olmo, W., 2001, Contouritas: Un excelente almacén casi desconocido (Golfo de Cadiz, SO de España), *in* 1er Congreso Técnico Exploración y Producción REPSOL-YPF, Madrid, p. 24–27.

Calvert, A., Sandvol, E., Seber, D., Barazangi, M., Roecker, S., Mourabit, T., Vidal, F., Alguacil, G., and Jabour, N., 2000, Geodynamic evolution of the lithosphere and upper mantle beneath the Alboran region of the western Mediterranean: Constraints from travel time tomography: Journal of Geophysical Research: Solid Earth, v. 105, p. 10871–10898, doi:10.1029/2000JB900024.

Camerlenghi, A., Urgeles, R., and Fantoni, L., 2010, A Database on Submarine Landslides of the Mediterranean Sea, *in* Submarine Mass Movements and Their Consequences, Dordrecht, Springer Netherlands, p. 503–513, doi:10.1007/978-90-481-3071-9_41.

Capella, W. et al., 2017a, Sandy contourite drift in the late Miocene Rifian Corridor (Morocco): Reconstruction of depositional environments in a foreland-basin seaway: Sedimentary Geology, v. 355, p. 31–57, doi:10.1016/j.sedgeo.2017.04.004.

Capella, W., Barhoun, N., Flecker, R., Hilgen, F.J., Kouwenhoven, T., Matenco, L.C., Sierro, F.J., Tulbure, M.A., Yousfi, M.Z., and Krijgsman, W., 2018, Palaeogeographic evolution of the late Miocene Rifian Corridor (Morocco): Reconstructions from surface and subsurface data: Earth-Science Reviews, v. 180, p. 37–59, doi:10.1016/j.earscirev.2018.02.017.

Capella, W., Flecker, R., Hernández-Molina, F.J., Simon, D., Meijer, P.Th., Rogerson, M., Sierro, F.J., and Krijgsman, W., 2019, Mediterranean isolation preconditioning the Earth System for late Miocene climate cooling: Scientific Reports, v. 9, p. 3795, doi:10.1038/s41598-019-40208-2.

Capella, W., Matenco, L., Dmitrieva, E., Roest, W.M.J., Hessels, S., Hssain, M., Chakor-Alami, A., Sierro, F.J., and Krijgsman, W., 2017b, Thick-skinned tectonics closing the Rifian Corridor: Tectonophysics, v. 710–711, p. 249–265, doi:10.1016/j.tecto.2016.09.028.

Cherubin, L., Carton, X., Paillet, J., Morel, Y., and Serpette, A., 2000, Instability of the Mediterranean Water undercurrents southwest of Portugal: effects of baroclinicity and of topography: Oceanologica Acta, v. 23, p. 551–573, doi:10.1016/S0399-1784(00)01105-1.

Civiero, C., Custódio, S., Duarte, J.C., Mendes, V.B., and Faccenna, C., 2020, Dynamics of the Gibraltar Arc System: A Complex Interaction Between Plate Convergence, Slab Pull, and Mantle Flow: Journal of Geophysical Research: Solid Earth, v. 125, doi:10.1029/2019JB018873.

Comas, M.C., Platt, J.P., Soto, J.I., and Watts, A.B., 1999, The origin and tectonic history of the Alboran Basin: insights from Leg 161 results, *in* Proceedings of the Ocean Drilling Program, 161 Scientific Results, Ocean Drilling Program, v. 12, p. 157–164, doi:10.2973/odp.proc.sr.161.262.1999.

Corbí, H., Lancis, C., García-García, F., Pina, J.-A., Soria, J.M., Tent-Manclús, J.E., and Viseras, C., 2012, Updating the marine biostratigraphy of the Granada Basin (central Betic Cordillera). Insight for the Late Miocene palaeogeographic evolution of the Atlantic – Mediterranean seaway: Geobios, v. 45, p. 249–263, doi:10.1016/j.geobios.2011.10.006.

Cosentino, D., Buchwaldt, R., Sampalmieri, G., Iadanza, A., Cipollari, P., Schildgen, T.F., Hinnov, L.A., Ramezani, J., and Bowring, S.A., 2013, Refining the Mediterranean "Messinian gap" with high-precision U-Pb zircon geochronology, central and northern Italy: Geology, v. 41, p. 323–326, doi:10.1130/G33820.1.

Creaser, A., Hernández-Molina, F.J., Badalini, G., Thompson, P., Walker, R., Soto, M., and Conti, B., 2017, A Late Cretaceous mixed (turbidite-contourite) system along the Uruguayan Margin: Sedimentary and palaeoceanographic implications: Marine Geology, v. 390, p. 234–253, doi:10.1016/j.margeo.2017.07.004.

Criado-Aldeanueva, F., García-Lafuente, J., Vargas, J.M., Del Río, J., Vázquez, A., Reul, A., and Sánchez, A., 2006, Distribution and circulation of water masses in the Gulf of Cadiz from in situ observations: Deep Sea Research Part II: Topical Studies in Oceanography, v. 53, p. 1144–1160, doi:10.1016/j.dsr2.2006.04.012.

de Castro, S., Hernández-Molina, F.J., Rodríguez-Tovar, F.J., Llave, E., Ng, Z.L., Nishida, N., and Mena, A., 2020, Contourites and bottom current reworked sands:

Bed facies model and implications: Marine Geology,
doi:10.1016/j.margeo.2020.106267.

de Castro, S., Hernández-Molina, F.J., de Weger, W., Jiménez-Espejo, F.J., Rodríguez-
Tovar, F.J., Mena, A., Llave, E., and Sierro, F.J., 2021a, Contourite
characterization and its discrimination from other deep-water deposits in the Gulf
of Cadiz contourite depositional system: Sedimentology, v. 68, p. 987–1027,
doi:10.1111/sed.12813.

de Castro, S., Miramontes, E., Dorador, J., Jouet, G., Cattaneo, A., Rodríguez-Tovar,
F.J., and Hernández-Molina, F.J., 2021b, Siliciclastic and bioclastic contouritic
sands: Textural and geochemical characterisation: Marine and Petroleum Geology,
v. 128, p. 105002, doi:10.1016/j.marpetgeo.2021.105002.

de Weger, W., Hernández-Molina, F.J., Flecker, R., Sierro, F.J., Chiarella, D.,
Krijgsman, W., and Manar, M.A., 2020, Late Miocene contourite channel system
reveals intermittent overflow behavior: Geology, v. 48, p. 1194–1199,
doi:10.1130/G47944.1.

de Weger, W., Hernández-Molina, F.J., Miguez-Salas, O., de Castro, S., Bruno, M.,
Chiarella, D., Sierro, F.J., Blackbourn, G., and Manar, M.A., 2021, Contourite
depositional system after the exit of a strait: Case study from the late Miocene
South Rifian Corridor, Morocco: Sedimentology, v. 68, p. 2996–3032,
doi:10.1111/sed.12882.

Dewey, J.F., Helman, M.L., Knott, S.D., Turco, E., and Hutton, D.H.W., 1989,
Kinematics of the western Mediterranean: Geological Society, London, Special
Publications, v. 45, p. 265–283, doi:10.1144/GSL.SP.1989.045.01.15.

Dott, R.H., Jr., 1963, Dynamics of Subaqueous Gravity Depositional Processes: AAPG
Bulletin, v. 47, doi:10.1306/BC743973-16BE-11D7-8645000102C1865D.

Duarte, D., Roque, C., Hernández-Molina, F.J., Ng, Z.L., Magalhães, V.H., Llave, E.,
and Sierro, F.J., 2020, Tectonic domains of the Betic Foreland System, SW Iberian
Margin: Implications for the Gulf of Cadiz Contourite System, *in* EGU General
Assembly 2020, Vienna.

Duarte, D. et al., 2021, Salt-sediment interaction during the Late Miocene-Quaternary
evolution of the SW Iberian margin, Betics foreland. Manuscript in preparation.

Duarte, J.C., Rosas, F.M., Terrinha, P., Gutscher, M.-A., Malavieille, J., Silva, S., and
Matias, L., 2011, Thrust–wrench interference tectonics in the Gulf of Cadiz

(Africa–Iberia plate boundary in the North-East Atlantic): Insights from analog models: Marine Geology, v. 289, p. 135–149, doi:10.1016/j.margeo.2011.09.014.

Ducassou, E., Fournier, L., Sierro, F.J., Alvarez Zarikian, C.A., Lofi, J., Flores, J.A., and Roque, C., 2016, Origin of the large Pliocene and Pleistocene debris flows on the Algarve margin: Marine Geology, v. 377, p. 58–76, doi:10.1016/j.margeo.2015.08.018.

Duggen, S., Hoernle, K., van den Bogaard, P., Rüpke, L., and Phipps Morgan, J., 2003, Deep roots of the Messinian salinity crisis: Nature, v. 422, p. 602–606, doi:10.1038/nature01553.

Embley, R.W., 1980, The role of mass transport in the distribution and character of deep-ocean sediments with special reference to the North Atlantic: Marine Geology, v. 38, p. 23–50, doi:10.1016/0025-3227(80)90050-X.

Esteras, M., Izquierdo, J., Sandoval, N.G., and Bahmad, A., 2000, Evolución morfológica y estratigráfica Plio-Cuaternaria del Umbral de Camarinal (Estrecho de Gibraltar) basada en sondeos marinos: Revista de la Sociedad Geológica de España, v. 13, p. 539–550.

Expedition 339 Scientists, 2013. Expedition 339 summary. In Stow, D.A.V., Hernández-Molina, F.J., Alvarez Zarikian, C.A., and the Expedition 339 Scientists, Proc. IODP, 339: Tokyo (Integrated Ocean Drilling Program Management International, Inc.). doi:10.2204/iodp.proc.339.101.2013

Faugères, J.-C., Gonthier, E., and Stow, D.A. v., 1984, Contourite drift molded by deep Mediterranean outflow: Geology, v. 12, p. 296, doi:10.1130/0091-7613(1984)12<296:CDMBDM>2.0.CO;2.

Faugères, J.-C., and Stow, D.A.V., 2008, Contourite Drifts: Nature, Evolution and Controls, *in* Rebesco, M. and Camerlenghi, A. eds., Developments in Sedimentology, Elsevier, v. 60, p. 257–288, doi:10.1016/S0070-4571(08)10014-0.

Faugères, J.-C., Stow, D.A.V., Imbert, P., and Viana, A., 1999, Seismic features diagnostic of contourite drifts: Marine Geology, v. 162, p. 1–38, doi:10.1016/S0025-3227(99)00068-7.

Fernandes, P., Rodrigues, B., Borges, M., Matos, V., and Clayton, G., 2013, Organic maturation of the Algarve Basin (southern Portugal) and its bearing on thermal history and hydrocarbon exploration: Marine and Petroleum Geology, v. 46, p. 210–233, doi:10.1016/j.marpetgeo.2013.06.015.

Fernández-Ibáñez, F., Soto, J.I., Zoback, M.D., and Morales, J., 2007, Present-day stress field in the Gibraltar Arc (western Mediterranean): Journal of Geophysical Research, v. 112, p. B08404, doi:10.1029/2006JB004683.

Flecker, R. et al., 2015, Evolution of the Late Miocene Mediterranean–Atlantic gateways and their impact on regional and global environmental change: Earth-Science Reviews, v. 150, p. 365–392, doi:10.1016/j.earscirev.2015.08.007.

Flinch, J.F., and Vail, P.R., 1998, Plio-Pleistocene Sequence Stratigraphy and Tectonics of the Gibraltar Arc, *in* de Graciansky, P.-C., Hardenbol, J., Jacquin, T., and Vail, P.R. eds., Mesozoic and Cenozoic Sequence Stratigraphy of European Basins, SEPM (Society for Sedimentary Geology), v. 60, p. 199–208, doi:10.2110/pec.98.02.0199.

Fonnesu, M., Palermo, D., Galbiati, M., Marchesini, M., Bonamini, E., and Bendias, D., 2020, A new world-class deep-water play-type, deposited by the syndepositional interaction of turbidity flows and bottom currents: The giant Eocene Coral Field in northern Mozambique: Marine and Petroleum Geology, v. 111, p. 179–201, doi:10.1016/j.marpetgeo.2019.07.047.

Fuhrmann, A., Kane, I.A., Clare, M.A., Ferguson, R.A., Schomacker, E., Bonamini, E., and Contreras, F.A., 2020, Hybrid turbidite-drift channel complexes: An integrated multiscale model: Geology, v. 48, p. 562–568, doi:10.1130/G47179.1.

Gamberi, F., Rovere, M., Marani, M.P., and Dykstra, M., 2015, Modern submarine canyon feeder-system and deep-sea fan growth in a tectonically active margin (northern Sicily): Geosphere, v. 11, p. 307–319, doi:10.1130/GES01030.1.

Gamberi, F., Rovere, M., Mercorella, A., and Leidi, E., 2014, The Influence of a Lateral Slope on Turbidite Lobe Development on A Modern Deep-Sea Slope Fan (Villafranca Deep-Sea Fan, Tyrrhenian Sea): Journal of Sedimentary Research, v. 84, p. 475–486, doi:10.2110/jsr.2014.37.

Garcés, M., Krijgsman, W., and Agusti, J., 2001, Chronostratigraphic framework and evolution of the Fortuna basin (Eastern Betics) since the Late Miocene: Basin Research, v. 13, p. 199–216, doi:10.1046/j.1365-2117.2001.00144.x.

García, M., 2002, Caracterización morfológica del sistema de canales y valles submarinos del talud medio del Golfo de Cádiz (SO de la Península Ibérica): Implicaciones oceanograficas. PhD Thesis. Universidad de Cádiz, Cádiz, 114 p.

García, M., Hernández-Molina, F.J., Alonso, B., Vázquez, J.T., Ercilla, G., Llave, E., and Casas, D., 2016, Erosive sub-circular depressions on the Guadalquivir Bank

(Gulf of Cadiz): Interaction between bottom current, mass-wasting, and tectonic processes: Marine Geology, v. 378, p. 5–19, doi:10.1016/j.margeo.2015.10.004.

Garcia-Castellanos, D., Estrada, F., Jiménez-Munt, I., Gorini, C., Fernàndez, M., Vergés, J., and De Vicente, R., 2009, Catastrophic flood of the Mediterranean after the Messinian salinity crisis: Nature, v. 462, p. 778–781, doi:10.1038/nature08555.

Garcia-Castellanos, D., and Villaseñor, A., 2011, Messinian salinity crisis regulated by competing tectonics and erosion at the Gibraltar arc: Nature, v. 480, p. 359–363, doi:10.1038/nature10651.

Garcia-Garcia, F., Soria, J.M., Viseras, C., and Fernandez, J., 2009, High-Frequency Rhythmicity in a Mixed Siliciclastic-Carbonate Shelf (Late Miocene, Guadix Basin, Spain): A Model of Interplay Between Climatic Oscillations, Subsidence, and Sediment Dispersal: Journal of Sedimentary Research, v. 79, p. 302–315, doi:10.2110/jsr.2009.028.

Garziglia, S., Migeon, S., Ducassou, E., Loncke, L., and Mascle, J., 2008, Mass-transport deposits on the Rosetta province (NW Nile deep-sea turbidite system, Egyptian margin): Characteristics, distribution, and potential causal processes: Marine Geology, v. 250, p. 180–198, doi:10.1016/j.margeo.2008.01.016.

Gong, C., Wang, Y., Hodgson, D.M., Zhu, W., Li, W., Xu, Q., and Li, D., 2014, Origin and anatomy of two different types of mass–transport complexes: A 3D seismic case study from the northern South China Sea margin: Marine and Petroleum Geology, v. 54, p. 198–215, doi:10.1016/j.marpetgeo.2014.03.006.

Gong, C., Wang, Y., Rebesco, M., Salon, S., and Steel, R.J., 2018, How do turbidity flows interact with contour currents in unidirectionally migrating deep-water channels? Geology, v. 46, p. 551–554, doi:10.1130/G40204.1.

Gong, C., Wang, Y., Zhu, W., Li, W., and Xu, Q., 2013, Upper Miocene to Quaternary unidirectionally migrating deep-water channels in the Pearl River Mouth Basin, northern South China Sea: AAPG Bulletin, v. 97, p. 285–308, doi:10.1306/07121211159.

Gonthier, E.G., Faugères, J.-C., and Stow, D.A. v., 1984, Contourite facies of the Faro Drift, Gulf of Cadiz: Geological Society, London, Special Publications, v. 15, p. 275–292, doi:10.1144/GSL.SP.1984.015.01.18.

González, A., Córdoba, D., Vegas, R., and Matias, L.M., 1998, Seismic crustal structure in the southwest of the Iberian Peninsula and the Gulf of Cadiz: Tectonophysics, v. 296, p. 317–331, doi:10.1016/S0040-1951(98)00151-6.

Gràcia, E., Dañobeitia, J., Vergés, J., Bartolomé, R., and Córdoba, D., 2003, Crustal architecture and tectonic evolution of the Gulf of Cadiz (SW Iberian margin) at the convergence of the Eurasian and African plates: Tectonics, v. 22, p. n/a-n/a, doi:10.1029/2001TC901045.

Gutscher, M.-A., Malod, J., Rehault, J.-P., Contrucci, I., Klingelhoefer, F., Mendes-Victor, L., and Spakman, W., 2002, Evidence for active subduction beneath Gibraltar: Geology, v. 30, p. 1071, doi:10.1130/0091-7613(2002)030<1071:EFASBG>2.0.CO;2.

Hamon, N., Sepulchre, P., Lefebvre, V., and Ramstein, G., 2013, The role of eastern Tethys seaway closure in the Middle Miocene Climatic Transition (ca. 14 Ma): Climate of the Past, v. 9, p. 2687–2702, doi:10.5194/cp-9-2687-2013.

Haughton, P., Davis, C., McCaffrey, W., and Barker, S., 2009, Hybrid sediment gravity flow deposits – Classification, origin, and significance: Marine and Petroleum Geology, v. 26, p. 1900–1918, doi:10.1016/j.marpetgeo.2009.02.012.

Herbert, T.D., Lawrence, K.T., Tzanova, A., Peterson, L.C., Caballero-Gill, R., and Kelly, C.S., 2016, Late Miocene global cooling and the rise of modern ecosystems: Nature Geoscience, v. 9, p. 843–847, doi:10.1038/ngeo2813.

Hernández-Molina, F.J. et al., 2014, Contourite processes associated with the Mediterranean Outflow Water after its exit from the Strait of Gibraltar: Global and conceptual implications: Geology, v. 42, p. 227–230, doi:10.1130/G35083.1.

Hernández-Molina, F.J. et al., 2016, Evolution of the gulf of Cadiz margin and southwest Portugal contourite depositional system: Tectonic, sedimentary and paleoceanographic implications from IODP expedition 339: Marine Geology, v. 377, p. 7–39, doi:10.1016/j.margeo.2015.09.013.

Hernández-Molina, F.J. et al., 2018, Large bedforms on contourite terraces: Sedimentary and conceptual implications: Geology, v. 46, p. 27–30, doi:10.1130/G39655.1.

Hernández-Molina, J. et al., 2003, Looking for clues to paleoceanographic imprints: A diagnosis of the Gulf of Cadiz contourite depositional systems: Geology, v. 31, p. 19, doi:10.1130/0091-7613(2003)031<0019:LFCTPI>2.0.CO;2.

Hernandez-Molina, F.J. et al., 2014, Onset of Mediterranean outflow into the North Atlantic: Science, v. 344, p. 1244–1250, doi:10.1126/science.1251306.

Hernández-Molina, F.J. et al., 2006, The contourite depositional system of the Gulf of Cádiz: A sedimentary model related to the bottom current activity of the

Mediterranean outflow water and its interaction with the continental margin: Deep Sea Research Part II: Topical Studies in Oceanography, v. 53, p. 1420–1463, doi:10.1016/j.dsr2.2006.04.016.

Hernández-Molina, F.J., Llave, E., and Stow, D.A.V., 2008, Continental Slope Contourites, *in* Rebesco, M. and Camerlenghi, A. eds., Contourites. Developments in Sedimentology, Elsevier, v. 60, p. 379–408, doi:10.1016/S0070-4571(08)10019-X.

Hernández-Molina, F.J., Paterlini, M., Violante, R., Marshall, P., de Isasi, M., Somoza, L., and Rebesco, M., 2009, Contourite depositional system on the Argentine Slope: An exceptional record of the influence of Antarctic water masses: Geology, v. 37, p. 507–510, doi:10.1130/G25578A.1.

Hernández-Molina, F.J., Stow, D., and Alvarez-Zarikian, C., 2013, IODP Expedition 339 in the Gulf of Cadiz and off West Iberia: decoding the environmental significance of the Mediterranean outflow water and its global influence: Scientific Drilling, v. 16, p. 1–11, doi:10.5194/sd-16-1-2013.

Hilgen, F., Kuiper, K., Krijgsman, W., Snel, E., and van der Laan, E., 2007, Astronomical tuning as the basis for high resolution chronostratigraphy: the intricate history of the Messinian Salinity Crisis: Stratigraphy, v. 4, p. 231–238.

Hodell, D.A., Benson, R.H., Kent, D. V, Boersma, A., and Rakic-El Bied, K., 1994, Magnetostratigraphic, biostratigraphic, and stable isotope stratigraphy of an Upper Miocene drill core from the Salé Briqueterie (northwestern Morocco): A high-resolution chronology for the Messinian stage: Paleoceanography, v. 9, p. 835–855, doi:10.1029/94PA01838.

Hollister, C.D., 1967, Sediment distribution and deep circulation in the western North Atlantic. PhD Thesis, Columbia University, New York, 467 p.

Hsü, K.J., Ryan, W.B.F., and Cita, M.B., 1973, Late Miocene Desiccation of the Mediterranean: Nature, v. 242, p. 240–244, doi:10.1038/242240a0.

Hüneke, H., and Stow, D.A.V., 2008, Identification of Ancient Contourites: Problems and Palaeoceanographic Significance, *in* Rebesco, M. and Camerlenghi, A. eds., Contourites. Developments in Sedimentology, Elsevier, v. 60, p. 323–344, doi:10.1016/S0070-4571(08)10017-6.

Hüsing, S.K., Oms, O., Agustí, J., Garcés, M., Kouwenhoven, T.J., Krijgsman, W., and Zachariasse, W.-J., 2010, On the late Miocene closure of the Mediterranean–Atlantic gateway through the Guadix basin (southern Spain): Palaeogeography,

Palaeoclimatology, Palaeoecology, v. 291, p. 167–179, doi:10.1016/j.palaeo.2010.02.005.

Hüsing, S.K., Zachariasse, W.-J., van Hinsbergen, D.J.J., Krijgsman, W., Inceöz, M., Harzhauser, M., Mandic, O., and Kroh, A., 2009, Oligocene–Miocene basin evolution in SE Anatolia, Turkey: constraints on the closure of the eastern Tethys gateway: Geological Society, London, Special Publications, v. 311, p. 107–132, doi:10.1144/SP311.4.

Iribarren, L., Vergés, J., Camurri, F., Fullea, J., and Fernàndez, M., 2007, The structure of the Atlantic–Mediterranean transition zone from the Alboran Sea to the Horseshoe Abyssal Plain (Iberia–Africa plate boundary): Marine Geology, v. 243, p. 97–119, doi:10.1016/j.margeo.2007.05.011.

Iribarren, L., Vergés, J., and Fernàndez, M., 2009, Sediment supply from the Betic–Rif orogen to basins through Neogene: Tectonophysics, v. 475, p. 68–84, doi:10.1016/j.tecto.2008.11.029.

Ivanovic, R.F., Valdes, P.J., Flecker, R., and Gutjahr, M., 2014, Modelling global-scale climate impacts of the late Miocene Messinian Salinity Crisis: Climate of the Past, v. 10, p. 607–622, doi:10.5194/cp-10-607-2014.

Jackson, C.A.-L., Kane, K.E., 2000, 3D Seismic Interpretation Techniques: Applications to Basin Analysis, *in* Busby, C. and Azor, A. eds., Tectonics of Sedimentary Basins: Recent Advances, Blackwell, p.95-110, doi:10.1002/9781444347166.ch5

Jackson, C.A.-L., Zakaria, A.A., Johnson, H.D., Tongkul, F., and Crevello, P.D., 2009, Sedimentology, stratigraphic occurrence, and origin of linked debrites in the West Crocker Formation (Oligo-Miocene), Sabah, NW Borneo: Marine and Petroleum Geology, v. 26, p. 1957–1973, doi:10.1016/j.marpetgeo.2009.02.019.

Jiménez-Bonilla, A., Expósito, I., Balanyá, J.C., Díaz-Azpiroz, M., and Barcos, L., 2015, The role of strain partitioning on intermontane basin inception and isolation, External Western Gibraltar Arc: Journal of Geodynamics, v. 92, p. 1–17, doi:10.1016/j.jog.2015.09.001.

Kenyon, N.H., and Belderson, R.H., 1973, Bed forms of the Mediterranean undercurrent observed with side-scan sonar: Sedimentary Geology, v. 9, p. 77–99, doi:10.1016/0037-0738(73)90027-4.

Kenyon, N.H., Klaucke, I., Millington, J., and Ivanov, M.K., 2002, Sandy submarine canyon-mouth lobes on the western margin of Corsica and Sardinia, Mediterranean Sea: Marine Geology, v. 184, p. 69–84, doi:10.1016/S0025-3227(01)00282-1.

Kirby, A., Hernández-Molina, F.J., and Rodrigues, S., 2021a, Lateral migration of large sedimentary bodies in a deep-marine system offshore of Argentina: Scientific Reports, v. 11, p. 20291, doi:10.1038/s41598-021-99730-x.

Kirby, A., Hernández-Molina, F.J., Rodriguez, P., and Conti, B., 2021b, Sedimentary stacking pattern of plastered drifts: An example from the Cenozoic on the Uruguayan continental slope: Marine Geology, v. 440, p. 106567, doi:10.1016/j.margeo.2021.106567.

Krijgsman, W. et al., 2018, The Gibraltar Corridor: Watergate of the Messinian Salinity Crisis: Marine Geology, v. 403, p. 238–246, doi:10.1016/j.margeo.2018.06.008.

Krijgsman, W., Garcés, M., J., A., Raffi, I., Taberner, C., and Zachariasse, W.J., 2000, The "Tortonian salinity crisis" of the eastern Betics (Spain): Earth and Planetary Science Letters, v. 181, p. 497–511, doi:10.1016/S0012-821X(00)00224-7.

Krijgsman, W., Hilgen, F.J., Raffi, I., Sierro, F.J., and Wilson, D.S., 1999, Chronology, causes and progression of the Messinian salinity crisis: Nature, v. 400, p. 652–655, doi:10.1038/23231.

Krijgsman, W., Leewis, M.E., Garcés, M., Kouwenhoven, T.J., Kuiper, K.F., and Sierro, F.J., 2006, Tectonic control for evaporite formation in the Eastern Betics (Tortonian; Spain): Sedimentary Geology, v. 188–189, p. 155–170, doi:10.1016/j.sedgeo.2006.03.003.

Krijgsman, W., and Meijer, P.Th., 2008, Depositional environments of the Mediterranean "Lower Evaporites" of the Messinian salinity crisis: Constraints from quantitative analyses: Marine Geology, v. 253, p. 73–81, doi:10.1016/j.margeo.2008.04.010.

Kuenen, Ph.H., 1937, Experiments in connection with Daly's hypothesis on the formation of submarine canyons: Leidse Geologische Mededelingen, v. 8, p. 327–351.

Kuenen, Ph.H., and Migliorini, C.I., 1950, Turbidity Currents as a Cause of Graded Bedding: The Journal of Geology, v. 58, p. 91–127, doi:10.1086/625710.

Laskar, J., Robutel, P., Joutel, F., Gastineau, M, Correia, A. C. M., and Levrard., B., 2004, A long-term numerical solution for the insolation quantities of the Earth: Astronomy and Astrophysics, v. 428, p. 261-285, doi:10.1051/0004-6361:20041335.

Ledesma, S., 2000, Astrobiocronología y estratigrafía de alta resolución del Neógeno de la Cuenca del Guadalquivir-Golfo De Cádiz. PhD Thesis. Universidad de Salamanca, Salamanca. 464 pp.

Liu, S., Hernández-Molina, F.J., Ercilla, G., and van Rooij, D., 2020, Sedimentary evolution of the Le Danois contourite drift systems (southern Bay of Biscay, NE Atlantic): A reconstruction of the Atlantic Mediterranean Water circulation since the Pliocene: Marine Geology, v. 427, p. 106217, doi:10.1016/j.margeo.2020.106217.

Liu, J.-Y., and Watkins, J.S., 1992, Seismic Facies and Depositional Processes on the Lower Continental Slope, in the Mississippi Canyon Area, Gulf of Mexico: Gulf Coast Association of Geological Societies Transactions, v. 42, p. 831.

Llave, E., 2004, Análisis morfosedimentario y estratigráfico de los depositos contorníticos del Golfo de Cádiz: implicaciones pleaoceanográficas. PhD Thesis. Universidad de Cádiz, Cádiz, 294 p.

Llave, E. et al., 2020, Contourites along the Iberian continental margins: conceptual and economic implications: Geological Society, London, Special Publications, v. 476, p. 403–436, doi:10.1144/SP476-2017-46.

Llave, E., Hernández-Molina, F.J., Somoza, L., Díaz-del-Río, V., Stow, D.A.V., Maestro, A., and Alveirinho Dias, J.M., 2001, Seismic stacking pattern of the Faro-Albufeira contourite system (Gulf of Cadiz): A Quaternary record of paleoceanographic and tectonic influences: Marine Geophysical Researches, v. 22, p. 487–508, doi:10.1023/1016355801344.

Llave, E., Hernández-Molina, F.J., Stow, D.A. v., Fernández-Puga, M.C., García, M., Vázquez, J.T., Maestro, A., Somoza, L., and Díaz del Río, V., 2007, Reconstructions of the Mediterranean Outflow Water during the quaternary based on the study of changes in buried mounded drift stacking pattern in the Gulf of Cadiz: Marine Geophysical Researches, v. 28, p. 379–394, doi:10.1007/s11001-007-9040-7.

Llave, E., Matias, H., Hernández-Molina, F.J., Ercilla, G., Stow, D.A.V., and Medialdea, T., 2011, Pliocene–Quaternary contourites along the northern Gulf of Cadiz margin: sedimentary stacking pattern and regional distribution: Geo-Marine Letters, v. 31, p. 377–390, doi:10.1007/s00367-011-0241-3.

Llave, E., Schönfeld, J., Hernández-Molina, F.J., Mulder, T., Somoza, L., Díaz del Río, V., and Sánchez-Almazo, I., 2006, High-resolution stratigraphy of the

Mediterranean outflow contourite system in the Gulf of Cadiz during the late
Pleistocene: The impact of Heinrich events: Marine Geology, v. 227, p. 241–262,
doi:10.1016/j.margeo.2005.11.015.

Lofi, J. et al., 2016, Quaternary chronostratigraphic framework and sedimentary
processes for the Gulf of Cadiz and Portuguese Contourite Depositional Systems
derived from Natural Gamma Ray records: Marine Geology, v. 377, p. 40–57,
doi:10.1016/j.margeo.2015.12.005.

Lonergan, L., and White, N., 1997, Origin of the Betic-Rif Mountain belt: Tectonics, v.
16, p. 504–522, doi:10.1029/96TC03937.

Lopes, F.C., Cunha, P.P., and Le Gall, B., 2006, Cenozoic seismic stratigraphy and
tectonic evolution of the Algarve margin (offshore Portugal, southwestern Iberian
Peninsula): Marine Geology, v. 231, p. 1–36, doi:10.1016/j.margeo.2006.05.007.

Louarn, E., and Morin, P., 2011, Antarctic Intermediate Water influence on
Mediterranean Sea Water outflow: Deep-Sea Research Part I: Oceanographic
Research Papers, v. 58, p. 932–942, doi:10.1016/j.dsr.2011.05.009.

Lowe, D.R., 1982, Sediment Gravity Flows: II Depositional Models with Special
Reference to the Deposits of High-Density Turbidity Currents: SEPM Journal of
Sedimentary Research, v. Vol. 52, doi:10.1306/212F7F31-2B24-11D7-
8648000102C1865D.

Lugli, S., Manzi, V., Roveri, M., and Schreiber, B.C., 2015, The deep record of the
Messinian salinity crisis: Evidence of a non-desiccated Mediterranean Sea:
Palaeogeography, Palaeoclimatology, Palaeoecology, v. 433, p. 201–218,
doi:10.1016/j.palaeo.2015.05.017.

Madelain, F., 1970, Influence de la topographie de fond sur l'ecoulement mediterraneen
entre le detroit de Gibraltar et le cap Saint Vincent: Cahiers Oceanographiques, v.
22, p. 43–61.

Maestro, A., Somoza, L., Medialdea, T., Talbot, C.J., Lowrie, A., Vazquez, J.T., and
Diaz-del-Rio, V., 2003, Large-scale slope failure involving Triassic and Middle
Miocene salt and shale in the Gulf of Cadiz (Atlantic Iberian Margin): Terra Nova,
v. 15, p. 380–391, doi:10.1046/j.1365-3121.2003.00513.x.

Maldonado, A., Somoza, L., and Pallarés, L., 1999, The Betic orogen and the Iberian–
African boundary in the Gulf of Cadiz: geological evolution (central North
Atlantic): Marine Geology, v. 155, p. 9–43, doi:10.1016/S0025-3227(98)00139-X.

Marchès, E., Mulder, T., Cremer, M., Bonnel, C., Hanquiez, V., Gonthier, E., and
Lecroart, P., 2007, Contourite drift construction influenced by capture of

Mediterranean Outflow Water deep-sea current by the Portimão submarine canyon (Gulf of Cadiz, South Portugal): Marine Geology, v. 242, p. 247–260, doi:10.1016/j.margeo.2007.03.013.

Marchès, E., Mulder, T., Gonthier, E., Cremer, M., Hanquiez, V., Garlan, T., and Lecroart, P., 2010, Perched lobe formation in the Gulf of Cadiz: Interactions between gravity processes and contour currents (Algarve Margin, Southern Portugal): Sedimentary Geology, v. 229, p. 81–94, doi:10.1016/j.sedgeo.2009.03.008.

Martín, J.M., Braga, J.C., Aguirre, J., and Puga-Bernabéu, Á., 2009, History and evolution of the North-Betic Strait (Prebetic Zone, Betic Cordillera): A narrow, early Tortonian, tidal-dominated, Atlantic–Mediterranean marine passage: Sedimentary Geology, v. 216, p. 80–90, doi:10.1016/j.sedgeo.2009.01.005.

Martin, J.M., Braga, J.C., and Betzler, C., 2001, The Messinian Guadalhorce corridor: the last northern, Atlantic-Mediterranean gateway: Terra Nova, v. 13, p. 418–424, doi:10.1046/j.1365-3121.2001.00376.x.

Martín–Chivelet, J., Fregenal–Martínez, M.A., and Chacón, B., 2008, Traction Structures in Contourites, *in* Rebesco, M. and Camerlenghi, A. eds., Contourites. Developments in Sedimentology, Elsevier, v. 60, p. 157–182, doi:10.1016/S0070-4571(08)10010-3.

Martínez del Olmo, W., and Comas, M.C., 2008, Arquitectura sísmica, olistostromas y fallas extensionales en el norte de la cuenca oeste del Mar de Albrán: Revista de la Sociedad Geologica de Espana, v. 21, p. 151–167.

Matias, H., Kress, P., Terrinha, P., Mohriak, W., Menezes, P.T.L., Matias, L., Santos, F., and Sandnes, F., 2011, Salt tectonics in the western Gulf of Cadiz, southwest Iberia: AAPG Bulletin, v. 95, p. 1667–1698, doi:10.1306/01271110032.

Matte, P., 1986, Tectonics and plate tectonics model for the Variscan belt of Europe: Tectonophysics, v. 126, p. 329–374, doi:10.1016/0040-1951(86)90237-4.

McKenzie, D.P., 1969, Speculations on the Consequences and Causes of Plate Motions: Geophysical Journal International, v. 18, p. 1–32, doi:10.1111/j.1365-246X.1969.tb00259.x.

Medialdea, T., Vegas, R., Somoza, L., Vázquez, J.T., Maldonado, A., Díaz-del-Río, V., Maestro, A., Córdoba, D., and Fernández-Puga, M.C., 2004, Structure and evolution of the "Olistostrome" complex of the Gibraltar Arc in the Gulf of Cádiz

(eastern Central Atlantic): evidence from two long seismic cross-sections: Marine Geology, v. 209, p. 173–198, doi:10.1016/j.margeo.2004.05.029.

Meiburg, E., and Kneller, B., 2010, Turbidity Currents and Their Deposits: Annual Review of Fluid Mechanics, v. 42, p. 135–156, doi:10.1146/annurev-fluid-121108-145618.

Meilijson, A., Steinberg, J., Hilgen, F.J, Bialik, O.M., Waldmann, N.D., and Makovsky, Y., 2018, Deep-basin evidence resolves a 50-year-old debate and demonstrates synchronous onset of Messinian evaporite deposition in a non-desiccated Mediterranean: Geology, v. 46, p. 243–246. doi:10.1130/G39868.1.

Mencaroni, D., Urgeles, R., Camerlenghi, A., Llopart, J., Ford, J., Sanchez Serra, C., Meservy, W., Gràcia, E., Rebesco, M., and Zitellini, N., 2021, A mixed turbidite – contourite system related to a major submarine canyon: The Marquês de Pombal Drift (south-west Iberian margin): Sedimentology, v. 68, p. 2069–2096, doi:10.1111/sed.12844.

Mestdagh, T., Lobo, F.J., Llave, E., Hernández-Molina, F.J., García Ledesma, A., Puga-Bernabéu, Á., Fernández-Salas, L.-M., and Rooij, D. van, 2020, Late Quaternary multi-genetic processes and products on the northern Gulf of Cadiz upper continental slope (SW Iberian Peninsula): Marine Geology, v. 427, p. 106214, doi:10.1016/j.margeo.2020.106214.

Middleton, G.V., and Hampton M.A., 1973, Sediment gravity flows: mechanics of flow and deposition, *in* Turbidites and deep-water sedimentation, SEPM.

Migeon, S., Cattaneo, A., Hassoun, V., Larroque, C., Corradi, N., Fanucci, F., Dano, A., Mercier de Lepinay, B., Sage, F., and Gorini, C., 2011, Morphology, distribution, and origin of recent submarine landslides of the Ligurian Margin (North-western Mediterranean): some insights into geohazard assessment: Marine Geophysical Research, v. 32, p. 225–243, doi:10.1007/s11001-011-9123-3.

Migeon, S., Mulder, T., Savoye, B., and Sage, F., 2012, Hydrodynamic processes, velocity structure and stratification in natural turbidity currents: Results inferred from field data in the Var Turbidite System: Sedimentary Geology, v. 245–246, p. 48–62, doi:10.1016/j.sedgeo.2011.12.007.

Migliorini, C.I., 1943, Sul modo di formazione dei complessi tipo macigno: Bollettino della Società Geologica Italiana, v. 62, p. 48–49.

Miller, K.G., Mountain, G.S., Wright, J.D., and Browning, J.V., 2011, A 180-million-year record of sea level and ice volume variations from continental margin and

deep-sea isotopic records: Oceanography, v. 24, p. 40–53,
doi:10.5670/oceanog.2011.26.

Millot, C., 2009, Another description of the Mediterranean Sea outflow: Progress in
Oceanography, v. 82, p. 101–124, doi:10.1016/j.pocean.2009.04.016.

Mitchum, R.M., Jr., 1985, Seismic stratigraphic expression of submarine fans, *in* Berg,
O.R. and Woolverton, D.G. eds., Seismic stratigraphy II - An integrated approach.
AAPG Memoir, American Association of Petroleum Geologist, v. 39, p. 117–136.

Mitchum, R.M., Vail, P.R., and Sangree, J.B., 1977, Seismic stratigraphy and global
changes of sea level, part 6: Seismic stratigraphy interpretation of seismic
reflection patterns in depositional sequence., *in* Payton, C.E. ed., Seismic
stratigraphy – applications to hydrocarbon exploration. AAPG Memoir 26.,
Michigan, Edwards Brothers Inc., p. 117–133.

Mojonero, C.G., and Martinez del Olmo, W., 2001, One Sea Level Fall and Four
Different Gas Plays: The Gulf of Cadiz Basin, SW Spain, *in* Petroleum Systems of
Deep-Water Basins: Global and Gulf of Mexico Experience: 21st Annual, Society
of Economic Paleontologists and Mineralogists, p. 357–368,
doi:10.5724/gcs.01.21.0357.

Moscardelli, L., and Wood, L., 2008, New classification system for mass transport
complexes in offshore Trinidad: Basin Research, v. 20, p. 73–98,
doi:10.1111/j.1365-2117.2007.00340.x.

Moscardelli, L., Wood, L., and Mann, P., 2006, Mass-transport complexes and
associated processes in the offshore area of Trinidad and Venezuela: AAPG
Bulletin, v. 90, p. 1059–1088, doi:10.1306/02210605052.

Mulder, T., 2011, Gravity Processes and Deposits on Continental Slope, Rise, and
Abyssal Plains, *in* Hüneke, H. and Mulder, T. eds., Deep Sea Sediments.
Developments in Sedimentology, Amsterdam, Elsevier, v. 63, p. 25–148,
doi:10.1016/B978-0-444-53000-4.00002-0.

Mulder, T. et al., 2003, The Gulf of Cadiz: an unstable giant contouritic levee: Geo-
Marine Letters, v. 23, p. 7–18, doi:10.1007/s00367-003-0119-0.

Mulder, T., and Etienne, S., 2010, Lobes in deep-sea turbidite systems: State of the art:
Sedimentary Geology, v. 229, p. 75–80, doi:10.1016/j.sedgeo.2010.06.011.

Mulder, T., Hassan, R., Ducassou, E., Zaragosi, S., Gonthier, E., Hanquiez, V.,
Marchès, E., and Toucanne, S., 2013, Contourites in the Gulf of Cadiz: a

cautionary note on potentially ambiguous indicators of bottom current velocity: Geo-Marine Letters, v. 33, p. 357–367, doi:10.1007/s00367-013-0332-4.

Mulder, T., Migeon, S., Savoye, B., and Faugeres, J.-C., 2001, Inversely graded turbidite sequences in the deep Mediterranean: a record of deposits from flood-generated turbidity currents? Geo-Marine Letters, v. 21, p. 86–93, doi:10.1007/s003670100071.

Mutti, E., 1985, Turbidite systems and their relations to depositional sequences, *in* Zuffa, G.G. ed., Provenance of arenites. NATO-ASI Series, Dordrecht, Reidel, p. 65–93.

Mutti, E., Bernulli, D., Ricci Lucchi, F., and Tinterri, R., 2009, Turbidites and turbidity currents from Alpine 'flysch' to the exploration of continental margins: Sedimentology, v. 56, p. 267–318, doi:10.1111/j.1365-3091.2008.01019.x.

Mutti, E., and Ricci Lucchi, F., 1972, Le torbiditi dell'Appennino settentrionale: introduzione all'ananisi di facies: Memoirs Società Geologica Italiana, v. 11, p. 161–199.

Mutti, E., Tinterri, R., Remacha, E., Mavilla, N., Angella, S., and Fava, L., 1999, An introduction to the analysis of ancient turbidite basins from an outcrop perspective, *in* AAPG Continuing Education Course Note Series, Tulsa, American Association of Petroleum Geologists, v. 39.

O'Neill-Baringer, M., and Price, J. F., 1997, Mixing and spreading of the Mediterranean outflow: Journal of Physical Oceanography, v. 27, p. 1654-1677, doi:10.1175/1520-0485(1997)027<1654:MASOTM>2.0.CO;2.

O'Neill-Baringer, M., and Price, J. F., 1999, A review of the physical oceanography of the Mediterranean outflow: Marine Geology, v. 155, p. 63-82, doi:10.1016/S0025-3227(98)00141-8.

Nardin, T.R., Hein, F.J., Gorsline, D.S., and Edwards, B.D., 1979, A review of mass movement processes, sediment and acoustic characteristics and contrasts in slope and base-of-slope systems versus canyon-fan-basin-floor basins, *in* Doyle, L.J. and Pilkey, O.H. eds., Geology of Continental Slopes. SEPM Special Publication, SEPM, v. 27, p. 61–73.

Negro, F., Agard, P., Goffe, B., and Saddiqi, O., 2007, Tectonic and metamorphic evolution of the Temsamane units, External Rif (northern Morocco): implications for the evolution of the Rif and the Betic-Rif arc: Journal of the Geological Society, v. 164, p. 829–842, doi:10.1144/0016-76492006-112.

Nelson, C.H., Baraza, J., and Maldonado, A., 1993, Mediterranean undercurrent sandy contourites, Gulf of Cadiz, Spain: Sedimentary Geology, v. 82, p. 103–131, doi:10.1016/0037-0738(93)90116-M.

Nelson, C.H., Baraza, J., Maldonado, A., Rodero, J., Escutia, C., and Barber, J.H., 1999, Influence of the Atlantic inflow and Mediterranean outflow currents on late Quaternary sedimentary facies of the Gulf of Cadiz continental margin: Marine Geology, v. 155, p. 99–129, doi:10.1016/S0025-3227(98)00143-1.

Normark, W.R., 1970, Growth Patterns of Deep-Sea Fans: AAPG Bulletin, v. 54, p. 2170–2195, doi:10.1306/5D25CC79-16C1-11D7-8645000102C1865D.

Pais, J., Legoinha, P., Elderfield, H., Sousa, L., and Estevens, M., 2000, The Neogene of Algarve (Portugal): Ciências da Terra, v. 14, p. 277–288.

Palermo, D., Galbiati, M., Famiglietti, M., Marchesini, M., Mezzapesa, D., and Fonnesu, F., 2014, Insights into a New Super-Giant Gas Field - Sedimentology and Reservoir Modeling of the Coral Reservoir Complex, Offshore Northern Mozambique, *in* All Days, OTC, doi:10.4043/24907-MS.

Palomeras, I., Villaseñor, A., Thurner, S., Levander, A., Gallart, J., and Harnafi, M., 2017, Lithospheric structure of Iberia and Morocco using finite-frequency Rayleigh wave tomography from earthquakes and seismic ambient noise: Geochemistry, Geophysics, Geosystems, v. 18, p. 1824–1840, doi:10.1002/2016GC006657.

Perconig, E., 1960, Sur la constitution géologique de l'Andalousie Occidentale en particulier du Bassin du Guadalquivir (Espagne méridionale): Livre Mémoir du Professor Paul Fallot, Mémoires hors-Série de la Société géologique de France., p. 229–256.

Pereira, R., Alves, T.M., and Cartwright, J., 2011, Post-rift compression on the SW Iberian margin (eastern North Atlantic): a case for prolonged inversion in the ocean-continent transition zone: Journal of the Geological Society, v. 168, p. 1249–1263, doi:10.1144/0016-76492010-151.

Pereira, P., Ribeiro, C., and Carneiro, J., 2021, Identification and characterization of geological formations with CO_2 storage potential in Portugal: Petroleum Geoscience, v. 27, p. petgeo2020-123, doi:10.1144/petgeo2020-123.

Pérez-Asensio, J.N., Aguirre, J., Schmiedl, G., and Civis, J., 2012, Impact of restriction of the Atlantic-Mediterranean gateway on the Mediterranean Outflow Water and

eastern Atlantic circulation during the Messinian: Paleoceanography, v. 27, p. n/a-n/a, doi:10.1029/2012PA002309.

Piper, D.J.W., 1985, Turbidite muds and silts on deep sea fans and abyssal plains, *in* Stanley, D.J. and Kelling, G. eds., Submarine Canyon and Fan Sedimentation, Stroudsburgh, Dowden, Hutchinson and Ross.

Piper, D.J.W., and Savoye, B., 1993, Processes of late Quaternary turbidity current flow and deposition on the Var deep-sea fan, north-west Mediterranean Sea: Sedimentology, v. 40, p. 557–582, doi:10.1111/j.1365-3091.1993.tb01350.x.

Platt, J.P., and Vissers, R.L.M., 1989, Extensional collapse of thickened continental lithosphere: A working hypothesis for the Alboran Sea and Gibraltar arc: Geology, v. 17, p. 540, doi:10.1130/0091-7613(1989)017<0540:ECOTCL>2.3.CO;2.

Pohl, F., Eggenhuisen, J.T., Tilston, M., and Cartigny, M.J.B., 2019, New flow relaxation mechanism explains scour fields at the end of submarine channels: Nature Communications, v. 10, p. 4425, doi:10.1038/s41467-019-12389-x.

Posamentier, H.W., and Erskine, R.D., 1991, Seismic Expression and Recognition Criteria of Ancient Submarine Fans, *in* Weimar, P. and Link, M.H., eds., Seismic Facies and Sedimentary Processes of Submarine Fans and Turbidite Systems, p. 197–222, doi:10.1007/978-1-4684-8276-8_10.

Posamentier, H.W., and Martinsen, O.J., 2011, The Character and Genesis of Submarine Mass-Transport Deposits: Insights from Outcrop and 3D Seismic Data, *in* Mass-Transport Deposits in Deepwater Settings, SEPM (Society for Sedimentary Geology), p. 7–38, doi:10.2110/sepmsp.096.007.

Postma, G., and Cartigny, M.J.B., 2014, Supercritical and subcritical turbidity currents and their deposits--A synthesis: Geology, v. 42, p. 987–990, doi:10.1130/G35957.1.

Prather, B.E., Booth, J.R., Steffens, G.S., and Craig, P.A., 1998, Classification, lithologic calibration, and stratigraphic succession of seismic facies from intraslope basins, deep water Gulf of Mexico, U.S.A: AAPG Bulletin , v. 82, p. 701–728.

Ramos, A., Fernández, O., Terrinha, P., and Muñoz, J.A., 2016, Extension and inversion structures in the Tethys–Atlantic linkage zone, Algarve Basin, Portugal: International Journal of Earth Sciences, v. 105, p. 1663–1679, doi:10.1007/s00531-015-1280-1.

Ramos, A., Fernández, O., Terrinha, P., and Muñoz, J.A., 2017, Neogene to recent contraction and basin inversion along the Nubia-Iberia boundary in SW Iberia: Tectonics, v. 36, p. 257–286, doi:10.1002/2016TC004262.

Rebesco, M., Camerlenghi, A., and Van Loon, A.J., 2008, Contourite Research: A Field in Full Development, *in* Rebesco, M. and Camerlenghi, A. eds., Contourites. Developments in Sedimentology, Elsevier, v. 60, p. 1–10, doi:10.1016/S0070-4571(08)10001-2.

Rebesco, M., Hernández-Molina, F.J., Van Rooij, D., and Wåhlin, A., 2014, Contourites and associated sediments controlled by deep-water circulation processes: State-of-the-art and future considerations: Marine Geology, v. 352, p. 111–154, doi:10.1016/j.margeo.2014.03.011.

Rebesco, M., Pudsey, C.J., Canals, M., Camerlenghi, A., Barker, P.F., Estrada, F., and Giorgetti, A., 2002, Sediment drifts and deep-sea channel systems, Antarctic Peninsula Pacific Margin: Geological Society, London, Memoirs, v. 22, p. 353–371, doi:10.1144/GSL.MEM.2002.022.01.25.

Riaza, C., and Martínez del Olmo, W., 1996, Depositional model of the Guadalquivir – Gulf of Cadiz Tertiary basin, *in* Friend, P.F. and Dabrio, C.J. eds., Tertiary basins of Spain: The Stratigraphic Record of Crustal Kinematics, Cambridge, Cambridge University Press, p. 330–338, doi:10.1017/CBO9780511524851.047.

Rodero, J., Pallarés, L., and Maldonado, A., 1999, Late Quaternary seismic facies of the Gulf of Cadiz Spanish margin: depositional processes influenced by sea-level change and tectonic controls: Marine Geology, v. 155, p. 131–156, doi:10.1016/S0025-3227(98)00144-3.

Rodrigues, S., 2021, Sedimentary model for mixed depositional systems: Conceptual and economic implications. PhD Thesis. Royal Holloway University of London, Egham.

Rodrigues, S., Roque, C., Hernández-Molina, F.J., Llave, E., and Terrinha, P., 2020, The sines contourite depositional system along the SW Portuguese margin: Onset, evolution, and conceptual implications: Marine Geology, v. 430, p. 106357, doi:10.1016/j.margeo.2020.106357.

Rogerson, M., Rohling, E.J., Bigg, G.R., and Ramirez, J., 2012, Paleoceanography of the Atlantic-Mediterranean exchange: Overview and first quantitative assessment of climatic forcing: Reviews of Geophysics, v. 50, doi:10.1029/2011RG000376.

Rogerson, M., Rohling, E.J., and Weaver, P.P.E., 2006, Promotion of meridional overturning by Mediterranean-derived salt during the last deglaciation: Paleoceanography, v. 21, doi:10.1029/2006PA001306.

Rögl, F., 1999, Mediterranean and Paratethys. Facts and hypotheses of an Oligocene to Miocene Paleogeography (short overview): Geologica Carpathica, v. 50, p. 339–349.

Roque, C., Duarte, H., Terrinha, P., Valadares, V., Noiva, J., Cachão, M., Ferreira, J., Legoinha, P., and Zitellini, N., 2012, Pliocene and Quaternary depositional model of the Algarve margin contourite drifts (Gulf of Cadiz, SW Iberia): Seismic architecture, tectonic control and paleoceanographic insights: Marine Geology, v. 303–306, p. 42–62, doi:10.1016/j.margeo.2011.11.001.

Rosas, F.M., Duarte, J.C., Terrinha, P., Valadares, V., Matias, L., 2009, Morphotectonic characterization of major bathymetric lineaments in Gulf of Cadiz (Africa–Iberia plate boundary): Insights from analogue modelling experiments: Marine Geology, v. 261, p. 33-47, doi:10.1016/j.margeo.2008.08.002.

Rouchy, J.M., Suc, J.-P., Ferrandini, J., and Ferrandini, M., 2006, The Messinian Salinity Crisis revisited: Sedimentary Geology, v. 188–189, p. 1–8, doi:10.1016/j.sedgeo.2006.02.003.

Roveri, M. et al., 2014, The Messinian Salinity Crisis: Past and future of a great challenge for marine sciences: Marine Geology, v. 352, p. 25–58, doi:10.1016/j.margeo.2014.02.002.

Sallarès, V., Gailler, A., Gutscher, M.-A., Graindorge, D., Bartolomé, R., Gràcia, E., Díaz, J., Dañobeitia, J.J., and Zitellini, N., 2011, Seismic evidence for the presence of Jurassic oceanic crust in the central Gulf of Cadiz (SW Iberian margin): Earth and Planetary Science Letters, v. 311, p. 112–123, doi:10.1016/j.epsl.2011.09.003.

Sallarès, V., Martínez-Loriente, S., Prada, M., Gràcia, E., Ranero, C., Gutscher, M.-A., Bartolome, R., Gailler, A., Dañobeitia, J.J., and Zitellini, N., 2013, Seismic evidence of exhumed mantle rock basement at the Gorringe Bank and the adjacent Horseshoe and Tagus abyssal plains (SW Iberia): Earth and Planetary Science Letters, v. 365, p. 120–131, doi:10.1016/j.epsl.2013.01.021.

Sánchez-Leal, R.F. et al., 2017, The Mediterranean Overflow in the Gulf of Cadiz: A rugged journey: Science Advances, v. 3, doi:10.1126/sciadv.aao0609.

Sanders, J.E., 1965, Primary sedimentary structures formed by turbidity currents and related resedimentation mechanisms, *in* Primary Sedimentary Structures and Their Hydrodynamic Interpretation, SEPM (Society for Sedimentary Geology), p. 192–219, doi:10.2110/pec.65.08.0192.

Sansom, P., 2018, Hybrid turbidite–contourite systems of the Tanzanian margin: Petroleum Geoscience, v. 24, p. 258–276, doi:10.1144/petgeo2018-044.

Santisteban, C., and Taberner, C., 1983, Shallow marine and continental conglomerates derived from coral reef complexes after desiccation of a deep marine basin: the Tortonian-Messinian deposits of the Fortuna Basin, SE Spain: Journal of the Geological Society, v. 140, p. 401–411, doi:10.1144/gsjgs.140.3.0401.

Sartori, R., Torelli, L., Zitellini, N., Peis, D., and Lodolo, E., 1994, Eastern segment of the Azores-Gibraltar line (central-eastern Atlantic) : An oceanic plate boundary with diffuse compressional deformation: Geology, v. 22, p. 555, doi:10.1130/0091-7613(1994)022<0555:ESOTAG>2.3.CO;2.

Seber, D., Barazangi, M., Ibenbrahim, A., and Demnati, A., 1996, Geophysical evidence for lithospheric delamination beneath the Alboran Sea and Rif–Betic mountains: Nature, v. 379, p. 785–790, doi:10.1038/379785a0.

Serra, C.S. et al., 2020, Tectonic evolution, geomorphology, and influence of bottom currents along a large submarine canyon system: The São Vicente Canyon (SW Iberian margin): Marine Geology, v. 426, p. 106219, doi:10.1016/j.margeo.2020.106219.

Serra, N., Ambar, I., Boutov, D., 2010, Surface expression of Mediterranean Water dipoles and their contribution to the shelf/slope - open ocean exchange: Ocean Science, v. 6, p. 191-209, doi:10.5194/os-6-191-2010.

Shanmugam, G., 2000, 50 years of the turbidite paradigm (1950s—1990s): deep-water processes and facies models—a critical perspective: Marine and Petroleum Geology, v. 17, p. 285–342, doi:10.1016/S0264-8172(99)00011-2.

Shanmugam, G., 2003, Deep-marine tidal bottom currents and their reworked sands in modern and ancient submarine canyons: Marine and Petroleum Geology, v. 20, p. 471–491, doi:10.1016/S0264-8172(03)00063-1.

Shanmugam, G., 2008, Deep-water Bottom Currents and their Deposits, *in* Rebesco, M.C.A. ed., Contourites. Developments in Sedimentology, Amsterdam, Elsevier, v. 60, p. 59–81, doi:10.1016/S0070-4571(08)10005-X.

Shanmugam, G., 2012, New Perspectives on Deep-water Sandstones Origin, Recognition, Initiation and Reservoir Quality, *in* Handbook of petroleum exploration and production, Amsterdam, Elsevier, v. 9, p. 524.

Shanmugam, G., 2016, Submarine fans: A critical retrospective (1950–2015): Journal of Palaeogeography, v. 5, p. 110–184, doi:10.1016/j.jop.2015.08.011.

Shanmugam, G., 2017, The Contourite Problem, *in* Sediment Provenance, Elsevier, p. 183–254, doi:10.1016/B978-0-12-803386-9.00009-5.

Sibuet, J.-C., Rouzo, S., and Srivastava, S., 2012, Plate tectonic reconstructions and paleogeographic maps of the central and North Atlantic oceans 1 This article is one of a series of papers published in this CJES Special Issue on the theme of Mesozoic–Cenozoic geology of the Scotian Basin. 2 Earth Scie (S. Dehler, M. Deptuck, & A. Karim, Eds.): Canadian Journal of Earth Sciences, v. 49, p. 1395–1415, doi:10.1139/e2012-071.

Sierro, F.J. et al., 2020, Mediterranean Overflow Over the Last 250 kyr: Freshwater Forcing from the Tropics to the Ice Sheets: Paleoceanography and Paleoclimatology, v. 35, doi:10.1029/2020PA003931.

Simon, D., 2017, Gateway exchange , climatic forcing, and circulation of the Mediterranean Sea during the late Miocene : A model perspective. PhD Thesis. Utrecht University, Utrecht.

Simon, D., and Meijer, P., 2015, Dimensions of the Atlantic-Mediterranean connection that caused the Messinian Salinity Crisis: Marine Geology, v. 364, p. 53–64, doi:10.1016/j.margeo.2015.02.004.

Somoza, L., Maestro, A., and Lowrie, A., 1999, Allochthonous Blocks as Hydrocarbon Traps in the Gulf of Cadiz, *in* All Days, OTC, doi:10.4043/10889-MS.

Southard, J.B., and Stanley, D.J., 1976, Shelf-break processes and sedimentation, *in* Stanley, D.J. and Swift, D.J.P. eds., Marine Sediment Transport and Environmental Management, New York, Wiley-Interscience, p. 351–377.

Spakman, W., Chertova, M. V., van den Berg, Arie., and van Hinsbergen, D.J.J., 2018, Puzzling features of western Mediterranean tectonics explained by slab dragging: Nature Geoscience, v. 11, p. 211–216, doi:10.1038/s41561-018-0066-z.

Spakman, W., and Wortel, M., 2004, The TRANSMED Atlas. The Mediterranean Region from Crust to Mantle (W. Cavazza, F. Roure, W. Spakman, G. M. Stampfli, & P. A. Ziegler, Eds.): Berlin, Heidelberg, Springer Berlin Heidelberg, doi:10.1007/978-3-642-18919-7.

Srivastava, S.P., Roest, W.R., Kovacs, L.C., Oakey, G., Lévesque, S., Verhoef, J., and Macnab, R., 1990, Motion of Iberia since the Late Jurassic: Results from detailed aeromagnetic measurements in the Newfoundland Basin: Tectonophysics, v. 184, p. 229–260, doi:10.1016/0040-1951(90)90442-B.

Stanley, D.J., 1988, Turbidites Reworked by Bottom Currents: Upper Cretaceous Examples from St. Croix, U.S. Virgin Islands: Smithsonian Contributions to the Marine Sciences, p. 1–79, doi:10.5479/si.01960768.33.

Stocker, S., 2021, Evolution of a Messinian turbiditic depositional system in the deep Algarve Basin: implications for hydrocarbon exploration and carbon capture and storage. MSc Independent Project Report.

Stow, D.A.V., and Faugères, J.-C., 2008, Contourite Facies and the Facies Model, *in* Rebesco, M. and Camerlenghi, A. eds., Contourites. Developments in Sedimentology, Elsevier, v. 60, p. 223–256, doi:10.1016/S0070-4571(08)10013-9.

Stow, D.A.V., Hernández-Molina, F.J., Llave, E., Sayago-Gil, M., Díaz del Río, V., and van Hinsbergen, D.J.J., Vissers, R.L.M., and Spakman, W., 2014, Origin and consequences of western Mediterranean subduction, rollback, and slab segmentation: Tectonics, v. 33, p. 393–419, doi:10.1002/2013TC003349.

Branson, A., 2009, Bedform-velocity matrix: The estimation of bottom current velocity from bedform observations: Geology, v. 37, p. 327–330, doi:10.1130/G25259A.1.

Stow, D.A.V., and Lovell, J.P.B., 1979, Contourites: Their recognition in modern and ancient sediments: Earth-Science Reviews, v. 14, p. 251–291, doi:10.1016/0012-8252(79)90002-3.

Stow, D.A.V., and Shanmugam, G., 1980, Sequence of structures in fine-grained turbidites: Comparison of recent deep-sea and ancient flysch sediments: Sedimentary Geology, v. 25, p. 23–42, doi:10.1016/0037-0738(80)90052-4.

Stow, D., and Smillie, Z., 2020, Distinguishing between Deep-Water Sediment Facies: Turbidites, Contourites and Hemipelagites: Geosciences, v. 10, p. 68, doi:10.3390/geosciences10020068.

Stow, D.A. v., and Tabrez, A.R., 1998, Hemipelagites: processes, facies, and model: Geological Society, London, Special Publications, v. 129, p. 317–337, doi:10.1144/GSL.SP.1998.129.01.19.

Teixeira, M., Terrinha, P., Roque, C., Rosa, M., Ercilla, G., Casas, D., 2019, Interaction of alongslope and downslope processes in the Alentejo Margin (SW Iberia) – Implications on slope stability: Marine Geology, v. 410, p. 88-108, doi:10.1016/j.margeo.2018.12.011.

Teixeira, M., Terrinha, P., Roque, C., Voelker, A.H.L., Silva, P., Salgueiro, E., Abrantes, F., Naughton, F., Mena, A., Ercilla, G., Casas, D., 2020, The Late Pleistocene-Holocene sedimentary evolution of the Sines Contourite Drift (SW Portuguese Margin): A multiproxy approach: Sedimentary Geology, v. 407, p. 105737, doi:10.1016/j.sedgeo.2020.105737.

Terrinha, P., et al., 2019a. Rifting of the Southwest and West Iberia Continental Margins. In. Quesada, C., Oliveira, J.T. (Eds.), The Geology of Iberia: A Geodynamic Approach. Regional Geology Reviews. Springer, Cham. pp. 251-283. doi:10.1007/978-3-030-11295-0_6

Terrinha, P., et al., 2019b. The Alpine Orogeny in the West and Southwest Iberia Margins. In: Quesada C., Oliveira J. (Eds.) The Geology of Iberia: A Geodynamic Approach. Regional Geology Reviews. Springer, Cham. pp. 487-505. doi:10.1007/978-3-030-11295-0_11

Terrinha, P. et al., 2009, Morphotectonics and strain partitioning at the Iberia–Africa plate boundary from multibeam and seismic reflection data: Marine Geology, v. 267, p. 156–174, doi:10.1016/j.margeo.2009.09.012.

Terrinha, P., 1998, Structural Geology and Tectonic Evolution of the Algarve Basin, South Portugal. PhD Thesis. Imperial College London (University of London), London. https://spiral.imperial.ac.uk:8443/handle/10044/1/7544.

Terrinha, P. et al., 2003, Tsunamigenic-seismogenic structures, neotectonics, sedimentary processes and slope instability on the southwest Portuguese Margin: Marine Geology, v. 195, p. 55–73, doi:10.1016/S0025-3227(02)00682-5.

Terrinha, P., Ribeiro, C., Kullberg, J.C., Lopes, C., Rocha, R., and Ribeiro, A., 2002, Compressive Episodes and Faunal Isolation during Rifting, Southwest Iberia: The Journal of Geology, v. 110, p. 101–113, doi:10.1086/324206.

Thiéblemont, A., Hernández-Molina, F.J., Ponte, J.-P., Robin, C., Guillocheau, F., Cazzola, C., and Raisson, F., 2020, Seismic stratigraphic framework and depositional history for Cretaceous and Cenozoic contourite depositional systems of the Mozambique Channel, SW Indian Ocean: Marine Geology, v. 425, p. 106192, doi:10.1016/j.margeo.2020.106192.

Topper, R.P.M., Flecker, R., Meijer, P.Th., and Wortel, M.J.R., 2011, A box model of the Late Miocene Mediterranean Sea: Implications from combined 87Sr/86Sr and salinity data: Paleoceanography, v. 26, p. PA3223, doi:10.1029/2010PA002063.

Torelli, L., Sartori, R., and Zitellini, N., 1997, The giant chaotic body in the Atlantic Ocean off Gibraltar: new results from a deep seismic reflection survey: Marine and Petroleum Geology, v. 14, p. 125–138, doi:10.1016/S0264-8172(96)00060-8.

Tripsanas, E.K., Piper David J. W., Jenner, K.A., and Bryant, W.R., 2007, Submarine mass-transport facies: new perspectives on flow processes from cores on the eastern North American margin: Sedimentology, v. 0, p. 070916035251003-???, doi:10.1111/j.1365-3091.2007.00894.x.

Tulbure, M.A., Capella, W., Barhoun, N., Flores, J.A., Hilgen, F.J., Krijgsman, W., Kouwenhoven, T., Sierro, F.J., and Yousfi, M.Z., 2017, Age refinement and basin evolution of the North Rifian Corridor (Morocco): No evidence for a marine connection during the Messinian Salinity Crisis: Palaeogeography, Palaeoclimatology, Palaeoecology, v. 485, p. 416–432, doi:10.1016/j.palaeo.2017.06.031.

Vail, P.R., Audemard, F., Bowman, S.A., Eisner, P.N., and Perez Cruz, C., 1991, The Stratigraphic Signatures of Tectonics, Eustacy and Sedimentology: An Overview, *in* Eisele, G., Rieken, W., and Seilacher, A. eds., Cycles and Events in Stratigraphy, Springer, p. 617–659.

van der Laan, E., Hilgen, F.J., Lourens, L.J., de Kaenel, E., Gaboardi, S., and Iaccarino, S., 2012, Astronomical forcing of Northwest African climate and glacial history during the late Messinian (6.5–5.5Ma): Palaeogeography, Palaeoclimatology, Palaeoecology, v. 313–314, p. 107–126, doi:10.1016/j.palaeo.2011.10.013.

van der Schee, M. et al., 2016, Evidence of early bottom water current flow after the Messinian Salinity Crisis in the Gulf of Cadiz: Marine Geology, v. 380, p. 315–329, doi:10.1016/j.margeo.2016.04.005.

van der Schee, M., van den Berg, B.C.J., Capella, W., Simon, D., Sierro, F.J., and Krijgsman, W., 2018, New age constraints on the western Betic intramontane basins: a late Tortonian closure of the Guadalhorce Corridor? Terra Nova, v. 30 p. 325–332, doi:10.1111/ter.12347.

van Hinsbergen, D.J.J., Vissers, R.L.M., and Spakman, W., 2014, Origin and consequences of western Mediterranean subduction, rollback, and slab segmentation: Tectonics, v. 33, p. 393–419, doi:10.1002/2013TC003349.

van Rooij, D. et al., 2010, The Le Danois Contourite Depositional System: Interactions between the Mediterranean Outflow Water and the upper Cantabrian slope (North Iberian margin): Marine Geology, v. 274, p. 1–20, doi:10.1016/j.margeo.2010.03.001.

Vergés, J., and Fernàndez, M., 2012, Tethys–Atlantic interaction along the Iberia–Africa plate boundary: The Betic–Rif orogenic system: Tectonophysics, v. 579, p. 144–172, doi:10.1016/j.tecto.2012.08.032.

Viana, A.R., 2008, Economic Relevance of Contourites, *in* Rebesco, M. and Camerlenghi, A. eds., Contourites. Developments in Sedimentology, Amsterdam, Elsevier, v. 60, p. 491–510, doi:10.1016/S0070-4571(08)10023-1.

Viana, A.R., 2001, Seismic expression of shallow- to deep-water contourites along the south-eastern Brazilian margin: Marine Geophysical Researches, v. 22, p. 509–521, doi:10.1023/A:1016307918182.

Viana, A.R., and Rebesco, M., 2007, Economic and Palaeoceanographic Significance of Contourite Deposits: Geological Society, London, Special Publications, v. 276.

Walker, R.G., 1984, Shelf and shallow-marine sands, *in* Walker, R.G. ed., Facies Models. Geoscience Canada Reprint Series, v. 1, p. 141–170.

Weijermars, R., 1988, Neogene tectonics in the Western Mediterranean may have caused the Messinian salinity crisis and an associated glacial event: Tectonophysics, v. 148, p. 211–219, doi:10.1016/0040-1951(88)90129-1.

Weimer, P., and Shipp, C., 2004, Mass Transport Complex: Musing on Past Uses and Suggestions for Future Directions, *in* All Days, OTC, doi:10.4043/16752-MS.

Woodruff, F., and Savin, S.M., 1989, Miocene deepwater oceanography: Paleoceanography, v. 4, p. 87–140, doi:10.1029/PA004i001p00087.

Wortel, M.J.R., and Spakman, W., 2000, Subduction and Slab Detachment in the Mediterranean-Carpathian Region: Science, v. 290, p. 1910–1917, doi:10.1126/science.290.5498.1910.

Würtz, M., 2012, Mediterranean Submarine Canyons: Ecology and Governance.: Gland, Málaga, IUCN.

Zeck, H.P., 1997, Mantle peridotites outlining the Gibraltar Arc — centrifugal extensional allochthons derived from the earlier Alpine, westward subducted nappe pile: Tectonophysics, v. 281, p. 195–207, doi:10.1016/S0040-1951(97)00067-X.

Zitellini, N., Gràcia, E., Matias, L., Terrinha, P., Abreu, M.A., DeAlteriis, G., Henriet, J.P., Dañobeitia, J.J., Masson, D.G., and Mulder, T., 2009, The quest for the Africa–Eurasia plate boundary west of the Strait of Gibraltar: Earth and Planetary Science Letters, v. 280, p. 13–50, doi:10.1016/j.epsl.2008.12.005.

Zitellini, N., Rovere, M., Terrinha, P., Chierici, F., and Matias, L., 2004, Neogene Through Quaternary Tectonic Reactivation of SW Iberian Passive Margin: Pure and Applied Geophysics, v. 161, p. 565–587, doi:10.1007/s00024-003-2463-4.